

UNIVERSITY OF OKLAHOMA
GRADUATE COLLEGE

GEOCHEMICAL CHARACTERIZATION OF ORGANIC MATTER
IN VICTORIA HARBOUR SEDIMENTS, HONG KONG

A Dissertation

SUBMITTED TO THE GRADUATE FACULTY

in partial fulfillment of the requirements for the

degree of

Doctor of Philosophy

By

MICHAEL HSIEH
Norman, Oklahoma
2006

UMI Number: 3207060



UMI Microform 3207060


Copyright 2006 by ProQuest Information and Learning Company.
All rights reserved. This microform edition is protected against
unauthorized copying under Title 17, United States Code.

ProQuest Information and Learning Company
300 North Zeeb Road
P.O. Box 1346
Ann Arbor, MI 48106-1346

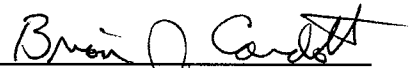
GEOCHEMICAL CHARACTERIZATION OF ORGANIC MATTER
IN VICTORIA HARBOUR SEDIMENTS, HONG KONG

A Dissertation APPROVED FOR THE
SCHOOL OF GEOLOGY & GEOPHYSICS

BY



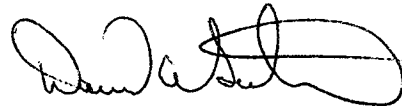
Dr. R. Paul Philp



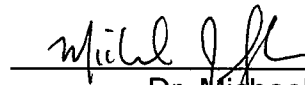
Mr. Brian J. Cardott



Dr. Michael H. Engel



Dr. David A. Sabatini



Dr. Michael J. Soreghan

ACKNOWLEDGEMENTS

I would like to thank my advisor, Dr. Paul Philp, for his guidance, encouragement, and financial support throughout the duration of my studies. Dr. Wyss Yim, at the University of Hong Kong, supplied the piston core used in this study and was a valuable source of information on topics related to Victoria Harbour. I am thankful for the hospitality and assistance that was extended to me during my visit to Hong Kong. I would also like to express my appreciation to Dr. Mike Engel, Dr. Mike Soreghan, Mr. Brian Cardott, and Dr. David Sabatini, for their comments to improve my dissertation and for serving on my committee.

Special thanks to Jon Allen and Tomasz Kuder for their help with analytical instruments, guidance, and friendship. Barbara Smallwood and Brian Jones helped with elemental and bulk stable isotope measurements at Texas A & M University. I want to thank the Hong Kong Department of Environmental Protection for allowing me to spend a day collecting samples with them throughout Victoria Harbour. Several of the SGG staff members have helped me in many ways over the year: Donna Mullins, Nancy Leonard, Therese Stone, Terry Brady, Carol Drayton, Brian Silver, and Claren Kidd.

The Geological Society of America is acknowledged for providing me with graduate student research grants, and also many thanks to the OU-School of Geology & Geophysics for the use of their facilities and resources.

My friends from Virginia Tech (Jon Kane, Greg Corder, and Scott Avery) still manage to make me laugh and relax. I appreciate the support they have

given me over the years. My parents, Dr. Hsin H. Hsieh and Yi-Jong Hsieh, have always supported and encouraged my pursuits. I thank them and my sisters, Arlene and Minnie, for their love and for always being there for me. My Oklahoma host families, Drs. Tom and Patti Landers, and Hal and Clara Jefferies, have been a positive influence in my life. I will always value their friendship.

I would like to dedicate this work to my wife, Shwu-Tzy Jiang, who has always been there for me. Her patience, encouragement, and love have helped sustain me throughout the Ph.D. program.

TABLE OF CONTENTS

LIST OF TABLES	x
LIST OF FIGURES	xi
LIST OF APPENDICES	xvi
ABSTRACT	xviii
 CHAPTER 1. INTRODUCTION	
1.1 Project Rationale and Objectives	1
1.2 Study Area – Victoria Harbour, Hong Kong SAR	7
1.2.1 Hong Kong – Late Pleistocene to Holocene	8
1.2.2 Sedimentation Rates (Based on ²¹⁰ Pb-Dating) and Approximate Age of Sediments	12
1.2.3 Tropical Cyclones (Typhoons) in Hong Kong	14
1.2.4 Sewage Dumping in Victoria Harbour	15
1.3 Summary Remarks	17
1.4 References	18
 CHAPTER 2. SAMPLES AND METHODOLOGY	
2.1 Core Samples	23
2.1.1 Sediment Core Description – MBH 54/2	24
2.2 Overview of Experimental Method	24
2.3 Free Lipid Extraction and Fractionation	25
2.3.1 Separation of Total Free Lipid Extracts into Non- Saponifiable and Saponifiable Fractions	26
2.3.2 Fractionation of Non-Saponifiable Lipids to Saturate, Aromatic, and Polar Fractions	27
2.4 Extraction of Ester- and Amide-Bound Lipids	28
2.5 Derivatization of Functionalized Lipids	29
2.5.1 Methylation of Saponifiable, Ester- and Amide-Bound Lipids ..	30

2.5.2 Silylation of Non-Saponifiable, Ester- and Amide-Bound Lipids	30
2.6 Gas Chromatography	31
2.7 Gas Chromatography-Mass Spectrometry	31
2.8 Gas Chromatography-Isotope Ratio Mass Spectrometry (GCIRMS)	32
2.9 Elemental Analysis, and Bulk Organic Carbon ($\delta^{13}\text{C}_{\text{org}}$) and Total Nitrogen ($\delta^{15}\text{N}$) Stable Isotope Measurements	34
2.10 References	35

CHAPTER 3. ELEMENTAL AND STABLE ISOTOPE ANALYSES OF ORGANIC CARBON AND TOTAL NITROGEN IN SEDIMENTS FROM KOWLOON BAY, HONG KONG

3.1 Introduction	37
3.2 Review of Literature	38
3.2.1 Organic Carbon and Total Nitrogen in Marine Sediments	38
3.2.2 Carbon-to-Nitrogen Ratio (C/N Ratio)	40
3.2.3 Bulk Stable Isotope Analyses	41
3.2.4 Sewage Derived Carbon and Nitrogen in Marine Sediments ..	43
3.3 Results and Discussion	47
3.3.1 Elemental Analyses	47
3.3.2 Ratio of Organic Carbon to Total Nitrogen	51
3.3.3 Bulk Stable Isotope Composition of Organic Carbon and Total Nitrogen	55
3.4 Summary Remarks	63
3.5 References	65

CHAPTER 4. SOURCES AND DISTRIBUTION OF EXTRACTABLE ORGANIC MATTER IN KOWLOON BAY SEDIMENTS, HONG KONG SAR, CHINA

4.1 Introduction	70
4.2 Review of Literature	71
4.2.1 Sterols in Marine Sediments	71
4.2.2 Fatty Alcohols in Marine Sediments	76

4.2.3 Fatty Acids in Marine Sediments	77
4.2.4 Hydrocarbons in Recent Sediments	78
4.3 Results and Discussion	79
4.3.1 Sterols and Stanols	80
4.3.2 Fatty Acids	85
4.3.3 Alcohols	90
4.3.4 Hydrocarbons	92
4.4 Summary Remarks	94
4.5 References	96
CHAPTER 5. THE OCCURRENCE AND DISTRIBUTION OF MICROBIAL MARKERS IN ESTER- AND AMIDE-BOUND LIPID FRACTIONS FROM KOWLOON BAY, HONG KONG SAR, CHINA	
5.1 Introduction	102
5.2 Literature Review	104
5.2.1 Ester- and Amide-Bound Lipids in Sedimentary Organic Matter	104
5.2.2 Carboxylic Acids	106
5.2.3 α - and β -Hydroxy Fatty Acids	107
5.2.4 ω - and (ω -1)-Hydroxy Fatty Acids	108
5.2.5 α,ω -Dicarboxylic Acids	109
5.2.6 Ester- and Amide-Bound Lipids in Bacteria	110
5.2.7 Carbon Isotopic Composition of Fatty Acids	112
5.3 Results and Discussion	115
5.3.1 n-Carboxylic Acids in the Ester-Bound Lipid Fraction	117
5.3.2 Branched-Carboxylic Acids in the Ester-Bound Lipid Fraction	124
5.3.3 Unsaturated-Carboxylic Acids in the Ester-Bound Lipid Fraction	130
5.3.4 α - and β -Hydroxy Fatty Acids in the Ester-Bound Lipid Fraction	131
5.3.5 Ester-Bound ω -Hydroxy Fatty Acids and n-Alcohols	134
5.3.6 Amide-Bound Carboxylic Acids	138
5.3.7 Amide-Linked β -Hydroxy Fatty Acids	142
5.3.8 Compound-Specific Carbon Isotope Composition of Ester- and Amide-Bound Fatty Acids	144
5.4 Summary Remarks	152

5.5 References	155
----------------------	-----

CHAPTER 6. CONCLUSIONS AND RECOMMENDATIONS FOR FUTURE WORK

6.1 Concluding Remarks	164
6.1.1 Summary of Bulk Parameter Measurements	165
6.1.2 Summary of Free Lipid Composition and Profiles	166
6.1.3 Summary of Ester- and Amide-Bound Lipids	168
6.2 Recommendations for Future Work	170
6.3 References	172

LIST OF TABLES

Table		Page
1.1	Estimated population in Hong Kong, 1841-2004	4
3.1	Summary of elemental and bulk stable isotope measurements of carbon and nitrogen in marine sediments, sewage sludge/ effluents, particulate organic matter, and plankton-derived particulate organic carbon	46
3.2	Summary of elemental analyses and bulk stable isotope measurements of carbon and nitrogen in sediments from core MBH 54/2	48
5.1	Summary of lipid composition in the ester-bound fraction in core MBH 54/2	116

LIST OF FIGURES

Fig.		Page
1.1	Map illustrating the location of Victoria Harbour, relative to the Pearl River, in the Hong Kong Special Administrative Region of China (map taken from Fyfe <i>et al.</i> , 2000)	2
1.2	Maps illustrating changes to the land area surrounding Victoria Harbour, 1903 to 1980, as a result of coastal reclamation (from Chalmers, 1984)	5
1.3	Coastal reclamation history in Victoria Harbour (modified from Yim 2000). MBH 54/2 refers to the piston core used in this study. Sedimentation rates, based on ²¹⁰ Pb data from MVC 74 (Tanner <i>et al.</i> , 2000), were used to estimate sediment ages in core MBH 54/2	6
1.4	Ancient river channels and delta plain, extending out into the continental shelf of the South China Sea, during the late Pleistocene (from Feng and Shi, 1997)	9
1.5	Reconstructed environment around Hong Kong, during the late Pleistocene (from Fyfe <i>et al.</i> , 2000)	10
1.6	Map illustrating the pathways of typhoons, with wind speeds of at least 118 km/hr, that passed over Hong Kong (map taken from http://www.hko.gov.hk/informtc/historical_tc/no10track.htm)	14
1.7	Location of sewage outfalls (↗) in Hong Kong, up to 1981 (modified from Yim, 1984 and 1993)	16
1.8	Submarine-type sewage outfalls in Victoria Harbour, Hong Kong (from Yim, 1984)	17
2.1	Core MBH 54/2-Kwun Tong Typhoon Shelter, Kowloon Bay. Estimated sedimentation rates were reported by Tanner <i>et al.</i> (2000) for MVC 74.....	23
2.2	Flowchart summarizing methodology for separating and isolating lipid groups from marine sediments	25
3.1	Incorporation of carbon into organic matter utilizing the C3 pathway (from Fogel and Cifuentes, 1993)	42

3.2	Photosynthetic pathway of C4 plants, utilizing the enzyme phosphoenolpyruvate carboxylase (from Fogel and Cifuentes, 1993)	42
3.3	Downcore profiles of %C _{org} and %N in sediment from core MBH 54/2, from Kowloon Bay, Victoria Harbour, Hong Kong SAR	49
3.4	Graph of %C _{org} versus %N in sediment intervals from core sample MBH 54/2, Kowloon Bay, Victoria Harbour. The trend line shows a positive correlation between organic carbon and total nitrogen	51
3.5	Downcore profile of C/N (wt. % ratio) in core MBH 54/2, from Kowloon Bay, Victoria Harbour, Hong Kong SAR. “○” indicates possible flux of terrigenous-derived organic matter	52
3.6	(a) Downcore profile of δ ¹³ C _{org} and C/N (wt. % ratio); (b) Downcore profile of δ ¹⁵ N and C/N ratio	56
3.7	Crossplot of atomic C/N mass ratio to δ ¹³ C of plant material, for differentiating sources of organic matter (from Meyers, 1994)	60
3.8	Crossplot of C/N to δ ¹³ C of sediments from Kowloon Bay (core MBH 54/2)	61
3.9	Overlay of the atomic C/N mass ratio vs δ ¹³ C _{org} of sediments from core MBH 54/2, and the Meyers (1994) plot for differentiating sources of organic matter	61
3.10	Discrimination of sewage contaminated sediments from uncontaminated sediments using the plot of %C _{org} versus C/N ratio	62
3.11	Crossplot of δ ¹⁵ N versus δ ¹³ C _{org} of sediments from Kowloon Bay, (core MBH 54/2)	63
4.1	Cholesterol structure illustrating an example of the numbering scheme for sterols	71
4.2	Sterol transformation pathways (from Mackenzie <i>et al.</i> , 1982)	72
4.3	Fecal sterol profiles from (a) sewage waste and (b) human feces (figures provided via personal communications with Dr. Rhys Leeming, CSIRO)	74
4.4	Biohydrogenation of cholesterol to coprostanol in the human digestive tract (based on Björkhem and Gustafsson, 1971)	75

4.5	Distribution of sterols and stanols in sediment samples from core MBH 54/2. (1) coprostanol; (2) epicoprostanol; (3) cholesterol; (4) cholestanol; (5) brassicasterol; (6) 24-ethylcoprostanol; (7) 24-ethylepicoprostanol; (8) campesterol; (9) ergostanol (campestanol); (10) β -sitosterol; (11) stigmastanol	81
4.6	Stanol and sterol ratios in sediment samples from core MBH 54/2 .	83
4.7	Hydrogenation of sterols to stanols in sediments deposited in Kowloon Bay	85
4.8	n-Alkanoic acids (as methyl esters) in the saponifiable fraction of extractable lipids from two depth intervals in core MBH 54/2	86
4.9	Aquatic-to-Terrigenous ratio for free n-alkanoic acids in the (a) saponifiable and (b) non-saponifiable fractions. Short-chain alkanolic acids are typically more abundant than long-chain alkanolic acids, and are attributed to planktonic and bacterial input. A greater abundance of short-chain acids is observed at 1.1m and 1.6m	87
4.10	n-Alkanoic acids (as trimethylsilyl ethers) in the non-saponifiable fraction of extractable lipids from two depth intervals in core MBH 54/2	89
4.11	Fatty alcohols (as trimethylsilyl ethers) in the non-saponifiable fraction of extractable lipids, from core MBH 54/2 (CPI~8)	91
4.12	Aquatic-to-Terrigenous ratio for free fatty alcohols. Downcore distribution indicates cuticle waxes of higher plants are the primary source for alcohols	91
4.13	n-Alkane distribution in the extractable lipid fraction from core MBH 54/2, illustrating a distinct odd-over-even predominance pattern (CPI~3.0)	93
4.14	(a) Aquatic-to-Terrigenous ratio for free n-alkanes; (b) Downcore profile illustrating shifts in predominance of macrophyte versus terrigenous plant material; (c) Downcore shifts in vegetation type, based on the mean carbon number ranging between C_{27} - C_{31}	93
5.1	Generic reactions summarizing steps in the remineralization of organic matter (from Jørgensen, 2000)	103

5.2	Example of structures and nomenclature of lipids commonly observed in bound lipids	105
5.3	Cellular structure of a Gram-negative bacterium (from http://www.bmb.leeds.ac.uk/mbiology/ug/ugteach/icu8/introduction/bacteria.html#cell_wall)	111
5.4	Components of phospholipids in bacterial cellular membranes (from http://cellbio.utmb.edu/cellbio/membrane_intro.htm)	111
5.5	Structure of Lipid-A in Gram-negative bacteria (from http://www.cyberlipid.org/glycolip/glyl0005.htm)	112
5.6	Downcore profile of fatty acids as methyl esters in the ester-bound lipid fraction of core section MBH 54/2. * indicates iso- branched fatty acids, and • indicates anteiso- branched fatty acids	118
5.7	Downcore distribution illustrating the abundance of short- and long-chain n-alkanoic acids in the ester-bound lipid fraction	119
5.8	Ratio of short to long chain ester-bound fatty acids as methyl esters. Downcore variations and shifts in contributions of organic source material are illustrated in this diagram	120
5.9	Carbon preference index for ester-bound fatty acids as methyl esters, relative to depth, in core MBH 54/2	122
5.10	Plot illustrating the relative proportion of bacterial components in the ester-bound fraction of sediments from core MBH 54/2, using the ratio of $(i-C_{15:0} + ai-C_{15:0})/C_{16:0}$ vs depth	125
5.11	Percent composition of branched chain fatty acids within the $C_{12:0}$ to $C_{20:0}$ range of ester-bound lipids	126
5.12	Partial chromatogram illustrating an example bacterial lipid profile, distributed in the ester-bound short chain fatty acids ($C_{12:0} - C_{20:0}$), extracted from a sediment sample (core MBH 54/2, ~1.6m depth) .	128
5.13	Iso-/Anteiso-ratio of $C_{15:0}$ and $C_{17:0}$ fatty acids in the ester-linked fraction of sediments from core MBH 54/2	129
5.14	Fragmentogram illustrating the distribution of β -hydroxy fatty acids in the ester-bound lipid fraction of core MBH 54/2	132

5.15	Downcore profile of straight chain and branched β -hydroxy fatty acids ($\mu\text{g/g}$ dry sediment weight), in the ester-bound lipid fraction of core MBH 54/2	133
5.16	Downcore distribution of ω -hydroxy fatty acids in the ester-bound lipid fraction of core MBH 54/2	136
5.17	Downcore distribution of n-alcohols in the ester-bound lipid fraction of core MBH 54/2	137
5.18	Downcore profile of fatty acids as methyl esters in the amide-bound lipid fraction of core MBH 54/2. * indicates iso- branched fatty acids, and • indicates anteiso- branched fatty acids	139
5.19	Average CPI of fatty acids in the amide-bound lipid fraction, relative to depth. CPIs were calculated using eq. 5.1 , eq. 5.2 , eq. 5.3	140
5.20	Aquatic-to-Terrigenous ratio using n-alkanoic acids in the amide-bound lipid fraction	141
5.21	Downcore abundance of ester- and amide-bound β -hydroxy fatty acids in core MBH 54/2	142
5.22	Fragmentogram illustrating the distribution of β -hydroxy fatty acids in the amide-bound lipid fraction of core MBH 54/2	143
5.23	Average carbon isotopic composition of ester-bound fatty acids at depths ranging from 0.8m to 2.6m, and the average isotopic composition at 3.3m and 3.9m	144
5.24	Downcore carbon isotopic composition of ester-bound fatty acids ..	145
5.25	Carbon isotopic composition of i- and ai- $\text{C}_{15:0}$ and $\text{C}_{17:0}$ ester-bound fatty acids in core MBH 54/2	147
5.26	Carbon isotopic composition of amide-bound fatty acids in core MBH 54/2	148
5.27	Isotopic composition of amide-bound fatty acids, at increasing depth intervals in core MBH 54/2	149

LIST OF APPENDICES

Appendix I	Page
A1.1 Bulk measurements of sediments from core MBH 54/2: total organic carbon (%C _{org}) and total nitrogen (%N)	173
A1.2 Bulk measurements of sediments from core MBH 54/2: δ ¹³ C _{org} (‰) and δ ¹⁵ N (‰)	174
Appendix II	
A2.1 Sterol structures, common names, IUPAC names, and chemical formula	175
Appendix III	
A3.1 Representative mass spectra for carboxylic acids, β-hydroxy fatty acids, α-hydroxy fatty acids, ω-hydroxy fatty acids, sterols, and stanols	176
Appendix IV	
A4.1 Summary of sterol ratios in free lipids in core MBH 54/2	194
A4.2 Summary of aquatic/terrigenous ratios for free lipids in core MBH 54/2	194
A4.3 Summary of carbon preference indices for free lipids in core MBH 54/2	194
A4.4 Chromatograms of free fatty acids in the saponifiable lipid fraction	195
A4.5 Chromatograms of free fatty acids in the non-saponifiable lipid fraction	196
A4.6 Chromatograms of free alcohols in the non-saponifiable lipid fraction	197
A4.7 Chromatograms of free n-alkanes in the non-saponifiable lipid fraction	198
Appendix V	
A5.1 Ester-bound fatty acid methyl esters (µg/g sediment dry weight) ..	199
A5.2 Ester-bound β-hydroxy fatty acids (ng/g sediment dry weight)	200
A5.3 Ester-bound ω-hydroxy fatty acids (ng/g sediment dry weight)	201

A5.4	Ester-bound n-alcohols (ng/g sediment dry weight)	201
A5.5	Amide-bound fatty acid methyl esters (ng/g sediment dry weight) .	202
A5.6	Amide-bound β -hydroxy fatty acids (ng/g sediment dry weight)	203
A5.7	Summary of carbon preference indices, aquatic-to-terrigenous ratio, and the (i-C _{15:0} + ai-C _{15:0})/C _{16:0} ratio for ester-bound fatty acids	204
A5.8	Summary of carbon preference indices, and the aquatic-to-terrigenous ratio for amide-bound fatty acids	204
Appendix VI		
A6.1	$\delta^{13}\text{C}$ (‰) composition of ester-bound fatty acids in core MBH 54/2	205
A6.2	$\delta^{13}\text{C}$ (‰) composition of amide-bound fatty acids in core MBH 54/2	206

ABSTRACT

Victoria Harbour is located between Kowloon and Hong Kong Island in the southeastern prodelta region of the Pearl River system. Since the mid-1900s, the population in Hong Kong has grown rapidly, coastal areas surrounding Victoria Harbour have been reclaimed, and excess raw sewage has been disposed into the Harbour. Release of methane from harbour sediments during dredging activities instigated interest in studying the sources of methane trapped in Victoria Harbour sediments. Core MBH 54/2, from a heavily polluted area in Victoria Harbour's Kowloon Bay, was selected for this study. However, no methane was detected in sediments from this core. The project was redefined, using a detailed organic geochemical characterization approach to determine the sources of organic matter, evaluate changes in environmental conditions, and to ascertain whether remnants of bacterial lipids might be present to enhance our understanding of processes contributing to methane generation. Bulk properties (e.g., %C_{org}, %N, $\delta^{13}\text{C}_{\text{org}}$, and $\delta^{15}\text{N}$), lipid composition and profiles were applied to delineate changes in organic matter sources deposited in the Kowloon Bay area during the late Quaternary.

The organic carbon-to-nitrogen ratio demonstrated fluctuations in the sources of organic matter throughout the Holocene unit of MBH 54/2. High fluxes in the carbon-to-nitrogen ratio may reflect strong storms, where excess terrigenous plant material is transported into the area. Sediment intervals impacted by sewage waste had isotopic compositions (*i.e.*, $\delta^{13}\text{C}_{\text{org}}$ and $\delta^{15}\text{N}$)

consistent with those reported in the literature for sewage in coastal environments.

Sources of organic matter could be differentiated using free lipids, which consisted of sterols, n-alcohols, fatty acids, and n-alkanes. Environmental conditions in Kowloon Bay were inferred to be anoxic based on the relative abundance of stanols-to-sterols. Sewage contaminated sediments were confirmed by the presence of fecal sterols. Periods of improved environmental conditions were noted by the occurrence of sterols common to aquatic organisms. Bound lipids appear to retain lipid profiles descriptive of bacterial communities in the sediments. More in-depth comparisons to lipid profiles of bacterial strains might allow bacterial remnants in sediments to be identified, allowing us to better speculate on their role in the remineralization of organic matter in Recent sediments.

CHAPTER 1

Introduction

1.1 Project Rationale and Objectives

Victoria Harbour is situated within the southeastern prodelta region of the Pearl River system (Fyfe *et al.*, 1999), between Kowloon and Hong Kong Island, in the Hong Kong Special Administrative Region (SAR) of China. A tidal channel runs west to east, through Victoria Harbour, with the mouth of the Pearl River to the west and the northern continental shelf of the South China Sea to the east (**Fig. 1.1**; Fyfe *et al.*, 1997; Yim *et al.*, 2002). The Pearl River system has played an important role in supplying sediments deposited in Victoria Harbour during the Quaternary (Chalmers, 1984; Davis, 1999; Fyfe *et al.*, 1999). Sediment transport in the harbour is controlled by tidal currents, with summer/autumn typhoons and winter/summer monsoons playing important roles in resuspending and redistributing sediments throughout the harbour (Huang and Yim, 1997; Yim *et al.*, 2002).

This region is of particular interest in that the Holocene unit of the inner-continental shelf in the Hong Kong SAR has been proposed to be a net carbon sink (Yim *et al.*, 2002). Continental margins, especially in regions in close proximity to deltas, are typically important reservoirs of sedimentary organic matter (Bernier, 1989; Hedges, 1992; Pernetta and Milliman, 1995; Hedges *et al.*, 1997; Mudge and Norris, 1997). In studies of the global carbon cycle, the ocean has been identified as preserving approximately one-third of the total organic

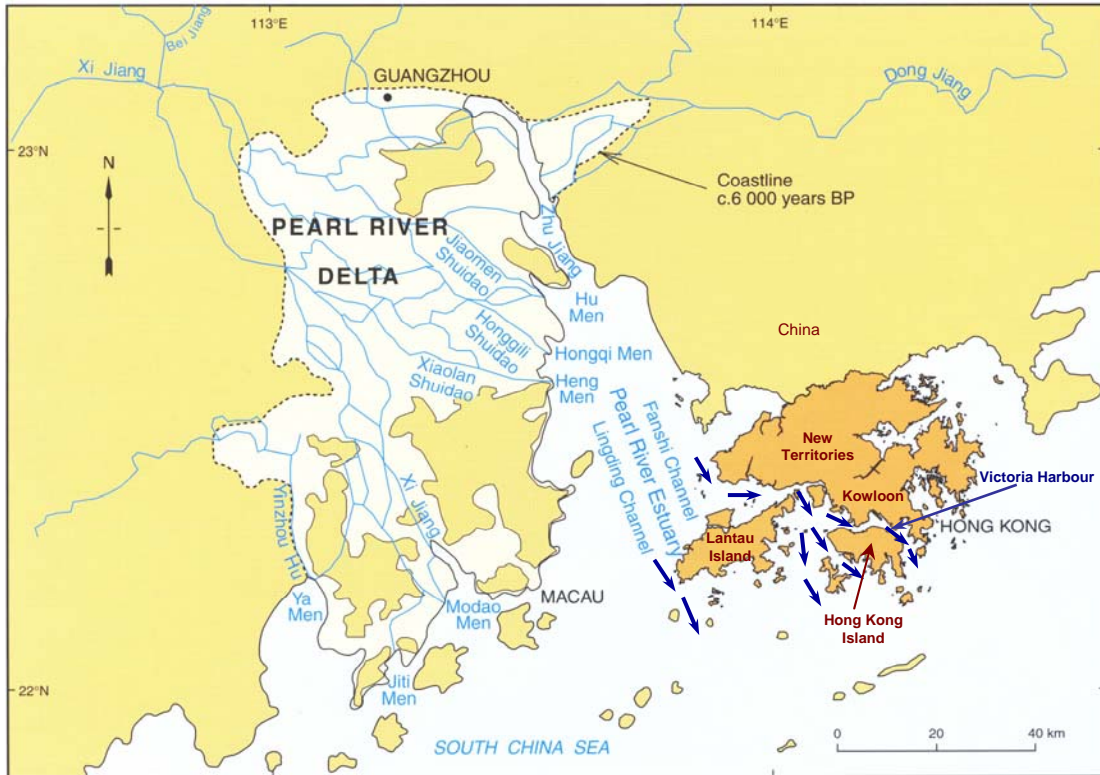


Fig. 1.1. Map illustrating the location of Victoria Harbour, relative to the Pearl River, in the Hong Kong Special Administrative Region of China (map taken from Fyfe *et al.*, 2000).

carbon inventory (Hedges *et al.*, 1997). An estimated 80% of the organic carbon in the ocean is buried and preserved in deltaic and continental shelf environments (Berner, 1989; Hedges, 1992; Hedges and Oades, 1997; Mudge and Norris, 1997). Factors controlling the preservation of organic carbon in marine sediments have been debated, with primary arguments being between anoxia versus productivity. Anoxia focuses on the idea that organic carbon is less efficiently degraded under anaerobic conditions compared to aerobic conditions. Whereas those supporting productivity argue that conditions favoring the growth of organisms (*e.g.*, areas of coastal upwelling) are more important for the

accumulation of organic matter (Demaison and Moore, 1980; Pedersen and Calvert, 1990; Calvert and Pedersen, 1993; Canfield, 1994). Additional parameters that have also been considered are the adsorption of organic matter to mineral surfaces and high sedimentation rates (Müller and Suess, 1979; Keil *et al.*, 1994; Rullkötter, 2000). It has been suggested that organic matter bound to mineral matrices is better protected from microbial attack and chemical alteration (Kawamura and Ishiwatari, 1984; Keil *et al.*, 1994). The thought behind better preservation of organic matter due to high sedimentation rate is that the organic matter will have a shorter residence time in the water column (where remineralization of organic matter to CO₂ typically occurs) and will be rapidly buried in bottom sediments (Didyk *et al.*, 1978). At the same time, high sedimentation rates can also result in the dilution of organic matter due to the deposition of clastic material (Rullkötter, 2000).

The present-day Victoria Harbour is a unique environment that has undergone many human-induced changes. Historical records indicate that the mid-1800s marked the beginning of reclamation activities and large-scale sewage discharge into Victoria Harbour. In the mid-1900s, the human population grew rapidly (**Table 1.1**) in Hong Kong, resulting in an increase of raw sewage and wastewater effluents being discharged into the harbour. This also led to the need for more land area resulting in large-scale dredging and coastal reclamation activities (Chalmers, 1984; Yim, 1984; Connell *et al.*, 1998; Lee and Liu, 1999; Tanner *et al.*, 2000; Yim *et al.*, 2002). During dredging of Victoria Harbour sediments, methane was observed escaping from the sediments to the surface

Table 1.1. Estimated population in Hong Kong, 1841-2004.

Year	Population
1841 ¹	7,500
1931 ¹	849,800
1945 ¹	750,000
1991 ^{2,3,4}	5.6×10^6
1996 ^{3,4}	6.3×10^6
1999 ⁵	6.6×10^6
2001 ^{3,4}	6.7×10^6
2003 ⁵	6.8×10^6
2004 ⁵	6.9×10^6

¹<http://www.answers.com/topic/demographics-of-hong-kong>

²<http://www.china-tour.cn/cityguides/hongkong.htm>

³<http://www.hk.cc.og.hk/eng/winter%202001/population%20Census.htm>

⁴http://www.jil.go.jp/foreign/event_r/event/documents/2004-sopemi_e_countryreport3.pdf

⁵http://www.info.gov.hk/censtatd/eng/hkstat/hkinf/population_index.html

raising concerns in this area for its potential impacts as a greenhouse gas (Yim *et al.*, 2002).

The increased sewage input has resulted in accelerated eutrophication of Victoria Harbour. Reclamation activities have not only reshaped the harbour (**Figs. 1.2** and **1.3**), but have also increased sedimentation rates in various parts of the harbour (Tanner *et al.*, 2000; Yim *et al.*, 2002). Based on the current amount of organic matter input, anoxic bottom waters, and high sedimentation rate, it would seem that marine sediments in Victoria Harbour should be well-suited for the deposition and preservation of organic carbon (Didyk *et al.*, 1978). Prior to human activities, the Pearl River, tidal currents, tropical storms and monsoons, and eustatic sea level changes were the likely factors controlling organic matter deposition in Victoria Harbour.

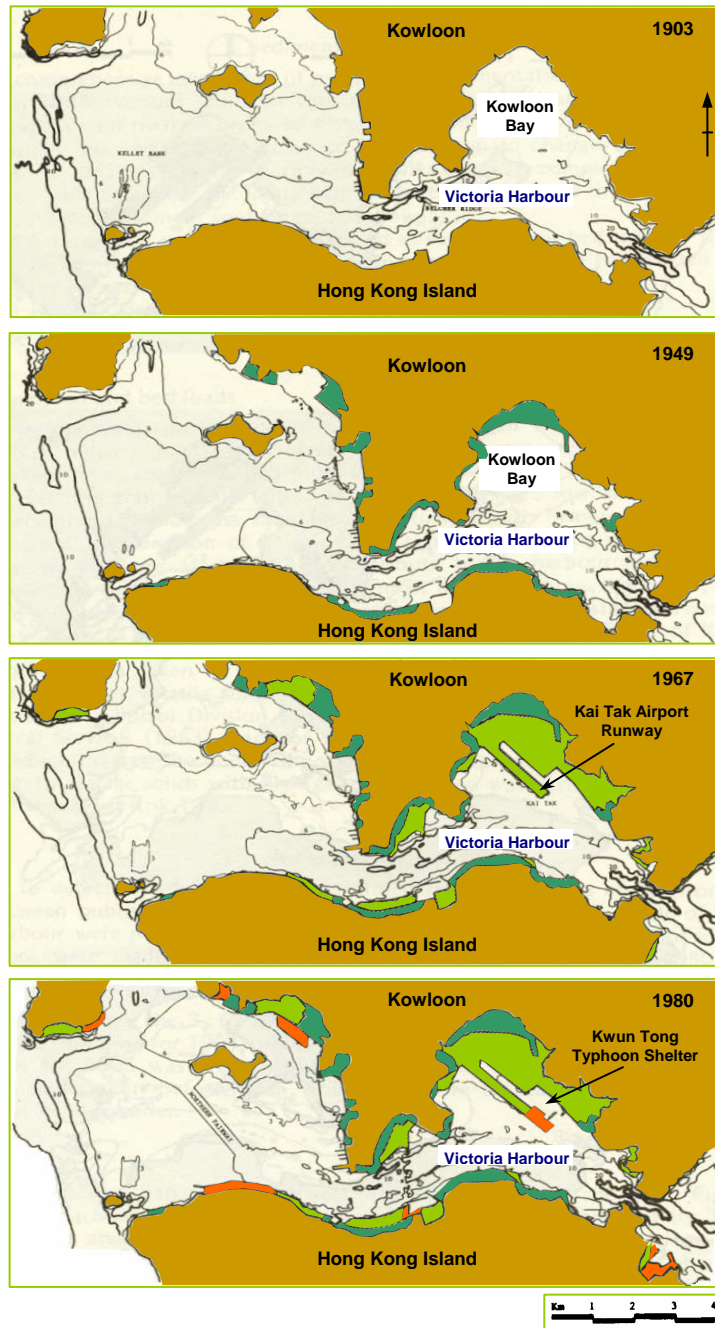


Fig. 1.2. Maps illustrating changes to the land area surrounding Victoria Harbour, 1903 to 1980, as a result of coastal reclamation (from Chalmers, 1984).

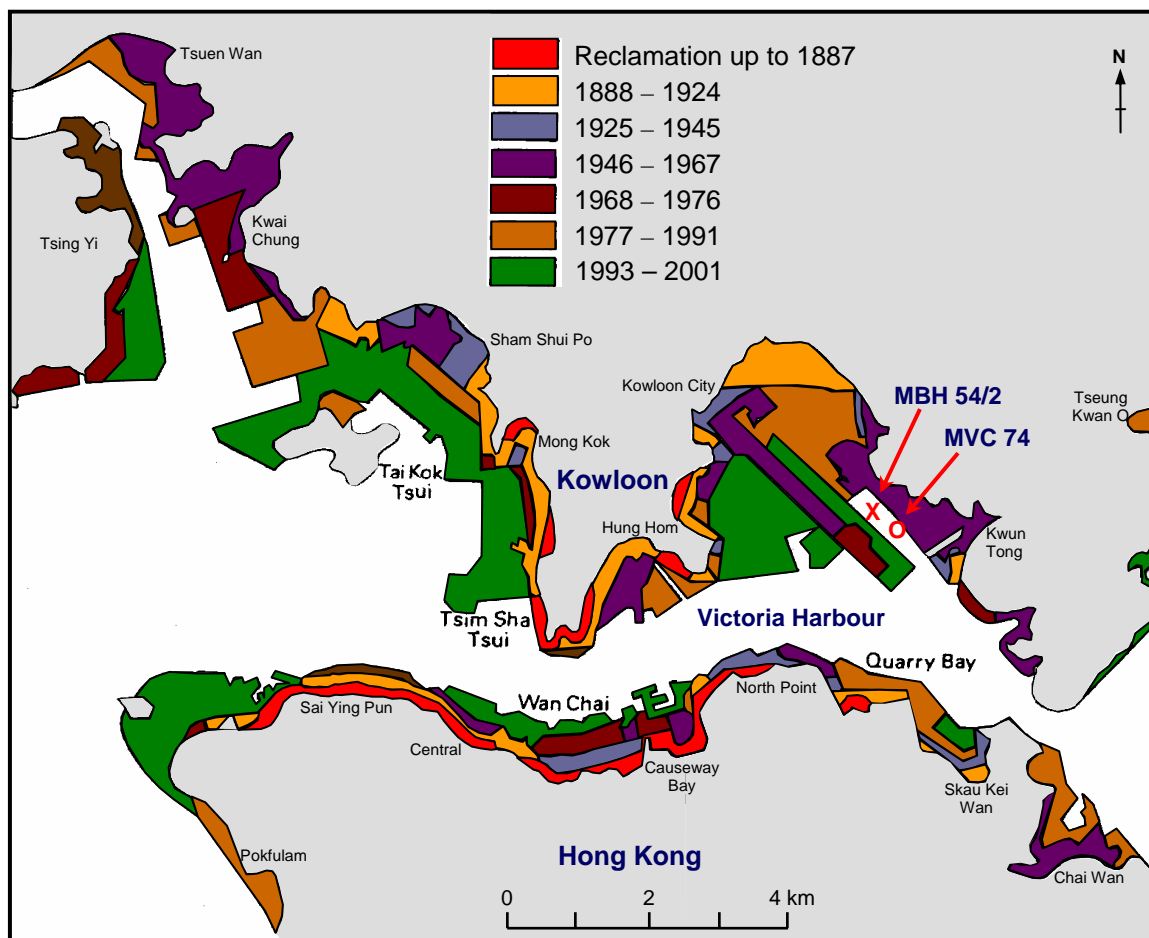


Fig. 1.3. Coastal reclamation history in Victoria Harbour (modified from Yim 2000). MBH 54/2 refers to the piston core used in this study. Sedimentation rates, based on ^{210}Pb data from MVC 74 (Tanner *et al.*, 2000), were used to estimate sediment ages in core MBH 54/2.

Lipid composition, elemental and isotopic measurements of organic matter at various depth intervals from a core in the inner-continental shelf region of Hong Kong have been used to reconstruct environmental changes and to speculate on the history of this region. The major objectives of this project were to: (1) characterize the various classes of lipids (*i.e.*, free-, ester-bound, and amide-bound lipids); (2) ascertain sources and changes in organic matter deposited and preserved during the late Quaternary in Victoria Harbour; (3) use elemental and bulk stable isotope compositions of carbon and nitrogen in sedimentary organic matter to infer changes in organic matter sources, to speculate on possible early diagenetic processes, and to identify periods of environmental change (*e.g.*, the interglacial-glacial boundary); (4) apply compound-specific carbon isotopes to differentiate sources of lipids in the core samples.

1.2 Study Area – Victoria Harbour, Hong Kong SAR

Victoria Harbour is located in the Hong Kong Special Administrative Region (SAR) of China, between Kowloon and Hong Kong Island, and is one of the busiest shipping ports in the world. The total area within the Hong Kong territorial boundaries is about 3400 km². Land coverage in this region, which is comprised of the New Territories, Kowloon, Hong Kong Island, Lantau Island, and other surrounding islands, totals an area of about 1100 km² (**Fig. 1.1**; Yim *et al.*, 2002). Victoria Harbour is in the southeastern prodelta region of the Pearl

River and has a tidal channel running west to east through the harbour into the northern continental shelf of the South China Sea (Fyfe *et al.*, 1997). Nearly all land surrounding Victoria Harbour has been reclaimed (**Fig. 1.3**).

1.2.1 Hong Kong – Late Pleistocene to Holocene

During the late Pleistocene, around the last glacial maximum (~25,000 years B.P.), the coastline along southern China was about 130 km south of Hong Kong (**Fig. 1.4**; Feng and Shi, 1997; Owen *et al.*, 1998). Shallow seismic profiles (Feng and Shi, 1997) unveiled buried ancient river channels demonstrating that the Pearl River palaeodelta once extended over a significant area on the continental shelf in the South China Sea (**Fig. 1.4**). Fyfe *et al.* (2000) and Owen (2005) have reported the occurrence of low sinuous braided river channels in the Hong Kong area, during the late Pleistocene (**Fig. 1.5**). Coarser grained sands were deposited in this area during this period of low sea level (Fyfe *et al.*, 2000).

After about 18,000 years B.P. sea level began rising, reaching at least -19.5m by around 8,080 years B.P. (Owen *et al.*, 1998; Owen, 2005). The rise in sea level resulted in a blanket of intertidal silty mud deposited over this area. By about 6,000 years B.P., the coastline along the southern shores of China extended as far north as Guangzhou, whereas the coastline surrounding Hong Kong was similar to what is seen in the present day (**Fig. 1.1**; Fyfe *et al.*, 1997; Owen *et al.*, 1998; Davis, 1999). Between 6,000 years B.P. and the present day,

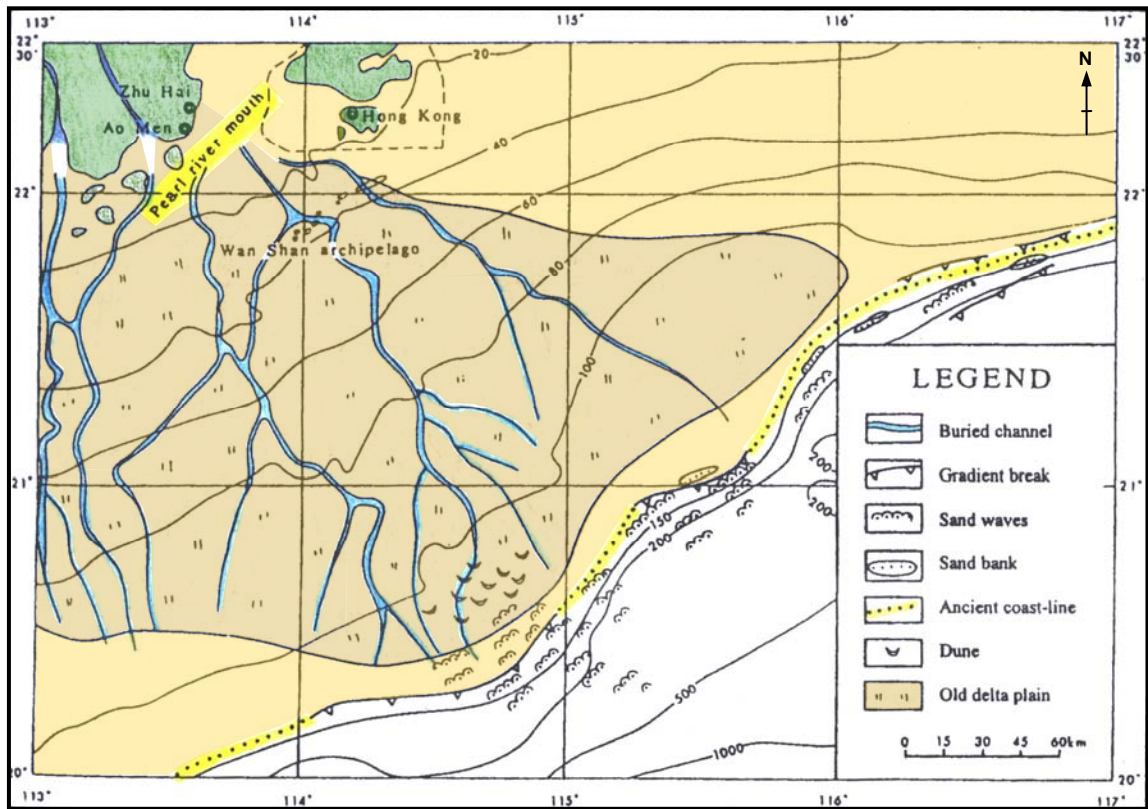


Fig. 1.4. Ancient river channels and delta plain, extending out into the continental shelf of the South China Sea, during the late Pleistocene (from Feng and Shi, 1997).

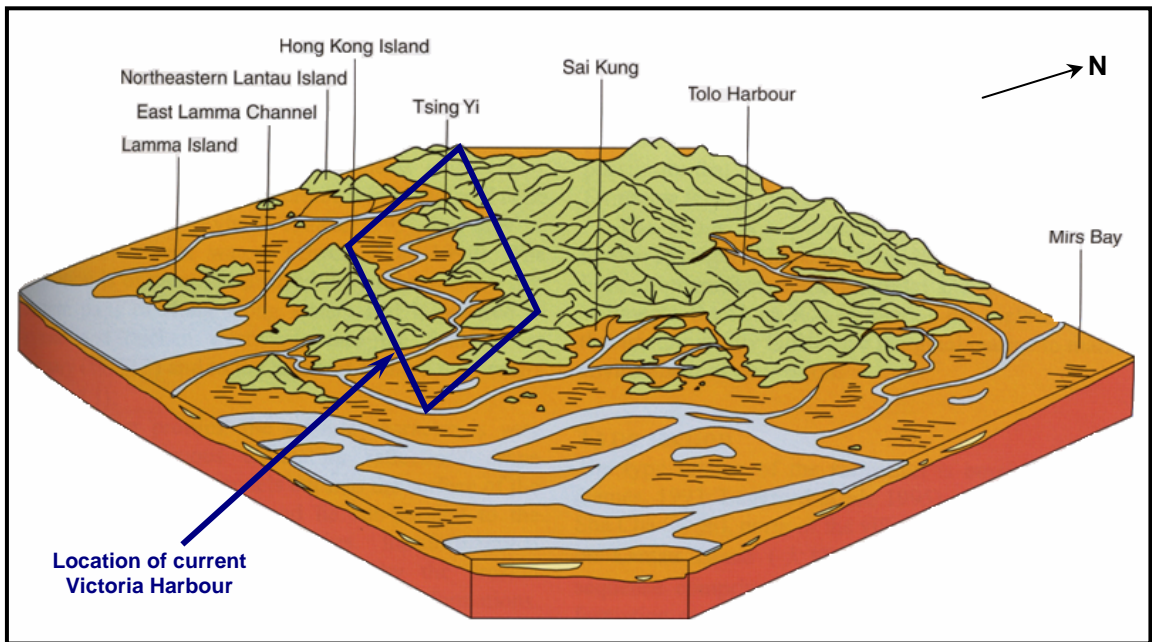


Fig. 1.5. Reconstructed environment around Hong Kong during the late Pleistocene (from Fyfe *et al.*, 2000).

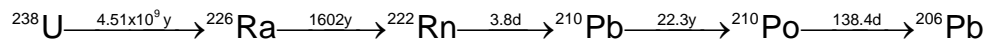
sea level fell slightly resulting in the development of the current Pearl River delta system (**Fig. 1.1**; Fyfe *et al.*, 1999).

The rise and fall in sea level throughout the Quaternary, in Hong Kong, has resulted in the deposition of alternating units of marine and terrestrial deposits (Yim, 1984; Yim, 1994; Owen *et al.*, 1998; Davis, 1999). The alternating units of marine sediments versus terrestrial sediments have been recognized by Yim (1994), based on selected features (*i.e.*, palaeontology, sedimentology, mineralogy, chemistry, and engineering properties). Using these parameters, Yim (1994) classified Quaternary sediments in Hong Kong as alternating units of marine and terrestrial sediments (denoted as “M” for marine, “T” for terrestrial, and numbered from 1 to 5). The youngest marine unit, “M1,” has a maximum age of 8,100 years B.P. and is comprised of soft green, gray, and/or black colored silty clay, with abundant shell remnants (Yim, 1984 and 1994). Throughout much of Hong Kong, the “T1” unit is missing. The “T1” unit represents terrestrial sediments of the last glacial period (8,100 to 70,000 years B.P.), deposited during a time of low sea level (Yim, 1994; Davis, 1999). It has been suggested that sediments of the T1 unit are missing because either they were never deposited, or during the lowstand the water levels were still high enough not to expose the sediments (Davis, 1999). The top of the “M2” unit, the marine unit of the last interglacial period (90,000 to 140,000 years B.P.), has been identified by the presence of a desiccated crust. The desiccated crust refers to marine sediments that have been subaerially exposed during periods of low sea level. Sediments that have undergone desiccation, in pre-Holocene marine sediments,

will have a mottled appearance (*i.e.*, a mixture of white, yellow, orange, red, and brown colors) (Yim, 1994; Tovey and Yim, 2002).

1.2.2 Sedimentation Rates (Based on ^{210}Pb -Dating) and Approximate Age of Sediments

Sedimentation rates in the Kwun Tong Typhoon Shelter area have been measured by Tanner *et al.* (2000), using ^{210}Pb -dating, for core MVC 74 (**Fig 1.3**). ^{210}Pb -dating is a technique commonly used for estimating sedimentation rates based on the radioactive decay of ^{210}Pb , where the half-life ($t_{1/2}$) is about 22.3y (Geyh and Schleicher, 1990). ^{210}Pb is a naturally occurring radionuclide which belongs to the ^{238}U decay series (see illustration below), and is produced in both the atmosphere and terrestrial environments.



Radionuclides formed in the ^{238}U decay series (from Appleby, 2001).

Atmospheric ^{210}Pb originates from ^{222}Rn , a radioactive gas which diffuses through the subsurface into the atmosphere. ^{222}Rn has a short half-life ($t_{1/2}=3.8\text{d}$) and decays to ^{210}Pb , which then easily binds to particulate material and is returned to sediments by dry deposition or rain. The ^{210}Pb is believed to be immobile once redeposited, and undergoes further decay. Terrestrially derived ^{210}Pb refers to ^{210}Pb occurring in the sampled sediment intervals where ^{222}Rn

undergoes *in situ* radioactive decay. ^{210}Pb -dating is calibrated using ^{137}Cs , an artificial radionuclide produced from the atmospheric testing of nuclear bombs. Peak deposition of ^{137}Cs in sediments occurred in 1964 (Noller, 2000; Appleby, 2001). Sedimentation rates, using ^{210}Pb , of recent sediments from lacustrine and marine environments have been estimated to be reliable between 5 to 150 years (Geyh and Schleicher, 1990; Noller, 2000).

The present-day sedimentation rate in Kwun Tong typhoon shelter (from the seafloor surface to 0.5m depth) was determined to be 3.5cm y^{-1} . The mean sedimentation rate for 0.5m to 1.5m was estimated to be about 4.4cm y^{-1} and corresponds to calendar years spanning 1957 to 1980. At depths of 1.5m to 2.1m, the sedimentation rate was estimated to be 1.9cm y^{-1} , representing sediments deposited between 1928 and 1957. Sedimentation rates at depths greater than 2.1m could not be determined due to uncertainties with excess ^{210}Pb activity (Tanner *et al.*, 2000). The maximum Holocene age has been reported to be about 8,100y. The base of the Holocene unit is marked by a desiccated crust, which represents the boundary between the M1 and M2 units (Yim, 1994). If the base of the Holocene unit occurs at 3.7m, and the maximum Holocene age is 8,100y, then the average sedimentation rate between 2.1m and 3.7m would be about 0.2mm y^{-1} .

1.2.3 Tropical Cyclones (Typhoons) in Hong Kong

Hong Kong is located on the northernmost region of the South China Sea and lies within the pathway commonly traversed by typhoons (Huang and Yim, 1997). Historical pathways of typhoons (also referred to as tropical cyclones) that have passed through Hong Kong (between 1957 and 1999), with wind speeds of at least 118km/hr, are summarized in **Fig. 1.6** (http://www.hko.gov.hk/informtc/historical_tc/no10track.htm). In general, the majority of typhoons tracked around the Hong Kong region approach Hong Kong from the southeast, and continues along a northwestern pathway (Huang and Yim, 1997).



Fig. 1.6. Map illustrating the pathways of typhoons, with wind speeds of at least 118 km/hr, that passed over Hong Kong between 1957 and 1999 (map taken from http://www.hko.gov.hk/informtc/historical_tc/no10track.htm).

1.2.4 Sewage Dumping in Victoria Harbour

The disposal of sewage waste into Hong Kong waters occurs on a rather large scale, primarily due to the immense population (~6.9 million people in 2004), and because existing sanitary landfill sites and sewage treatment plants are incapable of handling such large amounts of waste (Yim, 1984; World Wide Fund for Nature Hong Kong, 1993). In general, raw sewage is released into Hong Kong waters by seawall-type sewage outfalls (**Fig. 1.7**) and submarine-type sewage outfalls (**Fig. 1.8**), with minor or no treatment (Yim, 1984). About fifty percent of the raw sewage is released directly into Hong Kong waters. Of the remaining fifty percent of incoming sewage, about forty percent of larger size solid waste undergoes sedimentation (*i.e.*, “preliminary treatment”), and the remaining ten percent undergoes some type of further treatment (Wong and Tanner, 1997; World Wide Fund for Nature Hong Kong, 1993). Sometime after the mid-1970s, several of the seawall-type sewage outfalls were converted to submarine-type sewage outfalls and diverted further into the channel of Victoria Harbour. The goal was to dilute and better disperse sewage in Victoria Harbour (Yim, 1984). In a 1981 report, the two districts in Hong Kong generating and discharging the largest amount of sewage wastes were: Kwun Tong (~221,000 m³/day; via seawall-type sewage outfall) and Tsuen Wan/Kwai Chun (~243,000 m³/day; via submarine-type sewage outfall) (Yim, 1984). The total estimated raw sewage discharged throughout Victoria Harbour has been estimated to be at least 1.6×10^6 m³/day (Yim *et al.*, 2002). For comparison, the estimated daily sewage received by the waste water treatment facility in Norman, Oklahoma, is

about 38,611 m³/day, servicing a population of about 92,400 people (personal communications with Ralph Arnett, Darrell Schwartz, and Mark Daniels, from the Norman Waste Water Treatment Facility).

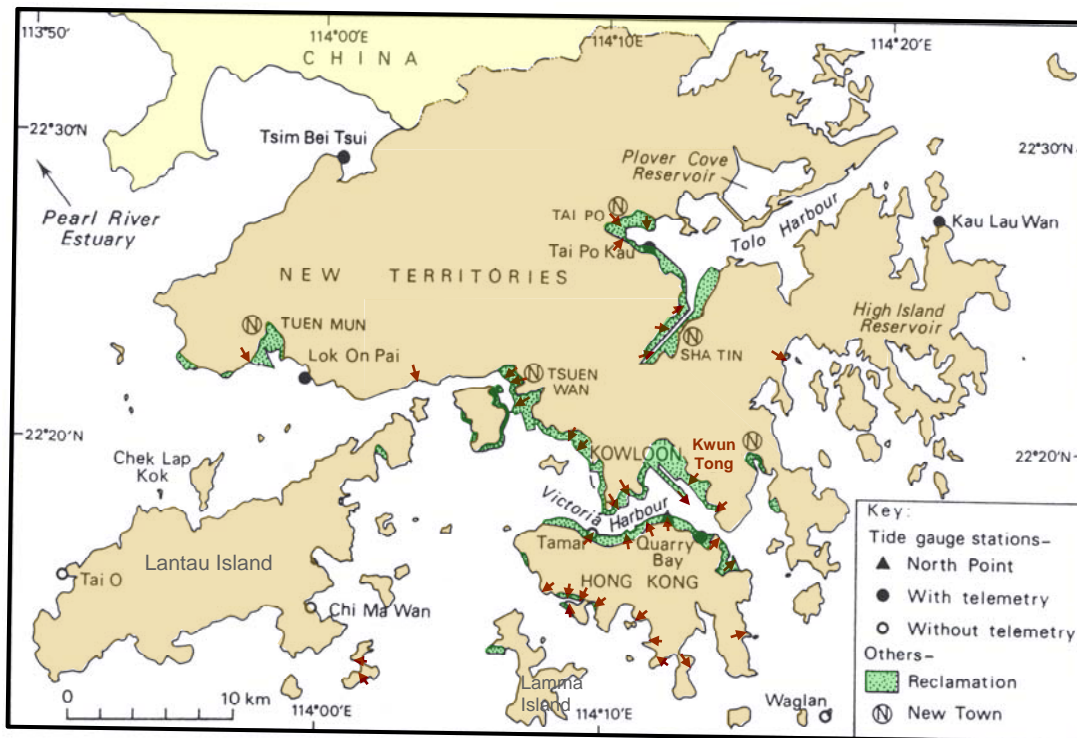


Fig. 1.7. Location of sewage outfalls (↗) in Hong Kong, up to 1981 (modified from Yim, 1984 and 1993).

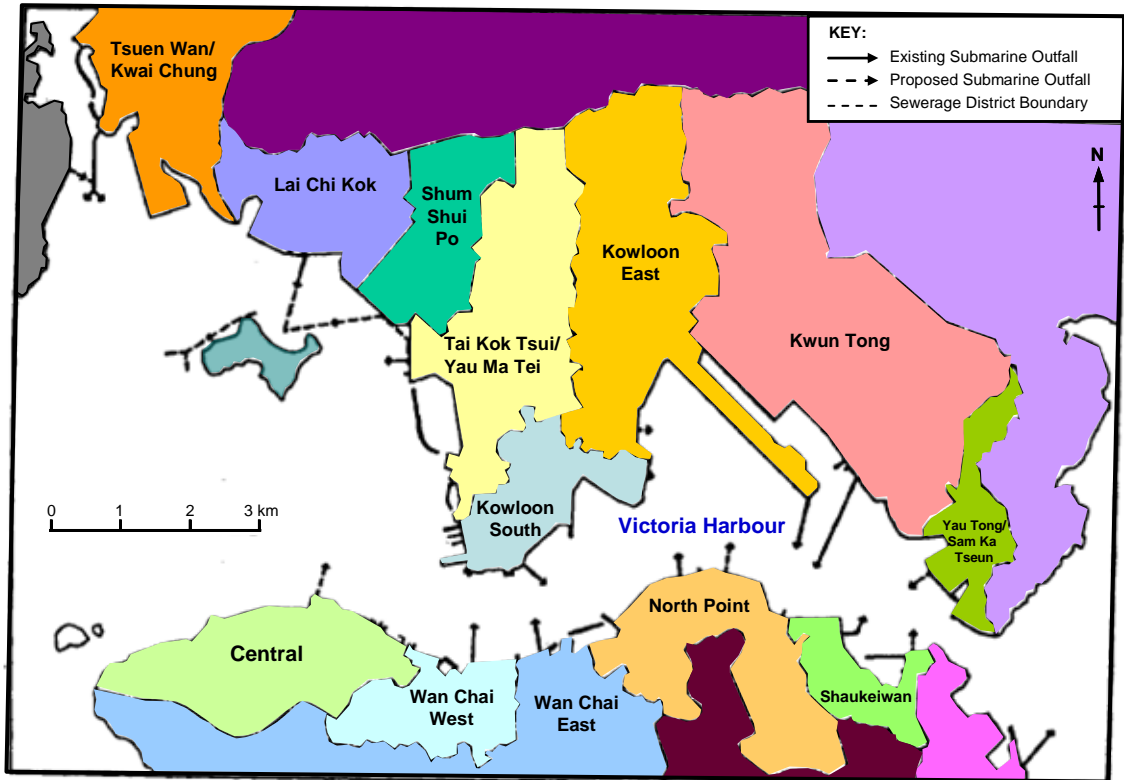


Fig. 1.8. Submarine-type sewage outfalls in Victoria Harbour, Hong Kong (from Yim, 1984).

1.3 Summary Remarks

The area where the modern-day Victoria Harbour is located has undergone many changes from the late Pleistocene through the Holocene. The coastline along the southern regions of China was about 130km south of Hong Kong during the late Pleistocene (during the last glacial max). During this period,

ancient river channels ran throughout the area, and a palaeodelta of the Pearl River extended over a significant region on the continental shelf in the South China Sea. Sea level began rising after ~18,000 years B.P., reaching at least -19.5m by ~8,080 years B.P. The coastline reached as far north as Guangzhou by about 6,000 years B.P., then receded slightly with the fall in sea level. With the rise in sea level, a blanket of Holocene intertidal silty mud was deposited throughout the area surrounding Hong Kong. Alternating layers of marine and terrestrial sediments, resulting from changes in sea level, can be observed in the Hong Kong marine sediments.

In more recent times, rapid population growth within Hong Kong has resulted in the need for more land, and the generation and disposal of significant amounts of raw sewage waste. Reclamation activities have altered the harbour profile and increased sedimentation rates in many areas around Hong Kong. Transitions of seawall-type sewage outfalls to submarine-type sewage outfalls further into the channel of Victoria Harbour have also had an impact on the concentration and dispersion of sewage waste in Hong Kong waters.

1.4 References

Appleby, P. G., 2001. Chronostratigraphic techniques in recent sediments. *In*: Last, W. M., Smol, J. P. (eds), *Tracking Environmental Change Using Lake Sediments. Volume 1: Basin Analysis, Coring, and Chronological Techniques*. Kluwer Academic Publishers, Dordrecht, The Netherlands, 171-203.

Berner, R. A., 1989. Biogeochemical cycles of carbon and sulfur and their effect on atmospheric oxygen over Phanerozoic time. *Palaeogeography*,

Palaeoclimatology, Palaeoecology (Global and Planetary Change Section), 75, 97-122.

Calvert, S. E., Pedersen, T. F., 1993. Geochemistry of recent oxic and anoxic marine sediments: implications for the geological record. *Marine Geology*, 113, 67-88.

Canfield, D. E., 1994. Factors influencing organic carbon preservation in marine sediments. *Chemical Geology*, 114, 315-329.

Chalmers, M. L., 1984. Preliminary assessment of sedimentation in Victoria Harbour, Hong Kong. *Geological Society Hong Kong Bulletin*, 1, 117-129.

Connell, D. W., Wu, R. S. S., Richardson, B. J., Leung, K., Lam, P. S. K., and Connell, P. A. 1998. Occurrence of persistent organic contaminants and related substances in Hong Kong marine areas: an overview. *Marine Pollution Bulletin*, 36, 376-384.

Davis, A. M., 1999. Quaternary stratigraphy of Hong Kong coastal sediments. *Journal of Asian Earth Sciences*, 17, 521-531.

Demaison, G. J., Moore, G. T., 1980. Anoxic environments and oil source bed genesis. *American Association of Petroleum Geologist Bulletin*, 64, 1179-1209.

Didyk, B. M., Simoneit, B. R. T., Brassell, S. C., Eglinton, G., 1978. Organic geochemical indicators of paleoenvironmental conditions of sedimentation. *Nature*, 272, 216-222.

Feng, W. K., Shi, W. J., 1997. Coastal remnants of the last glacial age in the continental shelf of the northern South China Sea. In: Jablonski, J. (Ed), *The Changing Face of East Asia During the Tertiary and Quaternary*, Centre of Asian Studies Occasional Papers and Monographs, 124, 150-155.

Fyfe, J. A., Selby, I. C., Shaw, R., James, J. W. C., Evans, C. D. R., 1997. Quaternary sea-level change on the continental shelf of Hong Kong. *Journal of the Geological Society*, 154, 1031-1038.

Fyfe, J. A., Selby, I. C., Plater, A. J., Wright, M. R., 1999. Erosion and sedimentation associated with the last sea level rise offshore Hong Kong, South China Sea. *Quaternary International*, 55, 93-100.

Fyfe, J. A., Shaw, R., Campbell, S. D. G., Lai, K. W., Kirk, P. A., 2000. The Quaternary Geology of Hong Kong. Geotechnical Engineering Office, Civil Engineering Department, The Government of the Hong Kong SAR. 209p.

- Geyh, M. A., Schleicher, H., 1990. *Absolute Age Determination: Physical and Chemical Dating Methods and Their Applications*. Springer-Verlag, New York, 503p.
- Hedges, J. I., 1992. Global biogeochemical cycles: progress and problems. *Marine Chemistry*, 39, 67-93.
- Hedges, J. I., Keil, R. G., Benner, R., 1997. What happens to terrestrial organic matter in the ocean? *Organic Geochemistry*, 27, 195-212.
- Hedges, J. I., Oades, J. M., 1997. Comparative organic geochemistries of soils and marine sediments. *Organic Geochemistry*, 27, 319-361.
- Huang, G., Yim, W. W. -S., 1997. Storm sedimentation in the Pearl River Estuary, China. *International Conference on the Evolution of the East Asian Environment. Centre of Asian Studies: Occasional Papers & Monographs*, 124, 156-177.
- Kawamura, K., Ishiwatari, R., 1984. Tightly bound aliphatic acids in Lake Biwa sediments: their origin and stability. *Organic Geochemistry*, 7, 121-126.
- Keil, R. G., Montlucon, D. B., Prahl, F. G., Hedges, J. I., 1994. Sorptive preservation of labile organic matter in marine sediments. *Nature*, 370, 549-552.
- Lee, A. H. M., Liu, J. W., 1999. *Marine Water Quality in Hong Kong in 1998*. Environmental Protection Department. Hong Kong SAR Government, Hong Kong.
- Mudge, S. M., Norris, C. E., 1997. Lipid biomarkers in the Conwy Estuary (North Wales, U. K.): Comparison between fatty alcohols and sterols. *Marine Chemistry*, 57, 61-84.
- Müller, P. J., Suess, E., 1979. Productivity, sedimentation rate and sedimentary organic matter in the oceans – Organic carbon preservation. *Deep Sea Research*, 26, 1347-1362.
- Noller, J. S., 2000. Lead-210 Geochronology. *In*: Noller, J. S., Sowers, J. M., Lettis, W. R. (eds), *Quaternary Geochronology: Methods and Applications*. American Geophysical Union Reference Shelf 4, Washington DC, 115-120.
- Owen, R. B., 2005. Modern fine-grained sedimentation – spatial variability and environmental controls on an inner pericontinental shelf, Hong Kong. *Marine Geology*, 214, 1-26.

Owen, R. B., Neller, R., Shaw, R., Cheung, P. C. T., 1998. Late Quaternary environmental changes in Hong Kong. *Palaeogeography, Palaeoclimatology and Palaeoecology*, 138, 151-173.

Pedersen, T. F., Calvert, S. E., 1990. Anoxia vs. Productivity: What controls the formation of organic-carbon-rich sediments and sedimentary rocks? *American Association of Petroleum Geologists Bulletin*, 74, 454-466.

Pernetta, J. C., Milliman, J. D., 1995. Land-ocean interactions in the coastal zone: implementation plan. *International Geosphere-Biosphere Programme, Stockholm; Report*, 33, 215p.

Rullkötter, J., 2000. Organic matter: the driving force for early diagenesis. In: Schulz, H. D., Zabel, M. (Eds), *Marine Geochemistry*, Springer, Berlin, 129-172.

Tanner, P. A., Leong, L. S., Pan, S. M., 2000. Contamination of heavy metals in marine sediment cores from Victoria Harbour, Hong Kong, *Marine Pollution Bulletin*, 40, 769-779.

Tovey, N. K., Yim, W. W. -S., 2002. Dessication of late Quaternary inner shelf sediments: micro fabric observations. *Quaternary International*, 92, 73-87.

Wong, A. Y. -S., Tanner, P. A, 1997. Monitoring environmental pollution in Hong Kong: trends and prospects. *Trends in Analytical Chemistry*, 16, 180-190.

World Wide Fund for Nature Hong Kong, 1993. Marine Pollution in Hong Kong. <http://www.wwf.org.hk/eng/pdf/references/factsheets/factsheet2.pdf>

Yim, W. W. -S., 1984. Evidence for Quaternary environmental changes from sea-floor sediments in Hong Kong. In: Whyte, R. O. (Ed), *The Evolution of the East Asian Environment, vol. 1. Geology and Palaeoclimatology*. Centre of Asian Studies, The University of Hong Kong, Hong Kong, 137-155.

Yim, W. W. -S., 1993. Future sea level rise in Hong Kong and possible environmental effects. In: Warrick, R. A., Barrow, E. M., Wigley, T. M. L. (Eds), *Climate and sea level change: observations, projections and implications*, 349-376.

Yim, W. W. -S., 1994. Offshore Quaternary sediments and their engineering significance in Hong Kong. *Engineering Geology*, 37, 31-50.

Yim, W. W. -S., 2000. Towards sustainable coastal development in Hong Kong. *Geological Society of Hong Kong Bulletin*, 6, 203-219.

Yim, W. W. S., Chan, L. S., Hsieh, M., Philp, R. P., Ridley Thomas, W. N., 2002. Carbon flux during the last interglacial cycle in the inner continental shelf of the South China Sea off Hong Kong. *Global and Planetary Change*, 33, 29-46.

CHAPTER 2

Samples and Methodology

2.1 Core Samples

Four intervals of a piston core section (MBH 54/2; 0.5m-4.2m) were obtained from the Kwun Tong Typhoon Shelter in Victoria Harbour's Kowloon Bay (Fig. 1.3). Core MBH 54/2 (Fig. 2.1) was supplied from the collection of Dr. W. W. -S. Yim, from the Department of Earth Sciences, at the University of Hong Kong. MBH 54/2 was collected in 1996 by rotary boring in stainless steel casings, wax sealed, and sent to the University of Oklahoma where it was stored in a freezer at -21°C .

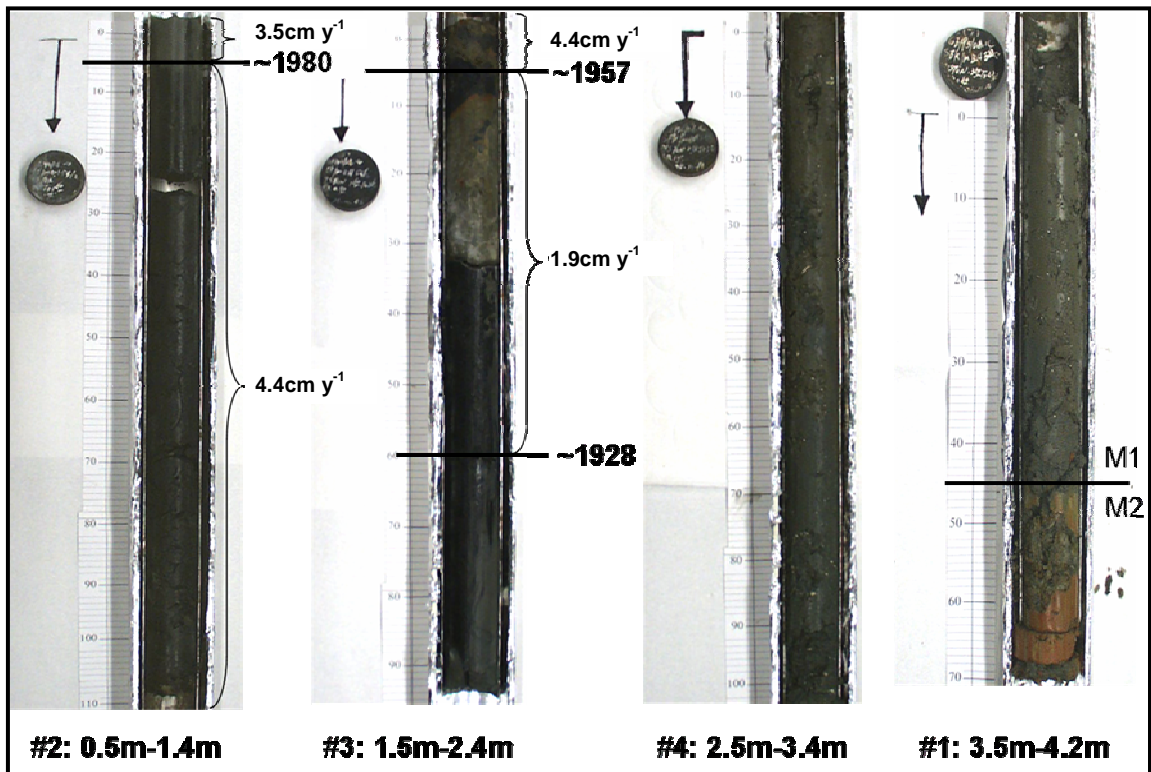


Fig. 2.1. Core MBH 54/2-Kwun Tong Typhoon Shelter, Kowloon Bay. Estimated sedimentation rates were reported by Tanner *et al.* (2000) for MVC 74.

2.1.1 Sediment Core Description – MBH 54/2

The majority of sediments in core MBH 54/2 (**Fig. 2.1**) are made up of dark greenish-gray to black, soft silty clays, with the presence of shell fragments. The base of the core section is composed of more compact, lighter colored, coarse grained sediments. Sediments in the uppermost unit (0.5m to 2.4m) were dark greenish-gray to black silty clays, underlain by light brownish-gray silty clays (2.5m to 3.1m), dark gray silty clays (3.1m to 3.5m) which transitioned into lighter gray sandy clays with red streaks and coarse quartz grains (3.9m to 4.2m). The dark greenish-gray to black sediment color observed throughout much of the core section is due to the presence of sulfides (*i.e.*, pyrite), from sulfate reduction. The light gray sandy clays with red streaks have been observed in desiccated pre-Holocene sediments formed during a low sea-level stand (Yim, 1994).

2.2 Overview of Experimental Method

Cores were sectioned into 5 cm intervals and stored at -21°C. Samples from various depths were freeze-dried using a Labconco Freeze Dryer 5. The following sections will provide detailed procedures used to isolate and analyze free, ester- and amide-bound lipids. Surrogate standards (cholestane and cholanic acid) were added to a small number of sediment samples prior to extraction. An external deuterated standard ($C_{24}D_{50}$) was added to the lipid extracts prior to analysis by gas chromatography (GC) and gas chromatography-

mass spectrometry (GCMS) to assess the extraction efficiency. Results summarizing surrogate standard recovery were misplaced. However, the percent recovered ranged between 90% and 110%. The flowchart in **Fig. 2.2** summarizes the experimental procedures.

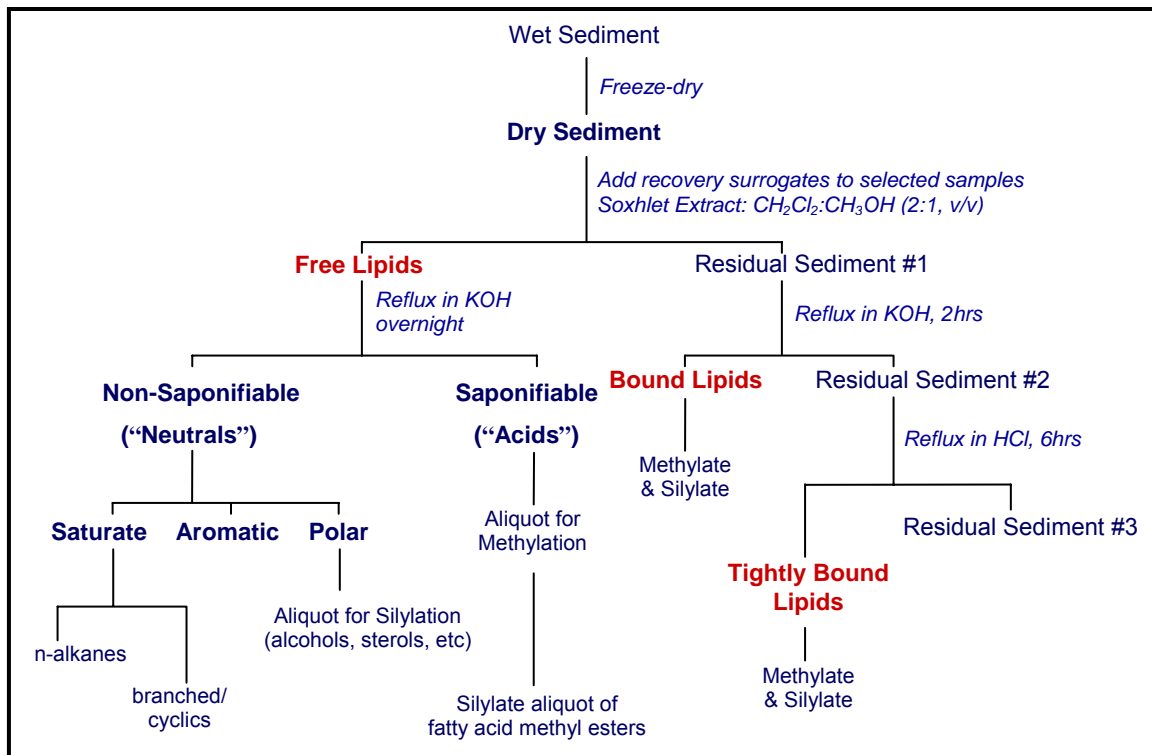


Fig. 2.2. Flowchart summarizing methodology for separating and isolating lipid groups from marine sediments.

2.3 Free Lipid Extraction and Fractionation

Cellulose extraction thimbles, glasswool, and boiling chips were pre-extracted with dichloromethane:methanol (1:1 v/v, at least 6hrs). Copper trimmings were activated in dilute hydrochloric acid (10% HCl), followed by ultrasonication in deionized water (3x), methanol (3x), and dichloromethane (3x).

Frozen sediments were transferred to Lyph-Lock flasks (100ml) with 24/40 joints and connected to valve ports on the drying chamber of a Labconco Freeze-Dry system (duration on the freeze-dry system was typically 24hrs). Dried sediments were ground to a fine powder using a ceramic mortar and pestle, weighed and transferred to pre-extracted cellulose thimbles for extraction of free lipids.

Free lipids were extracted from freeze-dried sediments using a mixture of dichloromethane:methanol (2:1 v/v, 48hrs). Activated copper was used to remove elemental sulfur extracted with the free lipid fraction. Excess solvent was removed using a Yamato RE-51 rotary evaporator under vacuum, and transferred to pre-weighed vials where solvents were completely evaporated under a stream of nitrogen gas. Sample weights were recorded.

2.3.1. Separation of Total Free Lipid Extracts into Non-Saponifiable and Saponifiable Fractions

A fraction of the total free lipid extract was saponified by refluxing with 6N potassium hydroxide (15ml; 6hrs) in 10% aqueous methanol. Non-saponifiable lipids, sometimes referred to as “neutral lipids,” were extracted with dichloromethane (5x30ml) in a separator funnel (vigorously shaken, 1min). The aqueous phase was acidified to pH~2 by the addition of 4N HCl to release saponifiable lipids (also referred to as “acidic lipids”). Saponifiable lipids were recovered from the aqueous phase by liquid-liquid extraction using dichloromethane. Excess solvent was removed from lipid fractions by rotary

evaporation under vacuum, transferred to pre-weighed 4ml vials, dried under a stream of nitrogen gas, and weighed.

2.3.2. Fractionation of Non-Saponifiable Lipids to Saturate, Aromatic, and Polar Fractions

Samples with sufficient total free lipid extracts were separated into saturate, aromatic, and polar fractions by column chromatography. Free non-saponifiable lipids were eluted through a 100ml glass column, packed with pre-conditioned alumina (14g; 80-200 mesh). Solvents of increasing polarity were used to elute saturate (n-pentane, 50ml), aromatic (n-pentane:dichloromethane 7:3 v/v, 50ml) and polar compounds (dichloromethane:methanol, 97:3 v/v, 50ml). Lipid fractions were concentrated by rotary evaporation and transferred to pre-weighed 4ml vials. Both saturate and aromatic fractions were screened by GC and GCMS.

The polar fraction was separated into three aliquots. The first aliquot was screened by GC and GCMS. The second aliquot was methylated using BF_3 -methanol (see section 2.5.1 for methylation procedure) and screened by GC and GCMS, followed by silylation (see section 2.5.2 for silylation procedure) of a small fraction of the methylated free non-saponifiable polar lipids. Free polar lipid compounds that were methylated and silylated were analyzed by GC and GCMS.

2.4 Extraction of Ester- and Amide-Bound Lipids

Ester- and amide-bound lipids were released and extracted from residual sediments using alkaline and acid hydrolysis, respectively. The technique used to extract the bound lipids is based on a slight modification of the procedure described by Lattuati *et al.* (2002). A Soxhlet extraction step was added at the end of each procedure to recover ester- or amide-bound lipids not extracted during the filtration step.

“Residual sediment-1” was refluxed in a solution of 1N potassium hydroxide (KOH) in methanol (30ml, 2hrs), to cleave ester-linkages of lipids present in the sediments. The reaction mixtures were filtered through vacuum flasks, using pre-combusted glass fiber filters (Whatman 934-AH). Residual sediment-1 was rinsed with methanol (100ml) and the combined filtrates were transferred to a large separator funnel (1000ml). Combined filtrates in the separator funnel were acidified using 10% aqueous HCl. Residual sediment-1 was then rinsed with dichloromethane (50ml), which was transferred to the separator funnel containing the combined filtrates. The solution mixture in the separator funnel was shaken vigorously (1min), producing a monophasic solution. The solution mixture was then diluted with deionized water (50ml) and additional dichloromethane (50ml). The solution mixture was shaken vigorously (1min), resulting in a biphasic solution, where the ester-bound lipids were extracted into the dichloromethane layer. The remaining residual sediment and glass fiber filter were transferred to a pre-extracted cellulose extraction thimble, and Soxhlet extracted with dichloromethane:methanol (2:1 v/v, 24hrs) to recover

any remaining released ester-bound lipids. All released ester-bound lipids were combined, concentrated, and weighed in 4ml vials, representing the total ester-bound lipid fraction.

“Residual sediment-2” (**Fig. 2.2**), was hydrolyzed by reflux in 4N HCl (40ml, 6hrs) to release amide-bound lipids. Hydrolyzed sediments were filtered through pre-combusted glass fiber filters (Whatman 934-AH) and rinsed with methanol (100ml). Combined filtrates were transferred to a large separator funnel (1000ml). The residual sediment was washed with dichloromethane (50ml), which was then transferred to the separator funnel and shaken vigorously (1min). Deionized water (50ml) and additional dichloromethane (50ml) were added to the separator funnel and shaken vigorously (1min), to recover the organic phase containing the amide-bound lipids. Any freed amide-bound lipids remaining in the sediment were recovered by Soxhlet extraction (dichloromethane:methanol; 2:1 v/v, 24hrs) and combined with the previously isolated amide-bound lipids. The total amide-bound lipid fraction was concentrated and weighed in 4ml vials.

2.5 Derivatization of Functionalized Lipids

Functionalized lipids (*e.g.*, alcohols, sterols, fatty acids, and hydroxy fatty acids) typically require derivatization procedures in order to produce less polar, more volatile compounds which can be separated on gas chromatographic columns. Methylation and silylation procedures, respectively, are commonly used in the derivatization of compounds with carboxyl or hydroxyl groups. Lipids

containing both carboxyl and hydroxyl groups are typically methylated, then silylated, to produce methyl ester-trimethylsilyl (TMS) ether compounds.

2.5.1 Methylation of Saponifiable, Ester- and Amide-Bound Lipids

Aliquots of saponifiable, ester- and amide-bound lipids were methylated using BF₃-methanol (14% borontrifluoride, 86% methanol). In general, for 5mg of lipids, 500µl of BF₃-methanol was used for methylation reactions. Lipid fractions (*i.e.* saponifiable, ester- and amide-bound lipids) were transferred and weighed in 4ml vials. BF₃-Methanol was added to the vials, capped, and heated at 60°C (15min). The reaction mixture was allowed to cool, transferred to a separatory funnel (125ml), and diluted with deionized water (20ml). Lipids, as methyl esters, were recovered by liquid-liquid extraction with dichloromethane (3x40ml). Samples were concentrated using a rotary evaporator, transferred to pre-weighed vials, and any remaining solvent removed under a stream of nitrogen gas. Sample weights were recorded and small aliquots of samples were set aside for GC, GCMS, and gas chromatography-isotope ratio mass spectrometry (GCIRMS) analyses. All methylated samples were stored in a refrigerator.

2.5.2 Silylation of Non-Saponifiable, Ester- and Amide-Bound Lipids

Non-saponifiable lipids, ester- and amide-bound lipid-methyl esters were silylated to produce trimethylsilyl ethers. Lipid samples (up to 1mg) were heated

to 50°C (30min) in N,O,-bis(trimethylsilyl)trifluoro-acetamide with 1% trimethylchlorosilane (BSTFA with 1%TMCS; 100µl) and pyridine (100µl), which was used as a catalyst for the reaction. After silylation, samples were dried under a flow of nitrogen gas, diluted in dichloromethane, and analyzed by GC and GCMS. Remaining samples were stored in a refrigerator.

2.6 Gas Chromatography

Lipid fractions were initially screened on a Hewlett-Packard 5890 gas chromatograph equipped with an on-column injector and a flame ionization detector (FID) set at 310°C. Samples were chromatographed on an Agilent/J&W HP-5MS fused silica capillary column (30m x 0.25mm i.d. x 0.5µm film thickness), which has a non-polar stationary phase composed of (5%-phenyl)-methylpolysiloxane. The oven temperature was programmed from 40°C to 310°C, at a rate of 4°C/min, and held isothermally at 310°C (32min). Data were acquired with a PE Nelson-900 series acquisition interface and transferred to a Windows-based computer at the end of the run. Chromatograms were processed and plotted using PE Nelson Chromatography Software.

2.7 Gas Chromatography – Mass Spectrometry

Lipid fractions were analyzed by gas chromatography-mass spectrometry with a Varian 3400 gas chromatograph interfaced via transfer line to a Finnigan

MAT triple stage quadrupole mass spectrometer (TSQ-70). Gas chromatography was performed on an Agilent/J&W Scientific DB-5MS fused silica capillary column (60m x 0.32mm i.d. x 0.25 μ m film thickness), which utilizes a (5%-phenyl)-methylpolysiloxane equivalent non-polar stationary phase. The split/splitless injector on the gas chromatograph was temperature programmed from 40°C to 310°C at a rate of 180°C/min, then held isothermal at 310°C (99min). The GC oven program was initially held at 40°C (1.5min), then heated to 310°C at a rate of 4°C/min, where it was held at 310°C (31min). The transfer line was isothermal (310°C) for the entire length of the run (100min). Analyses were completed in full-scan mode, where compounds were ionized by electron impact ionization (EI @ 70eV). The electron multiplier was set to detect and measure ions over the mass range of m/z 50 to m/z 550 each second. GCMS results were acquired, processed, and interpreted on a DEC Alpha Workstation, using the ICIS/ICL (*i.e.* “Interactive Chemical Information System”/“Interactive Control Language”) data acquisition software.

2.8 Gas Chromatography – Isotope Ratio Mass Spectrometry (GCIRMS)

Compound specific carbon isotopes were measured on two GCIRMS systems – a Varian 3410 GC interfaced via combustion reactor to a Finnigan MAT-252 isotope ratio mass spectrometer; and a HP6890A GC interfaced via ThermoQuest Finnigan GC Combustion III furnace to a ThermoQuest Delta^{plus}XL isotope ratio mass spectrometer. GCIRMS allows $\delta^{13}\text{C}$ values to be measured for

individual components in complex compound mixtures. In this project, fatty acids in the ester- and amide-bound lipid fractions were analyzed by GCIRMS as methyl esters. Samples were introduced into the GC, where the oven was temperature programmed from 40°C to 310°C at a rate of 4°C/min (total run time = 100min). The Varian 3410 was equipped with a DB-1 fused silica capillary column (60m x 0.32mm I.D. x 0.25µm film thickness), which has a non-polar stationary phase (100% dimethylpolysiloxane); and the HP6890A was equipped with a HP-5MS fused silica capillary column (30m x 0.25mm i.d. x 0.5µm film thickness), which has a non-polar stationary phase composed of (5%-phenyl)-methylpolysiloxane. Components separated on the GC columns passed through a ceramic combustion reactor (980°C), and completely combusted to CO₂ and H₂O. The water was removed with a water separator prior to introducing the CO₂ into the isotope ratio mass spectrometer, where the relative proportions of ¹³CO₂ to ¹²CO₂ were determined relative to the Pee Dee Belemnite (PDB) standard. The data acquisition system converted isotopic ratios of ¹³C/¹²C to delta (δ) notation, using **equation 2.8.1** (Hoefs, 1997).

$$\delta^{13}\text{C} = \left(\frac{{}^{13}\text{C}/{}^{12}\text{C}_{\text{sample}}}{{}^{13}\text{C}/{}^{12}\text{C}_{\text{standard}}} - 1 \right) \times 1000 \quad (\text{eq. 2.8.1})$$

δ¹³C values for fatty acids were corrected for the addition of a methanol carbon, from the methylating reagent BF₃-methanol. Bulk stable isotopes of a C_{24:0} fatty acid standard and fatty acid methyl ester product formed by the methylating reagent were measured by Rick Maynard from the Organic

Geochemistry Laboratory at the University of Oklahoma. The isotopic composition of the methanol carbon $\delta^{13}\text{C}_{\text{MEOH}}$ was determined using **equation 2.8.2**, where x is the fractional carbon contribution of fatty acid to fatty acid methyl ester (*e.g.* tetracosanoic acid would have a fractional carbon contribution where $x=24/25$) (Abrajano *et al.*, 1994) . The isotopic composition of fatty acids ($\delta^{13}\text{C}_{\text{FA}}$) was calculated (**equation 2.8.2**) using the known $\delta^{13}\text{C}_{\text{MEOH}}$ value and measured $\delta^{13}\text{C}_{\text{FAME}}$ compositions.

$$\delta^{13}\text{C}_{\text{FAME}} = [x]\delta^{13}\text{C}_{\text{FA}} + (1-x)\delta^{13}\text{C}_{\text{MEOH}} \quad (\text{eq. 2.8.2})$$

2.9. Elemental Analysis, and Bulk Organic Carbon ($\delta^{13}\text{C}_{\text{org}}$) and Total Nitrogen ($\delta^{15}\text{N}$) Stable Isotope Measurements

Freeze-dried sediment samples were sent to the Sedimentary Coastal and Oceanic Organic Biogeochemistry Laboratory at Texas A & M University for elemental analysis, and bulk stable isotope measurements of carbon and nitrogen. A Costech EA (Model # ECS4010), interfaced to a Finnigan MAT-252 dual inlet isotope ratio mass spectrometer via a Thermo-Finnigan Conflo III interface, was used to measure total organic carbon (% C_{org}), total nitrogen (%N), $\delta^{13}\text{C}_{\text{org}}$ and $\delta^{15}\text{N}$ of decarbonated sediment samples. The following temperature and flow parameters were used in the analyses: combustion furnace = 1020°C; reduction furnace = 650°C; column temperature = 40°C; and flow-rate = 98ml/min. $^{13}\text{C}/^{12}\text{C}$ and $^{15}\text{N}/^{14}\text{N}$ isotopic ratios were compared to standards (PDB and

atmospheric nitrogen, respectively), and converted to delta (δ) notation. $\delta^{13}\text{C}$ was calculated using **equation 2.8.1**, and $\delta^{15}\text{N}$ was calculated using **equation 2.9.1**.

$$\delta^{15}\text{N} = \left(\frac{{}^{15}\text{N}/{}^{14}\text{N}_{\text{sample}}}{{}^{15}\text{N}/{}^{14}\text{N}_{\text{standard}}} - 1 \right) \times 1000 \quad (\text{eq. 2.9.1})$$

Samples were weighed in silver boats and decarbonated in glass desiccators, with a small amount of 12N HCl at the base of the desiccator. After 72hrs, acid vapors were removed by placing samples in a vacuum oven (<30°C, 24hrs). Samples free of acid vapors were then placed into tin boats, crushed, closed and ready for analysis. Since nitrogen is typically present in low amounts relative to carbon, it is the limiting component. Thus, sample sizes were adjusted to obtain adequate measurements for $\delta^{15}\text{N}$ (*i.e.*, about 100 μg to 200 μg N is needed for an adequate signal on the isotope ratio mass spectrometer). Carbon, however, could be diluted with helium gas to reduce the signal (*i.e.*, to about 75 μg to 190 μg C) for a reliable $\delta^{13}\text{C}_{\text{Org}}$ measurement.

2.10. References

Abrajano Jr., T. A., Murphy, D. E., Fang, J., Comet, P., Brooks, J. M., 1994. $^{13}\text{C}/^{12}\text{C}$ ratios in individual fatty acids of marine mytilids with and without bacterial symbionts. *Organic Geochemistry*, 21, 611-617.

Hoefs, J., 1997. *Stable Isotope Geochemistry*. Springer, Berlin, 4th ed., 401p.

Lattuati, A., Metzger, P., Acquaviva, M., Bertrand, J. -C., Largeau, C., 2002. n-Alkane degradation by *Marinobacter hydrocarbonoclasticus* strain SP 17: long

chain β -hydroxy acids as indicators of bacterial activity. *Organic Geochemistry*, 33, 37-45.

Tanner, P. A., Leong, L. S., Pan, S. M., 2000. Contamination of heavy metals in marine sediment cores from Victoria Harbour, Hong Kong. *Marine Pollution Bulletin*, 40, 769-779.

Yim, W. W. -S., 1994. Offshore Quaternary sediments and their engineering significance in Hong Kong. *Engineering Geology*, 37, 31-50.

CHAPTER 3

Elemental and Stable Isotope Analyses of Organic Carbon and Total Nitrogen in Sediments from Kowloon Bay, Hong Kong

3.1 Introduction

Bulk properties of organic matter in marine sediments provide insights into the history and changes in environmental conditions in the sedimentary record. The piston core investigated in this study (*i.e.*, core MBH 54/2) provides a record of organic matter deposited during the late Quaternary, revealing changes in organic source material, periods affected by anthropogenic activities, and natural changes to this region. The bulk properties utilized include elemental and stable isotope compositions of organic carbon and total nitrogen in sedimentary organic matter. Sedimentary organic matter is comprised of complex mixtures which can include lipids, proteins, cellulose, lignin, and/or other components originating from various organisms or anthropogenic wastes. The majority of organic matter introduced into the marine environment undergoes remineralization (*i.e.*, organic matter is oxidized, resulting in the production of CO₂, H₂O, and nutrients) in the water column, where less than 10% of the original organic matter is incorporated and preserved in the sediments (Meyers and Lallier-Vergès, 1999; Meyers, 2003). While remineralization occurs during sedimentation, bulk properties of deposited sedimentary organic matter still retain important information for delineating the sources of organic matter and possible processes that may have occurred (*e.g.*,

denitrification or enhanced productivity; Teranes and Bernasconi, 2000; Bratton *et al.*, 2003; Meyers, 2003).

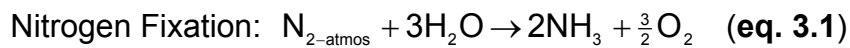
3.2 Review of Literature

3.2.1 Organic Carbon and Total Nitrogen in Marine Sediments

The total organic carbon (TOC) content in marine sediments measures the amount of organic matter that survived remineralization processes in the water column and was preserved in the sediments (Meyers and Lallier-Vergès, 1999). The amount of organic matter in sediments has been estimated to be twice the amount of measured TOC (*i.e.*, 50% of sedimentary organic matter is composed of carbon; Meyers, 2003). Changes in TOC content reflect periods of higher or lower influx of organic matter, which includes the total mixture of terrigenous plant material, algae, bacterial biomass, sewage effluents, and/or other sources of organic carbon.

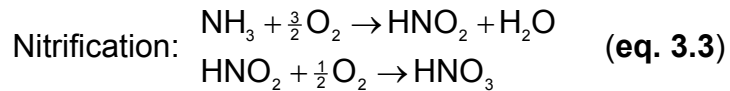
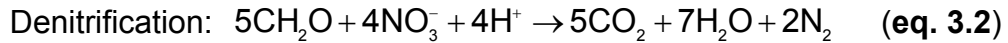
Nitrogen is an important nutrient and plays an important role in productivity in the marine environment (Minagawa and Wada, 1986; Teranes and Bernasconi, 2000; Talbot, 2001). If nitrogen availability is too low, then primary production is limited; if nitrogen is abundant this can result in intense algal blooms and eutrophication of the marine system (Sigleo and Macko, 2002). Nitrogen is typically characterized in sediments as total nitrogen, or as the ratio of organic carbon-to-nitrogen (C/N), and provides important information to aid in delineating sources and past variations of nitrogen in the environment (Meyers, 1994; Talbot,

2001). Atmospheric nitrogen is plentiful, comprising about 78% of the earth's atmosphere, and is the primary source of nitrogen for terrigenous plants (Peters *et al.*, 1978; Sweeney *et al.*, 1978; Hoefs, 1997; Meyers and Lallier-Vergès, 1999). Terrigenous plants are able to utilize atmospheric nitrogen after bacteria, located around the plant roots, convert the nitrogen to ammonia via nitrogen fixation (**eq. 3.1**; Peters *et al.*, 1978; Sweeney *et al.*, 1978; Whelan and Farrington, 1992; Bickert, 2000). Terrigenous plants can also uptake nitrogen, in the form of nitrates, around the plant roots (Moore, 2004).



Marine organisms assimilate dissolved inorganic nitrogen in the form of nitrate (NO_3^-), ammonium (NH_4^+), or nitrite (NO_2^-), although nitrate is the most common form of assimilated nitrogen (Peters *et al.*, 1978; Fogel and Cifuentes, 1993; Bickert, 2000; Talbot, 2001). Nitrate is reduced to nitrogen gas (N_2) by anaerobic bacteria via denitrification processes (**eq. 3.2**), returning nitrogen to the atmosphere (Hoefs, 1997; Bickert, 2000; Teranes and Bernasconi, 2000; Talbot, 2001). Denitrification is an important mechanism for balancing the natural processes of nitrogen fixation (Sweeney *et al.*, 1978). Ammonia (NH_3) and ammonium (NH_4^+) in aquatic environments are produced by bacterial decomposition of organic matter under anaerobic conditions (Teranes and Bernasconi, 2000; Talbot, 2001). The ammonia formed from the mineralization of organic nitrogen is an important component utilized by aerobic bacteria during

nitrification processes (Sweeney *et al.*, 1978). Conversion of ammonia to nitrate can be expressed by **equation 3.3** (Bickert, 2000).



3.2.2 Carbon-to-Nitrogen Ratio (C/N)

TOC and total nitrogen are commonly utilized together, where the ratio of organic carbon-to-total nitrogen functions as a tool for distinguishing the source of organic matter. The primary nitrogen components in marine organisms (*e.g.*, phytoplankton and zooplankton) are proteins. Vascular terrigenous plants, however, have low protein content and are enriched in cellulose and lignin. The low cellulose, high protein composition of phytoplankton results in C/N ratios between 4 and 10, whereas bacterioplankton have C/N ratios ranging between 2.6 and 4.3. High cellulose and lignin composition of vascular terrigenous plants, along with low protein content, results in C/N ratios greater than 15 (Sampei and Matsumoto, 2001; Meyers, 2003; Wu *et al.*, 2003). The downcore profile of the C/N ratio in a sediment core section can illustrate shifts through time as the principal contributor of organic matter changes between terrigenous and algal material. Preferential loss of nitrogen relative to carbon can occur as a result of the decomposition of algal biomass settling through the water column.

Consequently, organic matter deposited in the sediments may appear to have a higher C/N ratio (Sampei and Matsumoto, 2001).

3.2.3 Bulk Stable Isotope Analyses

Bulk stable isotope composition of organic carbon and total nitrogen complement the C/N ratio. Carbon and nitrogen each have two stable isotopes, ^{12}C (98.89%) and ^{13}C (1.11%), and ^{14}N (99.64%) and ^{15}N (0.36%) (Hoefs, 1997). Stable isotopes of carbon and nitrogen are expressed using the delta (δ) value, where the ratio of heavy-to-light isotope values (*i.e.*, $^{13}\text{C}/^{12}\text{C}$ and $^{15}\text{N}/^{14}\text{N}$) are calibrated relative to international standards (**eq. 2.8.1** and **eq. 2.9.1**; Hoefs, 1997).

$\delta^{13}\text{C}_{\text{org}}$ values have been used to determine the sources of sedimentary organic matter (*i.e.*, marine or terrigenous) and to identify photosynthetic pathways utilized by terrigenous plants (*i.e.*, C3 plants or C4 plants). C3 plants incorporate carbon into organic matter using the Calvin pathway, where a molecule of CO_2 reacts with the enzyme ribulose 1,5-bis-phosphate carboxylase to produce two molecules of 3-phosphoglycerate (**Fig. 3.1**; Fogel and Cifuentes, 1993; Hoefs, 1997).

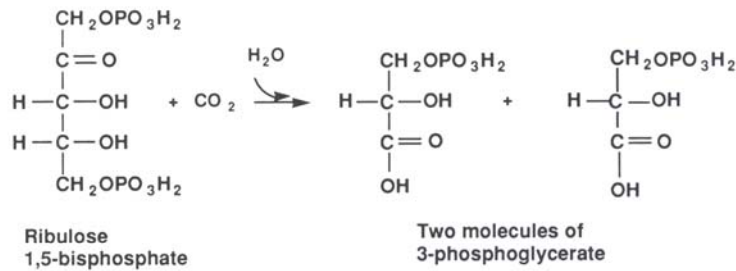


Fig. 3.1. Incorporation of carbon into organic matter utilizing the C3 pathway (from Fogel and Cifuentes, 1993).

C4 Plants follow the Hatch-Slack pathway, where the incorporation of carbon into organic matter occurs when CO_2 reacts with phosphoenolpyruvate carboxylase to form oxaloacetate (**Fig. 3.2**; Fogel and Cifuentes, 1993; Hoefs, 1997). $\delta^{13}\text{C}$ values of C3 terrigenous plants range between -33‰ and -22‰ ; whereas C4 terrigenous plants are more ^{13}C -enriched and range between -22‰ and -8‰ (Meyers, 1994; Hoefs, 1997; Huang *et al.*, 1999; Meyers and Teranes, 2001). Marine organic matter (*e.g.*, marine algae) is isotopically heavier than C3 terrigenous plants, and has $\delta^{13}\text{C}$ values ranging between -25‰ and -20‰ (Meyers, 1994).

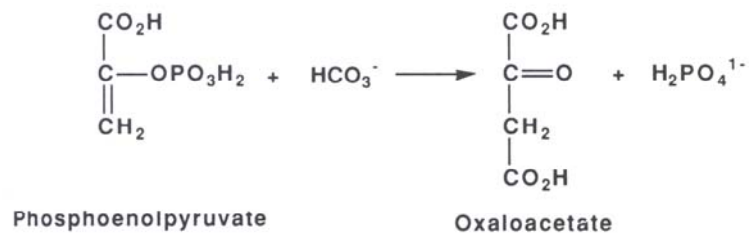


Fig. 3.2. Photosynthetic pathway of C4 plants, utilizing the enzyme phosphoenolpyruvate carboxylase (from Fogel and Cifuentes, 1993).

Nitrogen isotopes often supplement carbon isotope measurements for delineating source information, where the $\delta^{15}\text{N}$ value varies as a result of the form of inorganic nitrogen assimilated. The two primary forms of nitrogen utilized are nitrate (*i.e.*, for marine organisms; $\delta^{15}\text{N}_{\text{nitrate}} = 7\text{‰}$ to 10‰) and atmospheric nitrogen (*i.e.*, for terrigenous plants; $\delta^{15}\text{N}_{\text{atmos}} = \sim 0\text{‰}$) (Peters *et al.*, 1978; Meyers and Lallier-Vergès, 1999; Meyers and Teranes, 2001; Owen and Lee, 2004). Nitrates derived from anthropogenic activities (*e.g.*, human and/or animal waste products) are enriched in ^{15}N where $\delta^{15}\text{N}$ ranges from 10‰ to 25‰ (Teranes and Bernasconi, 2000; Meyers, 2003). These isotopic signatures can be traced in the environment where marine plankton or algae utilize NO_3^- and terrigenous plants utilize atmospheric nitrogen as their nitrogen source (Muzuka *et al.*, 1991; Meyers and Lallier-Vergès, 1999; Meyers and Teranes, 2001). Several factors, however, can affect the isotopic composition of nitrogen in organic matter, providing insights into nutrient cycling and processes such as nitrogen fixation or denitrification (Fogel and Cifuentes, 1993; Bickert, 2000).

3.2.4 Sewage Derived Carbon and Nitrogen in Marine Sediments

Nitrogen is an essential substrate needed for primary producer growth. The isotopic composition of the primary producers will be dependent on the isotopic composition of dissolved inorganic nitrogen components such as NO_3^- , NH_4^+ , or NO_2^- (Montoya, 1994). Potential sources of dissolved inorganic nitrogen in the aquatic environment include sewage and wastewater effluents. These

sources of nitrogen can serve as nutrients for marine organisms. When nutrient overloading occurs (*e.g.*, via excessive sewage waste disposal), algal blooms can be stimulated leading to eutrophication. Eutrophication results in increasing anoxic conditions whereby excessive denitrification processes can occur, enriching the ^{15}N in residual dissolved inorganic nitrogen (Muzuka *et al.*, 1991; Montoya, 1994; Teranes and Bernasconi, 2000; Bratton *et al.*, 2003). Conversely, as the phytoplankton assimilate and metabolize the dissolved inorganic nitrogen, the phytoplankton biomass becomes depleted in ^{15}N relative to that of the growth substrate (Montoya, 1994). In the early stages of algal blooms, phytoplankton biomass is isotopically lighter than the dissolved inorganic nitrogen being used as the substrate. As ^{14}N is selectively removed, the residual dissolved inorganic nitrogen becomes isotopically heavier. Progressive assimilation of the isotopically heavier nitrogen will be reflected in the phytoplankton biomass (Montoya, 1994). Bacterial remineralization of settling particulate organic matter in the water column can also lead to progressive enrichment of ^{15}N in the residual organic matter (Altabet and McCarthy, 1985; Bickert, 2000).

Offshore disposal of sewage waste has been common practice since the early occurrence of population growth in near-coast environments with the presumption that minimal sewage particulates would reach or accumulate on the seafloor due to dispersion and dilution effects in surface waters. Various research groups have utilized elemental and bulk stable isotope compositions of carbon and nitrogen in sewage effluents, particulate organic matter, marine sediments, and/or phytoplankton-derived organic matter to study the effects of

sewage-derived organic matter on marine sediments. **Table 3.1** summarizes the results of studies from various localities around the world. Sewage effluents, sewage sludges, and sewage-derived organic matter sampled around coastal regions have been reported with the following bulk properties: $\delta^{13}\text{C}_{\text{org}} = -28.5\text{‰}$ to -23.0‰ ; $\delta^{15}\text{N} = 1.8\text{‰}$ to 3.2‰ ; and C/N ratios = 11.0 to 13.4 (Burnett and Schaeffer, 1980; Sweeney *et al.*, 1980; Gearing *et al.*, 1991; van Dover *et al.*, 1992; Hunt *et al.*, 1992; Thornton and McManus, 1994; Rogers, 2003).

Organic matter derived from sewage effluents have been differentiated from terrigenous derived organic matter (Rogers, 2003) and organic matter derived from marine sediments unaffected by sewage (Burnett and Schaeffer, 1980; Sweeney *et al.*, 1980) using bulk stable isotope values of carbon and nitrogen. The proportion of sewage contributions can be estimated using isotopic measurements of sewage contaminated sites and pristine sites (Rogers, 2003). Burnett and Schaeffer (1980), for example, used **equation 3.5** to estimate the relative amount of sewage affected sediments at their study sites, where: $F_s = \%$ sewage sludge; $\delta^{13}\text{C} = \delta^{13}\text{C}$ value of C_{org} in the measured samples; $\delta^{13}\text{C}_m = \delta^{13}\text{C}$ value of C_{org} in uncontaminated marine shelf sediments “normal” to the area; $\delta^{13}\text{C}_s = \delta^{13}\text{C}$ value of the sewage sludge.

$$F_s = \frac{\delta^{13}\text{C} - \delta^{13}\text{C}_m}{\delta^{13}\text{C}_s - \delta^{13}\text{C}_m} \times 100 \quad (\text{eq. 3.5})$$

Table 3.1. Summary of elemental and bulk stable isotope measurements of carbon and nitrogen in marine sediments, sewage sludge/effluents, particulate organic matter, and plankton-derived particulate organic carbon.

Location	Sample	%C _{org}	%N	C/N Ratio	δ ¹³ C (‰)	δ ¹⁵ N (‰)	Reference
Western Hong Kong (estuarine-derived)	Sediment	0.4 to 1.2	-	6.0 to 18.5	-25.3 to -21.3	5.0 to 12.5	Owen, 2005
Central Hong Kong	Sediment	0.5 to 1.1	-	6.0 to 20.0	-	-	Owen, 2005
Eastern Hong Kong (marine-derived)	Sediment	0.6 to 3.0	-	6.0 to 25.5	-26.7 to -19.0	10.0 to 18.5	Owen, 2005
Lake Biwa	Sediment	-	-	-	-24.7 to -21.5	5.7 to 7.8	Mishima <i>et al.</i> , 1999
Yodo River	Sediment	-	-	-	-26.2 to -24.7	4.3 to 6.7	Mishima <i>et al.</i> , 1999
Ane River	Sediment	-	-	-	-28.3 to -26.6	-0.9 to 2.6	Mishima <i>et al.</i> , 1999
Tokyo Bay	POM	-	-	-	-15.0	-	Mishima <i>et al.</i> , 1999
Otuchi Bay	TOM	-	-	-	-26.5	-	Mishima <i>et al.</i> , 1999
S. California Bight	Marine PM	-	-	-	-21.0 to -19.0	8.0 to 12.0	Spies <i>et al.</i> , 1989
S. California Bight (Whites Point, CA)	Sewage PM	-	-	-	-16.5	1.8	Spies <i>et al.</i> , 1989
S. Calif. Coastal Area-1	Sewage Effluent	30.8	2.33	13.2*	-	3.0	Sweeney <i>et al.</i> , 1980
S. Calif. Coastal Area-2	Sewage Effluent	31.7	2.38	13.3*	-	2.0	Sweeney <i>et al.</i> , 1980
S. Calif. Coastal Area-3	Sewage Effluent	31.8	2.37	13.4*	-	2.4	Sweeney <i>et al.</i> , 1980
S. Calif. Coastal Area-4 (Whites Point, CA)	Sewage Effluent	31.7	2.36	13.4*	-	2.5	Sweeney <i>et al.</i> , 1980
Edinburgh (marine embayment)	Sewage Effluent	-	-	-	-25.2±0.9	10.7±0.7	Waldron <i>et al.</i> , 2001
Edinburgh (marine embayment)	Sediment	-	-	-	-22.9±0.2	6.1 to 6.7	Waldron <i>et al.</i> , 2001
Cranston, Ri	Sewage Sludge	-	-	-	-23.5±0.4	-	Gearing <i>et al.</i> , 1991
Los Angeles	Sewage Sludge	-	-	-	-23.5±0.5	-	Gearing <i>et al.</i> , 1991
New York	Sewage Sludge	-	-	-	-26.0 & -25.7	-	Gearing <i>et al.</i> , 1991
Moa Point, New Zealand	Sewage Effluent	-	-	-	-23.5	1.8 to 2.5	Rogers, 2003
Middlesex, NJ	Sewage derived OM	-	-	-	-24.7	-1.1	van Dover <i>et al.</i> , 1992
Mergen, NJ	Sewage derived OM	-	-	-	-23.2	6.1	van Dover <i>et al.</i> , 1992
Yonkers, NY	Sewage derived OM	-	-	-	-21.4	7.2	van Dover <i>et al.</i> , 1992
Providence, RI	Sewage derived OM	-	-	-	-23.7	-	van Dover <i>et al.</i> , 1992
Hunts Bay, Kingston Harbour, Jamaica	Sewage	-	-	11.0 to 13.0	-28.5 to -23.0	-	Andrews <i>et al.</i> , 1998
New York Bight-Newton Creek Treatment Plant	Sewage Sludge	-	-	-	-25.7	-	Burnett & Schaeffer, 1980
New York Bight- Ward Island Treatment Plant	Sewage Sludge	-	-	-	-26.0	-	Burnett & Schaeffer, 1980
Mangrove Creek, Hong Kong	Seston	-	-	-	-27.16±0.44	10.48±0.21	Lee, 2000
Pearl River Estuary	Seston (phytoplankton dominated)	-	-	-	-25.22±0.48	-1.06±0.98	Lee, 2000
Shan Pui River, Hong Kong	POM (primarily anthropogenic)	-	-	-	-24.13	5.23	Lee, 2000
New York/New Jersey	Sewage-derived OM	-	-	-	-23.0	3.2	Hunt <i>et al.</i> , 1992
North Atlantic	Phytoplankton-derived POM	-	-	-	-21.7	6.1	van Dover <i>et al.</i> , 1992
Western North Atlantic	Sed. POC (phytoplankton-derived)?	-	-	-	-21.6	-	Sayles & Curry, 1988; van Dover <i>et al.</i> , 1992
Pacific-Deepwater	PON	-	-	-	-	5.0 to 15.0	Saino & Hattori, 1987; van Dover <i>et al.</i> , 1992
Sargasso Sea	PON	-	-	-	-	5.0 to 7.0	Altabet, 1988; van Dover <i>et al.</i> , 1992
Invergowrie Bay, Tay Estuary, Scotland	Sewage Effluent	-	-	12.57	-26.7	2.3	Thorton & McManus, 1994

3.3 Results and Discussion

Bulk properties of sedimentary organic matter (*i.e.*, elemental and stable isotope compositions of carbon and nitrogen in sediments) have been measured in core MBH 54/2 to identify sources of organic matter, speculate on processes that affect carbon and nitrogen preservation and isotopic composition (*e.g.*, signatures resulting from microbial activity), and to infer processes that occurred as a result of raw sewage disposal in coastal environments. While the majority of organic matter (>90%) is remineralized during sedimentation, the C/N ratios and $\delta^{13}\text{C}_{\text{org}}$ values of the initial organic matter that survives the water column is preserved (Meyers and Ishiwatari, 1993; Meyers, 2003; Sifeddine *et al.*, 2004). Results of elemental and bulk stable isotope measurements are summarized in **Table 3.2**.

3.3.1 Elemental Analyses

Elemental analysis of organic carbon ($\%C_{\text{org}}$) and total nitrogen ($\%N$) content have been utilized to differentiate between terrigenous and aquatic sourced organic matter. The distribution of $\%C_{\text{org}}$ has been used in various studies to study changes in organic matter input and preservation in sediment core sections. One possible application has been to use organic carbon distributions to reflect periods of enhanced anthropogenic waste input (*e.g.*, sewage wastes, oil spills, and/or industrial waste effluents). Bulk measurements

Table 3.2. Summary of elemental analyses and bulk stable isotope measurements of carbon and nitrogen in sediments from core MBH 54/2.

Sed. Rate (cm/y)*	Approx. Calendar Year	Depth (m)	%C _{org}	%N	C/N (Weight %)	C/N (Atomic Mass)	δ ¹³ C _{org} (‰)	δ ¹⁵ N (‰)	
3.5cm/y	1981	0.5	0.75	0.07	10.71	12.50	-22.60	--	
		0.7	1.28	0.09	14.22	16.60	-23.86	6.19	
4.4cm/y	1971	0.9	1.68	0.12	14.00	16.34	-28.59	2.57	
		1.2	2.74	0.20	13.70	15.99	-26.62	3.44	
		1.4	2.83	0.15	18.87	22.02	-26.30	2.14	
1.9cm/y	1954	1.6	1.62	0.11	14.73	17.19	-27.49	3.13	
	1943	1.8	0.88	0.09	9.78	11.41	-27.74	4.49	
	1930	2.0	0.83	0.09	9.22	10.76	-27.99	3.05	
0.22mm/y		1428	0.59	0.07	8.43	9.84	-27.12	4.30	
		928	0.62	0.07	8.86	10.34	-26.92	4.27	
		604BC	2.6	0.94	0.06	15.67	18.28	-26.01	4.43
		1604BC	2.8	0.73	0.06	12.17	14.20	-27.25	3.61
		3104BC	3.1	0.63	0.06	10.50	12.25	-27.23	4.60
		4104BC	3.3	0.88	0.06	14.67	17.12	-24.74	4.57
		5104BC	3.5	0.83	0.07	11.86	13.84	-27.50	4.33
	M1	6104BC	3.7	0.86	0.05	17.20	20.07	-21.87	4.51
M2		3.9	0.42	0.04	10.50	12.25	-26.27	4.26	
		4.0	0.22	0.03	7.33	8.56	-30.18	2.53	
		4.1	0.39	0.03	13.00	15.17	-30.85	--	
		4.2	0.23	0.04	5.75	6.71	-33.17	--	

* Sedimentation rates from 0.5m to 2.1m are based on ²¹⁰Pb measurements reported by Tanner *et al.* (2000). At depths below 2.1m, the sedimentation rate is based on the maximum Holocene age of 8100y BP, which is marked by the dessicated crust which represents the boundary between the M1 and M2 layers (Yim, 1994); -- Indicates that measurements were below the detection limit; values in "**bold**" indicate an average of replicate runs. C/N (atomic mass ratio) was calculated by multiplying the C/N weight ratio by 1.167 (Meyers and Teranes, 2001). See **Appendix I** for a complete list of measurements and standard deviations.

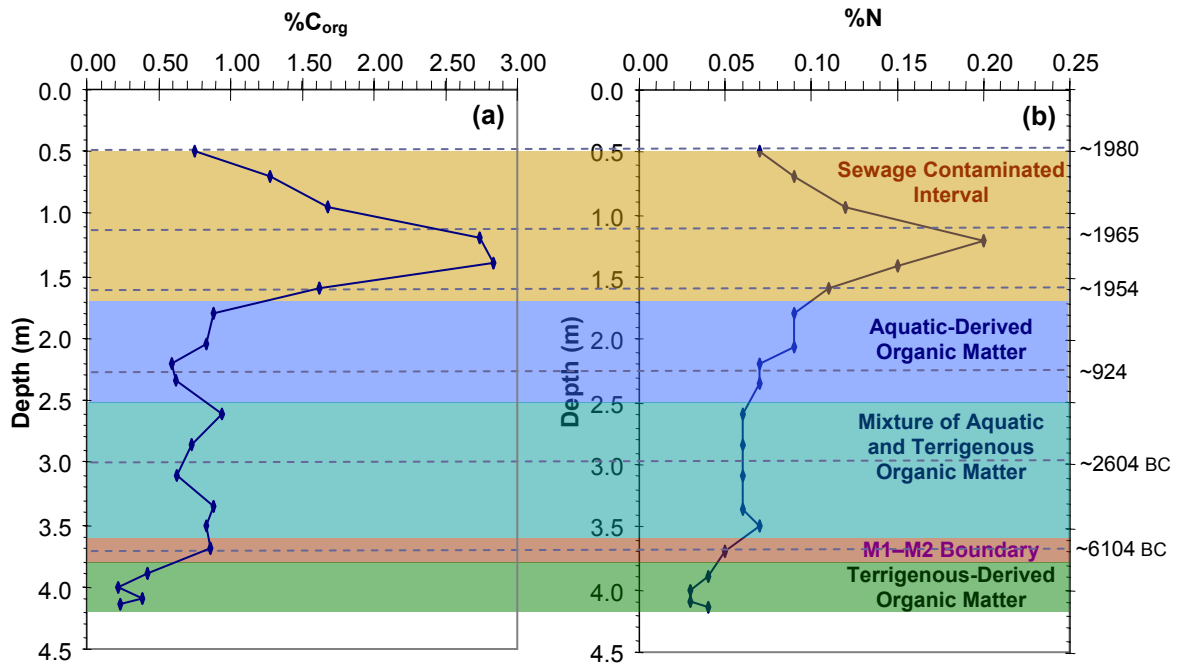


Fig. 3.3. Downcore profiles of %C_{org} and %N in sediment from core MBH 54/2, from Kowloon Bay, Victoria Harbour, Hong Kong SAR.

for several sediment samples were run in replicate and are summarized in

Appendix I. The average %C_{org} had standard deviations ranging up to ± 0.2 ;

average %N up to ± 0.01 ; average $\delta^{13}\text{C}_{\text{org}}$ compositions as high as ± 0.54 ; and

average $\delta^{15}\text{N}$ values within ± 0.3 . The downcore profile of organic carbon

deposited in Kowloon Bay during the Holocene and possible late Pleistocene is

shown in **Fig. 3.3a**. Three primary intervals can be observed, where the upper

unit (0.7m to 1.6m) consists of the highest organic carbon content ranging

between 1.28% and 2.83%. The maximum organic carbon content occurs

between 1.2m and 1.4m, where C_{org} is 2.74% and 2.83%, respectively. The

second unit (1.8m to 3.7m) is comprised of more intermediary organic carbon

compositions ranging between 0.59% and 0.94%. Within this unit (1.8m to 3.7m) there appear to be five subgroups marked by slight changes to the organic carbon content. The first subgroup occurs between 1.8m and 2.0m, where C_{org} is 0.83% and 0.88%, respectively. The organic carbon content decreases to between 0.59% and 0.73% at depths of 2.2m to 2.3m, and 2.8m and 3.1m; a sharp spike occurs at 2.6m where C_{org} is 0.94%. A slight rise in organic carbon content to between 0.83% and 0.88% occurs between 3.3m and 3.7m. The third unit is at the base of the core (3.9m to 4.1m) where C_{org} ranges between 0.22% and 0.42%.

The total nitrogen content reported in this study is positively correlated with organic carbon (**Fig. 3.4**), where the best fit line gives a correlation coefficient (R^2) of 0.8845. By extrapolating the organic carbon content to zero, the amount of inorganic nitrogen can be estimated (which was found to be ~0.02%). Thus, the total nitrogen content in sediments from MBH 54/2 can be assumed to be representative of organic nitrogen (Hedges *et al.*, 1986; Talbot and Johannessen, 1992; Andrews *et al.*, 1998; Talbot, 2001; Owen and Lee, 2004). The overall N content (**Fig. 3.3b**) is relatively low and ranges between 0.03% and 0.20%. In the same way as the organic carbon content, the nitrogen content can be divided into three major intervals. The upper unit (0.7m to 2.0m) has the highest N content ranging between 0.09% and 0.20% (maximum N occurs at 1.2m). The second unit extends from 2.2m to 3.7m and has a N composition ranging between 0.05% and 0.07%. The lowest N content occurs at

the base of the core (3.9m to 4.1m) with N values ranging between 0.03% and 0.04%.

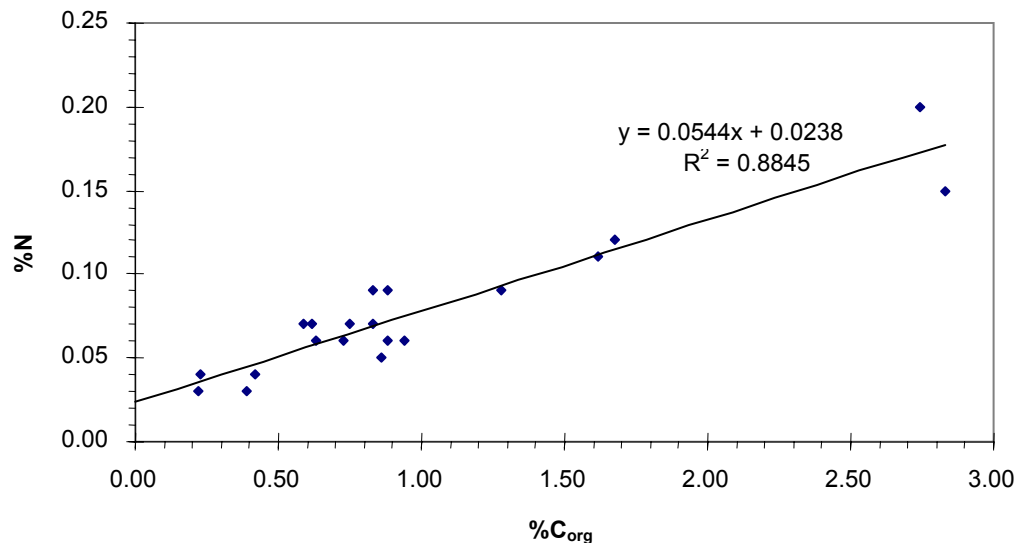


Fig. 3.4. Graph of %C_{org} versus %N in sediments from core MBH 54/2, Kowloon Bay, Victoria Harbour. The trend line shows a positive correlation between organic carbon and total nitrogen.

3.3.2 Ratio of Organic Carbon to Total Nitrogen

The weight % ratio of organic carbon to total nitrogen (C/N) is highly variable in the sediment core (**Fig. 3.5**). Fluctuations in the downcore profile documents shifts in the proportion of terrigenous, algal, and/or anthropogenically derived organic matter deposited during the Holocene and late Pleistocene. Early diagenesis may result in alterations in the C/N ratio. For example, microbial remineralization in the water column can cause the C/N value to decrease, or

increased productivity with limited nitrogen availability can result in higher C/N values (Meyers, 1994). Despite these changes in the water column, Meyers and Ishiwatari (1993) and Meyers (1994) have demonstrated that the C/N ratios and $\delta^{13}\text{C}_{\text{org}}$ signatures of organic matter do not undergo further diagenetic changes after burial, and that the overall source information is retained.

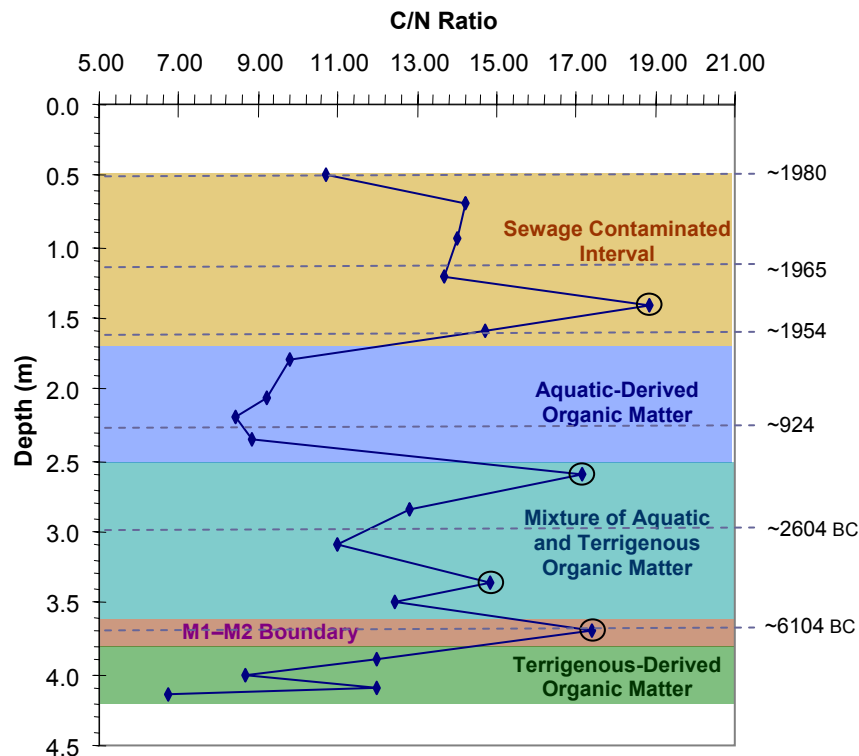


Fig 3.5. Downcore profile of the C/N (wt. % ratio) in core MBH 54/2, from Kowloon Bay, Victoria Harbour, Hong Kong SAR. “○” indicates possible flux of terrigenous-derived organic matter.

Four possible intervals are observed in **Fig. 3.5**. The first interval occurs between 0.7m and 1.6m with C/N ratios ranging between 13.7 and 14.7, except at 1.4m where the C/N ratio is 18.9. The relatively high C/N ratio between 0.7m and 1.6m occurs within a period known to have experienced a high influx of sewage waste. Higher disposal rates of sewage waste and nutrients lead to excessive algal blooms and this in turn could result in parts of Victoria Harbour becoming eutrophic. Phytoplankton and zooplankton typically have C/N ratios ranging between 4 and 10 (Meyers and Ishiwatari, 1993); however, the high C/N values observed in this interval indicates that other factors have affected this ratio. While the microbial denitrification of organic matter can result in the preferential loss of nitrogen, and increase the C/N values in sedimentary organic matter (Sarazin *et al.*, 1992; Sampei and Matsumoto, 2001; Owen and Lee, 2004), the high C/N values are likely due to contributions from sewage effluents.

The second interval occurs between 1.8m and 2.3m where the C/N ratio ranges between 8.4 and 9.8. The C/N ratio within this interval suggests that during this period Kowloon Bay received greater contributions of algal-derived organic matter compared to terrigenous-derived organic matter. These values are within the range for C/N ratios that have been used to implicate organic matter derived from phytoplankton, bacteria, and other single-celled organisms (Sigleo and Macko, 2002).

Intermediate C/N values are observed between 2.8m and 3.9m with values generally ranging between 10.5 and 12.2. Sedimentary organic matter in this region may reflect a mixture of both terrigenous- and algal-derived organic

matter. Spikes in the C/N ratio are observed at 2.6m (C/N=15.7), 3.3m (C/N=14.7), and 3.7m (C/N=17.2). The high C/N ratios at depths of 1.4m, 2.6m, 3.3m, and 3.7m (**Fig. 3.5**) resulted from higher organic carbon contents and were proposed to have been caused by the transport of terrigenous plant material by heavy monsoons or typhoons. At 1.4m, for example, a large spike in the C/N ratio (~18.9) was observed. Based on sedimentation rate data, sediments at this interval were deposited around 1961. Typhoons Mary (1960), Wanda (1962), Ruby (1964), and Dot (1964) passed through Hong Kong with Typhoon Wanda being the strongest typhoon to occur during this period (Yim, 1993; Huang and Yim, 1997). These events could have carried a greater abundance of terrigenous plant material into Kowloon Bay resulting in the spike in the C/N ratio observed at 1.4m. Owen (2005) reported spikes in the C/N ratio in two sediment core samples, corresponding to an event that occurred around 1910, from two locations in Tolo Harbour in northeastern Hong Kong. Heavy monsoons or typhoons were thought to have been responsible for the spike in the C/N ratio in his study. In core MBH 54/2, however, no spike in C/N ratio was observed in sediments deposited around depths corresponding to 1910 (*i.e.*, between 2.0m and 2.1m).

The fourth interval occurs at the base of the core, between 4.0m and 4.1m, where the C/N ratio is 7.3 and 5.8, respectively. A spike in the C/N ratio (13.0) is observed at 4.1m along with an elevated organic carbon content (0.39%). This may be indicative of an event where additional terrigenous organic matter was transported into Kowloon Bay.

3.3.3 Bulk Stable Isotope Composition of Organic Carbon and Total

Nitrogen

Sewage affected marine sediments can be discriminated from unaffected sediments using $\delta^{15}\text{N}$ signatures. Teranes and Bernasconi (2000) have reported isotopic values of sewage-derived nitrates to range between 10.00‰ and 25.00‰ . Bulk isotopic values for total nitrogen ranging between 1.8‰ and 3.2‰ have been reported in the literature for sewage effluent, sewage sludge, and sewage-derived organic matter (see **Table 3.1**). Bulk isotope values for organic carbon in these same samples were found to range between -28.5‰ and -23.0‰ .

Isotopically heavy organic carbon and nitrogen occur in sediments from the uppermost interval of core MBH 54/2 (0.5m to 0.7m), where $\delta^{13}\text{C}_{\text{org}}$ ranges between -23.86‰ to -22.60‰ , and $\delta^{15}\text{N}$ is 6.19‰ (**Fig. 3.6**). Higher influxes of raw sewage and nutrients can result in intense algal blooms, which ultimately would lead to eutrophication in Kowloon Bay. Under conditions of eutrophication, severe denitrification processes can occur, leading to the isotopic enrichment of ^{15}N (Teranes and Bernasconi, 2000; Bratton *et al.*, 2003). The increased productivity can also result in organic matter becoming enriched in ^{13}C . As phytoplankton preferentially consume ^{12}C from dissolved inorganic carbon, the residual inorganic carbon will become isotopically heavier. Utilization of ^{13}C enriched inorganic carbon by phytoplankton will result in the production of isotopically heavier organic matter (Meyers, 2003).

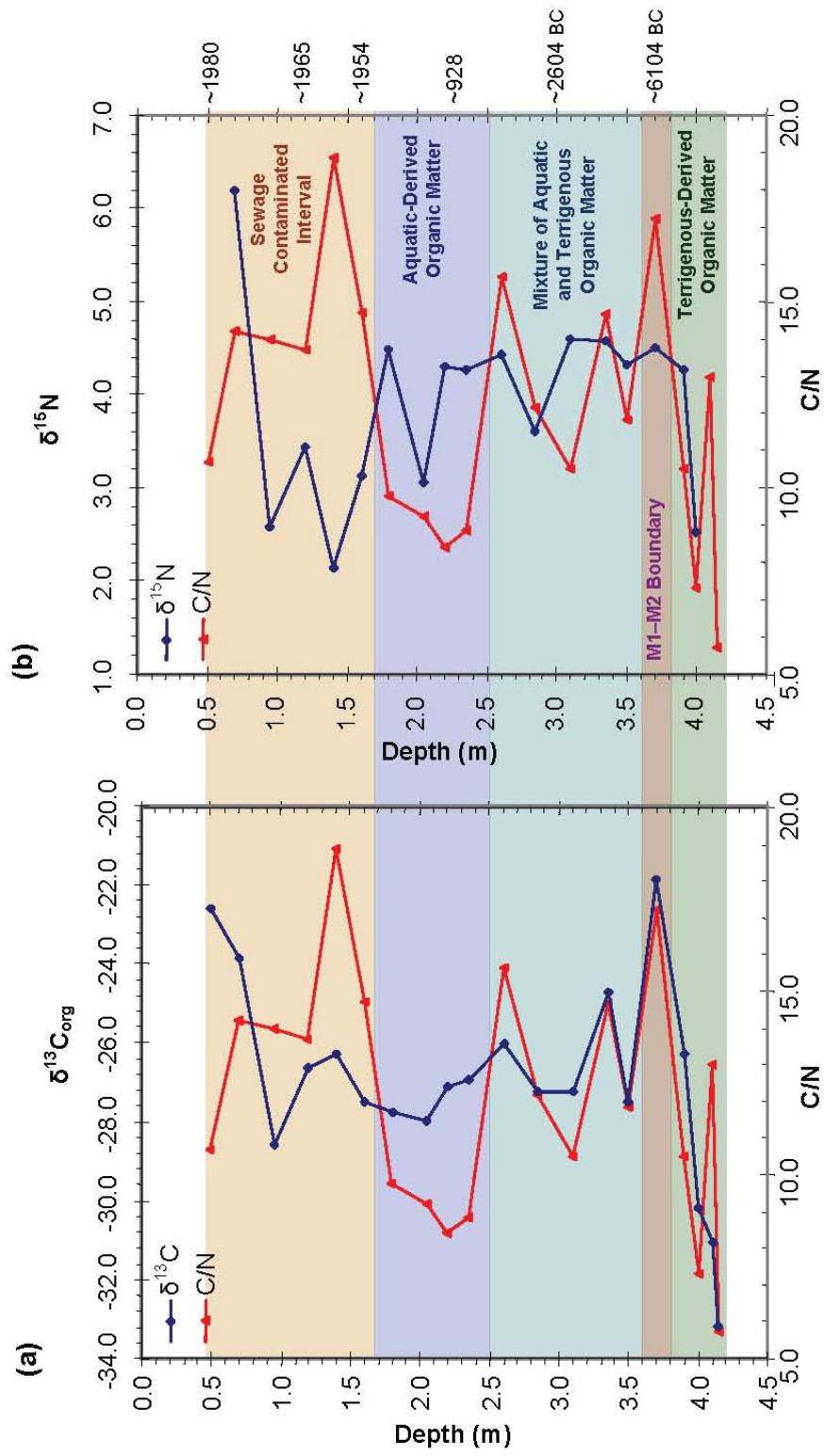


Fig. 3.6. (a) Downcore profile of $\delta^{13}C_{org}$ and C/N (wt. % ratio); **(b)** Downcore profile of $\delta^{15}N$ and C/N (wt. % ratio).

The interval between 0.7m and 1.6m represents a period most affected by raw sewage waste. The estimated calendar years for this interval fall between 1954 and 1977, a period of rapid population growth and increased dumping of raw sewage (seawall-type sewage outfall). Bulk properties (*i.e.*, $\delta^{13}\text{C}_{\text{org}}$, $\delta^{15}\text{N}$, and C/N ratio) of sediments in this interval are consistent with values reported in the literature for sewage contaminated sites, where sediments from MBH 54/2 have $\delta^{13}\text{C}_{\text{org}}$ compositions between -28.59‰ and -26.30‰ ; $\delta^{15}\text{N}$ values range between 2.14‰ and 3.44‰ ; and C/N ratio range between 13.7 and 14.7, except at 1.4m where the C/N ratio is 18.9.

The C/N ratio between 1.8m and 2.3m ranges between 8.4 and 9.8, suggesting that the sediments received greater contributions from algal-derived organic matter rather than terrigenous-derived organic matter during this time period. Bulk carbon isotope compositions, however, indicate values typical for C3 plants (-27.99‰ to -26.92‰). The carbon isotopic values in this interval were expected to be heavier, with values more characteristic of aquatic-derived organic matter (*i.e.*, around -25‰ to -20‰) since the C/N ratios indicated greater contributions from algal-derived organic matter. $\delta^{15}\text{N}$ values ranged between 4.27‰ and 4.49‰ , except at 2.0m where $\delta^{15}\text{N}$ was 3.05‰ . The relatively light $\delta^{13}\text{C}_{\text{org}}$ and $\delta^{15}\text{N}$ values may reflect the occurrence of excess bacterial biomass bound to the sediment (Bratton *et al.*, 2003).

The C/N ratio shifts between 10.5 and 15.7 at depths between 2.5m and 3.6m. Changes in the organic carbon content appear to be responsible for the variations observed in the C/N ratio. The nitrogen content is consistently around

0.06% between 2.5m and 3.6m. Spikes in C/N ratios are observed at 2.6m and 3.3m possibly reflecting a higher influx of terrigenous plant material transported into Kowloon Bay by strong storms. $\delta^{13}\text{C}_{\text{org}}$ compositions at these intervals are -26.01‰ and -24.73‰ , respectively, which are normal values for C3 terrigenous plants. At other measured intervals within this unit $\delta^{13}\text{C}_{\text{org}}$ values ranged between -27.50‰ and -27.23‰ . $\delta^{15}\text{N}$ values were relatively consistent between 4.33‰ and 4.60‰ , except at 2.8m, where $\delta^{15}\text{N}$ was 3.61‰ . This may suggest that, for the most part, there was not much variability in organic matter source input within this interval.

At 3.7m, there is a large spike in the C/N ratio (*i.e.*, C/N=17.2) and the bulk carbon isotope composition is enriched in ^{13}C (-21.87‰). While a $\delta^{13}\text{C}_{\text{org}}$ value of -21.87‰ falls within the range typical for marine-derived organic matter, the sediments in this part of the core appears to be part of the desiccated crust observed throughout most of Hong Kong Harbour. The desiccated crust represents a period when marine sediments were subaerially exposed during a low sea-level stand and mark the boundary between Holocene marine sediments (*i.e.*, the M1 layer) and pre-Holocene marine sediments (*i.e.*, the M2 layer), described by Yim (1994). The heavier $\delta^{13}\text{C}_{\text{org}}$ value observed at this interval may reflect contributions of C4 terrigenous plants (*e.g.*, C4 seagrasses) to the marine sediments. The $\delta^{13}\text{C}_{\text{org}}$ values become progressively lighter from 3.7m towards the base of the core, where $\delta^{13}\text{C}_{\text{org}}$ is -26.27‰ at 3.9m, and ranges from -33.17‰ to -30.18‰ between 4.0m and 4.1m. Isotopic values of organic carbon between 4.0m and 4.1m suggests predominant contributions of organic matter

from terrigenous plants. $\delta^{15}\text{N}$ values at 3.7m and 3.9m do not deviate much from $\delta^{15}\text{N}$ values measured in sediments deposited above these intervals, and range between 4.26‰ and 4.51‰ . At 4.0m, a sharp drop in $\delta^{15}\text{N}$ (2.53‰) is observed which may be reflective of terrigenous plants utilizing atmospheric nitrogen as their nitrogen source.

Crossplots of C/N (atomic mass ratio) to $\delta^{13}\text{C}_{\text{org}}$ of plant and algal material, from lake and marine environments, have been utilized for distinguishing sources of sedimentary organic matter (**Fig. 3.7**; Meyers, 1994). The C/N atomic mass ratio is calculated by multiplying the C/N weight % ratio by 1.167 (Meyers and Teranes, 2001). The C/N (atomic mass ratios) and $\delta^{13}\text{C}_{\text{org}}$ measurements from sediments in the Victoria Harbour core sample (MBH 54/2; **Fig. 3.8**) do not fall within the regions defined in **Fig. 3.7**. The majority of the samples have C/N (atomic mass ratios) less than 20, and have $\delta^{13}\text{C}_{\text{org}}$ values that fall within the range for C3 terrigenous plants (**Figs. 3.8 and 3.9**). Sediments from the interval between 1.8m and 2.3m have C/N (atomic mass ratios) that fall within the range for algal-derived organic matter. The $\delta^{13}\text{C}_{\text{org}}$ values within this interval, however, are much lighter than expected (-27.99‰ to -26.92‰).

Uncontaminated sediments with isotopic compositions suggesting contributions from C3 terrigenous plants (*i.e.*, $\delta^{13}\text{C}_{\text{org}}$ values ranging between -27.50‰ and -24.74‰) fall into two identifiable groups (**Fig. 3.8**). One group has C/N ratios ranging between 12.2 and 14.2, and the second group ranges between 17.1 and 18.3. Sewage contaminated sediments in the uppermost part of the core (0.5m to 0.7m) may have been affected by denitrification processes,

resulting in the enrichment of ^{13}C (*i.e.*, $\delta^{13}\text{C}_{\text{org}}$ values in this region range between -23.86‰ and -22.60‰). In general, $\delta^{13}\text{C}_{\text{org}}$ values of sewage contaminated sediments range from -28.59‰ to -26.30‰ , with C/N values between 16.0 and 17.2, except at 1.4m where there appears to have been a flux in organic matter input.

A plot of C_{org} versus atomic C/N mass ratio (**Fig. 3.10**) illustrates two envelopes separating those sediments affected or unaffected by sewage waste. Sediments in the upper 1.6m of the core are known to have been contaminated by sewage waste and contain the highest organic carbon content. Sediments contaminated

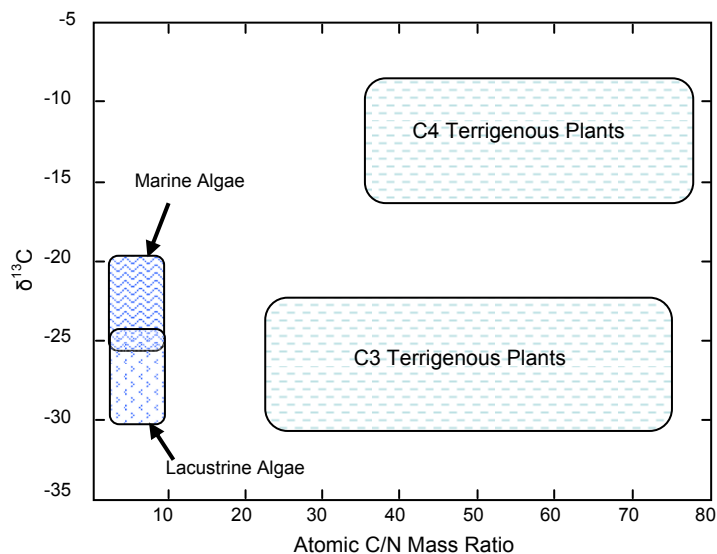


Fig. 3.7. Crossplot of atomic C/N mass ratio to $\delta^{13}\text{C}$ of terrigenous plant and algal material, for differentiating sources of organic matter (from Meyers, 1994).

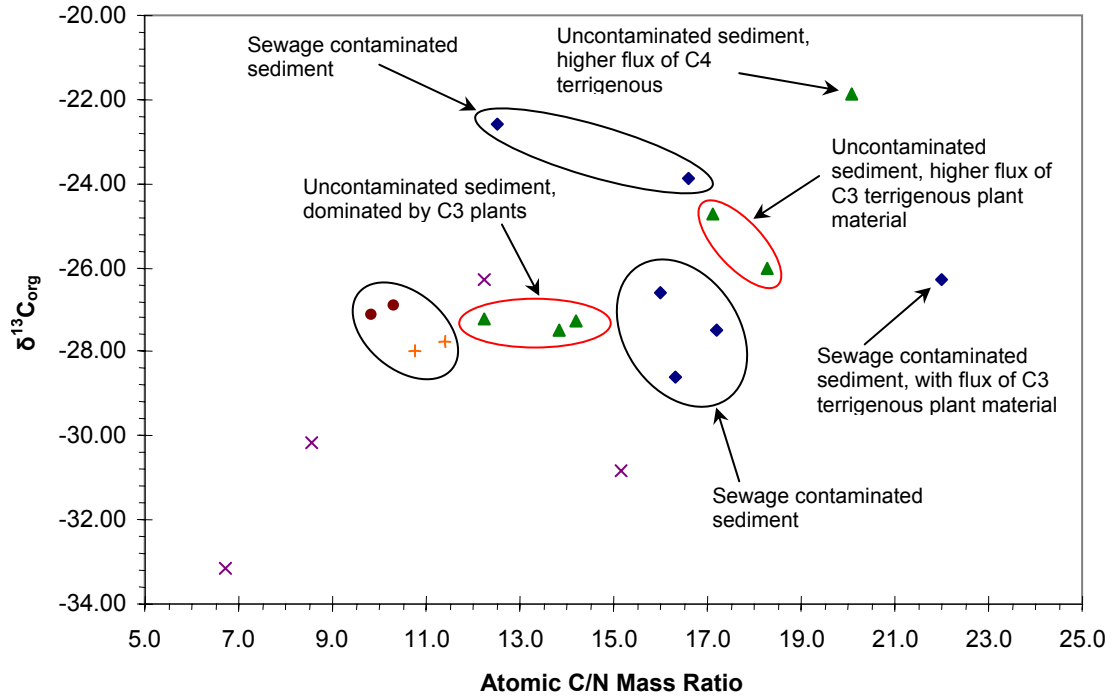


Fig. 3.8. Crossplot of C/N ratio to $\delta^{13}\text{C}_{\text{org}}$ of sediments from core MBH 54/2.

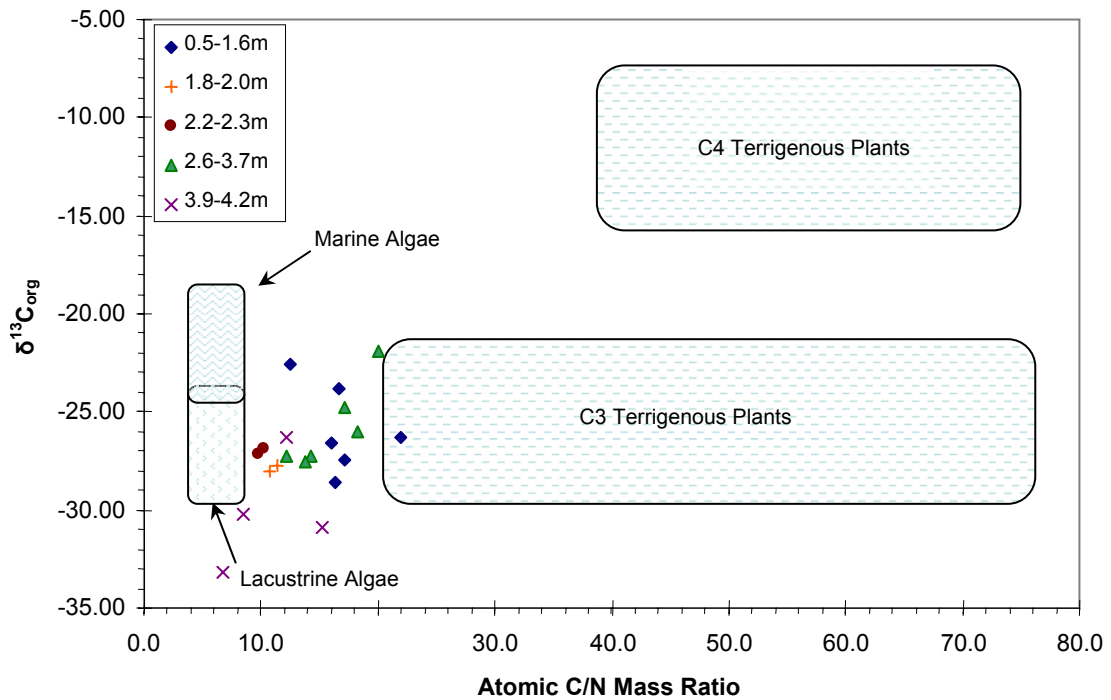


Fig. 3.9. Overlay of the atomic C/N mass ratio vs $\delta^{13}\text{C}_{\text{org}}$ of sediments from core MBH 54/2, and the Meyers (1994) plot for differentiating sources of organic matter.

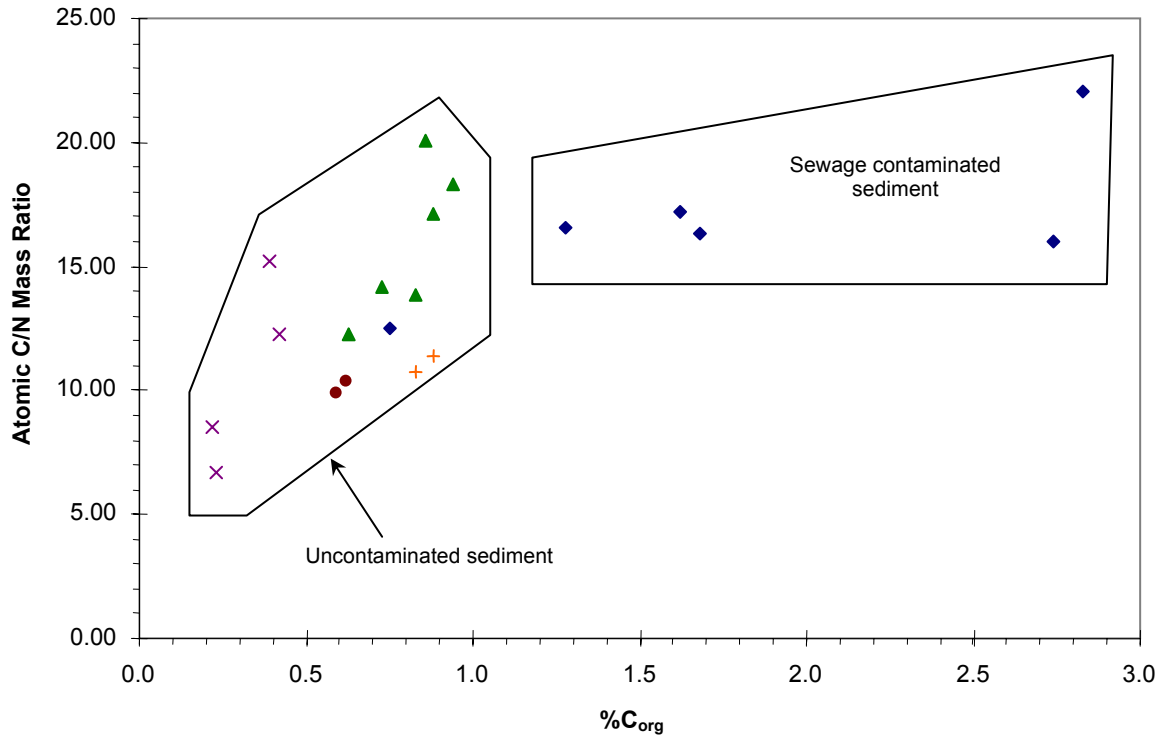


Fig. 3.10. Discrimination of sewage contaminated sediments from uncontaminated sediments using the plot of %C_{org} versus C/N ratio.

with sewage waste can not be differentiated from uncontaminated sediments using the plot of $\delta^{15}\text{N}$ versus $\delta^{13}\text{C}_{\text{org}}$ (**Fig. 3.11**). The envelopes drawn in **Fig. 3.11** are based on prior knowledge of sediments contaminated with sewage. The sewage affected sediments have $\delta^{15}\text{N}$ values ranging between 2.14‰ and 3.44‰, and $\delta^{13}\text{C}_{\text{org}}$ values ranging between -28.59‰ and -26.30‰. In the uppermost part of the core, the sewage contaminated sediment may have also been affected by denitrification processes, resulting in the enrichment of ^{15}N and ^{13}C .

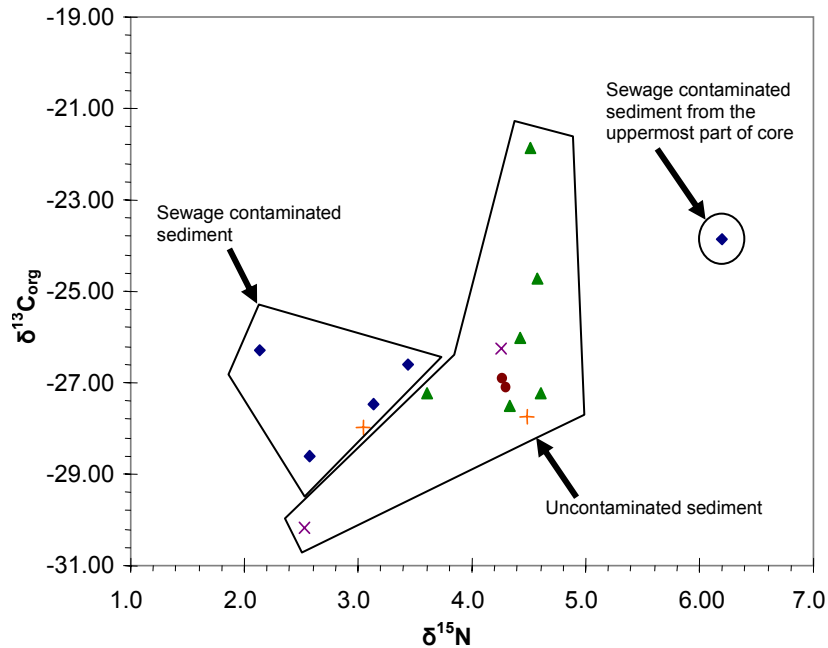


Fig. 3.11. Crossplot of $\delta^{15}\text{N}$ versus $\delta^{13}\text{C}_{\text{org}}$ of contaminated and uncontaminated sediments from Kowloon Bay (core MBH 54/2).

3.4 Summary Remarks

Elemental analyses and bulk stable isotope measurements of organic carbon and nitrogen in sediments from core MBH 54/2, Kowloon Bay, provide clues for delineating sources of organic matter and provide a means for speculating on processes and events that have occurred in this region.

Sediments in the upper 1.6m of the core are known to have been deposited during periods of rapid population growth and excessive disposal of raw sewage.

The highest flux in organic carbon and nitrogen occur within this interval and $\delta^{13}\text{C}_{\text{org}}$ and $\delta^{15}\text{N}$ values (*i.e.*, -28.59‰ to -26.30‰ and 2.14‰ to 3.44‰ , respectively) are consistent with bulk isotopic compositions reported in the

literature for sewage contaminated sites. The uppermost part of the core (0.5m to 0.7m) is more enriched in ^{13}C and ^{15}N , where $\delta^{13}\text{C}_{\text{org}}$ ranged between -23.86‰ to -22.60‰ , and $\delta^{15}\text{N}$ was 6.19‰ . It is speculated that this may be an indication that the organic matter was affected by denitrification processes as a result of eutrophication in Kowloon Bay. Enrichment of ^{13}C and ^{15}N in organic matter has been observed under conditions of eutrophication where increasing anoxicity results in intense denitrification processes.

Below the sewage contaminated sediments (1.8m to 2.3m), there is a shift in the C/N (weight % ratio) where organic carbon decreases relative to nitrogen. This may be an indication that the organic matter source has experienced a shift towards more aquatic-derived organic matter that would have a higher nitrogen content relative to C_{org} . Sediments deposited between 2.6m and 3.5m appear to be dominated by C3 terrigenous plant material with periodic shifts towards aquatic-derived organic matter (*e.g.*, at 3.1m and 3.5m). C/N ratios and $\delta^{13}\text{C}_{\text{org}}$ values within this interval range between 10.5 and 15.7, and -27.50‰ and -24.74‰ , respectively. The $\delta^{13}\text{C}_{\text{org}}$ value is enriched in ^{13}C at 3.7m (-21.87‰), which is located around the desiccated crust indicating the M1-M2 boundary. The heavier $\delta^{13}\text{C}_{\text{org}}$ value may represent contributions from C4 plants during the early Holocene/late Pleistocene, when sea level was approximately 130km south of Hong Kong. The isotopic signature at this depth may serve as a secondary parameter for identifying the boundary between Holocene marine sediments and pre-Holocene marine sediments (*i.e.*, the M1-M2 layer). Sediments at the base of the core (4.0m to 4.1m) are the most depleted in ^{13}C , where $\delta^{13}\text{C}_{\text{org}}$ ranges

between -33.17‰ to -30.18‰ . $\delta^{15}\text{N}$ was only measurable at 4.0m with a value of 2.53‰ . Isotopic compositions of the sedimentary organic matter at these intervals suggest origins from C3 terrigenous plant material where atmospheric nitrogen is utilized via nitrogen fixation.

3.5 References

Altabet, M. A., 1988. Variations in nitrogen isotopic composition between sinking and suspended particles – implications for nitrogen cycling and particle transformation in the open ocean. *Deep-Sea Research Part A-Oceanographic Research Papers*, 35, 535-554.

Altabet, M., McCarthy, J., 1985. Temporal and spatial variation in the natural abundance of ^{15}N in PON from a warm core ring. *Deep Sea Research*, 32, 755-772.

Andrews, J. E., Greenaway, A. M., Dennis, P. F., 1998. Combined carbon isotope and C/N ratios as indicators of source and fate of organic matter in a poorly flushed, tropical estuary: Hunts Bay, Kingston Harbour, Jamaica. *Estuarine, Coastal and Shelf Science*, 46, 743-756.

Bickert, T., 2000. Influence of geochemical processes on stable isotope distribution in marine sediments. In: Schulz, H. D., Zabel, M. (eds), *Marine Geochemistry*. Springer-Verlag, Berlin, 309-333.

Bratton, J. F., Colman, S. M., Seal II, R. R., 2003. Eutrophication and carbon source in Chesapeake Bay over the last 2700 yr: human impacts in context. *Geochimica et Cosmochimica Acta*, 67, 3385-3402.

Burnett, W. C., Schaeffer, O. A., 1980. Effect of Ocean Dumping on $^{13}\text{C}/^{12}\text{C}$ Ratios in Marine Sediments from the New York Bight. *Estuarine and Coastal Marine Science*, 11, 605-611.

van Dover, C. L., Grassle, J. F., Fry, B., Garritt, R. H., Starczak, V. R., 1992. Stable isotope evidence for entry of sewage-derived organic material into a deep-sea foodweb. *Nature*, 360, 153-156.

- Fogel, M. L., Cifuentes, L. A., 1993. Isotope fractionation during primary production. *In: Engel, M. H., Macko, S. A. (eds), Organic Geochemistry: Principles and Applications*, Plenum Press, New York, 73-98.
- Gearing, P. J., Gearing, J. N., Maughan, J. T., Ovlatt, C. A., 1991. Isotopic distribution of carbon from sewage sludge and eutrophication in the sediments and food web of estuarine ecosystems. *Environmental Science and Technology*, 25, 295-301.
- Hedges, J., Clark, W., Quay, P., Richey, J., Devol, A., Santos, U. D. M., 1986. Compositions and fluxes of particulate organic material in the Amazon River. *Limnology and Oceanography*, 31, 717-738.
- Hoefs, J., 1997. *Stable Isotope Geochemistry*. Springer, Berlin, 4th ed., 401p.
- Huang, G., Yim, W. W. -S., 1997. Storm sedimentation in the Pearl River Estuary, China. *International Conference on the Evolution of the East Asian Environment. Centre of Asian Studies: Occasional Papers and Monographs*, 124, 156-177.
- Huang, Y., Street-Perrott, F. A., Perrott, R. A., Metzger, P., Eglinton, G., 1999. Glacial-interglacial environmental changes inferred from molecular and compound-specific $\delta^{13}\text{C}$ analyses of sediments from Sacred Lake, Mt. Kenya. *Geochimica et Cosmochimica Acta*, 63, 1383-1404.
- Hunt, C. D., Ginsburg, L., West, D., Redford, D., 1992. The fate of sewage sludge dumped at the 106-mile site – preliminary results from sediment trap studies. *EOS Transactions American Geophysical Union*, 73, 165.
- Lee, S. Y., 2000. Carbon dynamics of Deep Bay, eastern Pearl River estuary, China. II: Trophic relationships based on carbon- and nitrogen- stable isotopes. *Marine Ecology Progress Series*, 205, 1-10.
- Meyers, P. A., 1994. Preservation of elemental and isotopic source identification of sedimentary organic matter. *Chemical Geology*, 114, 289-302.
- Meyers, P. A., 2003. Applications of organic geochemistry to paleolimnological reconstructions: a summary of examples from the Laurentian Great Lakes. *Organic Geochemistry*, 34, 261-289.
- Meyers, P. A., Ishiwatari, R., 1993. The early diagenesis of organic matter in lacustrine sediments. *In: Engel, M. H., Macko, S. A. (eds), Organic Geochemistry: Principles and Applications*. Plenum, New York, 185-209.
- Meyers, P. A., Lallier-Vergès, E., 1999. Lacustrine sedimentary organic matter records of Late Quaternary paleoclimates. *Journal of Paleolimnology*, 21, 345-372.

- Meyers, P. A., Teranes, J. L., 2001. Sediment organic matter. *In: Last, W. M., Smol, J. P. (eds), Tracking Environmental Change Using Lake Sediments. Vol. 2: Physical and Geochemical Methods.* Kluwer Academic Publishers, Dordrecht, The Netherlands, 239-269.
- Minagawa, M., Wada, E., 1986. Nitrogen isotope ratios of red tide organisms in the East China Sea: a characterization of biological nitrogen fixation. *Marine Chemistry*, 19, 245-259.
- Mishima, Y., Hoshika, A., Tanimoto, T., 1999. Deposition rates of terrestrial and marine organic carbon in the Osaka Bay, Seto Inland Sea, Japan, determined using carbon and nitrogen stable isotope ratios in the sediment. *Journal of Oceanography*, 55, 1-11.
- Montoya, J. P., 1994. Nitrogen isotope fractionation in the modern ocean: Implications for the sedimentary record. *In: Zahn, R., Pedersen, T. F., Kaminski, M. A., Labeyrie, L. (eds), Carbon Cycling in the Glacial Ocean: Constraints on the Oceans Role in Global Change. Nato ASI Series*, 117, 259-279.
- Moore, P. D., 2004. Isotopic biogeography. *Progress in Physical Geography*, 28, 145-151.
- Muzuka, A. N. N., Macko, S. A., Pedersen, T. F., 1991. Stable carbon and nitrogen isotope compositions of organic matter from sites 724 and 725, Oman Margin. *Proceedings of the Ocean Drilling Program, Scientific Results*, 117, 571-586.
- Owen, R. B., 2005. Modern fine-grained sedimentation – spatial variability and environmental controls on an inner pericontinental shelf, Hong Kong, *Marine Geology*, 214, 1-26.
- Owen, R. B., Lee, R. 2004. Human impacts on organic matter sedimentation in a proximal shelf setting, Hong Kong. *Continental Shelf Research*, 24, 583-602.
- Peters, K. E., Sweeney, R. E., Kaplan, I. R., 1978. Correlation of carbon and nitrogen stable isotope ratios in sedimentary organic matter. *Limnology and Oceanography*, 23, 598-604.
- Rogers, K. M., 2003. Stable carbon and nitrogen isotope signatures indicate recovery of marine biota from sewage pollution at Moa Point, New Zealand. *Marine Pollution Bulletin*, 46, 821-827.
- Sampei, Y., Matsumoto, E., 2001. C/N ratios in a sediment core from Nakaumi Lagoon, southwest Japan – usefulness as an organic source indicator. *Geochemical Journal*, 35, 189-205.

- Saino, T., Hattori, A., 1987. Geographical variation of the water column distribution of suspended particulate organic nitrogen and its N-15 natural abundance in the Pacific and its marginal seas. *Deep-Sea Research Part A-Oceanographic Research Papers*, 34, 807-827.
- Sarazin, G., Michard, G., Al Gharib, I., Bernet, M., 1992. Sedimentation rate and early diagenesis of particulate organic nitrogen and carbon in Aydat lake (Puy de Dome, France). *Chemical Geology*, 98, 307-316.
- Sayles, F. L., Curry, W. B., 1988. $\delta^{13}\text{C}$, TCO_2 , and the metabolism of organic-carbon in deep-sea sediments. *Geochimica et Cosmochimica Acta*, 52, 2963-2978.
- Sifeddine, A., Wirmann, D., Albuquerque, A. L. S., Turq, B., Cordeiro, R. C., Gurgel, M. H. C., Abrão, J. J., 2004. Bulk composition of sedimentary organic matter used in palaeoenvironmental reconstructions: examples from the tropical belt of South America and Africa. *Palaeogeography, Palaeoclimatology, Palaeoecology*, 214, 41-53.
- Sigleo, A. C., Macko, S. A., 2002. Carbon and nitrogen isotopes in suspended particles and colloids, Chesapeake and San Francisco Estuaries, USA. *Estuarine, Coastal and Shelf Science*, 54, 701-711.
- Spies, R. B., Kruger, H., Ireland, R., Rice Jr., D. W., 1989. Stable isotope ratios and contaminant concentrations in a sewage-distorted food web. *Marine Ecology Progress Series*, 54, 157-170.
- Sweeney, R. E., Kalil, E. K., Kaplan, I. R., 1980. Characterisation of domestic and industrial sewage in southern California Coastal Sediments using nitrogen, carbon, sulphur, and uranium tracers. *Marine Environmental Research*, 3, 225-243.
- Sweeney, R. E., Liu, K. K., Kaplan, I. R., 1978. Oceanic nitrogen isotopes and their uses in determining the source of sedimentary nitrogen. In: Robinson, B. W. (ed), *Stable Isotopes in the Earth Sciences*. New Zealand Department of Scientific and Industrial Research, *DSIR Bulletin*, 220, 9-26.
- Talbot, M. R., 2001. Nitrogen isotopes in palaeolimnology. In: Last, W. M., Smol, J. P. (eds), *Tracking Environmental Change Using Lake Sediments. Vol. 2: Physical and Geochemical Methods*. Kluwer Academic Publishers, Dordrecht, The Netherlands, 401-439.
- Talbot, M. R., Johannessen, T., 1992. A high resolution palaeoclimate record for the past 27,500 years in tropical west Africa from the carbon and nitrogen

isotopic composition of lacustrine organic matter. *Earth and Planetary Science Letters*, 110, 23-37.

Tanner, P. A., Leong, L. S., Pan, S. M., 2000. Contamination of heavy metals in marine sediment cores from Victoria Harbour, Hong Kong. *Marine Pollution Bulletin*, 40, 769-779.

Teranes, S. L., Bernasconi, S. M., 2000. The record of nitrate utilization and productivity limitation provided by $\delta^{15}\text{N}$ values in lake organic matter – a study of sediment trap and core sediments from Baldeggersee, Switzerland. *Limnology and Oceanography*, 45, 801-813.

Thornton, S. F., McManus, J., 1994. Applications of organic carbon and nitrogen stable isotope and C/N ratios as source indicators of organic matter provenance in estuarine systems: evidence from the Tay Estuary, Scotland. *Estuarine, Coastal and Shelf Science*, 38, 219-233.

Waldron, S., Tatner, P., Jack, I., Arnott, C., 2001. The impact of sewage discharge in a marine embayment: a stable isotope reconnaissance. *Estuarine, Coastal and Shelf Science*, 52, 111-115.

Whelan, J. K., Farrington, J. W., 1992. *Organic matter: productivity, accumulation, and preservation in recent and ancient sediments*. Columbia University Press, New York, 533p.

Wu, Y., Zhang, J., Li, D. J., Wei, H., Lu, R. X., 2003. Isotope variability of particulate organic matter at the PN section in the East China Sea. *Biogeochemistry*, 65, 31-49.

Yim, W. W. -S., 1993. Future sea level rise in Hong Kong and possible environmental effects. In: Warrick, R. A., Barrow, E. M., Wigley, T. M. L. (eds), *Climate and Sea Level Change: Observations, Projections and Implications*, 349-376.

Yim, W. W. -S., 1994. Offshore Quaternary sediments and their engineering significance in Hong Kong. *Engineering Geology*, 37, 31-50.

CHAPTER 4

Sources and Distribution of Extractable Organic Matter in Kowloon Bay Sediments, Hong Kong SAR, China

4.1 Introduction

Lipids are important constituents of sedimentary organic matter and can be used to delineate the sources of organic matter and transformation processes in Recent sediments. While lipids make up a minor fraction of the organic matter in Recent sediments (*i.e.*, proteins and carbohydrates are more abundant), they demonstrate a greater degree of resilience to environmental alteration (Killops and Killops, 1993; Wakeham *et al.*, 1997; Smallwood and Wolff, 2000; Gogou and Stephanou, 2004; Muri *et al.*, 2004). In general, lipids are defined as the fraction of organic matter extractable from biological material using organic solvents such as dichloromethane, methanol, toluene, ether, or hexane (Meyers and Ishiwatari, 1993; Rullkötter, 2000). It should be noted that a significant portion of lipids in sedimentary organic matter occur in bound form (discussed in Chapter 5) and require harsher treatments (*e.g.*, alkaline and acid hydrolysis) in order to release ester- and amide-bound lipids (Goosens *et al.*, 1986, 1989a,b; Cranwell, 1990; Fukushima *et al.*, 1992a,b; Wakeham, 1999; Killops and Killops, 2005). Lipids extractable from marine sediments are comprised of sterols, fatty alcohols, fatty acids, and hydrocarbons. Each of these lipid groups provides diagnostic information that can be used to reconstruct the origin of sedimentary organic matter and transformation processes.

4.2 Review of Literature

4.2.1 Sterols in Marine Sediments

Sterols are well preserved in the environment and have unique structures, making them favorable compounds as biological markers. The basic structure and numbering scheme for sterols, using cholesterol as an example, is shown in **Fig. 4.1**.

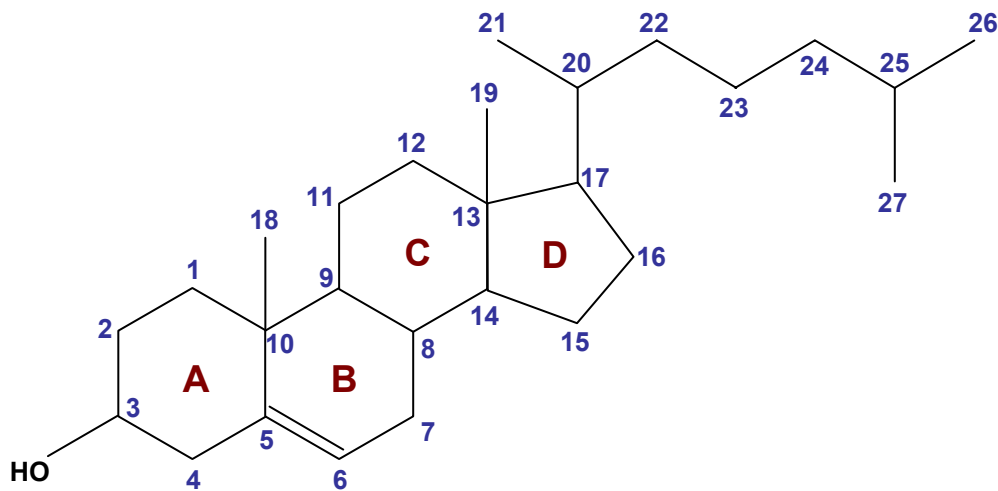


Fig. 4.1. Cholesterol structure illustrating an example of the numbering scheme for sterols.

Sterols and compounds derived from sterols (*e.g.*, stanols, stenones, stanones, sterenes, and steranes; **Fig. 4.2**) have been used as proxies to determine the proportions of algal and terrigenously derived organic matter in marine sediments, study transformation processes, and to trace the origin of fecal material in the

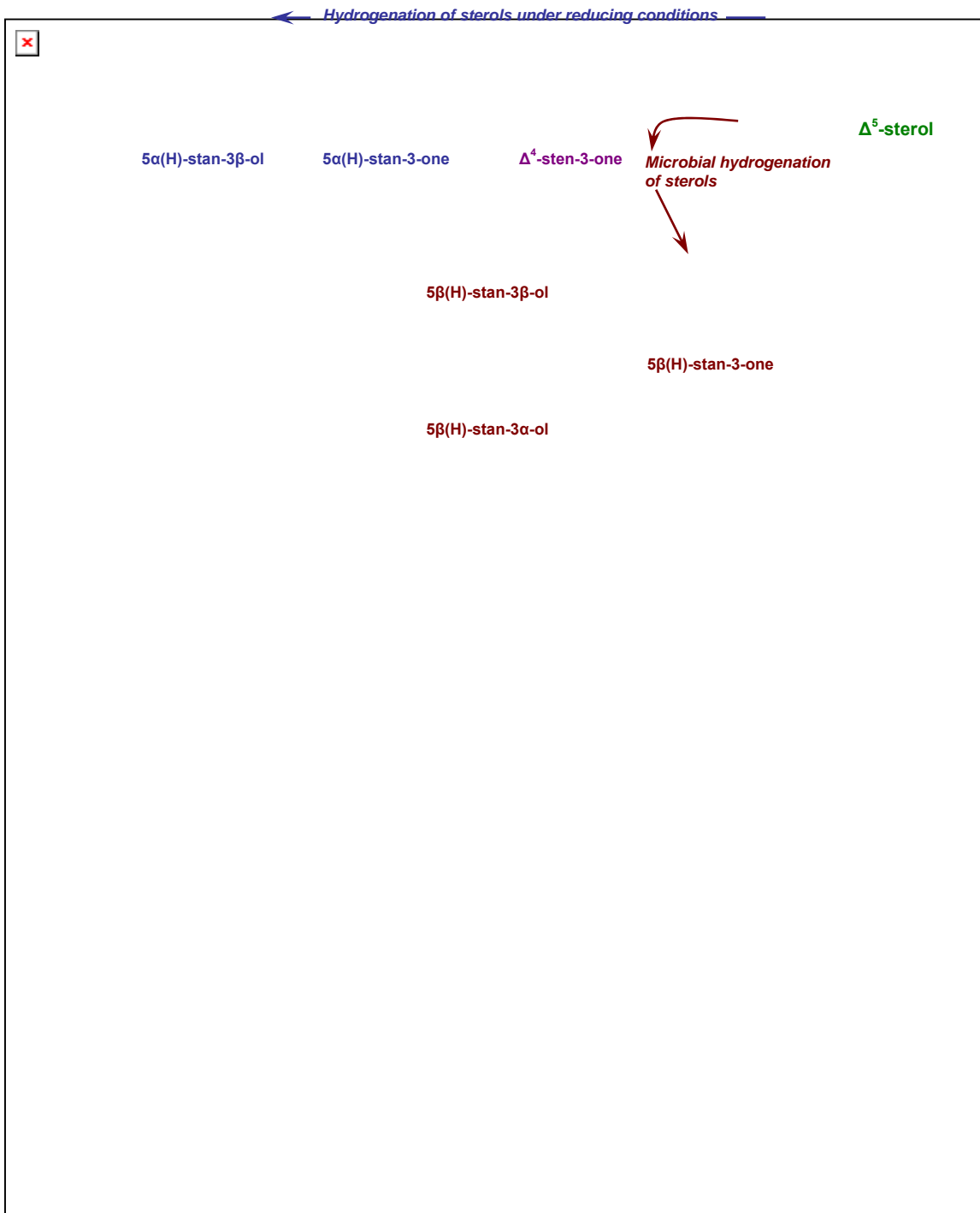


Fig. 4.2. Sterol transformation pathways (from Mackenzie *et al.*, 1982).

environment (Gagosian *et al.*, 1980; Mackenzie *et al.*, 1982; Readman *et al.*, 1986; Volkman, 1986; Mudge *et al.*, 1999; Meyers, 2003).

Sterols from algal and zooplankton derived organic matter are typically dominated by cholesterol (Volkman, 1986; Santos *et al.*, 1994; Burns *et al.*, 2003; Meyers, 2003). The key sterols in vascular terrigenous plants are the C₂₉ sterols, β -sitosterol and stigmasterol (Huang and Meinschein, 1979; Volkman, 1986; Saliot *et al.*, 1991; Mudge and Norris, 1997). Relative contributions of aquatic versus terrigenous plant material in Recent sediments have been estimated using the C₂₇ to C₂₉ sterol ratio (Huang and Meinschein, 1979; Meyers, 2003). This ratio should be used with caution, since C₂₉ sterols have been observed to occur in certain marine organisms (Volkman, 1986; Santos *et al.*, 1994; Gogou and Stephanou, 2004). Other unique sterols include brassicasterol, a common marker for diatoms and prymnesiophytes; and dinosterol, an indicator for dinoflagellates (Gagosian *et al.*, 1980; Volkman, 1986; Santos *et al.*, 1994; Smallwood and Wolff, 2000).

Sewage contamination in the environment has been monitored and traced using sterols. Human sewage waste can be monitored in the environment using the fecal sterol, coprostanol (5 β -cholestan-3 β -ol; **Fig. 4.3a**). Coprostanol is a unique marker formed by the bacterial reduction of cholesterol (cholest-5-en-3 β -ol) in the human digestive tract, and released into the environment in human feces (**Fig. 4.3b**; Readman *et al.*, 1986; Nichols and Leeming, 1991; Mudge *et al.*, 1999). The process for transforming cholesterol to coprostanol is illustrated in

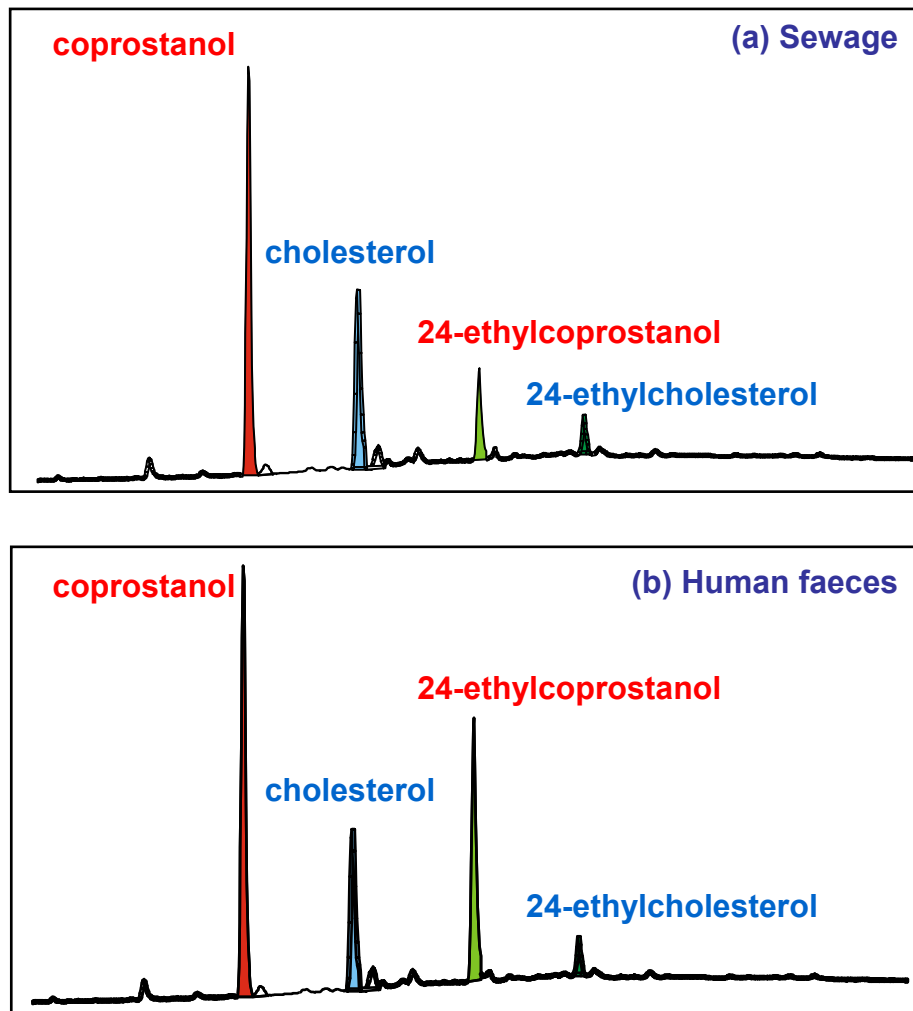


Fig. 4.3. Fecal sterol profiles from (a) sewage waste and (b) human feces (figures provided via personal communications with Dr. Rhys Leeming, CSIRO).

Fig. 4.4. During sewage treatment, coprostanol is transformed to its isomer epicoprostanol (5β -cholestan- 3α -ol). To date, epicoprostanol is only known to be present in treated sewage sludge (McCalley *et al.*, 1981; Mudge *et al.*, 1999; and personal communication with Rhys Leeming, 2003). Leeming *et al.* (1994, 1996 and 1997) and Sinton *et al.* (1998) have demonstrated that fecal sterols can be used to distinguish human and animal feces. Herbivores (e.g., sheep and cows) consume substantial amounts of plants enriched with C_{29} sterols (e.g., β -sitosterol and stigmasterol). Fecal matter released into the environment by herbivores are usually composed of considerable amounts of 24-ethylcoprostanol and 24-ethyl-epicoprostanol (Leeming *et al.*, 1997).

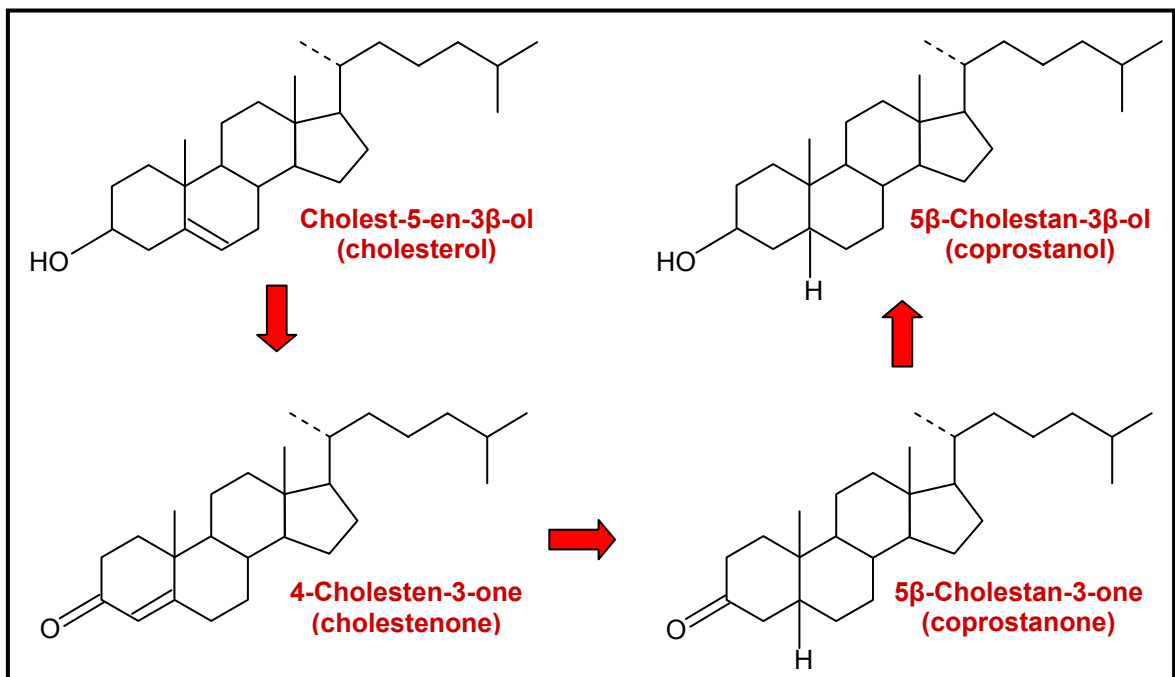


Fig. 4.4. Biohydrogenation of cholesterol to coprostanol in the human digestive tract (based on Björkhem and Gustafsson, 1971).

4.2.2 Fatty Alcohols in Marine Sediments

Fatty alcohols have been observed in marine sediments but have not been utilized to the same extent as fatty acids and aliphatic hydrocarbons (Mudge and Norris, 1997; Meyers, 2003). Organic matter derived from terrigenous or marine sources have been differentiated using fatty alcohols (Mudge and Norris, 1997; Mudge and Seguel, 1999; Meyer, 2003). In terrigenous plants, fatty alcohols (C_{22} to C_{30}) occur as wax esters in epicuticular waxes with an even-over-odd carbon preference (Grimalt and Albaigés, 1990; Mudge and Norris, 1997; Mudge and Seguel, 1999; Meyers, 2003). Leaf waxes are generally dominated by C_{24} , C_{26} , and C_{28} alcohols (Mudge and Norris, 1997; Fernandes *et al.*, 1999). Their primary function in terrigenous plant leaves is to retain water (Eglinton and Hamilton, 1967; Mudge and Norris, 1997; Mudge and Seguel, 1999).

Short chain fatty alcohols ($<C_{20}$) are associated with organic matter derived from aquatic algae and/or bacterial sources. It has been suggested that wax esters are synthesized by marine animals to serve as energy reserves during periods of food shortages (Lee and Hirota, 1976; Mudge and Norris, 1997). Fatty alcohols in marine wax esters are normally dominated by saturated alcohols (*i.e.*, $C_{14:0}$ and $C_{16:0}$) or monounsaturated alcohols (*e.g.*, $C_{16:1}$, $C_{18:1}$, $C_{20:1}$, and $C_{22:1}$) (Sargent *et al.*, 1977, 1981; Rajendran *et al.*, 1991; Mudge and Norris, 1997).

4.2.3 Fatty Acids in Marine Sediments

Fatty acids are ubiquitous in the environment and are common constituents in bacteria, microalgae, terrigenous plants, and marine plants (Volkman *et al.*, 1998; Mudge and Seguel, 1999; Meyers, 2003). They serve important roles in energy storage and are involved in the structure of cellular membranes (Ratledge and Wilkinson, 1988; Budge and Parrish, 1998). Two common applications of fatty acids include determination of the sources of organic matter and studying transformation processes (Budge and Parrish, 1998; Wakeham, 1999). Terrigenously derived fatty acids consist of long-chain monocarboxylic acids ($>C_{20:0}$; with an even-over-odd carbon preference), and are associated with epicuticular waxes of higher plants. Both n-alkanoic and n-alkenoic acids $<C_{20}$ (with an even-over-odd preference) have been used as indicators for planktonic and bacterial input (Grimalt and Albaigés, 1990; Saliot *et al.*, 1991; Budge and Parrish, 1998; Volkman *et al.*, 1998; Meyers, 2003).

The diverse range of fatty acid structures allow certain fatty acids to be used as markers for specific organisms (Budge and Parrish, 1998). Branched fatty acids, in particular iso- (i-) and anteiso- (ai-) $C_{15:0}$ and $C_{17:0}$, along with their corresponding unsaturated branched fatty acids are considered to be unique constituents of bacteria. Their occurrence in Recent sediments have been used as indications of bacterial activity (Cranwell, 1973; Saliot *et al.*, 1991; Budge and Parrish, 1998; Grimalt and Albaigés, 1990). Markers for planktonic input consist of mixtures of $C_{14:0}$, $C_{16:0}$, $C_{16:1\omega7}$, $C_{18:1\omega9}$, $C_{18:0}$, $C_{20:5\omega3}$, and $C_{22:6\omega3}$ fatty acids (Saliot *et al.*, 1991). Budge and Parrish (1998) have utilized the $C_{22:6\omega3}/C_{20:5\omega3}$

ratio to distinguish between dinoflagellates and diatoms, where $C_{22:6\omega3}/C_{20:5\omega3} > 1$ suggests the predominance of dinoflagellates and $C_{22:6\omega3}/C_{20:5\omega3} \ll 1$ is indicative of diatoms. Additional indicators of diatoms include the occurrence of $C_{16:4\omega1}$ (which is common in diatoms, but rare in other phytoplankton); an abundance of $C_{16:1}$ relative to $C_{16:0}$ (e.g., $C_{16:1}/C_{16:0} > 1.6$); and an abundance of C_{16} fatty acids relative to C_{18} fatty acids (i.e., $\Sigma C_{16(\text{saturated} + \text{unsaturated})}/\Sigma C_{18(\text{saturated} + \text{unsaturated})}$) (Saliot *et al.*, 1991; Mudge and Seguel, 1997; Budge and Parrish, 1998; Mudge and Seguel, 1999).

4.2.4 Hydrocarbons in Recent Sediments

Aliphatic hydrocarbons in Recent sediments are more resistant to microbial degradation than other types of organic matter and can be used to delineate source information. In studies, primarily around lakes, aliphatic hydrocarbons have been used to distinguish between sources of organic matter commonly found within lakes (e.g., algae, bacteria, and vascular plants) and vascular plants surrounding the lakes (Meyers, 2003). Marine phytoplankton and bacteria have hydrocarbons that maximize around C_{17} (Cranwell *et al.*, 1987; Mudge and Seguel, 1999; Meyers, 2003). Vascular plants, on the other hand, are dominated by longer chain n-alkanes with an odd-over-even predominance pattern (Cranwell, 1978; Santos *et al.*, 1994). The type of vascular plant can be differentiated based on alkane distributions. Submerged and floating macrophytes in lakes have n-alkanes that maximize around C_{21} , C_{23} , or C_{25}

(Cranwell, 1984; Ficken *et al.*, 2000; Meyers, 2003). Terrestrially derived vascular plants are dominated by C₂₇, C₂₉, and C₃₁ n-alkanes, where n-C₂₇ and n-C₂₉ are indicators for trees and n-C₃₁ is dominant in grasses (Meyers, 2003).

4.3 Results and Discussion

Free lipids were extracted from sediment samples taken from core MBH 54/2, from Kowloon Bay, in Victoria Harbour, Hong Kong. Procedures used to recover non-saponifiable and saponifiable fractions are discussed in Chapter 2. Samples were derivatized to produce trimethylsilyl ethers (for sterols, stanols, and alcohols) and methyl esters (for fatty acids), prior to analysis by gas chromatography-mass spectrometry. Identification of lipid components was based on mass spectra interpretation, comparison to published spectra, and retention times. The extractable lipids provide information that can be used to determine the sources of sedimentary organic matter and to infer environmental conditions. Identified lipids are discussed in the following sections. Sterol structures, spectra, chromatograms, and tables summarizing lipid ratios are located in **Appendix II, III, and IV**. Examples of fatty acid and alcohol structures can be found in Chapter 5, Fig. 5.2.

4.3.1 Sterols and Stanols

Sterols and stanols were detected in sediments from core MBH 54/2. This area in Kowloon Bay has received significant amounts of raw sewage and is thought to be highly anoxic. The downcore distribution of sterols and stanols is illustrated in **Fig. 4.5**. Sediments from the uppermost part of the core (**Fig. 4.5a**) were deposited after the sewage outfall in Hong Kong was converted to a submarine-type outfall and diverted further into the channel of Victoria Harbour. No significant amount of fecal sterols were identified at 0.5m, possibly suggesting that there were improvements in reducing sewage contamination in this part of the harbour. Cholesterol, cholestanol, brassicasterol, β -sitosterol, and stigmastanol were also identified at 0.5m.

Sediments deposited during a period of rapid population growth can be recognized by the chromatograms shown in **Figs. 4.5 b and c**. At the time sediments were deposited at 1.1m and 1.6m, raw sewage was discharged into the harbour via a seawall-type sewage outfall. Significant amounts of fecal sterols were observed in the extractable lipid fraction. Fecal material derived from human sewage waste is indicated by the occurrence of coprostanol. The isomer of coprostanol, epicoprostanol, is commonly used as a ratio with coprostanol as an indicator for the degree of sewage treatment (*i.e.* a higher epicoprostanol to coprostanol ratio would indicate that the majority of sewage is treated before being released into the environment) (McCalley *et al.*, 1981; Mudge and Seguel, 1999).

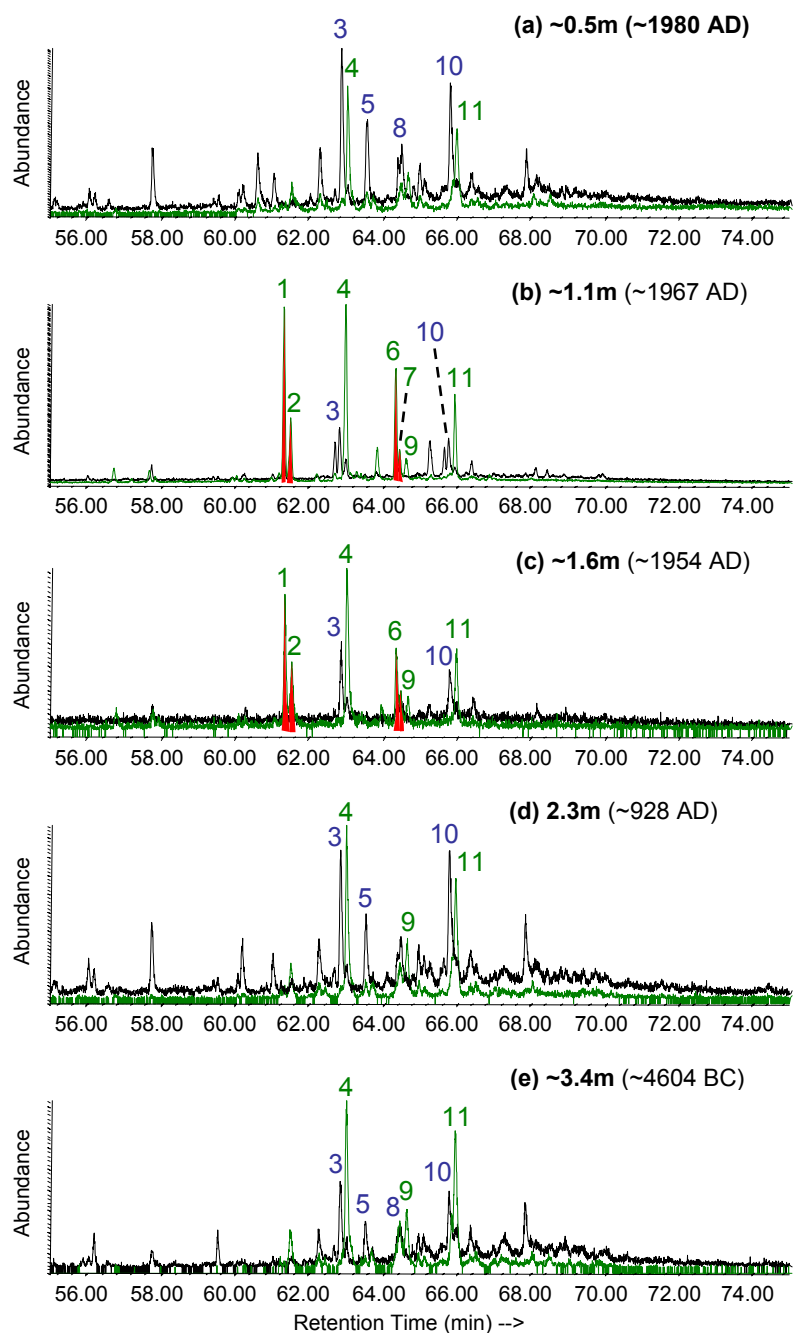


Fig. 4.5. Distribution of sterols and stanols in sediment samples from core MBH 54/2. (1) coprostanol; (2) epicoprostanol; (3) cholesterol; (4) cholestanol; (5) brassicasterol; (6) 24-ethylcoprostanol; (7) 24-ethylepicoprostanol; (8) campesterol; (9) ergostanol (campestanol); (10) β -sitosterol; (11) stigmasterol

The occurrence of epicoprostanol throughout the core is peculiar since there were no sewage treatment plants in Hong Kong during these periods. Bacterial populations in the human digestive tract preferentially mediate cholesterol to coprostanol, but not to epicoprostanol or cholestanol. The epicoprostanol in core MBH 54/2 was most likely produced by the anaerobic bacterial community within the sediments. Both coprostanol and epicoprostanol are more abundant than cholesterol at 1.1m and 1.6m (**Fig. 4.6a**). Similar to the human fecal sterols, 24-ethylcoprostanol and 24-ethylepicoprostanol (*i.e.*, fecal markers for herbivores) are more abundant than cholesterol at 1.1m and 1.6m.

Brassicasterol and campesterol were not detected at 1.1m or 1.6m (**Figs. 4.5 b, c; and Fig. 4.6b**). Brassicasterol is the major sterol in the algae Prymnesiophycean and is commonly used as a biomarker for diatoms (Volkman, 1986). Campesterol is widespread in vascular plants (Mudge and Seguel, 1999), but has also been observed in green algae and marine invertebrates (Goad and Akihisa, 1997). Both brassicasterol and campesterol were only observed at 0.5m, 2.3m, and 3.4m (**Figs. 4.5 b, d, and e**). Depth intervals around 2.3m and 3.4m represent periods when Victoria Harbour was not affected by sewage waste; around 0.5m the sewage was diverted away from the study site. The diminished sewage contamination appears to have improved conditions, allowing marine organisms to bloom.

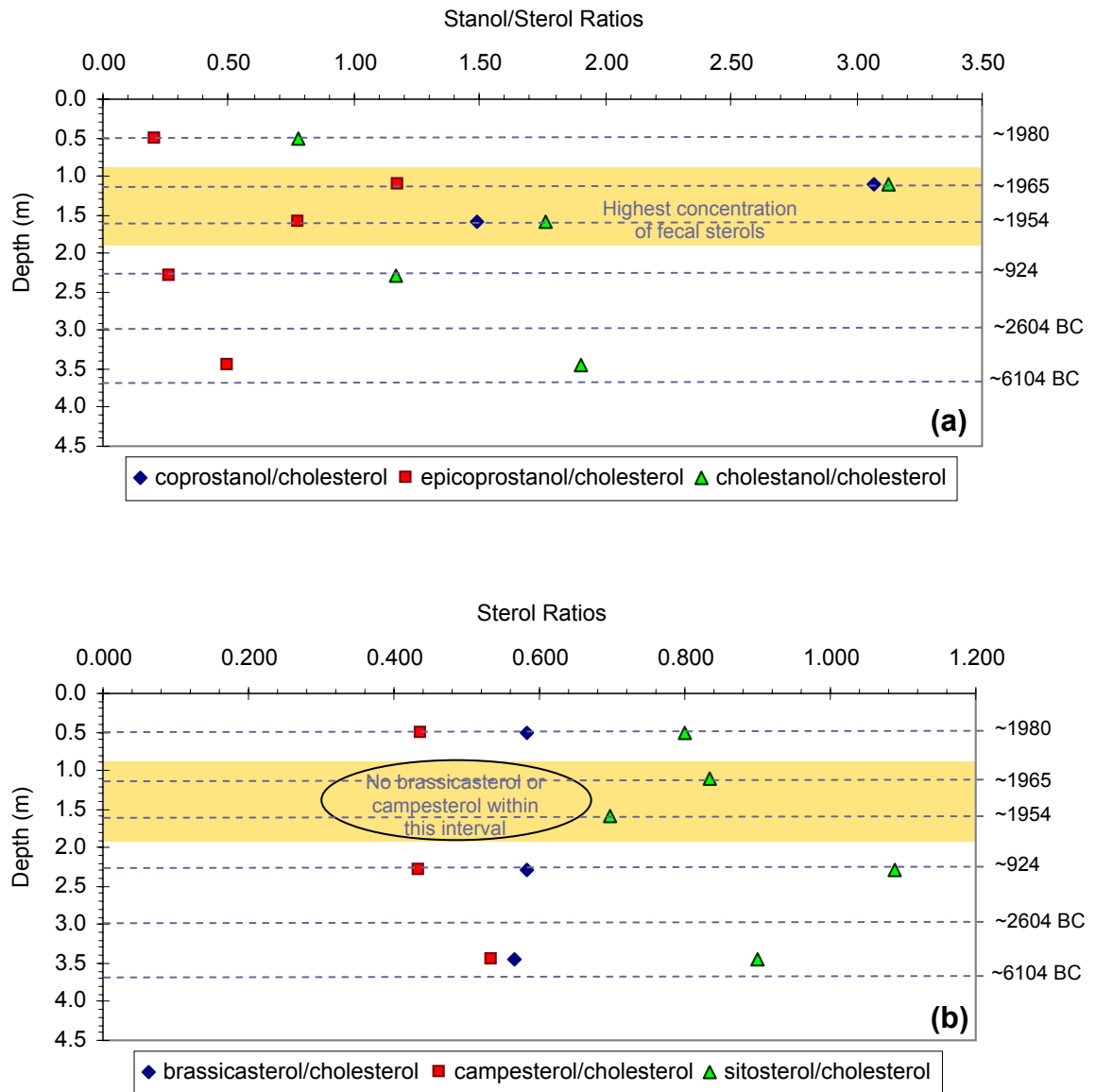


Fig. 4.6. Stanol and sterol ratios in sediment samples from core MBH 54/2.

Cholestanol and campestanol increase downcore (between 1.0m and 2.0m) relative to their corresponding sterols. The ratios of cholestanol/cholesterol and campestanol/campesterol show similar patterns downcore (**Fig. 4.7**). These stanols are likely derived from the hydrogenation of their corresponding sterols (Gaskell and Eglinton, 1975; Nishumira and Koyama, 1977; Pinturier-Geiss *et al.*, 2002). Gaskell and Eglinton (1975) have observed, and demonstrated experimentally with radiolabelled sterols, that sterols undergo rapid hydrogenation in anoxic Recent sediments. Gagosian *et al.* (1980) noted that while anaerobic conditions inhibit sterol degradation, sterol to stanol reduction is accelerated. At depth intervals between 1.0m and 2.0m, the study site received substantial amounts of raw sewage, which probably resulted in highly anoxic conditions. Between 2.0m and 3.0m, Kowloon Bay was an open bay and did not receive significant amounts of raw sewage. Conditions during this period may have been less anoxic resulting in the decrease in stanol/sterol ratios observed in **Fig. 4.7**. The slight increase in stanol/sterol ratio at 3.4m suggests a shift towards slightly more anoxic conditions.

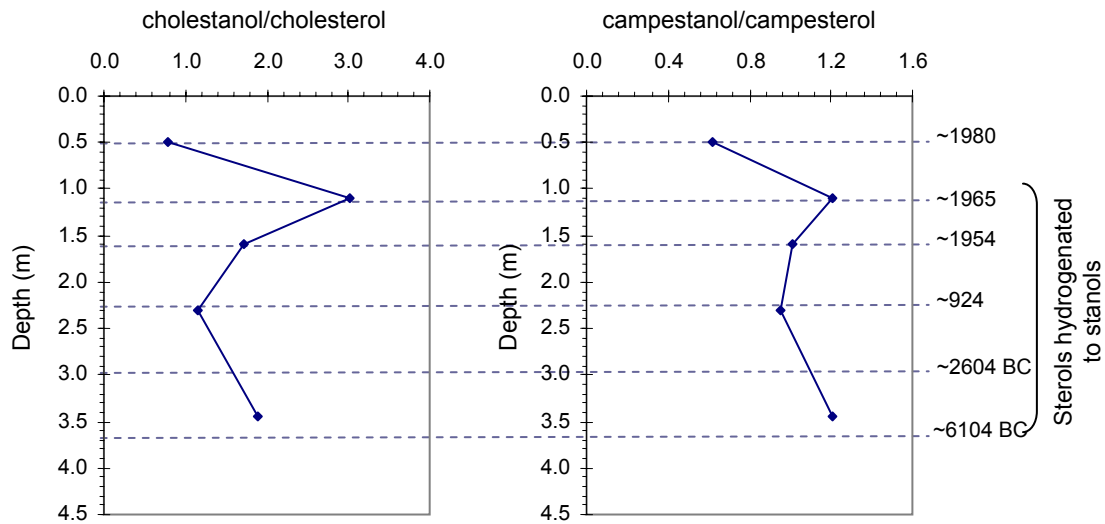


Fig. 4.7. Hydrogenation of sterols to stanols in sediments deposited in Kowloon Bay.

4.3.2 Fatty Acids

Free n-alkanoic acids were identified in both saponifiable and non-saponifiable fractions. In the saponifiable fraction (**Fig. 4.8**), n-alkanoic acids were distributed between $C_{12:0}$ and $C_{34:0}$, with a distinct even-over-odd predominance pattern (average CPI=7.8). A slightly higher even preference is observed at depths of 1.1m (CPI=10.4) and 1.6m (CPI=9.5). Throughout the core, a bimodal distribution is observed, with short chain n-alkanoic acids predominating over long chain n-alkanoic acids. The short chain n-alkanoic acids maximize at n- $C_{16:0}$, and long chain n-alkanoic acids at n- $C_{30:0}$ around 1.1m and n- $C_{22:0}$ or n- $C_{24:0}$ at all other depths. Short-chain n-alkanoic acids (<n- $C_{20:0}$) are

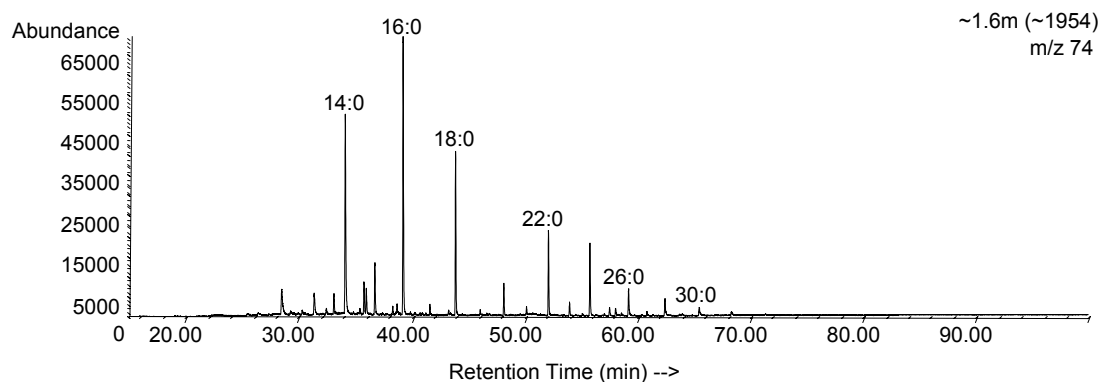
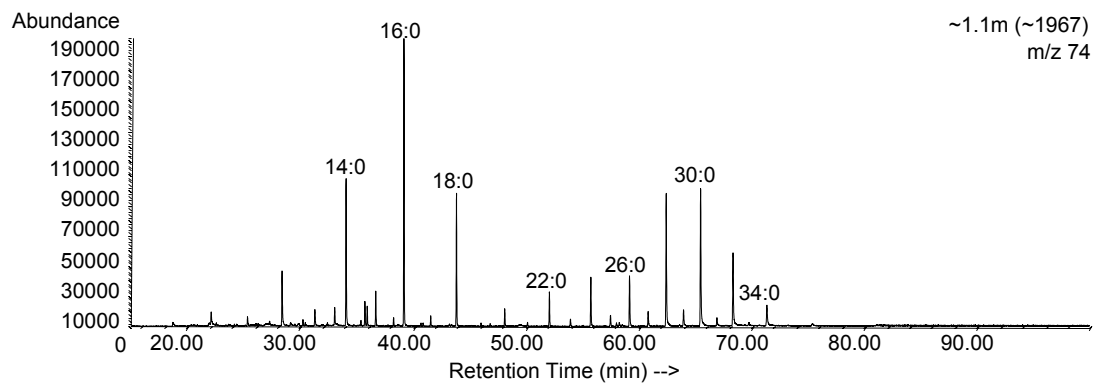


Fig. 4.8. n-Alkanoic acids (as methyl esters) in the saponifiable fraction of extractable lipids from two depth intervals in core MBH 54/2.

attributed to planktonic and bacterial input, whereas longer chain alkanolic acids (>n-C_{20:0}) originate from the cuticular waxes of terrigenous plant material (Grimalt and Albaigés, 1990).

A plot of the aquatic-to-terrigenous ratio (*i.e.*, short-chain to long-chain alkanolic acids; *e.g.*, $\Sigma(C_{12:0}-C_{18:0})/\Sigma(C_{22:0}-C_{28:0})$) downcore illustrates a higher aquatic input from the surface down to 1.6m ($\Sigma(C_{12:0}-C_{18:0})/\Sigma(C_{22:0}-C_{28:0}) > 1.5$). At depths below 2.3m, terrigenous plant material are more abundant than

aquatically-derived organic matter (**Fig. 4.9a**; $\Sigma(C_{12:0}-C_{18:0})/\Sigma(C_{22:0}-C_{28:0}) \leq 1$). Iso- and anteiso- alkanolic acids ($C_{13:0}$, $C_{15:0}$, and $C_{17:0}$) have been used as indicators of bacterial activity. The most abundant branched acids are *i*- and *ai*- $C_{15:0}$, where *i*- $C_{15:0}$ dominates over *ai*- $C_{15:0}$ downcore (avg *i*-/*ai*- $C_{15:0}$ ratio =1.2). Aside from indicating the presence of bacteria, the branched fatty acids identified in the free lipid fraction provide limited information about the bacteria types.

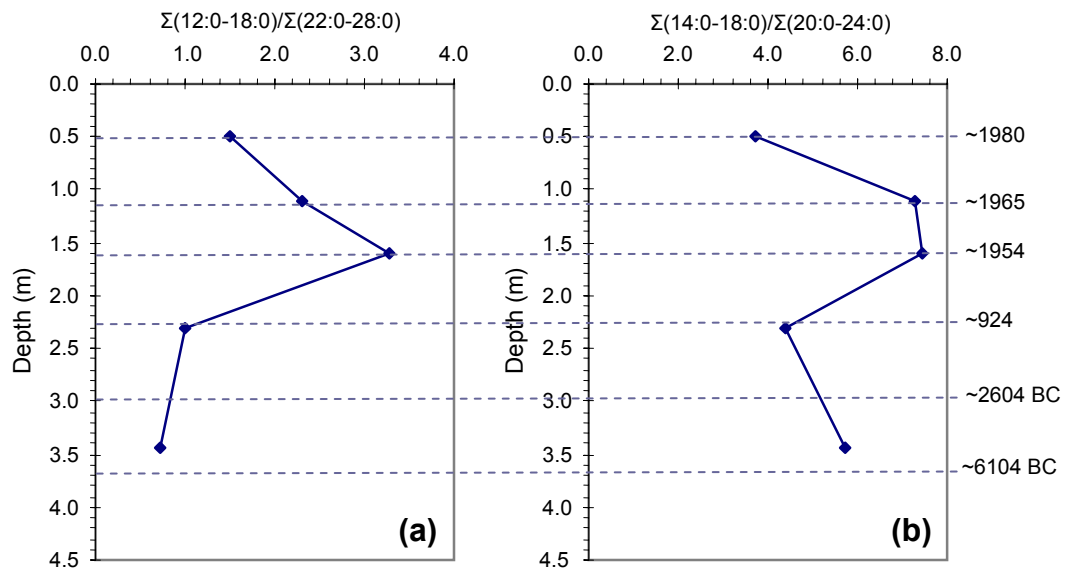


Fig. 4.9. Aquatic-to-Terrigenous ratio for free n-alkanoic acids in the (a) saponifiable and (b) non-saponifiable fractions. Short-chain alkanolic acids are typically more abundant than long-chain alkanolic acids, and are attributed to planktonic and bacterial input. A greater abundance of short-chain acids is observed at 1.1m and 1.6m.

Alkenoic acids ($C_{16:1}$ and $C_{18:1}$) were only observed in the upper 1.6m, and are present in low abundance relative to their corresponding *n*-alkanoic acids. Two peaks in the chromatograms were identified as C_{18} alkenoic acids with 1-degree of unsaturation (the location of the double bond was not determined). The $C_{16:1}/C_{16:0}$ and $\Sigma C_{18:1}/C_{18:0}$ ratios are lowest at 1.1m (0.006 and 0.018, respectively), and highest at 1.6m ($C_{16:1}/C_{16:0}=0.41$) and 0.5m ($\Sigma C_{18:1}/C_{18:0}=0.065$). The ratio of $C_{16:1}/C_{16:0}$ has been used to measure the predominance of diatoms in sediments (Saliot *et al.* 1991; Santos *et al.*, 1994; Budge and Parrish, 1998; Mudge and Seguel, 1999; Azevedo, 2003; Burns *et al.*, 2003) whereas $C_{18:1}$ is commonly used as an indicator for zooplankton (Santos *et al.*, 1994; Azevedo, 2003; Burns *et al.*, 2003). $C_{16:1}$ and $C_{18:1}$, however, have also been observed in certain species of sulfate-reducing bacteria (Edlund *et al.*, 1985; Wilkinson, 1988), which may be the primary source of these acids in sediments from Kowloon Bay.

Free *n*-alkanoic acids in the non-saponifiable fraction had carbon number distributions between *n*- $C_{14:0}$ to *n*- $C_{26:0}$ with an even carbon number preference (**Fig. 4.10**). CPI typically ranged between 7.0 and 9.6, except at 1.6m, where a more pronounced even preference is observed (CPI=15.9). Short-chain alkanolic acids (<*n*- $C_{20:0}$) are present at significantly higher abundance than long-chain alkanolic acids (>*n*- $C_{20:0}$), and typically show a high aquatic-to-terrigenous ratio ($(\Sigma(C_{14:0}-C_{18:0}))/\Sigma(C_{20:0}-C_{24:0}) >3.5$) downcore. Aquatic input is significantly higher between 1.1m and 1.6m, where the average aquatic/terrigenous ratio is 7.3 (**Fig. 4.9b**).

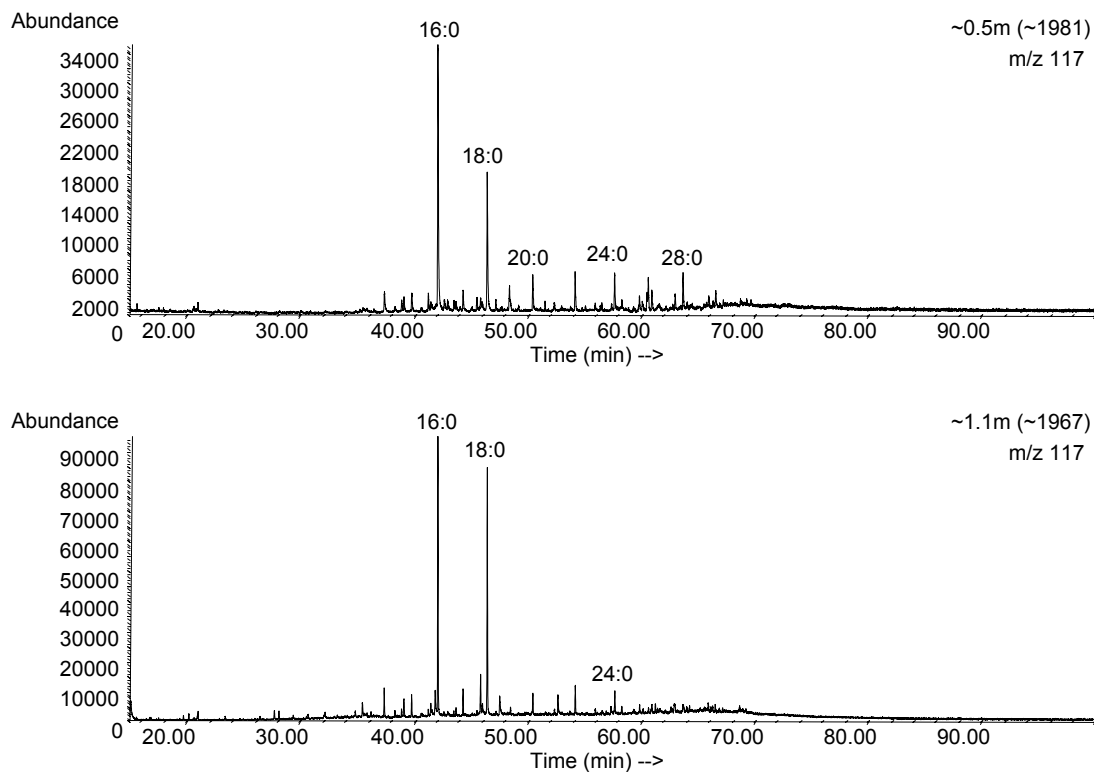


Fig. 4.10. n-Alkanoic acids (as trimethylsilyl ethers) in the non-saponifiable fraction of extractable lipids from two depth intervals in core MBH 54/2.

Monounsaturated fatty acids ($C_{16:1}$ and $C_{18:1}$) in the non-saponifiable fraction are more abundant than in the saponifiable fraction. Ratios of $C_{16:1}/C_{16:0}$ and $\Sigma C_{18:1}/C_{18:0}$ are significantly higher at a depth of 1.6m (0.07 and 0.3, respectively). $C_{16:1}$ is not observed in the non-saponifiable fraction below 2.3m. *i*- and *ai*- $C_{15:0}$ and $C_{17:0}$ are observed downcore with greater abundance of *i*- and *ai*- $C_{15:0}$. At all depths, *ai*- $C_{15:0}$ is more abundant than *i*- $C_{15:0}$ (where *i*-/*ai*- $C_{15:0}$ range between 0.5-0.8), except 2.3m (where *i*-/*ai*- $C_{15:0}$ =1.1), possibly indicating the presence of

the sulfate reducing bacteria *D. gigas* (Vainshtein *et al.*, 1992). The ratio of *i-ai-C*_{17:0} in the non-saponifiable fraction demonstrates a very similar pattern to that observed in the saponifiable fraction. In both fractions, *i-ai-C*_{17:0} ratio is about 1.1 at depths of 0.5m and 1.6m. At all other depths, the *i-ai-C*_{17:0} ratio ranges between 0.7-0.9. *i-* and *ai-C*_{17:0} are markers for sulfate reducing bacteria and other anaerobic bacteria (Rajendran *et al.*, 1992a and b).

4.3.3 Alcohols

Free *n*-alcohols (C₁₄ to C₃₂) in the non-saponifiable fraction (**Fig. 4.11**) have an even carbon-number preference downcore. Short-chain *n*-alcohols (C₁₄-C₂₀) represent a minor source of alcohols and may originate from zooplankton or other marine invertebrates (Grimalt and Albaigés, 1990). The long-chain *n*-alcohols (C₂₂-C₃₂) are more abundant and suggest cuticle waxes of terrigenous plant material (Grimalt and Albaigés, 1990; Santos *et al.*, 1994; Mudge and Norris, 1997; Mudge and Seguel, 1999) are more important sources of alcohols in these sediments. The aquatic-to-terrigenous ratio (C₁₈/C₂₈ <1) supports the idea that terrestrial plants are the primary source of alcohols in Kowloon Bay. In general, the aquatic-to-terrigenous ratio ranged between 0.4 and 0.6, except at 1.1m where alcohols were dominated by C₂₈, C₃₀, and C₃₂ (**Fig. 4.12**). The C₁₆-C₂₆ alcohols were only present as very small peaks, near the baseline of the chromatogram, in sediments around 1.1m. At 1.6m, the alcohols may have been degraded, although C₁₆, C₁₈, C₂₈, and C₃₀ alcohols were still identifiable.

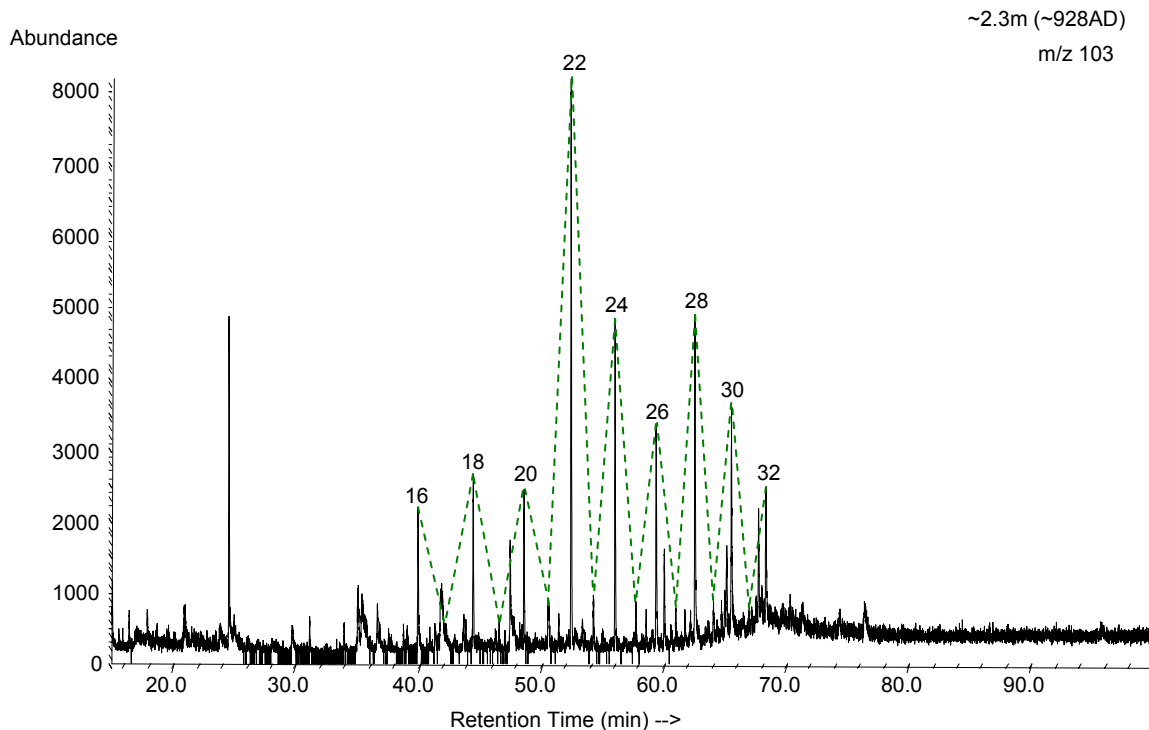


Fig. 4.11. Fatty alcohols (as trimethylsilyl ethers) in the non-saponifiable fraction of extractable lipids, from core MBH 54/2 (CPI~8).

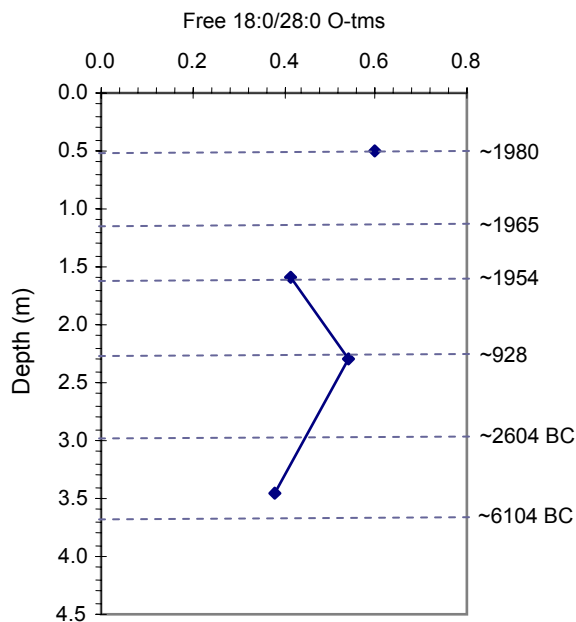


Fig. 4.12. Aquatic-to-Terrigenous ratio for free fatty alcohols. Downcore distribution indicates cuticle waxes of higher plants are the primary source for alcohols.

4.3.4 Hydrocarbons

A distinct odd-over-even preference is observed for n-alkanes (n-C₁₈ to n-C₃₇) at all depths (**Fig. 4.13**). CPI values for n-alkanes ranged between 2.2 and 3.0, except at 1.1m and 1.6m where CPI was about 1.2. The distinct odd predominance suggests that the free n-alkanes were most likely derived from biotic hydrocarbons rather than petroleum hydrocarbons. The aquatic-to-terrigenous ratio for free n-alkanes (n-C₁₉/n-C₃₁) ranged between 0.1 to 0.2, except at 1.1m and 1.6m where n-C₁₉/n-C₃₁ was about 0.6 (**Fig. 4.14a**). n-Alkanes in sediments around 1.1m and 1.6m were partially degraded, as was observed for n-alcohols at these depths. Cuticle waxes of higher plants appear to be the primary contributors of n-alkanes and can be further subdivided into those derived from terrigenous plants (maximum at n-C₂₉ and n-C₃₁) and macrophyte plant material (n-C₂₃ and n-C₂₅) (Ficken *et al.*, 2000; Filley *et al.*, 2001; Silliman and Schelske, 2003). Proxy ratios based on mid-chain (C₂₃, C₂₅) to long chain (C₂₉, C₃₁) n-alkanes have been used to distinguish between macrophyte and terrigenous plant input (Ficken *et al.*, 2000; Filley *et al.*, 2001; Silliman and Schelske, 2003). The downcore profile of this proxy shows a slight increase at 1.1m and 1.6m (0.8 and 1.0, respectively). All other depths appear to be dominated by free n-alkanes derived from terrigenous plants based on the (C₂₃+C₂₅)/(C₂₉+C₃₁) ratio between 0.3 to 0.6 (**Fig. 4.14b**). Fisher *et al.* (2003) have used the mean carbon number (MC#) parameter ($\frac{\sum([C_i] \cdot C_i)}{\sum[C_i]}$, where [C_i] is the amount of n-alkane with carbon number C_i, and C_i ranges between C₂₇-C₃₁) to reflect slight changes in vegetation. Grasses are dominated by C₃₁ n-alkanes,

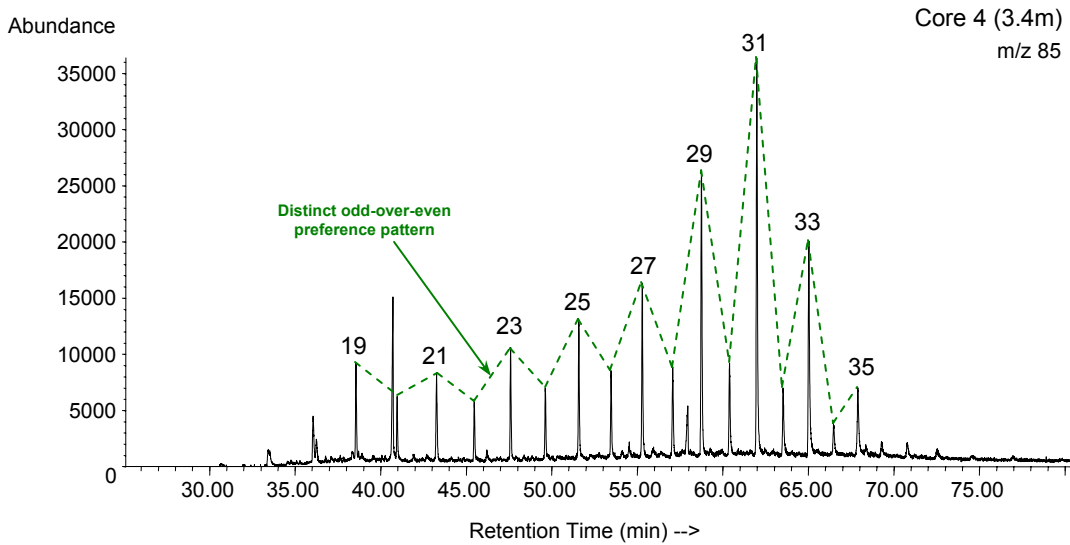


Fig. 4.13. n-Alkane distribution in the extractable lipid fraction from core MBH 54/2, illustrating a pronounced odd-over-even predominance pattern (CPI ~ 3.0).

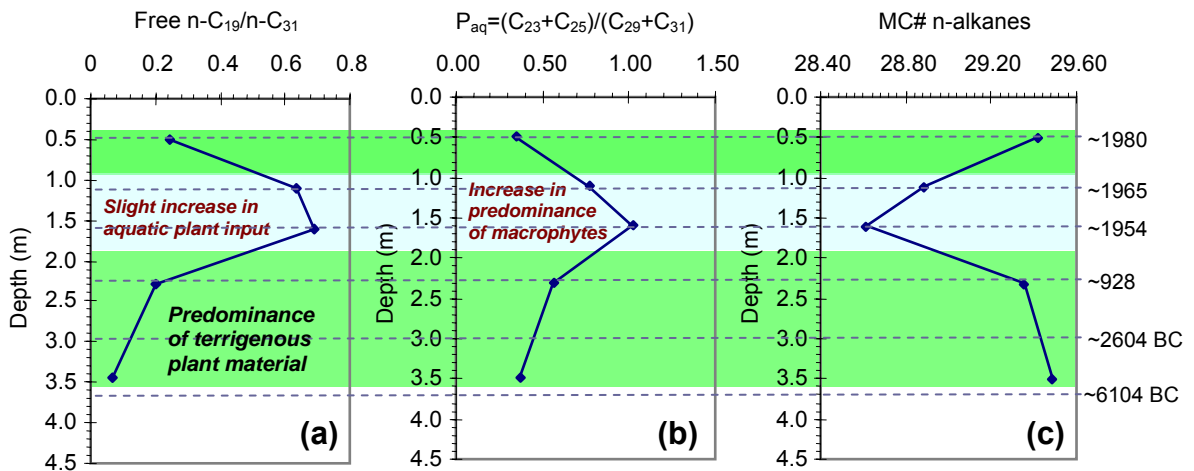


Fig. 4.14. (a) Aquatic-to-Terrigenous ratio for free n-alkanes; (b) Downcore profile illustrating shifts in predominance of macrophyte versus terrigenous plant material; (c) Downcore shifts in vegetation type, based on the mean carbon number ranging between C_{27} - C_{31} .

while trees tend to contribute leaves with significant amounts of C₂₇ and C₂₉ n-alkanes (Cranwell, 1973; Fisher *et al.*, 2003; Meyers, 2003). A plot of the MC# downcore shows a shift from 29.4 to about 28.7 between 1.1m and 1.6m (**Fig. 4.14c**). The shift towards a MC# of 28.7 is due to a decrease in the C₃₁ n-alkane compared to C₂₇ and C₂₉. Less grass and possibly more terrestrial plant leaves were transported into Kowloon Bay between 1.1m and 1.6m. This may support the idea of storms transporting higher plant material into this area, indicated by a spike in the C/N ratio around 1.4m (discussed in Chapter 3).

4.4 Summary Remarks

Extractable lipids in core MBH 54/2, Kowloon Bay, are comprised of sterols, fatty alcohols, fatty acids, and hydrocarbons. Each of these lipid groups (*i.e.*, the lipid composition and profile) provide information that allow the sources of sedimentary organic matter to be determined, and to also infer conditions and transformation processes that may have occurred. Stanols were more abundant than their corresponding sterols suggesting that the sterols had been hydrogenated to stanols under anaerobic conditions.

Significant amounts of fecal sterols (*i.e.*, coprostanol, epicoprostanol, 24-ethylcoprostanol, and 24-ethylepicoprostanol) were identified in the upper 2m of the core, maximizing at 1.1m and 1.6m. These depth intervals correspond to periods of rapid population growth in Hong Kong and also during a time when

raw sewage was disposed directly over the sample site via seawall-type sewage outfall. Of the fecal sterols extracted, coprostanol (a marker for human feces) was most abundant. 24-Ethylcoprostanol, a lipid marker for herbivores (e.g., cows and sheep), was also very abundant in the sediment. The occurrence of epicoprostanol in the sediments was unusual since it has only been observed in treated sewage. Microbes in the human intestine are not known to be able to hydrogenate cholesterol to epicoprostanol and no direct evidence of bacteria mediating cholesterol to epicoprostanol has been documented in the literature. Since sewage treatment plants were not operating in Hong Kong when epicoprostanol was detected in the sediments, it is proposed that the microbes in the anaerobic sediments were probably responsible for transforming cholesterol to epicoprostanol.

n-Alkanoic acids were identified in both saponifiable and non-saponifiable fractions of extractable lipids. A bimodal distribution of even carbon numbered n-alkanoic acids ($C_{12:0}$ to $C_{34:0}$) were detected in the saponifiable lipid fraction. The short chain components ($<C_{20:0}$) are attributed to bacterial and/or planktonic input, and the long chain components ($>C_{20:0}$) are associated with cuticular waxes of terrigenous plants. Iso- and anteiso-alkanoic acids ($C_{13:0}$, $C_{15:0}$, and $C_{17:0}$) were identified in the sediments and are used as general markers for bacteria. In the non-saponifiable fraction, n-alkanoic acids ranged between $C_{14:0}$ to $C_{26:0}$. However, $C_{16:0}$ and $C_{18:0}$ were dominant in each of the samples.

n-Alcohols ranged between C_{14} and C_{32} , with an even carbon preference. The longer chain n-alcohols (C_{22} to C_{32}) were more abundant throughout the core,

suggesting that terrigenous plants are the primary source of alcohols in Kowloon Bay. n-Alkanes ranged between C₁₈ and C₃₇, with distinct odd carbon preference. The n-alkanes are derived from a biotic source where cuticular waxes of terrigenous plants (e.g., terrestrial plant leaves and grasses) are the likely contributors.

4.5 References

- Azevedo, D. A., 2003. A preliminary investigation of the polar lipids in Recent tropical sediments from aquatic environments at Campos do Goytacazes, Brazil. *Journal of the Brazilian Chemical Society*, 14, 97-106.
- Björkhem, I., Gustafsson, J. A., 1971. Mechanisms of microbial transformation of cholesterol into coprostanol. *European Journal of Biochemistry*, 21, 428-432.
- Budge, S. M., Parrish, C. C. 1998. Lipid biogeochemistry of plankton, settling matter and sediments in Trinity Bay, Newfoundland. II. Fatty acids. *Organic Geochemistry*, 29, 1547-1559.
- Burns, K. A., Volkman, J. K., Cavanagh, J., Brinkman, D., 2003. Lipids as biomarkers for carbon cycling on the northwest shelf of Australia: results from a sediment trap study. *Marine Chemistry*, 80, 103-128.
- Cranwell, P. A., 1973. Branched-chain and cyclopropanoid acids in a recent sediment. *Chemical Geology*, 11, 307-313.
- Cranwell, P. A., 1978. Extractable and bound lipid components in a freshwater sediment. *Geochimica et Cosmochimica Acta*, 42, 1523-1532.
- Cranwell, P. A., 1984. Lipid geochemistry of sediments from Upton Broad, a small productive lake. *Organic Geochemistry*, 7, 25-37.
- Cranwell, P. A., 1990. Paleolimnological studies using sequential lipid extraction from recent lacustrine sediment: recognition of source organisms from biomarkers. *Hydrobiologia*, 23, 293-303.

- Cranwell, P. A., Eglinton, G., Robinson, N., 1987. Lipids of aquatic organisms as potential contributors to lacustrine sediments – II. *Organic Geochemistry*, 11, 513-527.
- Edlund, A., Nichols, P. D., Roffey, R., White, D. C., 1985. Extractable and lipopolysaccharide fatty acid and hydroxyl acid profiles from *Desulfovibrio* species. *Journal of Lipid Research*, 26, 982-988.
- Eglinton, G., Hamilton, R. J., 1967. Leaf epicuticular waxes. *Science*, 156, 1322-1335.
- Fernandes, M. B., Elias, V. O., Cardoso, J. N., Carvalho, M. S., 1999. Sources and fate of n-alkanols and sterols in sediments of the Amazon Shelf. *Organic Geochemistry*, 30, 1075-1087.
- Ficken, K. J., Li, B., Swain, D. L., Eglinton, G., 2000. An n-alkane proxy for the sedimentary input of submerged/floating freshwater aquatic macrophytes. *Organic Geochemistry*, 31, 745-749.
- Filley, T. R., Freeman, K. H., Bianchi, T. S., Baskaran, M., Colarusso, L. A., Hatcher, P. G., 2001. An isotopic biogeochemical assessment of shifts in organic matter input to Holocene sediments from Mud Lake, Florida. *Organic Geochemistry*, 32, 1153-1167.
- Fisher, E., Oldfield, F., Wake, R., Boyle, J., Appleby, P., Wolff, G. A., 2003. Molecular marker records of land use change. *Organic Geochemistry*, 34, 105-119.
- Fukushima, K., Kondo, H., Sakata, S., 1992a. Geochemistry of hydroxyl acids in sediments – I. Some freshwater and brackish water lakes in Japan. *Organic Geochemistry*, 18, 913-922.
- Fukushima, K., Uzaki, M., Sakata, S., 1992b. Geochemistry of hydroxyl acids in sediments: I. Freshwater and brackish water lake in Japan. *Organic Geochemistry*, 18, 923-932.
- Gagosian, R. B., Smith, S. O., Lee, C., Farrington, J. W., Frew, N. M., 1980. Steroid transformations in Recent marine sediments. In: Douglass A. C., Maxwell, J. R. (Eds), *Advances in Organic Geochemistry 1979*, Pergamon Press, Oxford, 407-419.
- Gaskell, S. J., Eglinton, G., 1975. Rapid hydrogenation of sterols in a contemporary lacustrine sediment. *Nature*, 254, 209-211.
- Goad, L. J., Akihisa, T., 1997. *Analysis of Sterols*, Blackie Academic and Professional, Chapman Hall, London, 437p.

Gogou, A., Stephanou, E. G., 2004. Marine organic geochemistry of the Eastern Mediterranean: 2. Polar biomarkers in Cretan Sea surficial sediments. *Marine Chemistry*, 85, 1-25.

Goosens, H., Rijpstra, W. I. C., Düren, R. R., de Leeuw, J. W., 1986. Bacterial contribution to sedimentary organic matter; a comparative study of lipid moieties in bacteria and Recent sediments. *In: Leythäeuser, D., Rullkötter, J. (Eds), Advances in Organic Geochemistry 1985*. Pergamon Press, Oxford. *Organic Geochemistry*, 10, 683-696.

Goosens, H., de Leeuw, J. W., Rijpstra, W. I. C., Meyburg, G. J., Schenck, P. A., 1989a. Lipids and their mode of occurrence in bacteria and sediments – I. A methodological study of the lipid composition of *Acinetobacter calcoeticus* LMD 79-41. *Organic Geochemistry*, 14, 15-25

Goosens, H., Düren, R. R., de Leeuw, J. W., Schenck, P. A., 1989b. Lipids and their mode of occurrence in bacteria and sediments – II. Lipids in the sediment of a stratified, freshwater lake. *Organic Geochemistry*, 14, 27-41.

Grimalt, J. O., Albaigés, J., 1990. Characterization of the depositional environments of the Ebro Delta (Western Mediterranean) by the study of sedimentary lipid markers. *Marine Geology*, 95, 207-224.

Huang, W. -Y., Meinschein, W. G., 1979. Sterols as ecological indicators. *Geochimica et Cosmochimica Acta*, 43, 739-745.

Killops, S. D., Killops, V. J., 1993. *An Introduction to Organic Geochemistry*, Longman Scientific & Technical and John Wiley & Sons, Inc, New York, 248p.

Killops, S. D., Killops, V. J., 2005. *An Introduction to Organic Geochemistry 2nd ed.*, Blackwell Publishing, Oxford, 393p.

Lee, R. F., Hirota, J., 1976. Wax esters in tropical zooplankton and nekton and the geographical distribution of wax esters in marine copepods. *Limnology and Oceanography*, 18, 227-239.

Leeming, R., Ball, A., Ashbolt, N. J., Jones, G., Nichols, P., 1994. Distinguishing between human and animal sources of faecal pollution. *Chemistry in Australia Waters (supplement)*, 434-435.

Leeming, R., Ball, A., Ashbolt, N. J., Nichols, P., 1996. Using faecal sterols from humans and animals to distinguish faecal pollution in receiving waters. *Water Research*, 30, 2893-2900.

- Leeming, R., Latham, V., Rayner, M., Nichols, P., 1997. Detecting and distinguishing sources of sewage pollution in Australian inland and coastal waters and sediments. *ACS Symposium Series*, 671, 306-319.
- Mackenzie, A. S., Brassell, S. C., Eglinton, G., Maxwell, J. R., 1982. Chemical fossils: The geological fate of steroids. *Science*, 217, 491-504.
- McCalley, D. V., Cooke, M., Nickless, G., 1981. The effect of sewage treatment on fecal sterols. *Water Research*, 15, 1019-1025.
- Meyers, P. A., 2003. Applications of organic geochemistry to paleolimnological reconstructions: a summary of examples from the Laurentian Great Lakes. *Organic Geochemistry*, 34, 261-289.
- Meyers, P. A., Ishiwatari, 1993. The early diagenesis of organic matter in lacustrine sediments. In: Engel, M. H., Macko, S. A. (Eds), *Organic Geochemistry: Principles and Applications*, Plenum Press, New York, 185-209.
- Mudge, S. M., Norris, C. E. 1997. Lipid biomarkers in the Conwy Estuary (North Wales, UK): a comparison between fatty alcohols and sterols. *Marine Chemistry*, 57, 61-84.
- Mudge, S. M., Seguel, C. G., 1997. Trace organic contaminants and lipid biomarkers in Concepcion and San Vicente Bays. *Boletín de la Sociedad Chilena de Química*, 42, 5-15.
- Mudge, S. M., Seguel, C. G., 1999. Organic contamination of San Vicente Bay, Chile. *Marine Pollution Bulletin*, 38, 1011-1021.
- Mudge, S. M., Bebianno, M. J. A. F., East, J. A., Barreira, L. A., 1999. Sterols in the Rio Formosa Lagoon, Portugal. *Water Research*, 33, 1038-1048.
- Muri, G., Wakeham, S. G., Pease, T. K., Faganeli, J., 2004. Evaluation of lipid biomarkers as indicators of changes in organic matter delivery to sediments from Lake Planina, a remote mountain lake in NW Slovenia. *Organic Geochemistry*, 35, 1083-1093.
- Nichols, P. D., Leeming, R., 1991. Tracing sewage in the marine environment. *Chem. Aust.*, 58, 274-276.
- Nishumira, M., Koyama, T., 1977. The occurrence of stanols in various living organisms and the behavior of sterols in contemporary sediments. *Geochimica et Cosmochimica Acta*, 41, 379-385.

- Pinturier-Geiss, L., Mejanelle, L., Dale, B., Karlsen, D. A., 2002. Lipids as indicators of eutrophication in marine coastal sediments., *Journal of Microbiological Methods*, 48, 239-258.
- Rajendran, N., Fujiyoshi, E., Matsuda, O., 1991. Fatty acids and fatty alcohols of zooplankton from coastal upwelling area of Hyuga Nada, Japan. *Bulletin of the Japanese Society of Fisheries*, 57, 2277-2284.
- Rajendran, N., Matsuda, O., Urushigawa, Y., 1992a. Distribution of polar lipid fatty acid biomarkers for bacteria in sediments of a polluted bay. *Microbios*, 72, 143-152.
- Rajendran, N., Suwa, Y., Urushigawa, Y., 1992b. Microbial community structure in sediments of a polluted bay as determined by phospholipid ester-linked fatty acids. *Marine Pollution Bulletin*, 24, 305-309.
- Ratledge, C., Wilkinson, S. G., 1988. An overview of microbial lipids. *In: Ratledge, C., Wilkinson, S. G. (Eds), Microbial Lipids Vol. 1, Academic Press, London, 3-22.*
- Readman, J. W., Preston, M. R., Mantoura, R. F. C., 1986. An integrated technique to quantify sewage, oil and PAH pollution in estuarine and coastal environments. *Marine Pollution Bulletin*, 17, 298-308.
- Rullkötter, J., 2000. Organic matter: The driving force for early diagenesis. *In: Schulz, H. D., Zabel, M. (Eds), Marine Geochemistry, Springer-Verlag, Berlin, 129-172.*
- Saliot, A., Laureillard, J., Scribe, P., Sicre, M. A., 1991 Evolutionary trends in the lipid biomarker approach for investigating the biogeochemistry of organic matter in the marine environment. *Marine Chemistry*, 36, 233-248.
- Santos, V., Billett, D. S. M., Rice, A. L., Wolff, G. A., 1994. Organic matter in deep-sea sediments from the Porcupine Abyssal Plain in the northeast Atlantic Ocean. I – Lipids. *Deep Sea Research I.*, 41, 787-819.
- Sargent, J. R., Gatten, R. R., Henderson, R. J., 1981. Marine wax esters. *Pure Applied Chemistry*, 53, 867-871.
- Sargent, J. R., Gatten, R. R., McIntosh, R., 1977. Wax esters in the marine environment – their occurrence, formation, transformation and fates. *Marine Chemistry*, 5, 573-584.
- Silliman, J. E., Schelske, C. L., 2003. Saturated hydrocarbons in the sediments of Lake Apopka, Florida, *Organic Geochemistry*, 34, 253-260.

- Sinton, L. W., Finlay, R. K., Hannah, D. H., 1998. Distinguishing human from animal faecal contamination in water: a review. *New Zealand Journal of Marine and Freshwater Research*, 32, 323-348.
- Smallwood, B. J., Wolff, G. A., 2000. Molecular characterization of organic matter in sediments underlying the oxygen minimum zone at the Oman Margin, Arabian Sea. *Deep Sea Research II*, 47, 353-375.
- Vainshtein, M., Hippe, H., Kroppenstedt, R. M., 1992. Cellular fatty acid composition of *Desulfovibrio* species and its use in classification of sulfate-reducing bacteria. *Systematics of Applied Microbiology*, 15, 554-566.
- Volkman, J. K., 1986. A review of sterol markers for marine and terrigenous organic matter. *Organic Geochemistry*, 9, 83-99.
- Volkman, J. K., Barrett, S. M., Blackburn, S. I., Mansour, M. P., Sikes, E. L. Gelin, F., 1998. Microalgal biomarkers: a review of recent research developments. *Organic Geochemistry*, 29, 1163-1179.
- Wakeham, S. G., 1999. Monocarboxylic, dicarboxylic and hydroxyl acids released by sequential treatments of suspended particles and sediments of the Black Sea. *Organic Geochemistry*, 30, 1059-1074.
- Wakeham, S. G., Hedges, J. I., Lee, C., Peterson, M. L., Hernes, P. J., 1997. Composition and transport of lipid biomarkers through the water column and surficial sediments of the equatorial Pacific Ocean. *Deep Sea Research II*, 44, 2131-2162.
- Wilkinson, S. G., 1988. Gram-negative bacteria. *In*: Ratledge, C., Wilkinson, S. G. (Eds), *Microbial Lipids vol. 1*, Academic Press, London, 299-488.

CHAPTER 5

The Occurrence and Distribution of Microbial Markers in Ester- and Amide-Bound Lipid Fractions from Kowloon Bay, Hong Kong SAR, China

5.1 Introduction

Ester- and amide-bound lipids in Recent sediments are well preserved in sedimentary organic matter and provide a record of different sources of input in the biogeochemical record. While various research groups have suggested that bound lipids can provide more detailed information than freely extractable lipids for characterizing sedimentary organic matter, bound lipids have not been widely utilized (Wakeham, 1999; Stefanova and Disnar, 2000; Zegouagh *et al.*, 2000; Garcette-Lepecq *et al.*, 2004). Recovery of bound lipids from Recent sediments requires harsher treatments than conventional solvent extraction. Ester-bound lipids are freed from solvent extracted sediments via alkaline hydrolysis followed by solvent extraction. The amide-bound lipids are freed by acid hydrolysis and subsequent solvent extraction (Goosens *et al.*, 1986, 1989a,b; Cranwell, 1990; Fukushima *et al.*, 1992a,b; Wakeham 1999; Garcette-Lepecq *et al.*, 2004). Unlike free lipids, bound lipids are sterically protected and resilient to chemical and diagenetic degradation (Kawamura and Ishiwatari, 1984; Kawamura *et al.*, 1986; Zegouagh *et al.*, 2000). Preserved organic material in sediments can be utilized to reconstruct the origin and diagenetic pathways from which the organic matter was derived.

A key interest in identifying the types of bacteria present in sediments from core MBH 54/2 is that significant amounts of methane have been released from sediments in Victoria Harbour during dredging activities. Since no methane was detected in sediments from core MBH 54/2, markers identifying the bacterial community may provide a better understanding of organic matter remineralization and possible methane generation. The general sequence of organic matter remineralization processes is summarized in **Fig. 5.1**, starting with aerobic respiration. Once O₂ has been consumed, denitrification occurs followed by manganese and iron respiration. Methane generation via methanogenesis will occur after the sulfate oxygen has been consumed by sulfate reduction (Froelich *et al.*, 1979; Jørgensen, 2000).

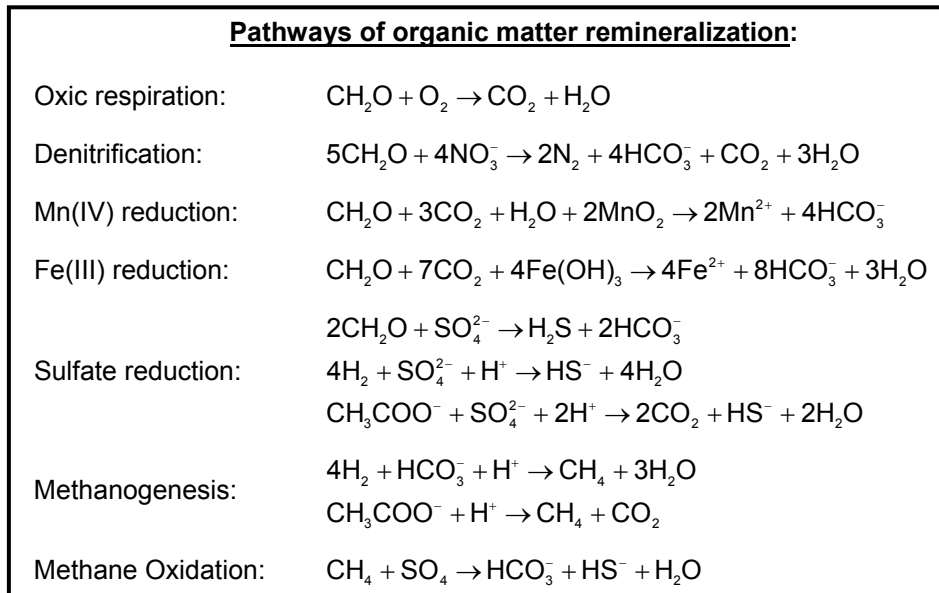


Fig. 5.1. Generic reactions summarizing steps in the remineralization of organic matter (from Jørgensen, 2000).

Sulfate reducing and methanogenic bacteria often coexist in anoxic marine sediments (Martens and Berner, 1974; Barnes and Goldberg, 1976) where the sulfate reducing bacteria play two important roles. First, sulfate reducing bacteria are important for removing sulfate from the system, allowing methanogenesis to proceed (Martens and Berner, 1974; Barnes and Goldberg, 1976; Martens and Klump, 1984). Secondly, sulfate reducing bacteria (along with other methanogens) can also reduce the flux of methane from marine sediments by anaerobic methane oxidation (Barnes and Goldberg, 1976; Reeburgh, 1980; Valentine and Reeburgh, 2000). This chapter discusses the occurrence and distribution of ester- and amide-bound lipids recovered from sediments in core MBH 54/2, from Kowloon Bay, in the Hong Kong Special Administrative Region of China. Lipid groups in the ester- and amide-bound lipid fractions may provide insights into the types of bacterial communities that were present and possible roles they may have played in the remineralization of organic matter.

5.2 Literature Review

5.2.1 Ester- and Amide-Bound Lipids in Sedimentary Organic Matter

Bound lipids in sedimentary organic matter are typically dominated by bacterial lipids. Compounds observed in ester- and amide-bound lipid fractions include carboxylic acids, alcohols, β -hydroxy fatty acids, α -hydroxy fatty acids, ω -hydroxy fatty acids, (ω -1)-hydroxy fatty acids, and α,ω -dicarboxylic fatty acids (**Fig. 5.2**; Kawamura and Ishiwatari, 1984; Goosens *et al.*, 1989b; Fukushima *et*

al., 1992a; Skerratt *et al.*, 1992; Wakeham, 1999). Bacterial fatty acid profiles have been described by Boon *et al.* (1977), Edlund *et al.* (1985), Dowling *et al.* (1986), Ratledge and Wilkinson (1988), Vainshtein *et al.* (1992), and others. However, limited information has been documented for bacterial fatty acid profiles isolated from

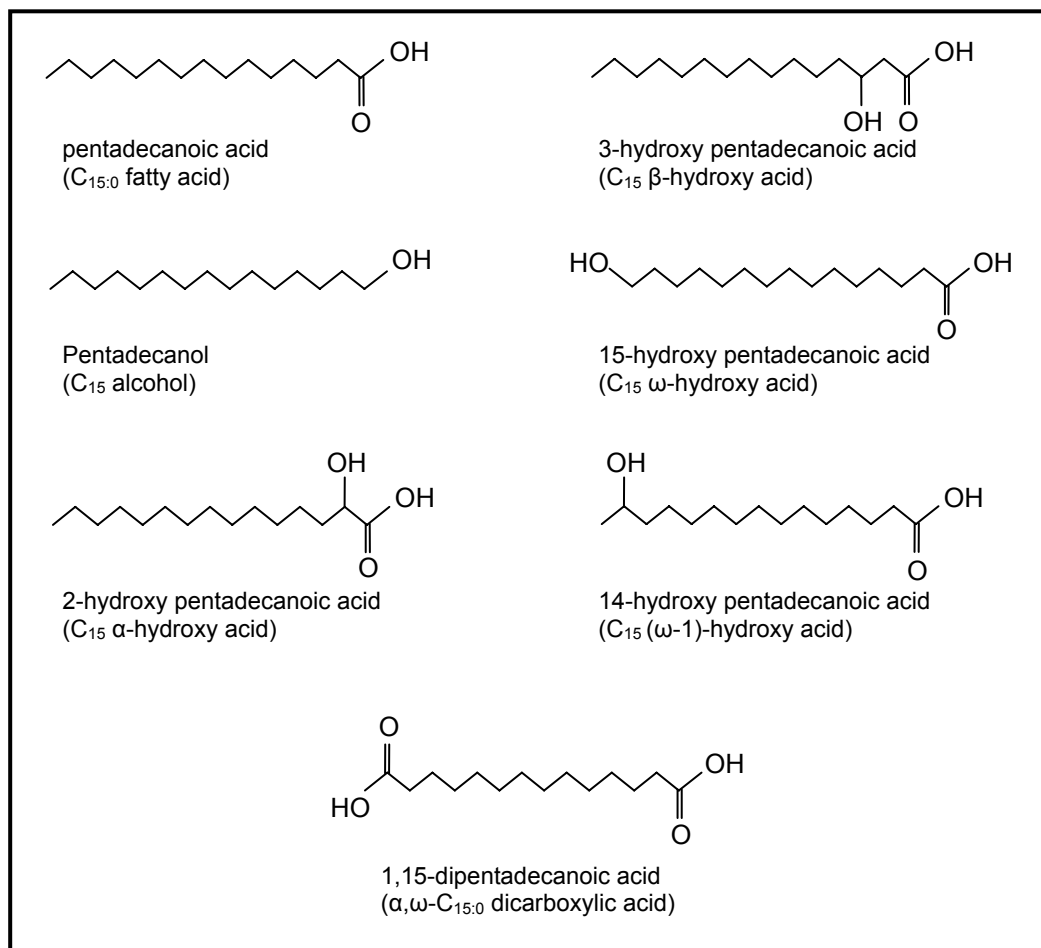


Fig. 5.2. Example of structures and nomenclature of lipids commonly observed in bound lipids.

sediments (Zelles *et al.*, 1995). Other sources of bound lipids that have been recognized include those derived from terrigenous plant material, algae, and formed as intermediaries during oxidative transformations (Cardoso *et al.*, 1977; Albaigés *et al.*, 1984; Cranwell, 1984; Kawamura and Ishiwatari, 1984; Fukushima *et al.*, 1992a,b; Wakeham, 1999; Garcette-Lepecq *et al.*, 2004).

5.2.2 Carboxylic Acids

Carboxylic acids are ubiquitous in the environment and occur in free, ester-, and amide-bound forms. In free form, the low molecular weight monocarboxylic acids (<C_{20:0}) are more susceptible to degradation and can appear to be less abundant than the high molecular weight monocarboxylic acids (>C_{20:0}; Wünsche *et al.*, 1988). Carboxylic acids in the ester- or amide-bound forms are more resilient to degradation, and when utilized with free carboxylic acids can provide a better assessment of the original source material (Farrington and Quinn, 1973; Cranwell, 1984; Goosens *et al.*, 1989b; Garcette-Lepecq *et al.*, 2004). General source information can be obtained by the distribution and abundance of monocarboxylic acids in the ester- and amide-bound forms. Low molecular weight monocarboxylic acids (C_{12:0} to C_{20:0}) have been used as indicators for bacterial and algal source material, whereas iso- and anteiso-carboxylic acids (*e.g.*, i- and ai-C_{13:0}, C_{15:0}, and C_{17:0}) have been utilized as evidence for bacterial input (Cranwell, 1978; Kawamura and Ishiwatari, 1984). As was the case for free lipids, high molecular weight monocarboxylic acids (C_{20:0} to

C_{30:0}) are derived from terrigenous sources (Cranwell, 1978; Kawamura and Ishiwatari, 1984).

5.2.3 α - and β -Hydroxy Fatty Acids

α - and β -Hydroxy fatty acids (**Fig. 5.2**) are more abundant in sediments in ester- and amide-bound form than as free lipids (Kawamura and Ishiwatari, 1984; Fukushima *et al.*, 1992b; Wakeham, 1999). In free lipids, the occurrence of α - and β -hydroxy fatty acids is typically attributed to intermediates formed during the oxidative degradation of fatty acids (Goosens *et al.*, 1986; Wakeham, 1999).

Hydroxy acids, formed as intermediates in the oxidative degradation of fatty acids, preferentially follow the β -oxidation pathway rather than the α -oxidation pathway (Lehninger, 1975; Wakeham, 1999; Garcette-Lepecq, 2004). Distribution patterns of α - and β -hydroxy fatty acids, formed as intermediates, will parallel those of their precursor monocarboxylic fatty acids (Wakeham, 1999).

Significant amounts of α - and β -hydroxy fatty acids bound by ester-linkages are released by saponification of solvent extracted sediments (Cranwell, 1978; Kawamura and Ishiwatari, 1984; Goosens *et al.*, 1986; Garcette-Lepecq *et al.*, 2004). Ester-bound hydroxy acids are thought to originate from biotic sources, where short-chain α - and β -hydroxy fatty acids are representative of bacterial sources and the longer chain homologues are characteristic of terrigenous sources (Kawamura and Ishiwatari, 1984; Wünsche *et al.*, 1987). Further acid hydrolysis of residual sediments releases amide-bound lipid

moieties (Klok *et al.*, 1984; Goosens *et al.*, 1986, 1989a,b; Mendoza *et al.*, 1987; Fukushima *et al.*, 1992a; Garcette-Lepecq *et al.*, 2004). In general, β -hydroxy fatty acids in sediments are more abundant in the amide-bound form than as ester-linked compounds, and are thought to be intact cellular remains of bacteria (Kawamura and Ishiwatari, 1982; Goosens *et al.*, 1986; Wakeham, 1999).

5.2.4 ω - and (ω -1)-Hydroxy Fatty Acids

Fatty acids hydroxylated at the ω - and (ω -1)- positions (**Fig. 5.2**) have been observed in the ester- or amide-bound lipid fractions in sediments. The ω -hydroxy fatty acids are common constituents of cutin and suberin, and have been used as indicators for terrigenous plant material (Kawamura and Ishiwatari, 1984; Wünsche *et al.*, 1987; Fukushima *et al.*, 1992a,b; Garcette-Lepecq *et al.*, 2004). C_{16} and C_{18} ω -hydroxy fatty acids are the most common acids in cutin, whereas the longer chain ω -hydroxy fatty acids (*e.g.*, C_{22} and C_{24}) are more prevalent in suberin (Cardoso *et al.*, 1977). An alternative source of ω -hydroxy fatty acids is the microbial oxidation of *n*-carboxylic acids at the terminal end. ω -Hydroxy fatty acids derived from microbial oxidation reactions can be recognized by distribution patterns analogous to the distribution patterns of their precursor *n*-carboxylic acids (Wakeham, 1999; Garcette-Lepecq *et al.*, 2004).

Even numbered (ω -1)-hydroxy fatty acids in sediments are thought to be derived directly from methanotrophic bacteria or indirectly through the microbial hydroxylation of monocarboxylic acids at the carbon adjacent to the terminal end (typically via some type of aerobic microorganism; Skerratt *et al.*, 1992; Wakeham, 1999). Seagrasses and cuticles of bryophytes have also been speculated as possible sources of (ω -1)-hydroxy fatty acids (Skerratt *et al.*, 1992).

5.2.5 α,ω -Dicarboxylic Acids

α,ω -Dicarboxylic acids (**Fig. 5.2**) with carbon numbers distributed between C₁₀ and C₃₀ have been observed in sediments (Cranwell, 1977; Wakeham, 1999; Stefanova and Disnar, 2000). Reported origins for α,ω -dicarboxylic acids include biosynthesis in seagrasses and higher plants, or as oxidation products of ω -hydroxy fatty acids and monocarboxylic acids (Cranwell, 1977; Wakeham, 1999; Stefanova and Disnar, 2000). In higher plants, α,ω -dicarboxylic acids typically occur as constituents of cuticular waxes, or as components in cutin and suberin (Cranwell, 1977; Wakeham, 1999). Formation of α,ω -dicarboxylic acids, via oxidative processes, will result in profiles similar to their precursor acids (Cranwell, 1977; Wakeham, 1999).

5.2.6 Ester- and Amide-Bound Lipids in Bacteria

Bacterial fatty acids typically occur in bound form as phospholipids, glycolipids, lipoproteins, lipopolysaccharides, and lipoteichoic acids (O'Leary, 1962; Zelles, 1999). The predominant components of bacteria, useful for characterizing microbial communities in sediments, are phospholipid fatty acids and lipopolysaccharides (Zelles, 1999; Rütters *et al.*, 2002). The ester- and amide-bound lipids can be utilized as unique markers for bacteria in the environment. The phospholipid fatty acids are predominantly located in the inner cellular membrane but also occur in the outer cellular membrane (**Fig. 5.3**). The illustration in **Fig. 5.4** represents the components of phospholipids in bacterial cellular membranes, where the head of the phospholipid is hydrophilic (polar end) and the tail is hydrophobic (non-polar end). Lipopolysaccharides make-up a significant portion of the outer cell-membrane of Gram-negative bacteria, where the most abundant fatty acids are the β -hydroxy fatty acids (Kawamura and Ishiwatari, 1984; Zelles, 1999). The β -hydroxy fatty acids are unique markers exclusive to a bacterial origin (Kawamura and Ishiwatari, 1984; Wakeham, 1999; Garette-Lepecq *et al.*, 2004). In the outer cell-membrane, n-carboxylic acids and β -hydroxy fatty acids occur as substituted constituents (via ester- and amide-linkages, respectively) on the phosphate-sugar backbone of Lipid-A of lipopolysaccharides (**Fig. 5.5**; Bhat and Carlson, 1992).

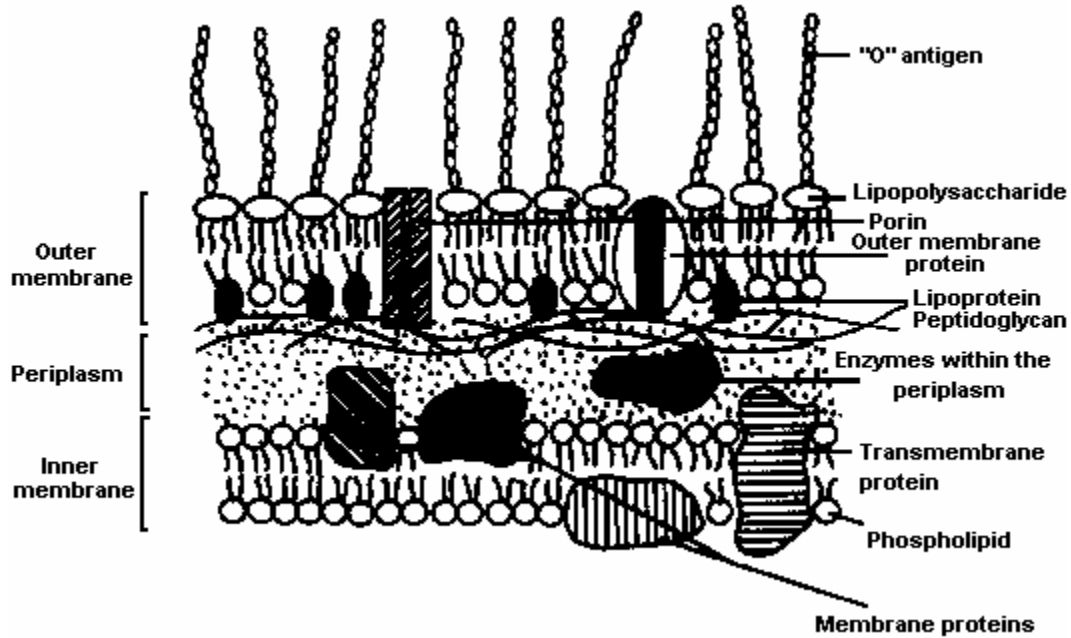


Fig. 5.3. Cellular structure of a Gram-negative bacterium (from http://www.bmb.leeds.ac.uk/mbiology/ug/ugteach/icu8/introduction/bacteria.html#cell_wall).

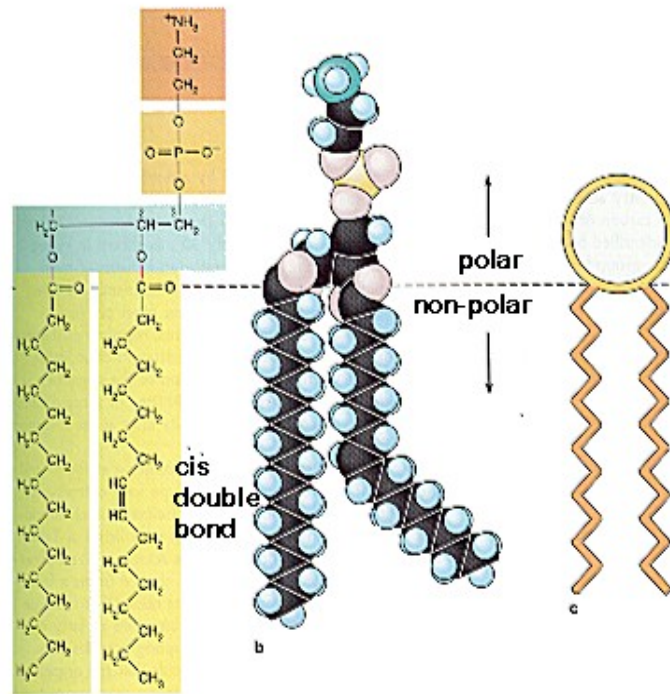


Fig. 5.4. Components of phospholipids in bacterial cellular membranes (from http://cellbio.utmb.edu/cellbio/membrane_intro.htm)

CAM pathways; see Chapter 3, Section 3.1.3). C3 plants are depleted in ^{13}C , C4 plants are more enriched in ^{13}C , and CAM plants (which can utilize both C3 and C4 pathways) have intermediate $\delta^{13}\text{C}$ values (Collister *et al.*, 1994). The $\delta^{13}\text{C}$ values of C3 plants range around -26‰ , C4 plants around -13‰ , and $\delta^{13}\text{C}$ values for CAM plants cover the range typical of C3 and C4 plants (Deines, 1980). Lipids, however, are commonly depleted in ^{13}C relative to the biomass by 3‰ to 12‰ (Deines, 1980; Monson and Hayes, 1982; Collister *et al.*, 1994; Abraham *et al.*, 1998; Naraoka and Ishiwatari, 1999). In a study by Naraoka and Ishiwatari (2000), fatty acids ($\text{C}_{20:0}$ to $\text{C}_{30:0}$) from leaves of C3 terrigenous plants ranged between -35‰ to -30‰ , whereas marine derived fatty acids (*e.g.*, $\text{C}_{14:0}$, $\text{C}_{16:0}$, and $\text{C}_{18:0}$) had an average $\delta^{13}\text{C}$ value of $-23.8 \pm 1.1\text{‰}$. Duan *et al.* (1997) measured the isotopic composition of fatty acids ($\text{C}_{16:0}$ to $\text{C}_{28:0}$) in sediment samples from Ruergai marsh, China. The average $\delta^{13}\text{C}$ composition for individual fatty acids was -33.7‰ , which was about 7.3‰ lighter than the average $\delta^{13}\text{C}$ composition of C3 plants (*i.e.*, -26.4‰) around the marsh. The 7.3‰ difference is consistent with levels of depletion observed between lipids and their associated biomass. Knowledge of end-member isotopic compositions of fatty acids would allow the proportion of source contributors to be estimated in marine sediments (Naraoka and Ishiwatari, 2000).

More recently, carbon pathways within microbial communities have been investigated using compound-specific carbon isotope analysis of fatty acids derived from cellular membranes of bacteria (Boschker *et al.*, 1998, 1999; Abraham *et al.*, 1998; Boschker and Middleburg, 2002; Petsch *et al.*, 2003;

Londry and Des Marais, 2003; Londry *et al.*, 2004). Carbon isotopic fractionation of bacterial lipids is affected by the mode of growth (*i.e.*, heterotrophic or autotrophic growth in the environment), growth substrate (*e.g.*, acetate, mannose, lactose, or glycerol), and metabolic pathway (*e.g.*, the acetyl-CoA pathway or tricarboxylic acid cycle) (Abraham *et al.*, 1998; Boschker *et al.*, 1998; Londry and Des Marais, 2003; Londry *et al.*, 2004). However, it has been demonstrated that the isotopic composition of fatty acids is not dependent on the growth stage of the bacteria (Summons *et al.*, 1994; Abraham *et al.*, 1998; and Londry and Des Marais, 2003).

Sulfate-reducing bacteria, for example, are ubiquitous in coastal sediments and can mineralize as much as 50% of the total organic carbon (Jørgensen, 1982; Boschker *et al.*, 1998). The primary substrate used by sulfate-reducing bacteria, during the anaerobic decomposition of organic matter, is acetate (Parkes *et al.*, 1989; Boschker *et al.*, 1998). In a study by Boschker *et al.* (1998), the isotopic composition of fatty acids was measured for sulfate-reducing bacteria, using ^{13}C -labelled acetate as the substrate. The isotopic composition of key phospholipid fatty acids associated with the Gram-positive bacteria *Desulfotomaculum acetoxidans*, indicated that these bacteria consumed a significant portion of the ^{13}C -labelled acetate. ^{13}C -Labelled acetate, however, was not significantly utilized by the Gram-negative bacteria of the *Desulfobacter* species (Boschker *et al.*, 1998).

Methanotrophs (*i.e.*, methane-oxidizing bacteria) in anaerobic sediments utilize methane as their carbon and energy source. They play an important role in

limiting the amount of methane released from anaerobic environments (Boschker *et al.*, 1998). Biogenic methane has isotopic compositions depleted in ^{13}C in the range of -110‰ to -60‰ (Hunt, 1996). Bacteria utilizing biogenic methane will reflect biomass depleted in ^{13}C , by as much as 20‰ (Boschker *et al.*, 1998; Boschker and Middelburg, 2002).

5.3 Results and Discussion

In the following sections, compound classes identified in the ester- and amide-bound lipid fractions from core MBH 54/2 will be discussed. Ester- and amide-bound lipids were isolated by the saponification and acid hydrolysis of solvent extracted sediments. Techniques used to release and extract ester- and amide-bound lipids are discussed in more detail in Chapter 2. Lipids were identified based on mass spectra, retention time, and comparison to literature data (see **Appendix III** for representative spectra from identified lipid classes). Ester-bound lipids in sediments from core MBH 54/2 include carboxylic acids, α -hydroxy fatty acids, β -hydroxy fatty acids, ω -hydroxy fatty acids, and n-alcohols, and are summarized in **Table 5.1**. The amide-bound lipid fraction consists of carboxylic acids and β -hydroxy fatty acids. The quantitative data for the lipid constituents from ester- and amide-bound lipid fractions are summarized in **Appendix V**.

Table 5.1. Summary of lipid composition in the ester-bound fraction in core MBH 54/2.

Core #	Depth (m)	Carboxylic acids	β -FAOH	α -FAOH	ω -FAOH	n-alcohols
Core 2 (0-5)	0.5	12,i13,ai13,13,i14,14,i15, ai15,15,i16,16,i17,ai17,17, 18,19,20-30	10,i12,12,i13,ai13,i14,14 i15,ai15,15,i16,16,i17,ai17,17 18,19,20,21,22,23	16,17,18,20,22,24	16,22,24	16,18,20, 22,24,26
Core 2 (20-25)	0.7	12,i13,ai13,13,i14,14,i15, ai15,15,i16,16,i17,ai17, 17,18:1 ^a ,18:1 ^b ,18,19,20-30	i13,i14,14,i15,ai15,15,i16,16, i17,ai17,17,18	16,18,20,22	--	--
Core 2 (70-75)	1.2	12,i13,ai13,13,i14,14,i15, ai15,15,i16,16:i1,16,i17,ai17, 17,18:1 ^a ,18:1 ^b ,18,19,20-30	10,i12,12,i15,ai15,15,i16,16, i17,ai17,17,18	16,18,20,22,23,24	16	16,18,20, 22,24,26
Core 2 (95-100)	1.4	12,i13,ai13,13,i14,14,i15, ai15,15,i16,16, 10Me16:0 , i17, ai17, cy17 ,18:1 ^a ,18,19,20-30	10,12,i13,ai13,13,i14,14,i15, ai15,15,i16,16,i17,ai17,17	16	--	--
Core 3 (10-15)	1.6	12,i13,ai13,13,i14,14,i15,ai15, 15,i16,16:i1,16, 10Me16:0 ,i17, ai17, cy17 ,17,18:1 ^a ,18,19,20-32	10,11,i12,12,i13,ai13,13,i14, 14,i15,ai15,15,i16,16,i17,ai17, 17,18	16,18,20,22,23,24, 24:1,25,26	16,22,24,26	16,18,20, 22,24,26
Core 3 (80-85)	2.3	i13,ai13,13,i14,14,i15,ai15, 15,i16,i17,ai17,17,18,19,20-30	12,i13,ai13,13,i14,14,i15,ai15, 15,i16,16,i17,ai17,17,18,20	16,17,18,20	16,22	16,18,24
Core 4 (55-60)	3.0	12,i13,ai13,13,i14,14,i15, ai15,15,i16,16,i17,ai17,17, 18,19,20-30	10,12,i13,ai13,13,i14,14, i15,ai15,15,i16,16,i17,ai17, 17,18,20	16,17,18	--	16,18,22,24
Core 4 (80-85)	3.3	i14,14,i15,ai15,15,i16,16, i17,ai17,17,18,19,20-32	12,i13,ai13,13,i14,14,i15,ai15, 15,i16,16,i17,ai17,17,18,19, 20,21,22	16,18,20,22,24,26	16,18,20, 22,24,26	16,18,20, 22,24,26
Core 1 (5-10)	3.5	12,i13,ai13,13,i14,14,i15, ai15,15,i16,16,16:1, 10Me16:0 , i17,ai17,17,18,19,20-30	10,11,12,i13,ai13,13,i14,14, i15,ai15,15,i16,16,i17,ai17, 18,19,20,21,22	16,18,20	16,22	16,18,20, 22,24,26
Core 1 (40-45)	3.9	i14,14,i15,ai15,15,i16,16, i17,ai17,17,18,19,20-32	12,i13,ai13,13,i14,14,i15,ai15, 15,i16,16,i17,ai17,17,18,19, 20,21,22	16,18,22	16,18,20, 22,26	16,18,20, 22,24,26

Roman numerals indicate carbon chain-length.

5.3.1 n-Carboxylic Acids in the Ester-Bound Lipid Fraction

Carboxylic acids comprised of straight chain, branched, and monounsaturated fatty acids dominated the ester-bound lipid fraction in core MBH 54/2. Throughout the core, a bimodal distribution is observed for carboxylic acids (**Fig. 5.6**). Short-chain fatty acids ($C_{12:0}$ to $C_{20:0}$) are significantly more abundant than long-chain fatty acids ($C_{21:0}$ to $C_{30:0}$). On average, the short-chain fatty acids comprise ~78% of the ester-bound alkanolic acids and the long-chain fatty acids the remaining ~22%. The ester-bound short-chain fatty acids ($C_{12:0}$ to $C_{20:0}$) are most abundant between 0.7m and 2.3m, with amounts ranging between 81% and 89%. In general, short-chain alkanolic acids ($<C_{20:0}$) are associated with bacterial and planktonic input, whereas long-chain alkanolic acids ($>C_{20:0}$) are derived from cuticular waxes of terrigenous plants.

The concentrations of short- and long-chain fatty acids are plotted in **Fig. 5.7**. The long-chain alkanolic acids do not demonstrate much variation down the core (concentration ranges between 2-4 $\mu\text{g/g}$ dry sediment weight in the upper 3.5m). A slight enrichment, to about 6 $\mu\text{g/g}$ dry sediment weight, is observed at 1.2m and 1.6m; below 3.5m the concentration of long-chain alkanolic acids falls below 1 $\mu\text{g/g}$ dry sediment weight.

The degree of variation in fatty acid composition and shifts in source contributions preserved in core MBH 54/2 can be illustrated by plotting the aquatic-to-terrigenous ratio (*i.e.*, $\Sigma(C_{12:0}-C_{18:0})/\Sigma(C_{22:0}-C_{28:0})$); **Fig. 5.8**). The highest influx of aquatic derived organic matter is observed between 0.7m and 1.4m. A higher influx of terrigenously derived organic matter is observed

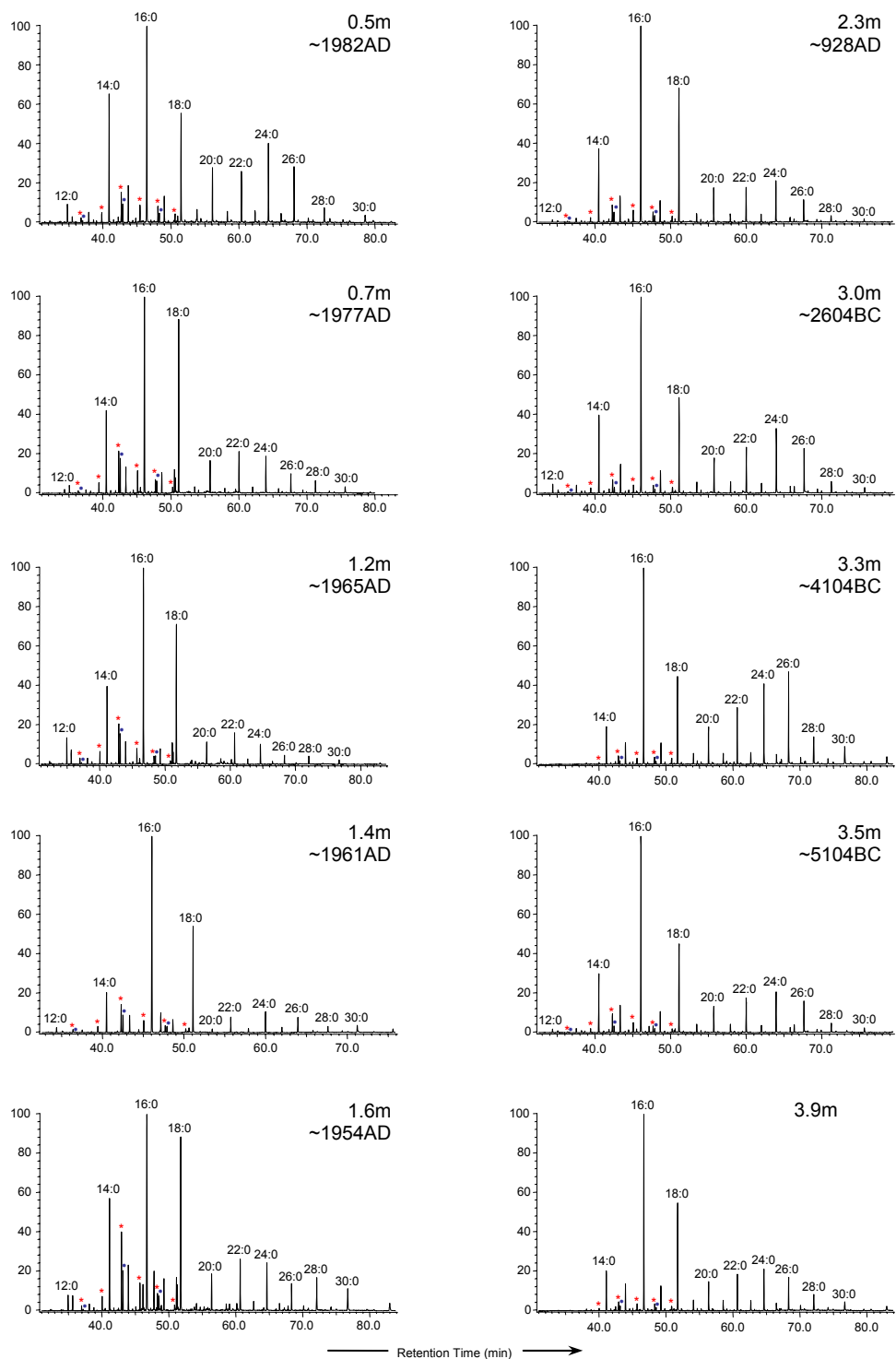


Fig. 5.6. Downcore profile of fatty acids as methyl esters in the ester-bound lipid fraction of core section MBH 54/2. * indicates iso- branched fatty acids, and • indicates anteiso- branched fatty acids.

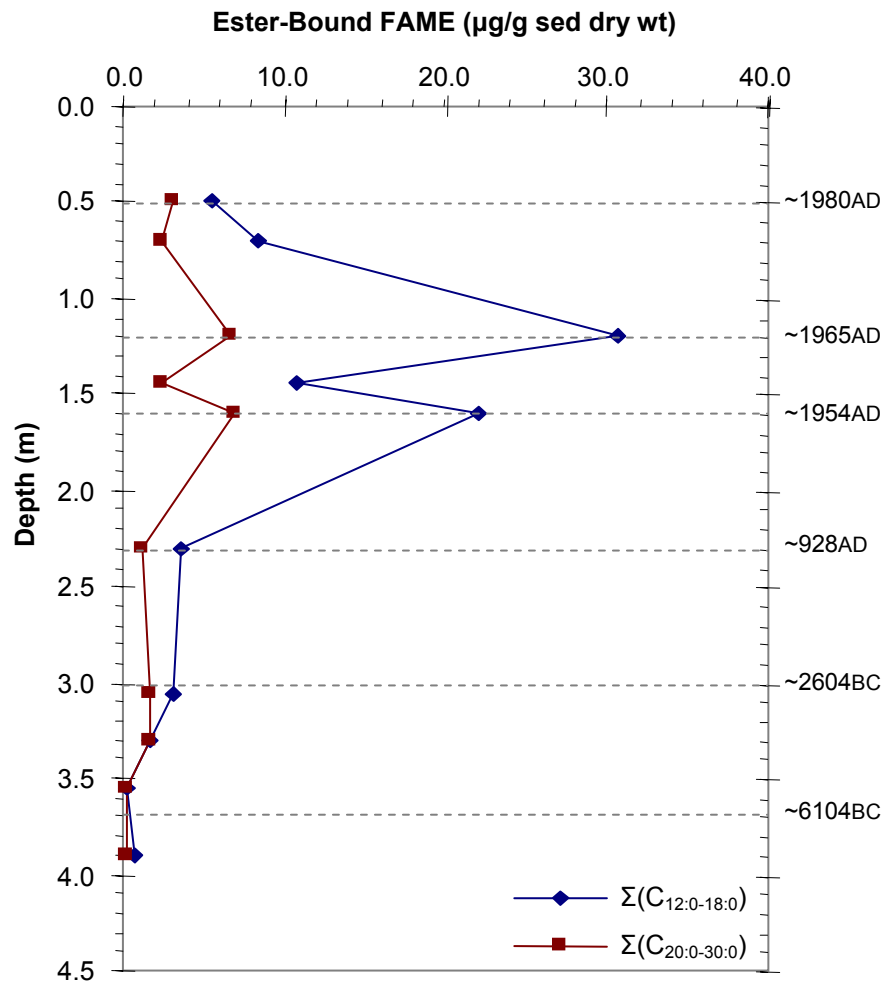


Fig. 5.7. Downcore distribution illustrating the abundance of short- and long-chain n-alkanoic acids in the ester-bound lipid fraction.

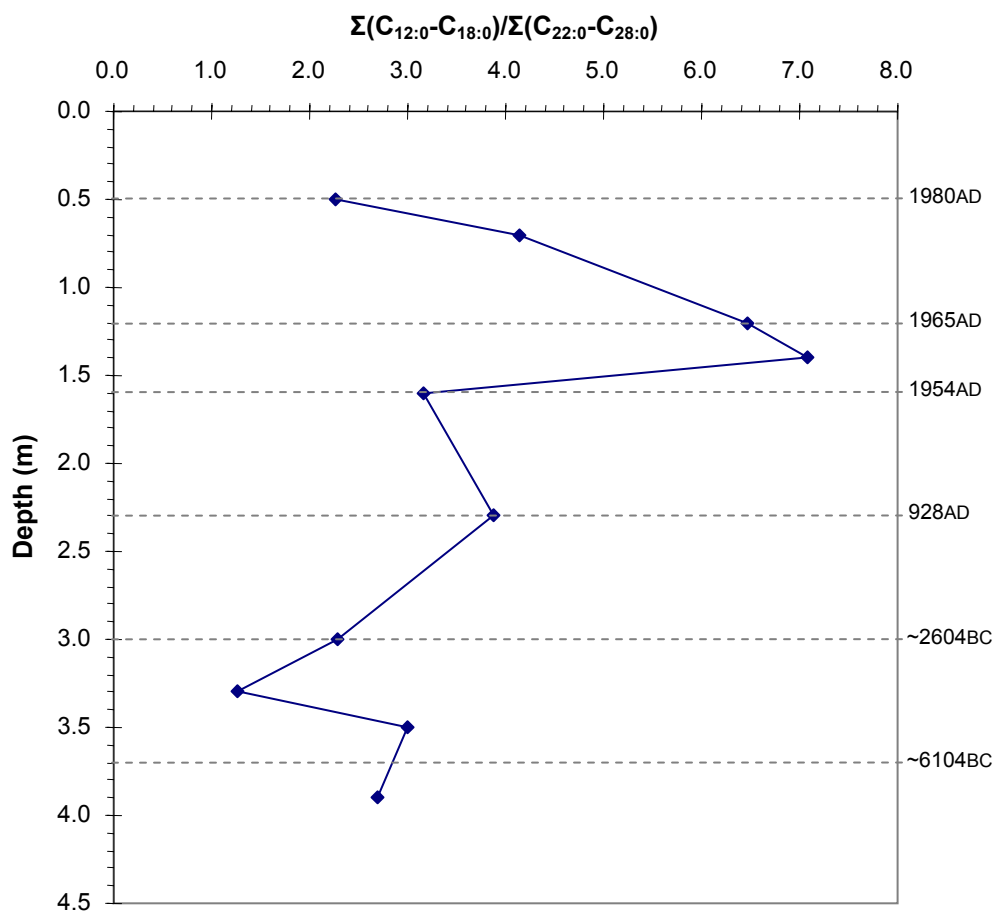


Fig. 5.8. Ratio of short to long chain ester-bound fatty acids as methyl esters. Downcore variations and shifts in contributions of organic source material are illustrated in this diagram.

at 1.6m, followed by increased contributions from aquatically derived organic matter around 2.3m. Between 2.3m and 3.3m, more abundant contributions from terrigenously derived organic matter are recorded in the sediment. A slight increase in aquatically derived organic matter is observed at 3.5m and 3.9m. Results of the C/N ratio (discussed in Chapter 3) support these observations where a higher C/N ratio at 1.6m shifts towards lower C/N ratios around 2.3m, followed by more intermediate C/N ratios between 2.3m and 3.3m (indicating a mixture of both terrigenous and aquatic derived organic matter).

The carbon preference index (CPI) was originally used to estimate the thermal maturity of source rocks and crude oils, based on the odd-over-even preference of n-alkanes (Bray and Evans, 1961). n-Alkanes with CPI values greater than or less than 1.0 suggest low thermal maturity, whereas CPI values closer to 1.0 indicate higher thermal maturity. In Recent sediments, which are immature, the CPI has been applied to n-alkanoic acids (even-over-odd preference) as an indicator for the degree of diagenetic alterations (Matsuda and Koyama, 1977; Meyers and Ishiwatari, 1993). CPI values of n-alkanoic acids that approach 1.0 suggest higher degrees of diagenetic alterations. In ester-bound lipid fractions from core MBH 54/2, an even-over-odd predominance pattern is observed over the total carbon number range ($C_{12:0}$ to $C_{30:0}$; **Fig. 5.9**), with an average CPI ~ 6.5 (**eq. 5.1**). The average CPI for short-chain fatty acids ($C_{12:0}$ to $C_{20:0}$) is 6.8 (**eq. 5.2**); long-chain fatty acids ($C_{20:0}$ and $C_{30:0}$) have an average CPI

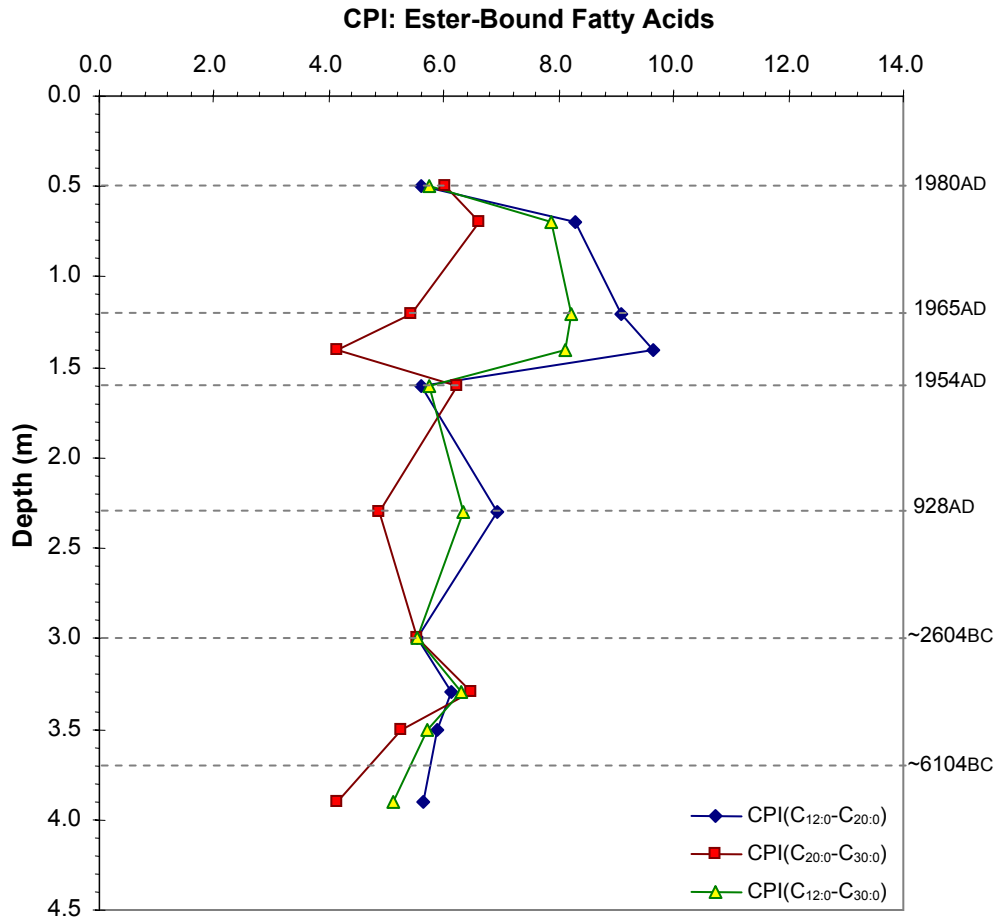


Fig. 5.9. Carbon preference index for ester-bound fatty acids as methyl esters, relative to depth, in core MBH 54/2.

$$\text{CPI}_{\text{C}_{12:0}\text{-C}_{30:0}} = \frac{(\text{C}_{12:0} + 2 * (\text{C}_{14:0} + \text{C}_{16:0} + \dots + \text{C}_{26:0} + \text{C}_{28:0}) + \text{C}_{30:0})}{2 * (\text{C}_{13:0} + \text{C}_{15:0} + \dots + \text{C}_{27:0} + \text{C}_{29:0})} \quad (\text{eq. 5.1})$$

$$\text{CPI}_{\text{C}_{12:0}\text{-C}_{20:0}} = \frac{(\text{C}_{12:0} + 2 * (\text{C}_{14:0} + \text{C}_{16:0} + \text{C}_{18:0}) + \text{C}_{20:0})}{2 * (\text{C}_{13:0} + \text{C}_{15:0} + \text{C}_{17:0} + \text{C}_{19:0})} \quad (\text{eq. 5.2})$$

$$\text{CPI}_{\text{C}_{20:0}\text{-C}_{30:0}} = \frac{(\text{C}_{20:0} + 2 * (\text{C}_{22:0} + \text{C}_{24:0} + \text{C}_{26:0} + \text{C}_{28:0}) + \text{C}_{30:0})}{2 * (\text{C}_{21:0} + \text{C}_{23:0} + \text{C}_{25:0} + \text{C}_{27:0} + \text{C}_{29:0})} \quad (\text{eq. 5.3})$$

of 5.5 (**eq. 5.3**). In the short chain fatty acid fraction, the highest CPI values are observed between 0.7m and 1.4m, where CPI values range between 8.3 and 9.6. Small spikes in the CPI values for short-chain fatty acids are observed at depths of 2.3m and 3.3m, where CPI values are 6.9 and 6.1, respectively. The long-chain fatty acids appear to demonstrate more variability in CPI values down the core, with CPI values shifting between 4.1 and 6.6. Peak CPI values occur at 0.7m, 1.6m, and 3.3m (where CPI values are 6.6, 6.2, and 6.5, respectively). The downcore plot of CPI values calculated over the total carbon number range closely parallel CPI values calculated for the short-chain fatty acids.

At depth intervals between 0.7m and 1.4m, CPI values for short-chain fatty acids are significantly greater than CPI values for long-chain fatty acids. Cellular fatty acids in bacteria are commonly dominated by short-chain even carbon numbers. The high CPI values of short-chain fatty acids between 0.7m and 1.4m may reflect an increase in bacteria in the region due to the excessive discharge of sewage into the harbour. The long-chain fatty acids, on the other hand, had much lower CPI values between 0.7m and 1.4m. Lower CPI values may reflect bacterial reworking of sedimentary organic matter. Around 2.3m, there is another slight rise in the CPI value for short-chain fatty acids, with a corresponding lower CPI value for long-chain fatty acids. Again, this may reflect a higher flux of bacteria in the sediment and increased reworking of the longer chain fatty acids. CPI values of long-chain fatty acids demonstrate a slight increase at 1.6m and 3.3m, and correspond to fluxes observed in the concentration of ω -hydroxy fatty acids and n-alcohols (discussed in **section 5.3.5**).

5.3.2 Branched-Carboxylic Acids in the Ester-Bound Lipid Fraction

Branched-carboxylic acids in sediments (*i.e.*, primarily *i*- and *ai*-C_{13:0}, C_{15:0}, and C_{17:0}) have been used as lipid markers providing evidence for bacterial input (Cranwell, 1973, 1978; Saliot *et al.*, 1991; Guezennec and Fiala-Medioni, 1996; Budge and Parrish, 1998). The proportion of bacteria in a sedimentary environment can be represented by the relative abundance of *i*-C_{15:0} and *ai*-C_{15:0} to C_{16:0}, since the C_{16:0} fatty acid is ubiquitous in most organisms (Nichols *et al.*, 1987; Mancuso *et al.*, 1990; and Rajendran *et al.*, 1992a). The ratio of *i*-C_{15:0} plus *ai*-C_{15:0} to C_{16:0} in the ester-bound lipid fraction in core MBH 54/2 is plotted relative to depth in **Fig. 5.10**. At depths between 2.0m and 4.0m, the (*i*-C_{15:0} + *ai*-C_{15:0})/C_{16:0} ratio ranges from 0.06 to 0.14. In the upper 2.0m, the (*i*-C_{15:0} + *ai*-C_{15:0})/C_{16:0} ratio ranges from 0.23 to 0.68. A significant increase in the proportion of bacterial components is observed in the uppermost section of the core (*i.e.*, peak occurrences at 0.7m, 1.2m, and 1.6m).

Throughout core MBH 54/2, branched fatty acids have been identified in the C_{12:0} to C_{20:0} range, comprising between 7.6% to 29.3% of the total short chain fatty acids (**Fig. 5.11**). Branched fatty acids are most abundant in the upper 2.0m of the core (*i.e.*, between 16.8% and 29.3%), with a maximum abundance at 1.6m. Between 2.3m and 3.9m, branched fatty acids become less abundant and consist of 7.6% to 12.7% of the short chain fatty acid fraction. Various groups have attempted to identify and classify bacteria types based on the carbon chain length of branched fatty acids and on the location of branching points (*e.g.*, Edlund *et al.*, 1985; Rajendran *et al.*, 1992c; Vainshtein *et al.*, 1992).

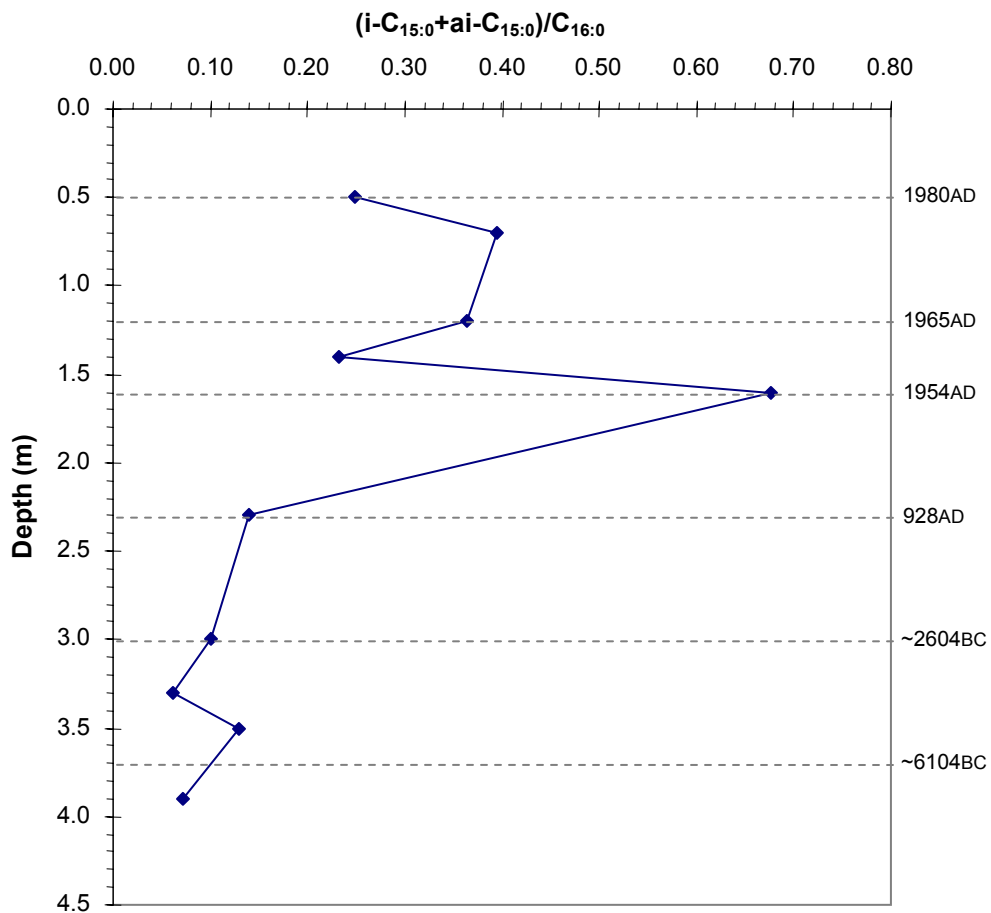


Fig. 5.10. Plot illustrating the relative proportion of bacterial components in the ester-bound fraction of sediments from core MBH 54/2, using the ratio of $(i-C_{15:0} + ai-C_{15:0})/C_{16:0}$ vs depth.

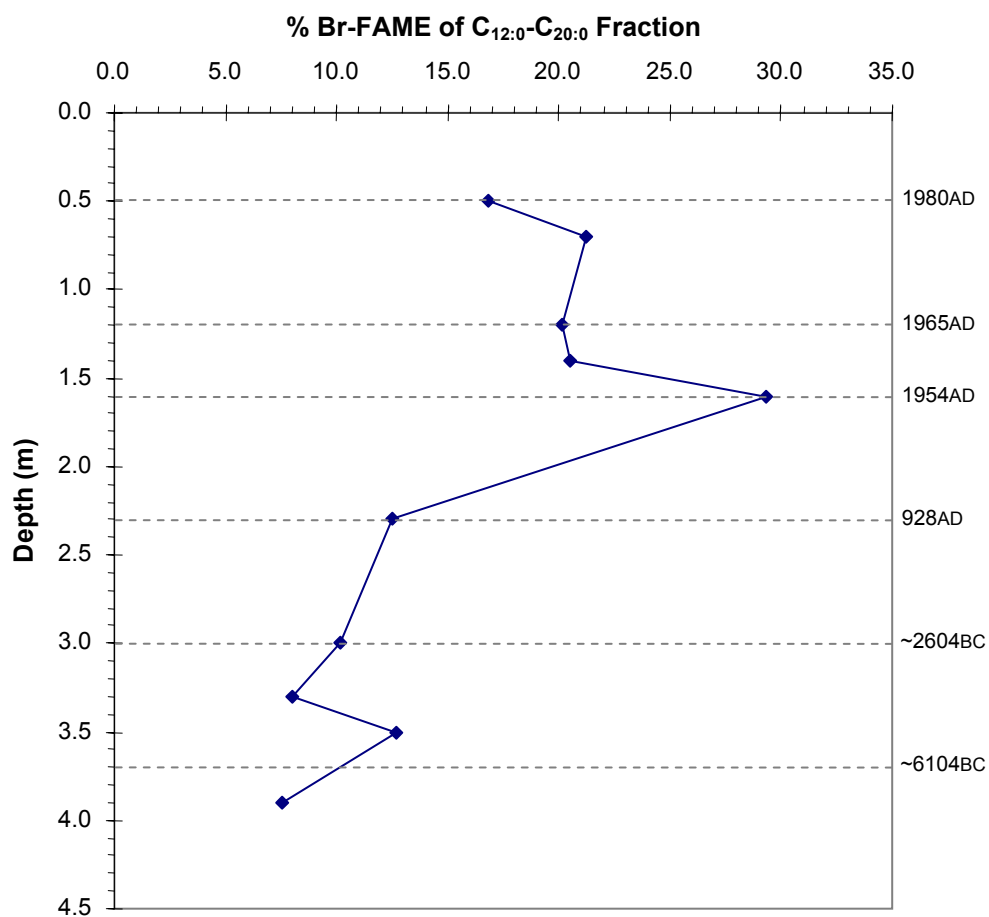


Fig. 5.11. Percent composition of branched chain fatty acids within the C_{12:0} to C_{20:0} range of ester-bound lipids.

The ester-bound branched fatty acids identified in sediments from core MBH 54/2 include i-C_{13:0}, ai-C_{13:0}, i-C_{14:0}, i-C_{15:0}, ai-C_{15:0}, i-C_{16:0}, 10Me16:0, i-C_{17:0}, ai-C_{17:0}, i-C_{18:0}, i-C_{19:0}, and ai-C_{19:0} (as illustrated in **Fig. 5.12**). A broader distribution of branched fatty acids is present in the ester-bound form, compared to free lipids, and has more specificity enabling the identification of bacteria types. Branched fatty acids, with carbon chain lengths ranging between C_{14:0} and C_{16:0} are commonly associated with Gram-positive and anaerobic bacteria. Branched fatty acids in the C_{16:0} to C_{19:0} range are attributed to sulfate reducing and anaerobic bacteria (Rajendran *et al.* 1992c). Each of these branched fatty acids was identified throughout core MBH 54/2. Vainshtein *et al.* (1992) observed that i-C_{15:0} fatty acids are predominant in most *Desulfovibrio* species of sulfate reducing bacteria (*e.g.*, *Desulfomicrobium* and *Desulfomomas*). i-C_{15:0} Fatty acids were observed to be less abundant than ai-C_{15:0} fatty acids in *D. sulfodismutans*, *D. alocoholorans*, *D. carbinolicus*, *D. fructosovorans*, *D. giganteus*, and *D. gigas* (Vainshtein *et al.*, 1992). Throughout the core section from Kowloon Bay, the i-C_{15:0} acid is the most abundant branched fatty acid. The iso-/anteiso- C_{15:0} ratio (**Fig. 5.13**) demonstrates that the iso- acid is more abundant than the anteiso- acid, with the greatest difference occurring below 3.0m. The *Desulfovibrio* species of bacteria were likely present throughout the core. In studies of fatty acid profiles of *Desulfovibrio* species of sulfate reducing bacteria, Edlund *et al.* (1985) observed i-C_{15:0}, C_{16:0}, and i-C_{17:0} saturated fatty acids to be major constituents of *D. desulfuricans*, *D. vulgaris*, and *D. africanus*. These

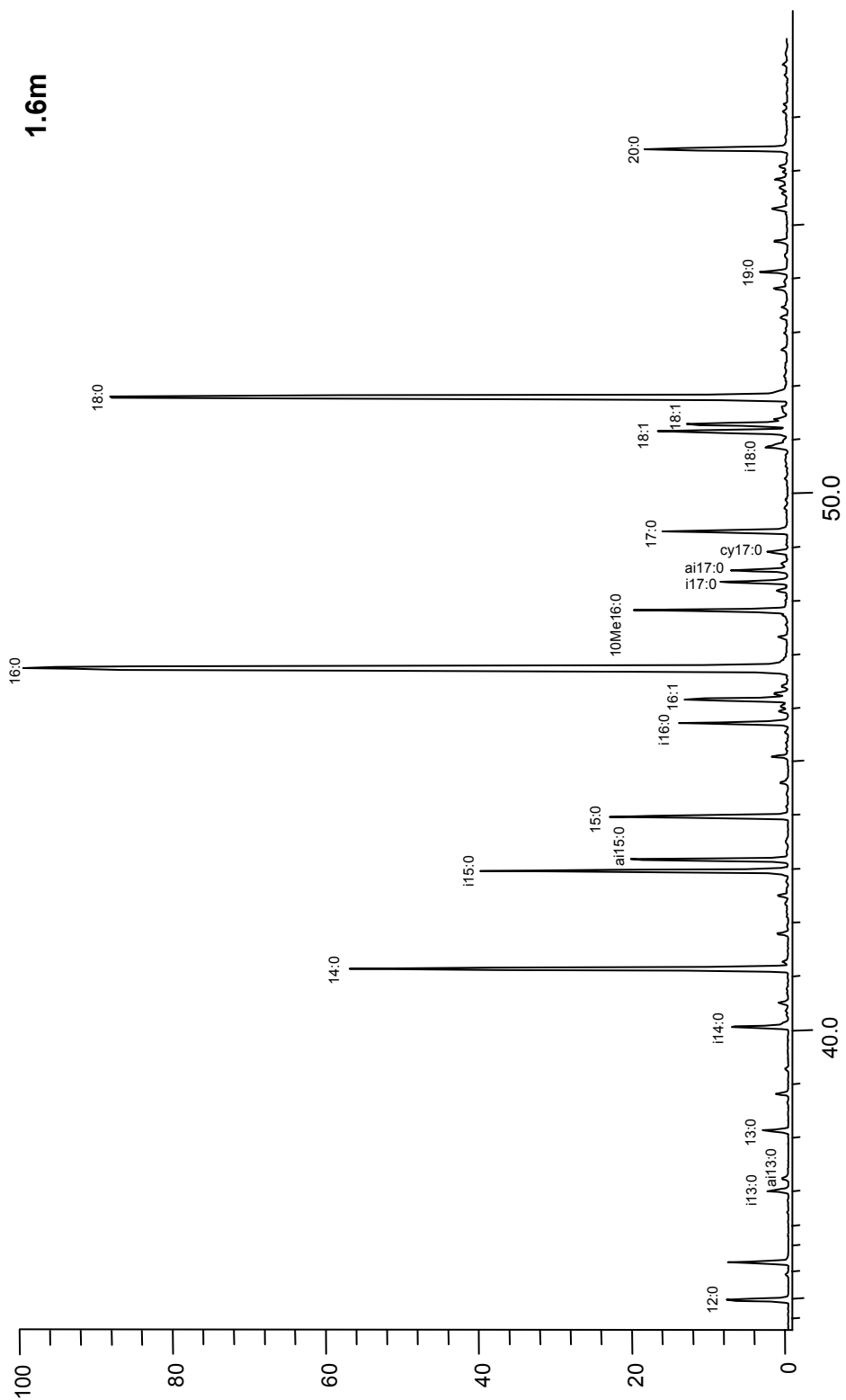


Fig. 5.12. Partial chromatogram illustrating an example bacterial lipid profile, distributed in the ester-bound short chain fatty acids ($C_{12:0}$ – $C_{20:0}$), extracted from a sediment sample (core MBH 54/2, ~1.6m depth).

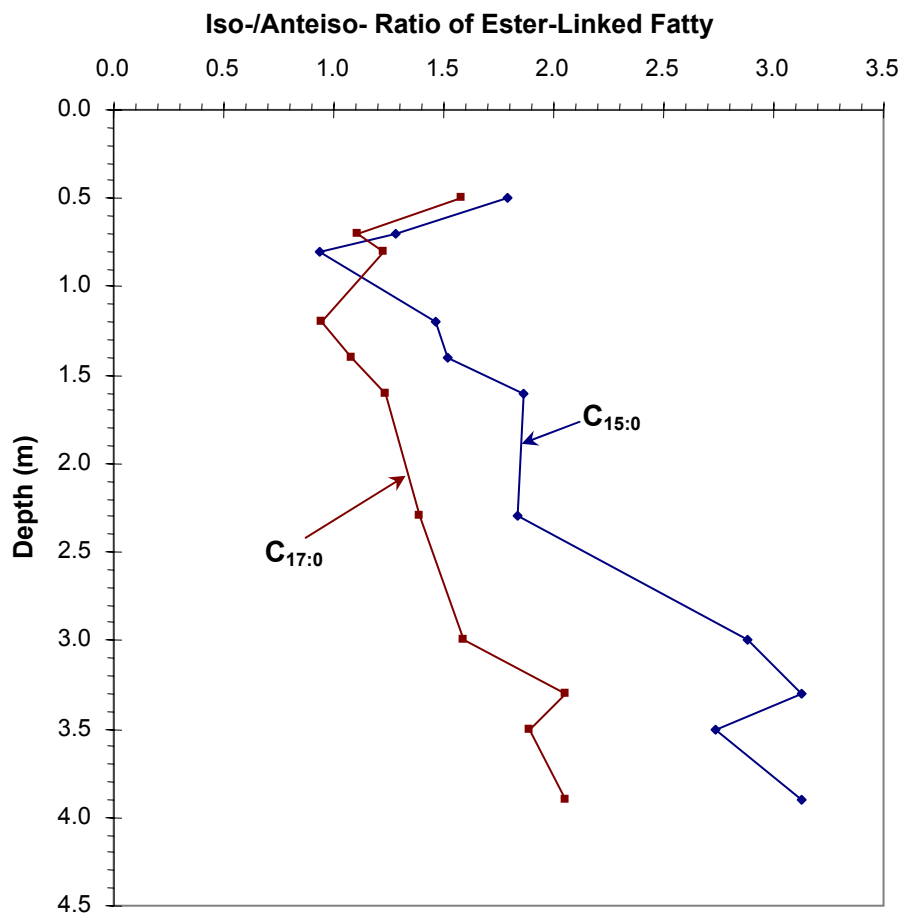


Fig. 5.13. Iso-/Anteiso-ratio of C_{15:0} and C_{17:0} fatty acids in the ester-linked fraction of sediments from core MBH 54/2.

bacteria also contain significant amounts of monounsaturated fatty acids (e.g., C_{16:1(n-7)c}, i-C_{17:1(n-7)c}, and C_{18:1(n-7)c}), and were only observed between 0.7m to 1.6m, and at 3.5m. Major components of *D. gigas* include i-C_{15:0}, ai-C_{15:0}, C_{16:0}, and i-C_{17:0} (Edlund *et al.*, 1985). The branched fatty acid, 10Me16:0 (*i.e.*, 10-methyl-hexadecanoic acid), has been identified as a signature compound for *Desulfobacter* species of sulfate reducing bacteria (Rajendran *et al.*, 1992b;

Rajendran *et al.*, 1992c; Vainshtein *et al.*, 1992). The marker for *Desulfobacter* species of sulfate reducing bacteria was only identified at 1.4m, 1.6m, and 3.5m. Each of these depths corresponds to periods with the greatest stanol/sterol ratio (discussed in Chapter 4).

5.3.3 Unsaturated-Carboxylic Acids in the Ester-Bound Lipid Fraction

Unsaturated fatty acids were not detected in significant amounts in the ester-bound lipid fraction of core MBH 54/2, and only C_{16:1}, C_{18:1}, and C_{18:2} unsaturated fatty acids were identified in relatively low concentrations. While monounsaturated fatty acids have been used as markers for aerobic bacteria and polyunsaturated fatty acids as markers for eukaryotes (Findlay *et al.*, 1990; Rajendran *et al.*, 1992b,c), certain unsaturated fatty acids have been detected in anaerobic bacteria (Perry *et al.*, 1979; Edlund *et al.*, 1985; Dowling *et al.*, 1986; Rajendran *et al.*, 1992b; Vainshtein *et al.*, 1992). In particular, C_{16:1 ω 7} and C_{18:1 ω 7} fatty acids have been observed as predominant components in anaerobic bacteria (Perry *et al.*, 1979; Summit *et al.*, 2000), and i- and ai-C_{15:1} and C_{17:1} fatty acids have been attributed to sulfate reducing bacteria and other anaerobic bacteria (Edlund *et al.*, 1985; Rajendran *et al.*, 1992b; Vainshtein *et al.*, 1992; Summit *et al.*, 2000). No branched unsaturated fatty acids (*i.e.*, i- and ai-C_{15:1} and C_{17:1}) were identified in core MBH 54/2. If any branched unsaturated fatty acids had been present in older sediments of Victoria Harbour, they may have been

hydrogenated to their saturated counterparts (e.g., i- and ai-C_{15:0} and C_{17:0}) due to the highly anoxic conditions around the study site.

5.3.4 α - and β -Hydroxy Fatty Acids in the Ester-Bound Lipid Fraction

α -Hydroxy fatty acids were less abundant in the ester-bound lipid fraction than β -hydroxy fatty acids. Only straight-chain, even numbered α -hydroxy fatty acids (C₁₆ to C₂₆), with variable distributions, were detected downcore (**Table 5.1**). Possible sources of α -hydroxy fatty acids (C₁₆ to C₂₆) include phytoplankton, bacteria, and cyanobacteria (Wakeham, 1999; Smallwood and Wolff, 2000).

Substantial amounts of β -hydroxy fatty acids (C₁₀ to C₂₀) were detected and identified in the ester-bound lipid fraction (**Fig. 5.14**). n- β -Hydroxy fatty acids comprised ~48% to ~75% of the total β -hydroxy fatty acids; whereas branched β -hydroxy fatty acids constituted ~25% to ~52% of the total β -hydroxy fatty acids. The total straight chain and branched β -hydroxy fatty acid contents (in $\mu\text{g/g}$ dry sediment weight) are plotted relative to depth in **Fig. 5.15**. Significant contributions of these compounds to the ester-bound lipid fraction of the sediments are observed between 0.8m and 2.0m, maximizing at 1.2m and 1.6m. A slight secondary flux of β -hydroxy fatty acids is observed at 3.5m. Ester-linked β -hydroxy fatty acids are unique markers for bacteria (Edlund *et al.*, 1985; Mendoza *et al.*, 1987; Skerratt *et al.*, 1992; Wakeham, 1999). They are important cellular components in lipopolysaccharides of Gram-negative bacteria, and are linked by ester- or amide-bonds (Weckesser and Drews, 1979; Edlund *et al.*,

2.3m

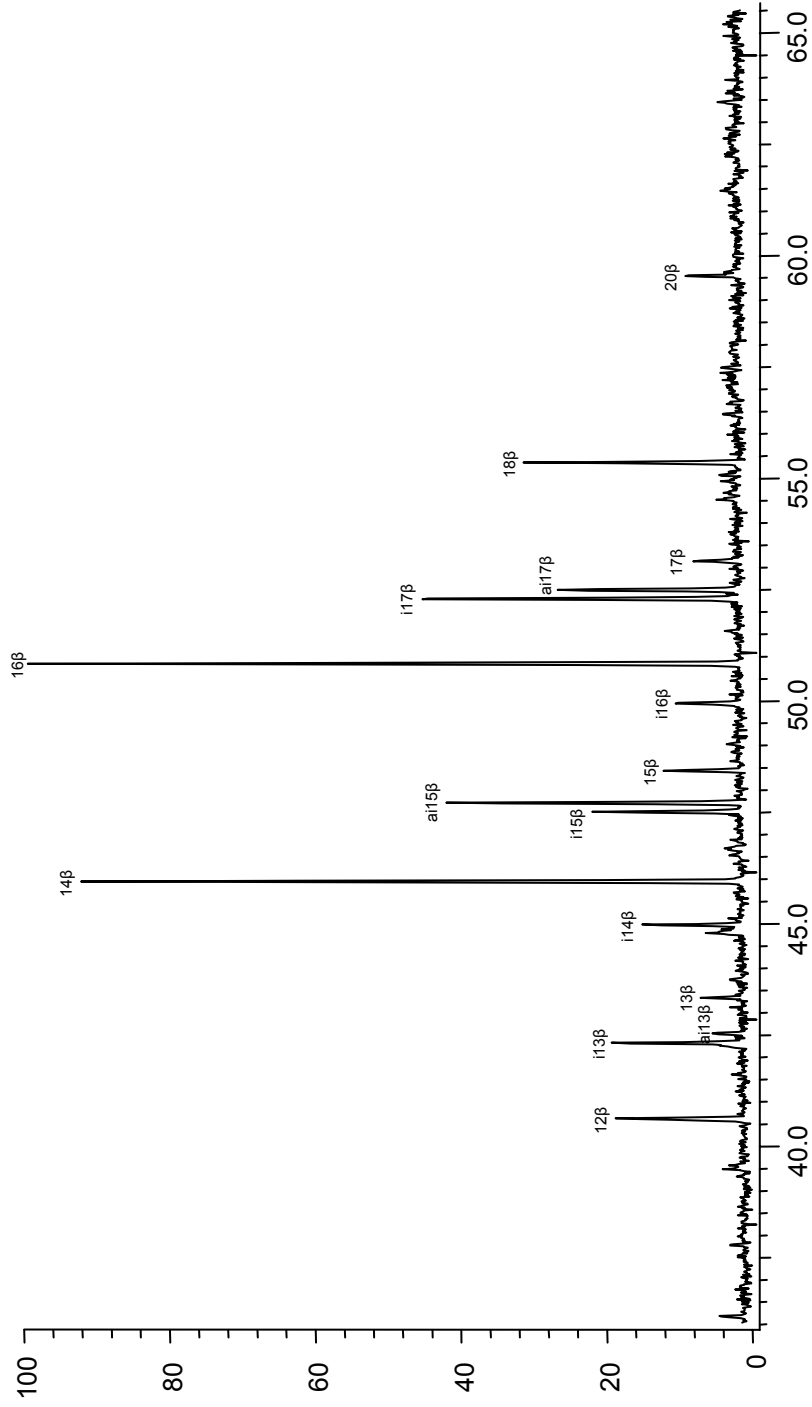


Fig. 5.14. Fragmentogram illustrating the distribution of β -hydroxy fatty acids in the ester-bound lipid fraction of core MBH 54/2.

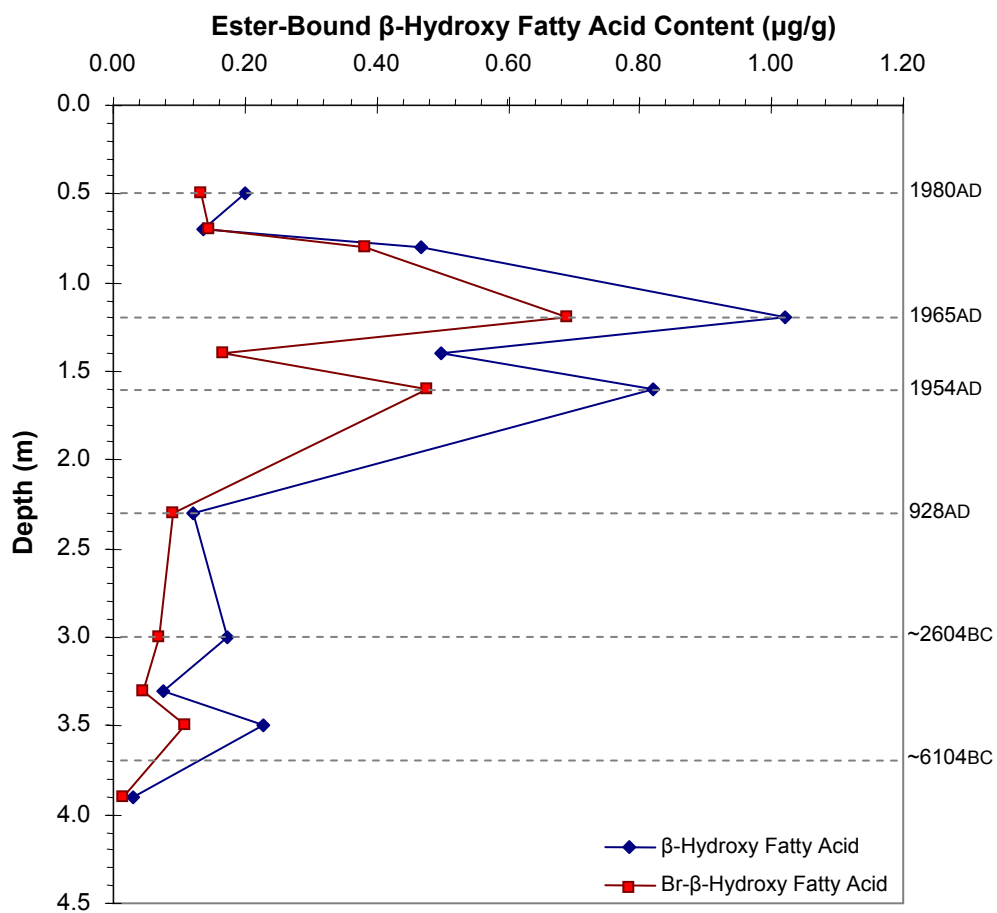


Fig. 5.15. Downcore profile of straight chain and branched β -hydroxy fatty acids ($\mu\text{g/g}$ dry sediment weight), in the ester-bound lipid fraction of core MBH 54/2.

1985; Mendoza *et al.*, 1987). The occurrence of β -hydroxy fatty acids in sediments is thought to reflect intact cellular remains of bacteria in the sediment (Klok *et al.*, 1988). The depth interval where a large flux in β -hydroxy fatty acids occurs (*i.e.*, 0.8m to 2.0m), corresponds to a period of rapid population growth in regions surrounding the study site. The rapid population growth, in turn, resulted in excess sewage waste discharged into Kowloon Bay. The increase in abundance of bacterially derived β -hydroxy fatty acids suggests that bacterial communities thrived during this period (between ~1933AD and 1974AD). The secondary flux at 3.5m probably indicates an event which led to an abundance of bacteria in the sediment. Similar fluxes suggesting the occurrence of bacterial remnants in sediments were observed in **Fig. 5.10** and **Fig. 5.11**, using branched-carboxylic acids as bacterial markers.

5.3.5 Ester-bound ω -Hydroxy Fatty Acids and n-Alcohols

Small amounts of even numbered ω -hydroxy fatty acids and n-alcohols were detected in the ester-bound lipid fraction of core MBH 54/2 (**Table 5.1**). Variable distributions of even numbered ω -hydroxy fatty acids (C_{16} to C_{26}) were identified in the ester-bound lipid fraction. The presence of ω -hydroxy fatty acids reflect contributions from vascular plant material, where C_{16} and C_{18} ω -hydroxy fatty acids are derived from cutin and C_{20+} ω -hydroxy fatty acids are likely derived from suberin (Cardoso *et al.*, 1977; Kawamura and Ishiwatari, 1984; Wünsche *et al.*, 1987; Fukushima *et al.*, 1992a,b). The downcore distribution of the total ω -

hydroxy fatty acid content in **Fig. 5.16** shows that there were at least two periods of high influx of terrigenous plant material (*i.e.*, around 1.6m and 3.3m).

The n-alcohols consisted of variable distributions of even numbered alcohols in the range C₁₆ to C₂₆. Short chain alcohols (*e.g.*, C₁₂, C₁₄, and C₁₆) are typically used as indicators of marine organisms, whereas long chain alcohols (C₂₀₊) originate from cuticular waxes of terrigenous plant material (Mudge and Norris, 1997; Mudge and Seguel, 1999). Terrigenous plant material may be the primary source of alcohols detected in the ester-bound lipid fraction. The downcore distribution pattern of the total n-alcohol content (**Fig. 5.17**) follows the pattern observed for the downcore distribution of the total ω -hydroxy fatty acid content. At least two periods of high influx of terrigenous plant material were seen at 1.6m and 3.3m, analogous to the ω -hydroxy fatty acids. The two periods with a high influx of terrigenous plant material may indicate periods of strong storms, which transported excess terrigenous plant material into the study site. The first spike occurred around 1.6m, which corresponds to a calendar date around 1954. Around this time period at least 7 typhoons were documented in this area (http://www.hko.gov.hk/informtc/historical_tc/no10track.htm).

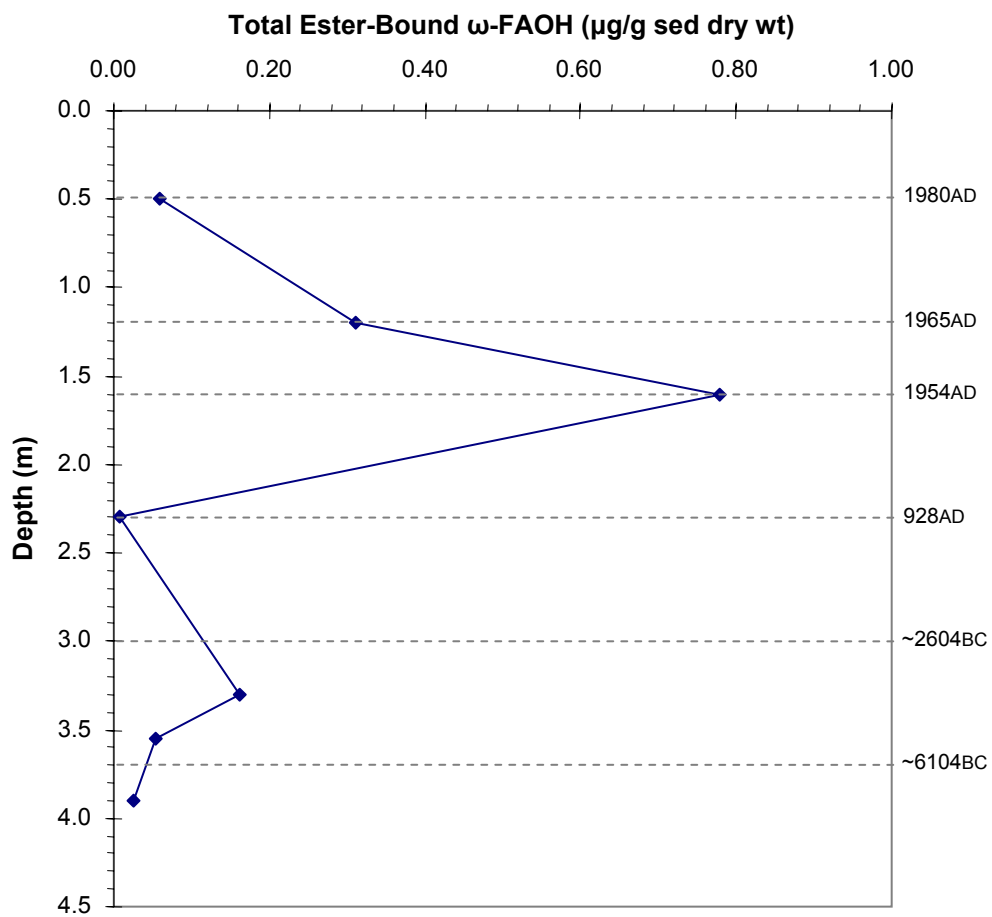


Fig. 5.16. Downcore distribution of ω -hydroxy fatty acids in the ester-bound lipid fraction of core MBH 54/2.

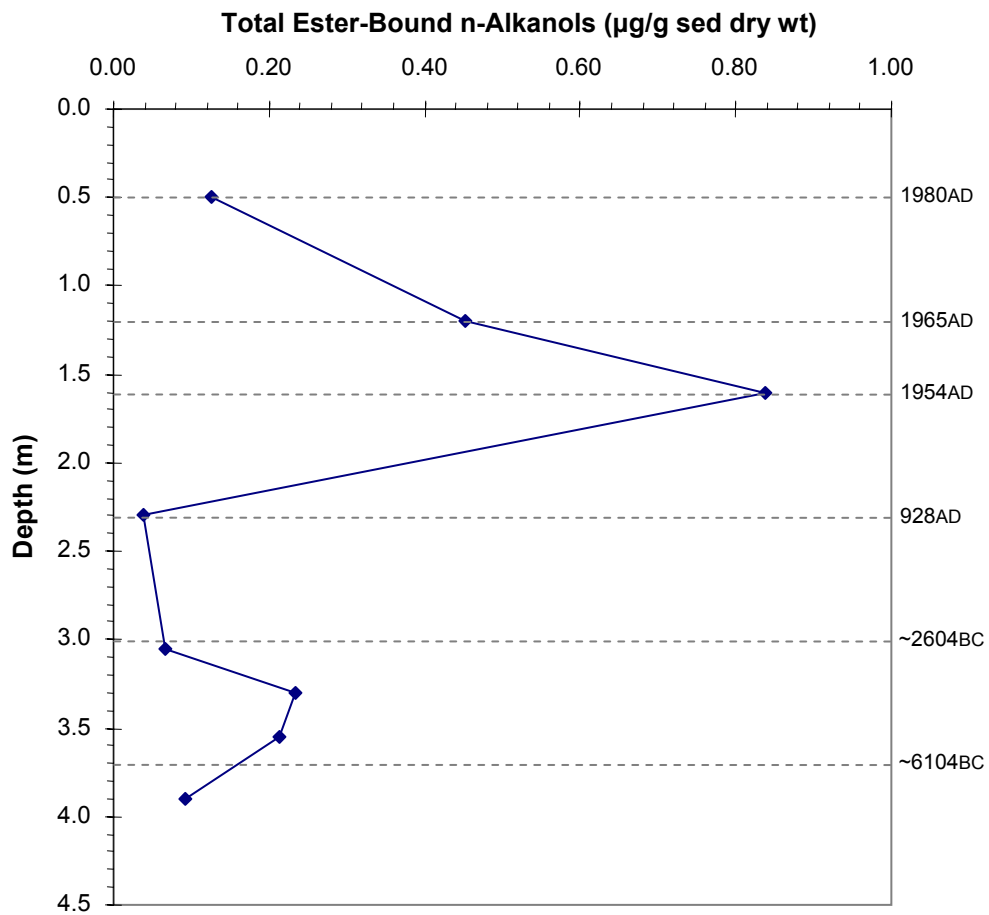


Fig. 5.17. Downcore distribution of n-alkohols in the ester-bound lipid fraction of core MBH 54/2.

5.3.6 Amide-Bound Carboxylic Acids

Amide-bound lipids consist of n-alkanoic acids and β -hydroxy fatty acids. The n-alkanoic acids are bimodally distributed between C_{12:0} and C_{30:0} (**Fig. 5.18**), and have an even-over-odd predominance pattern with an average CPI = 6.1. The short chain fatty acids (C_{12:0} to C_{20:0}) have an average CPI = 7.0, and the long chain fatty acids (C_{20:0} to C_{30:0}) have an average CPI = 4.9 (**Fig. 5.19**). In the uppermost interval of core MBH 54/2 (0.5m to 0.8m), the CPI over the total carbon number range (C_{12:0} to C_{30:0}) falls between 5.3 and 6.0. Between 1.0m and 2.0m, the CPI (C_{12:0} to C_{30:0}) increases to 10.2, decreases to 4.0 to 4.8 (between 3.0m and 3.8m), and increases slightly to 6.7 at 3.9m. The relatively high CPI values indicate that the n-alkanoic acids have not been significantly reworked by bacteria. The slight decrease in CPI values between 3.0m and 3.8m may indicate that slight alterations (e.g., bacterial degradation) may have occurred at these depths. An increase in the presence of bacterial lipids within this depth range supports alterations due to bacteria.

Analogous to the ester-bound lipid fraction, the short chain fatty acids (C_{12:0} to C_{20:0}) are more abundant than the long chain fatty acids (C_{21:0} to C_{30:0}). The downcore plot of the aquatic-to-terrigenous ratio (*i.e.*, $\Sigma(C_{12:0}-C_{18:0})/\Sigma(C_{22:0}-C_{28:0})$; **Fig. 5.20**) illustrates the change in contributions of organic source material. A high influx of aquatically derived organic matter is observed between 0.8m and 2.3m, and at 3.9m. The aquatic-to-terrigenous ratio then decreases between 2.6m and 3.3m, possibly due to a slight increase in contributions from terrigenous plant material.

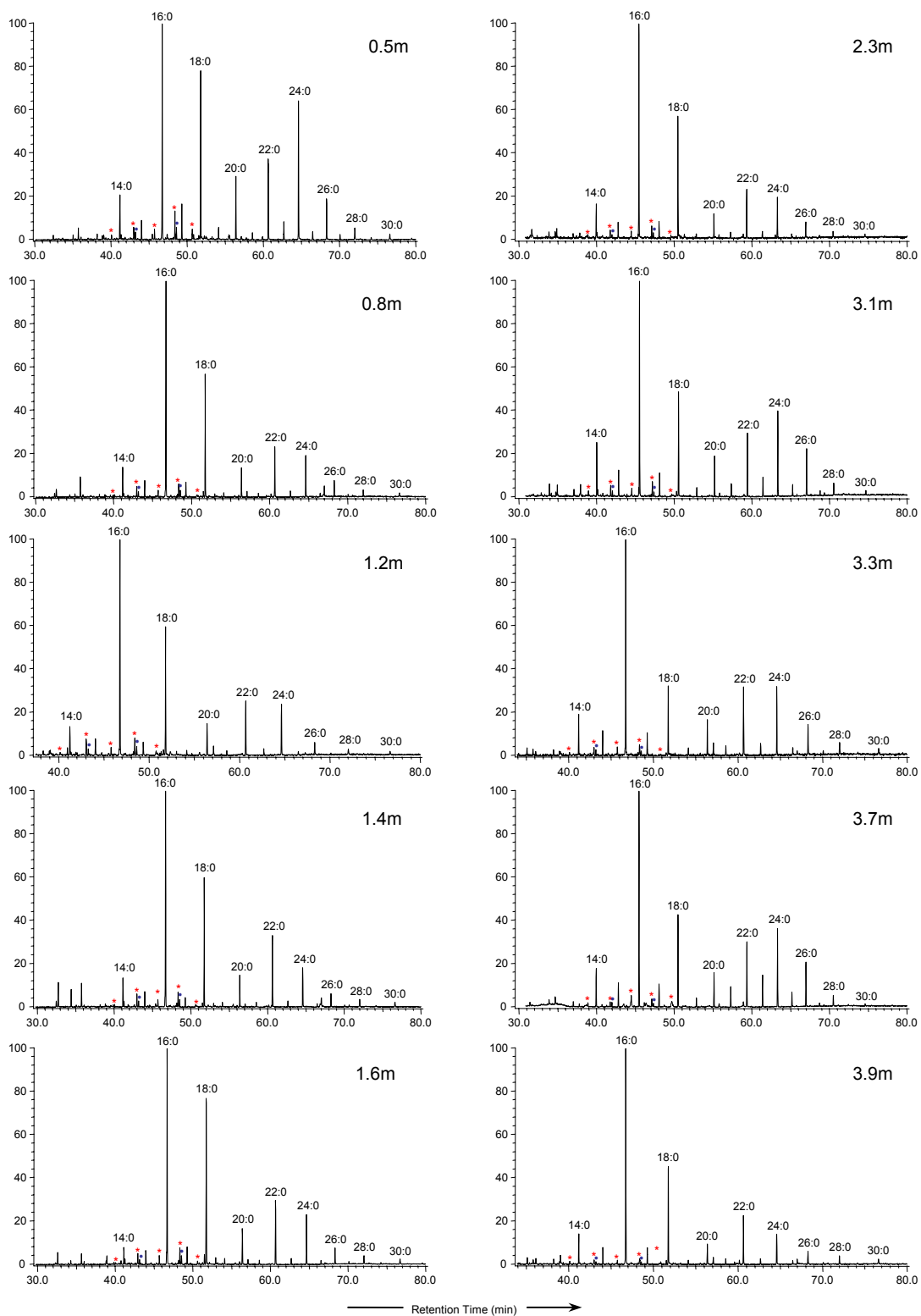


Fig. 5.18. Downcore profile of fatty acids as methyl esters in the amide-bound lipid fraction of core MBH 54/2. * indicates iso- branched fatty acids, and • indicates anteiso- branched fatty acids.

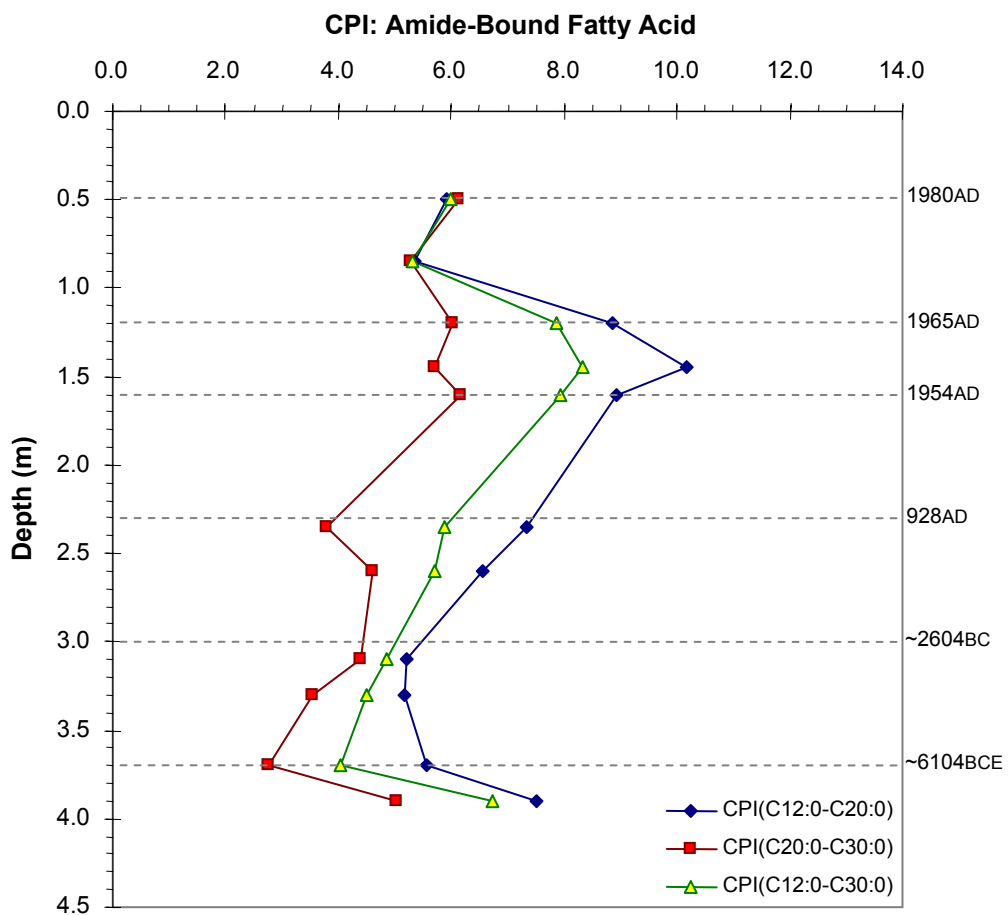


Fig. 5.19. Average CPI of fatty acids in the amide-bound lipid fraction, relative to depth. CPIs were calculated using eq. 5.1, eq. 5.2, eq. 5.3.

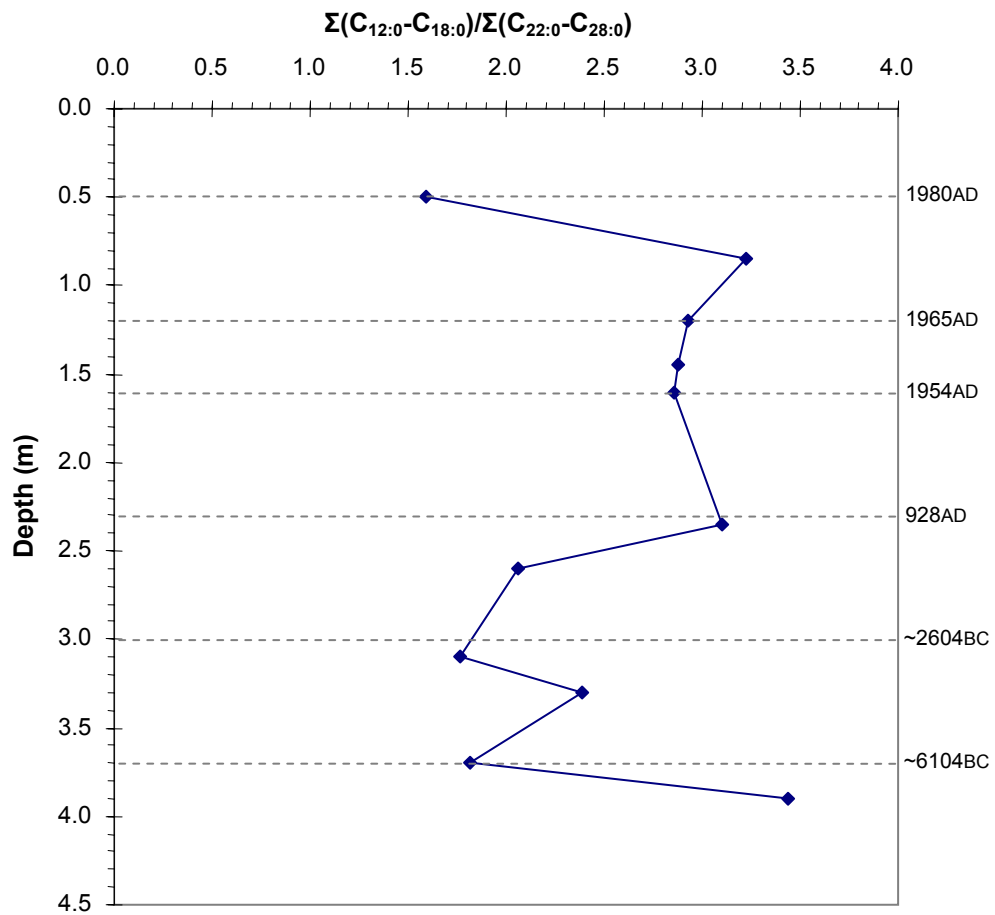


Fig. 5.20. Aquatic-to-Terrigenous ratio using n-alkanoic acids in the amide-bound lipid fraction.

5.3.7 Amide-Linked β -Hydroxy Fatty Acids

β -Hydroxy fatty acids are more abundant in the amide-bound lipid fraction, than in the ester-bound lipid fraction (**Fig. 5.21**). The β -hydroxy fatty acid profiles (C_{10} to C_{20}) consists of significant amounts of iso- and anteiso- β -hydroxy fatty acids (**Fig. 5.22**). β -Hydroxy fatty acids in the amide-bound lipid fraction are unique to bacteria and are widespread in Gram-negative bacteria (Edlund *et al.*, 1985; Mendoza *et al.*, 1987; Klok *et al.*, 1988; Kaneda, 1991; Bhat and Carlson, 1992; Wakeham, 1999; Garcette-Lepecq *et al.*, 2004).

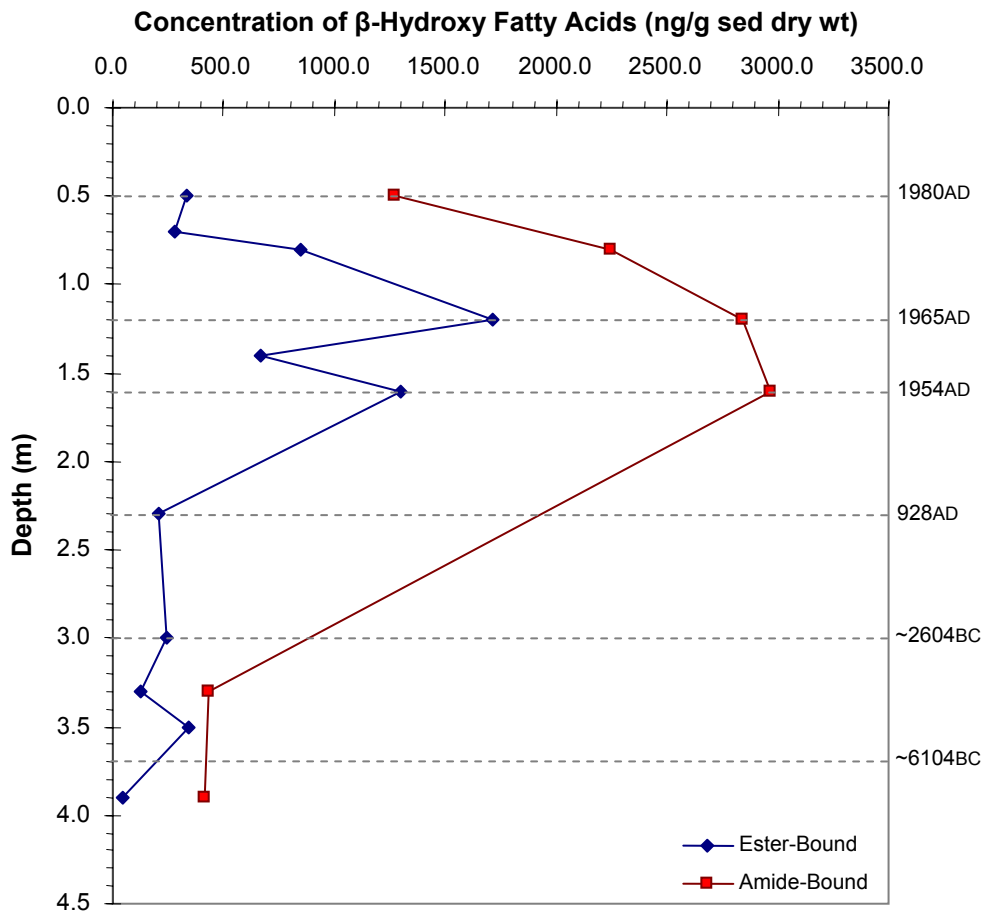


Fig. 5.21. Downcore abundance of ester- and amide-bound β -hydroxy fatty acids in core MBH 54/2.

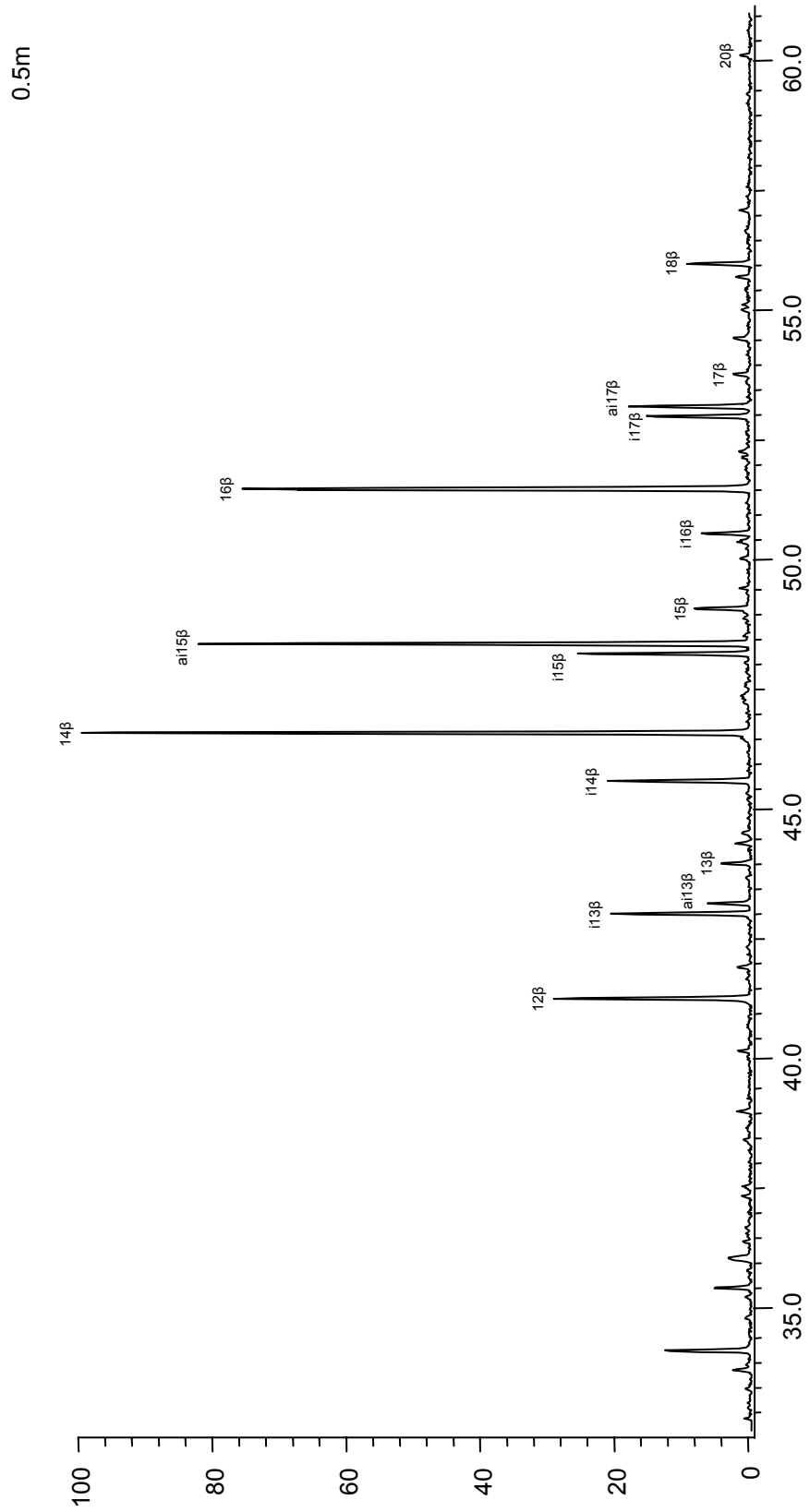


Fig. 5.22. Fragmentogram illustrating the distribution of β -hydroxy fatty acids in the amide-bound lipid fraction of core MBH 54/2.

5.3.8 Compound-Specific Carbon Isotope Composition of Ester- and Amide-Bound Fatty Acids

The carbon isotopic values for ester-bound fatty acids (C_{14:0} to C_{30:0}), at depths between 0.8m and 2.6m, are generally more depleted in ¹³C than corresponding values at 3.3m and 3.9m (**Fig. 5.23**). The δ¹³C compositions of fatty acids at 3.7m, however, are slightly isotopically lighter than at adjacent depth intervals (*i.e.*, 3.3m and 3.9m). In general, the isotopic composition of C_{15:0} and C_{18:0+} fatty acids at 3.7m are still enriched in ¹³C relative to the average isotopic compositions measured between 0.8m and 2.6m. Downcore distributions of δ¹³C compositions for individual ester-bound fatty acids (*i.e.*, C_{14:0} to C_{30:0}) are illustrated in **Figures 5.24a-c**. At depths between 0.8m and 3.1m, δ¹³C values ranged between -26‰ and -33‰. Each of the ester-bound fatty acids (C_{14:0} to C_{30:0}) demonstrated a general overall enrichment in ¹³C at depths below 3.1m.

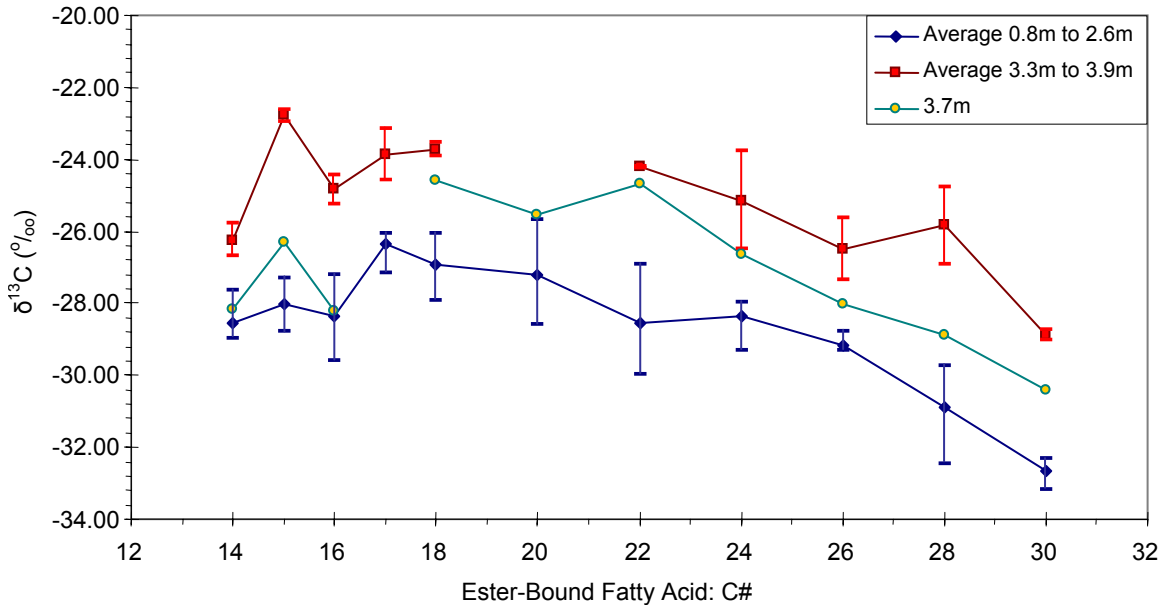


Fig. 5.23. Average carbon isotopic composition of ester-bound fatty acids at depths ranging from 0.8m to 2.6m, and the average isotopic composition at 3.3m and 3.9m.

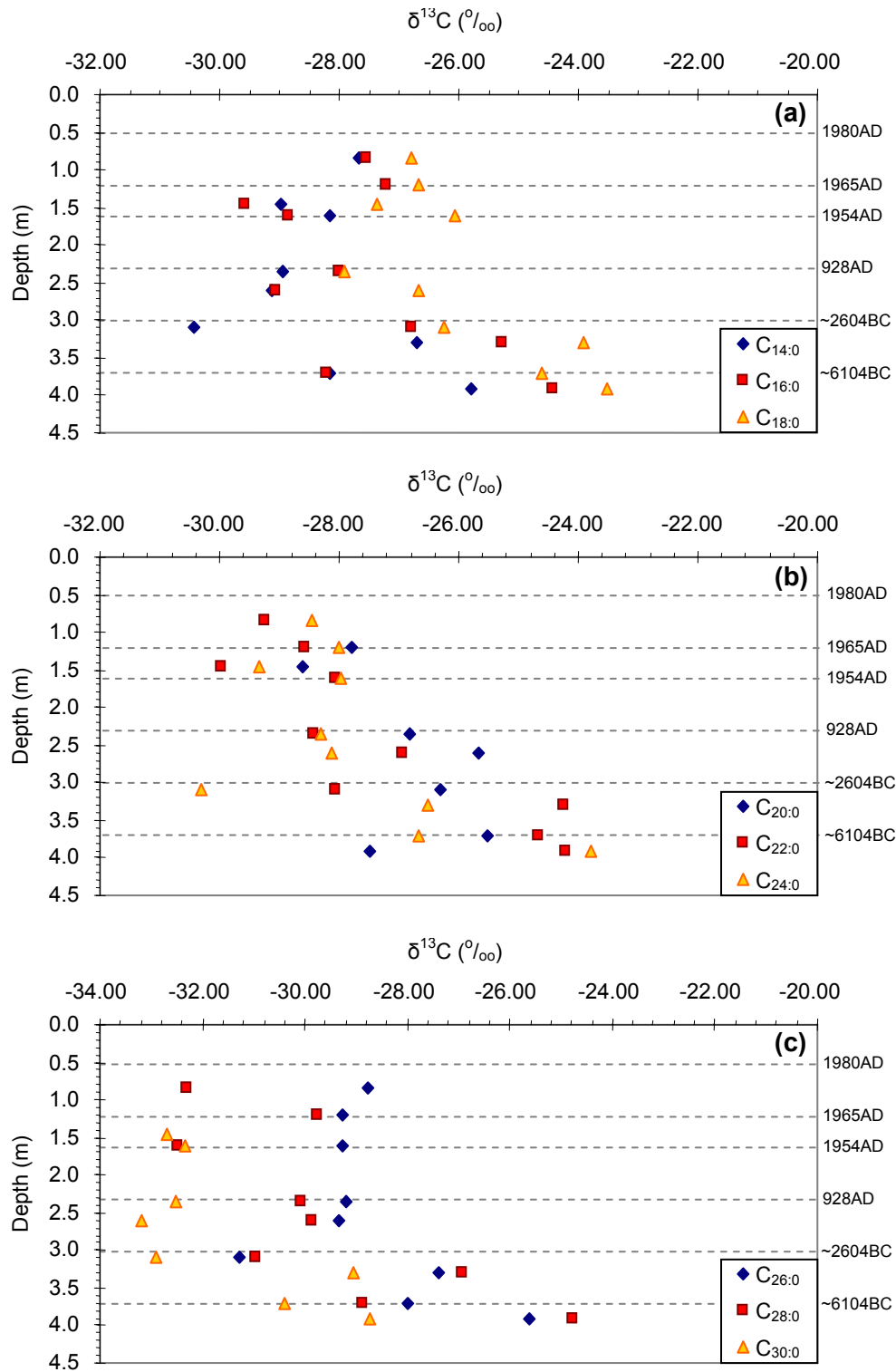


Fig. 5.24a-c. Downcore carbon isotopic composition of ester-bound fatty acids.

Throughout the core, C_{28:0} and C_{30:0} ester-bound fatty acids are more depleted in ¹³C, compared to ester-bound fatty acids <C_{28:0}. The isotopic composition of C_{28:0} fatty acids range between -29.76‰ and -32.49‰; whereas C_{30:0} fatty acids are isotopically lighter, with δ¹³C values ranging between -32.35‰ and -33.19‰. The C_{28:0} and C_{30:0} fatty acids are likely derived from C3 terrigenous plants. Slight enrichments in ¹³C were observed at depths of 3.3m and 3.9m, where δ¹³C values for C_{28:0} fatty acids are -26.92‰ and -24.76‰, respectively; and δ¹³C values for C_{30:0} fatty acids are -29.04‰ and -28.74‰, respectively. The slight enrichment in ¹³C observed at 3.3m and 3.9m may be due to mixing with C4 terrigenous plants.

Branched fatty acids (e.g., i- and ai-C_{15:0} and C_{17:0}) are typically used as markers for bacteria. In the ester-bound lipid fraction, i- and ai-C_{15:0} have δ¹³C values ranging between -28.11‰ to -30.59‰ (in the upper 2.6m), and are isotopically heavier at 3.3m and 3.9m with an average isotopic composition of -23.75‰ (**Fig. 5.25**). Similarly, i- and ai-C_{17:0} are isotopically lighter at shallower depths (i.e., upper 1.6m, where δ¹³C ranges between -27.08‰ and -28.02‰) and isotopically heavier deeper in the core (i.e., at 3.9m, δ¹³C = -24.66‰; **Fig. 5.25**). In general, however, each of the ester-bound fatty acids appear to be isotopically lighter in the upper half of the core, then systematically become enriched in ¹³C with increasing depth.

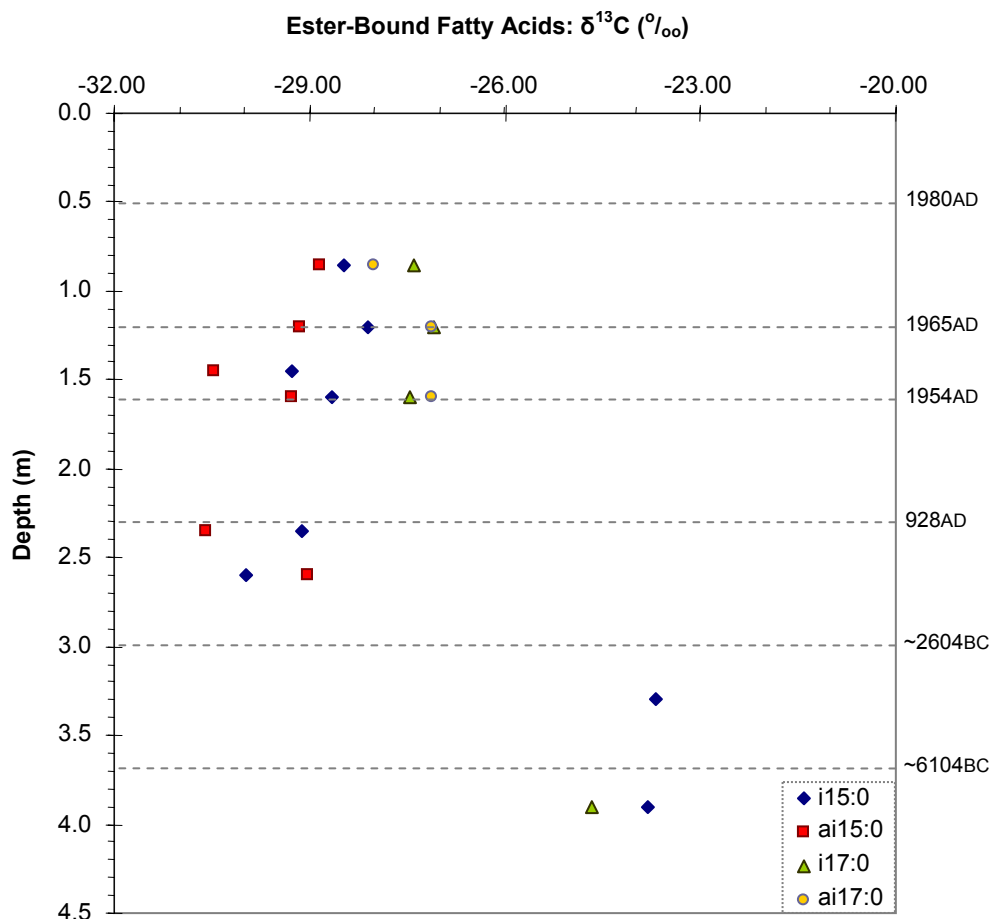


Fig. 5.25. Carbon isotopic composition of i- and ai-C_{15:0} and C_{17:0} ester-bound fatty acids in core MBH 54/2.

The isotopic compositions of amide-bound fatty acids demonstrate more variability downcore (**Fig. 5.26a-c**). C_{14:0} and C_{16:0} amide-bound fatty acids have $\delta^{13}\text{C}$ values ranging between -26.26‰ to -29.34‰ , and -25.50‰ to -29.12‰ , respectively; where C_{14:0} fatty acids are generally slightly lighter than C_{16:0} fatty acids. Amide-bound fatty acids (C_{18:0} to C_{30:0}) exhibit more shifts in isotopic compositions downcore, where $\delta^{13}\text{C}$ values at 0.5m are more enriched in ¹³C compared to all other depths (**Fig. 5.27**). The isotopic composition of C_{16:0} to C_{28:0}

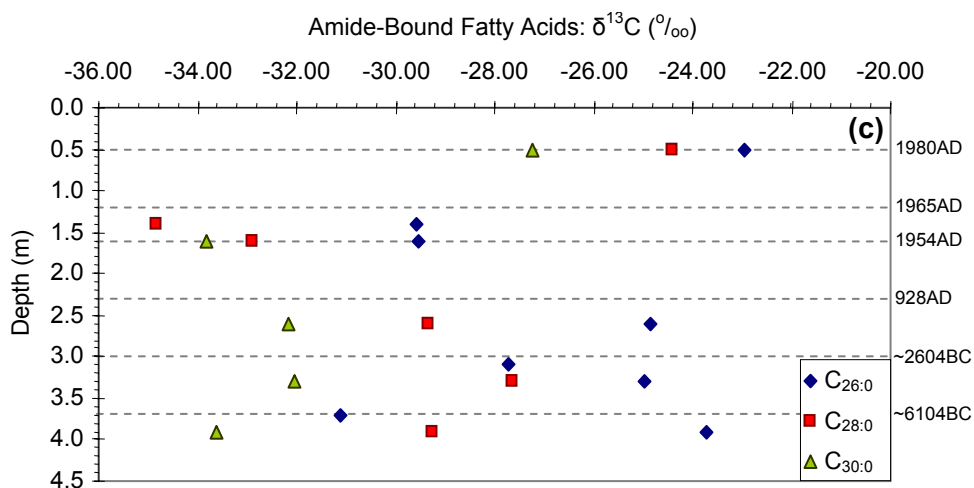
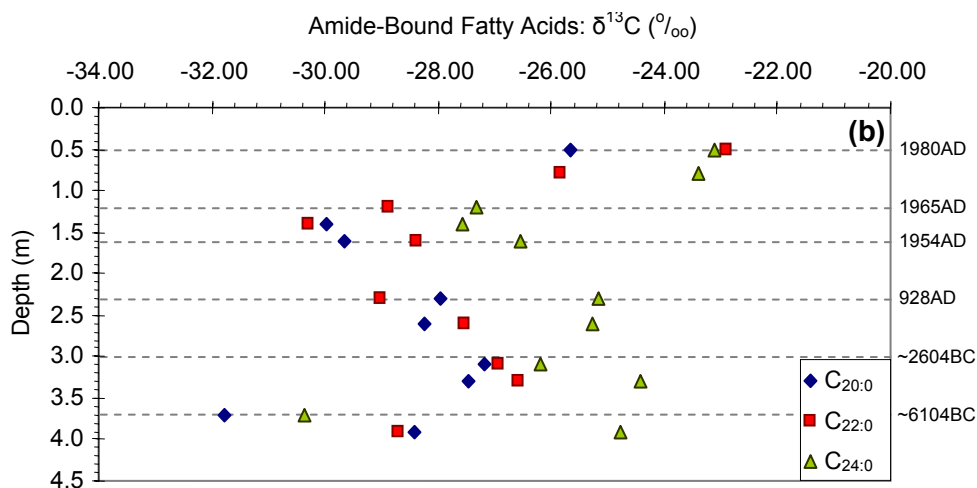
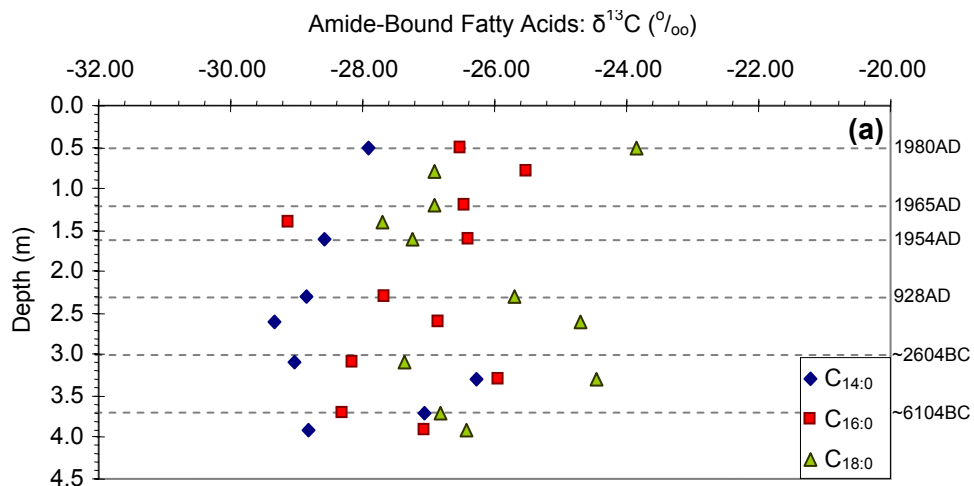


Fig. 5.26a-c. Carbon isotopic composition of amide-bound fatty acids in core MBH 54/2.

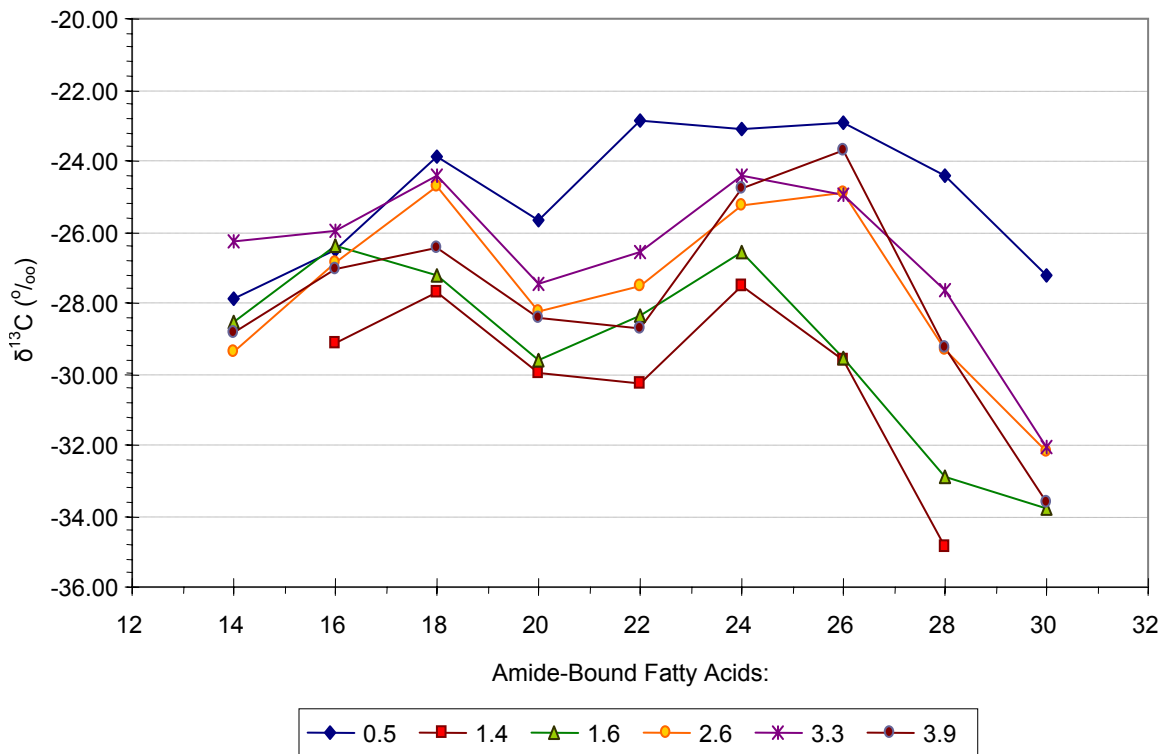


Fig. 5.27. Isotopic composition of amide-bound fatty acids, at increasing depth intervals in core MBH 54/2.

fatty acids are more depleted in ^{13}C at 1.4m, than at other depth intervals. $\text{C}_{18:0}$, $\text{C}_{24:0}$, and $\text{C}_{26:0}$ fatty acids demonstrate enrichments in ^{13}C at 2.3m, 2.6m, 3.3m, and 3.9m (**Fig. 5.26a-c**). At depths of 1.4m and 3.7m, $\delta^{13}\text{C}$ values are slightly lighter than isotopic compositions measured at adjacent depth intervals.

Limited information is currently available on the carbon isotopic composition of fatty acids in bacteria. Various groups (*e.g.*, Abraham *et al.*, 1998; Boschker *et al.*, 1999; Londry *et al.*, 2001; Boschker and Middelburg, 2002;

Londry and Des Marais, 2003) have proposed that the isotopic composition of bacterial fatty acids can be used to evaluate the substrate utilized or to determine if the bacteria were autotrophic or heterotrophic. In a study by Londry *et al.* (2004) the isotopic composition of fatty acids were measured for four types of sulfate reducing bacteria, grown autotrophically, heterotrophically, or mixotrophically, on substrates of known isotopic composition. No consistent fractionation pattern was observed between the isotopic composition of fatty acids relative to the biomass or substrate, where differences were dependent on growth mode or bacteria type. For example, Londry *et al.* (2004) reported that *Desulfovibrio desulfuricans* grown heterotrophically with lactate (-29.1‰) resulted in fatty acids (-41.0‰) that were 11.7‰ lighter than their biomass (-29.3‰) and 11.9‰ lighter than the substrate. When grown mixotrophically with acetate (-34.2‰), fatty acids (-36.2‰) were 4.1‰ lighter than biomass (-32.1‰) and 2.0‰ lighter than substrate. *Desulfobacter hydrogenophilus* grown autotrophically produced fatty acids (-52.2‰) that were 11.8‰ lighter than biomass (-40.4‰) and 24.4‰ lighter than substrate. *Desulfobacter hydrogenophilus* was also grown heterotrophically with acetate (-34.2‰), producing fatty acids (-48.1‰) that were 13.3‰ lighter than biomass (-34.9‰) and 13.9‰ lighter than substrate. Abraham *et al.* (1998) also compared the isotopic compositions of fatty acids in a set of bacteria grown with different substrates (*e.g.*, glycerol, glucose, mannose, lactose, and a complex medium). They found that the isotopic composition of fatty acids varied between bacterial strains based on the substrates being utilized. It is uncertain whether compound specific carbon isotopes can be used to

differentiate bacterial strains, substrates being utilized, or growth modes being followed, by measuring the isotopic composition of lipids in marine sediments. Under natural environmental settings, the situation is much more complex where multiple bacterial strains and substrates are present, and where each of the bacteria follows a different growth mode and competes for available substrate. This will require further investigation.

There have been reports of the isotopic composition of bacterial fatty acids measured around methane seeps (Hinrichs *et al.*, 2000; Orphan *et al.*, 2001; Zhang *et al.*, 2002; Pancost and Sinninghe Damsté, 2003). The isotopic compositions of lipids from bacteria, involved in anaerobic methane oxidation, were measured in these studies. In general, the $\delta^{13}\text{C}$ composition of fatty acids was depleted in ^{13}C , and had isotopic values within the range of the methane seeps. Pancost and Sinninghe Damsté (2003) used *i*- and *ai*- $\text{C}_{15:0}$ and $\text{C}_{17:0}$ fatty acids as markers for sulfate reducing bacteria. The isotopic composition of these branched fatty acids ranged between -60 and -90‰ , demonstrating that the sulfate reducing bacteria were involved in anaerobic methane oxidation. Fatty acids in sediments from core MBH 54/2, in Kowloon Bay, did not have isotopic compositions that were significantly depleted in ^{13}C . Isotopic values of bacterial fatty acids ranged between -22 and -34‰ , possibly suggesting that biogenic methane was not a significant carbon source or that the bacteria did not play a significant role in anaerobic methane oxidation.

The compound-specific carbon isotope measurement of ester- and amide-bound fatty acids will require more in-depth evaluation for potential future

applications. There are currently many uncertainties with potential fractionation effects that may occur with the cleaving of ester- and amide-linkages in bound fatty acids. Ester- and amide-bound fatty acids are likely derived from cellular membranes of a broad variety of bacteria, which follow different metabolic pathways, and metabolize carbon sources from different substrates. Each of these variables further complicates the interpretation of the compound-specific carbon isotope composition of bound fatty acids. Further work should be conducted to determine if fractionation occurs during the isolation of bound lipids, and to better understand possible fractionation effects due to the type of bacteria, metabolic pathways, and type of substrate utilized.

5.4 Summary Remarks

Ester- and amide-bound lipids in sediment core MBH 54/2 from Kowloon Bay are well preserved and provide a record of the sources of organic matter. Ester-bound lipids were dominated by n-alkanoic acids and smaller amounts of hydroxy fatty acids and n-alcohols. The n-alkanoic acids had bimodal distributions where the first modal ranged between C_{12:0} and C_{20:0}, maximizing at C_{16:0}; the second modal was distributed between C_{20:0} and C_{30:0}, maximizing at either C_{22:0}, C_{24:0}, or C_{26:0}. Relatively high CPI values (average CPI = 6.5) suggest that the n-alkanoic acids are well preserved and have not undergone significant diagenetic alteration. While short chain fatty acids were typically more abundant than long-chain fatty acids throughout the core, this was more evident

at depths between 0.7m and 1.4m. This depth interval corresponds to a period of rapid population growth in Hong Kong, which led to the substantial discharge of sewage waste into Kowloon Bay.

Branched fatty acids were very abundant, constituting between 7.6% to 29.3% of the total short-chain fatty acid fraction. Branched fatty acids in the carbon range $C_{14:0}$ to $C_{16:0}$ may have been derived from Gram-positive bacteria or some type of anaerobic bacteria, while branched fatty acids in the $C_{16:0}$ to $C_{19:0}$ range may have originated from either sulfate-reducing bacteria or some type of anaerobic bacteria. Iso- and anteiso- $C_{15:0}$ fatty acids are abundant in various species of *Desulfovibrio* type sulfate reducing bacteria. *Desulfobacter* species of sulfate reducing bacteria were identified at depths of 1.4m, 1.6m, and 3.5m, using the signature lipid marker 10Me $16:0$ fatty acid. Monounsaturated and polyunsaturated fatty acids were not detected in any significant amounts. Only $C_{16:1}$, $C_{18:1}$, and $C_{18:2}$ were identified in the ester-bound lipid fraction.

β -Hydroxy fatty acids (C_{10} and C_{20}) were identified throughout the core, with significant amounts of iso- and anteiso- β -hydroxy fatty acids. The β -hydroxy fatty acids are derived from bacterial sources and demonstrate two periods of higher influx (*i.e.*, between 0.8m and 2.0m, and around 3.5m). The substantial influx of bacterial material (0.8m to 2.0m) occurs during the period of rapid population growth and excess discharge of sewage waste.

ω -Hydroxy fatty acids and n-alcohols were detected in minor amounts and are likely derived from cuticle waxes of terrigenous plant material. At least two intervals in the downcore profile indicate significant contributions from

terrigenous plant material. The two fluxes may be indications for the occurrence of strong storms in the area which could transport excess terrigenous plant material into the area.

Amide-bound lipids were dominated by β -hydroxy fatty acids and smaller amounts of n-alkanoic fatty acids. The β -hydroxy fatty acids are derived directly from the outer cellular membrane of bacteria and have carbon number distributions between C_{10} and C_{20} . n-Alkanoic fatty acids in the amide-bound lipid fraction, like the ester-bound fatty acids, were bimodally distributed between $C_{12:0}$ and $C_{30:0}$. The short-chain fatty acids $<C_{20:0}$ were likely derived from bacterial sources, while the long-chain fatty acids $>C_{20:0}$ originated from terrigenous plant material. More detailed profiles of β -hydroxy fatty acids from various strains of sulfate reducing bacteria and other types of anaerobic bacteria may provide a means to better delineate the types of bacteria in marine sediments.

Carbon isotopic compositions were measured for ester- and amide-bound fatty acids. Fatty acids in the ester-bound lipid fraction were isotopically lighter in the upper 3m of the core ($\delta^{13}C$ values ranged between about -26‰ to -33‰) and became enriched in ^{13}C at 3.3m and 3.9m. Enrichment in ^{13}C at 3.3m and 3.9m may have been due to the presence of significant amounts of C4-type terrigenous plants. A slight decrease in $\delta^{13}C$ composition was observed at 1.4m and 3.7m, which corresponds to spikes observed in the C/N ratio (discussed in Chapter 3). This depletion in $\delta^{13}C$ composition may reflect the influx of C3-type terrigenous plant material thought to have been carried into the study site via strong storms. The isotopic composition of amide-bound fatty acids

demonstrated more varied distributions downcore. However, similar to the ester-bound fatty acids, a slight decrease in $\delta^{13}\text{C}$ composition was also observed at 1.4m and 3.7m. It is still uncertain how the isotopic composition might be affected when ester- and amide-bound fatty acids are freed from sediment samples. Since the short-chain fatty acids are thought to be derived from bacterial sources, the interpretation of isotopic compositions becomes more challenging. The fatty acids most likely represent a broad range of bacterial strains, feeding on different substrates, and which follow different metabolic pathways. Further work is necessary to address each of these uncertainties.

5.5 References

- Abraham, W., Hesse, C., Pelz, O., 1998. Ratios of carbon isotopes in microbial lipids as an indicator of substrate usage. *Applied and Environmental Microbiology*, 64, 4202-4209.
- Abrajano Jr., T. A., Murphy, D. E., Fang, J., Comet, P., Brooks, J. M., 1994. $^{13}\text{C}/^{12}\text{C}$ ratios in individual fatty acids of marine mytilids with and without bacterial symbionts. *Organic Geochemistry*, 21, 611-617.
- Albaigés, J., Algaba, J., Grimalt, J., 1984. Extractable and bound neutral lipids in some lacustrine sediments. *Organic Geochemistry*, 6, 223-236.
- Barnes, R. O., Goldberg, E. D., 1976. Methane production and consumption in anoxic marine sediments. *Geology*, 4, 297-300.
- Bhat, U. R., Carlson, R. W., 1992. A new method for the analysis of amide-linked hydroxy fatty acids in Lipid-A from gram-negative bacteria. *Glycobiology*, 2, 535-539.
- Boon, J. J., DeLeeuw, G. W., Hoek, G. J., Vosjan, J. H., 1977. Significance and taxonomic value of iso and anteiso monoenoic fatty acids and branched beta-acids in *Desulfovibrio desulfuricans*. *Journal of Bacteriology*, 129, 1183-1191.

- Boschker, H. T. S., de Brouwer, J. F. C., Cappenberg, T. E., 1999. The contribution of macrophyte-derived organic matter to microbial biomass in salt-marsh sediments: Stable carbon isotope analysis of microbial biomarkers. *Limnology and Oceanography*, 44, 309-319.
- Boschker, H. T. S., Middelburg, J. J., 2002. Stable isotopes and biomarkers in microbial ecology. *FEMS Microbiology Ecology*, 40, 85-95.
- Boschker, H. T. S., Nold, S. C., Wellsbury, P., Bos, D., de Graaf, W., Pel, R., Parkes, R. J., Cappenberg, T. E., 1998. Direct linking of microbial populations to specific biogeochemical processes by ¹³C-labelling of biomarkers. *Nature*, 392, 801-805.
- Bray, E. E., Evans, E. D., 1961. Distribution of n-paraffins as a clue to the recognition of source beds. *Geochimica et Cosmochimica Acta*, 27, 1113-1127.
- Budge, S. M., Parrish, C. C., 1998. Lipid biogeochemistry of plankton, settling matter and sediments in Trinity Bay, Newfoundland. II Fatty Acids. *Organic Geochemistry*, 29, 1547-1559.
- Cardoso, J. N., Eglinton, G., Holloway, P. J., 1977. The use of cutin acids in the recognition of higher plant contribution to recent sediments. In: Campos, R., Goñi, J. (Eds), *Advances in Organic Geochemistry 1975*, Enadimsa, Madrid, 273-287.
- Collister, J. W., Rieley, G., Stern, B., Eglinton, G., Fry, B., 1994. Compound-specific $\delta^{13}\text{C}$ analyses of leaf lipids from plants with carbon dioxide metabolisms. *Organic Geochemistry*, 21, 619-627.
- Cranwell, P. A., 1973. Branched-chain and cyclopropanoid acids in a recent sediment. *Chemical Geology*, 11, 307-313.
- Cranwell, P. A., 1977. Organic geochemistry of Cam Loch (Sutherland) sediments. *Chemical Geology*, 20, 205-221.
- Cranwell, P. A., 1978. Extractable and bound lipid components in a freshwater sediment. *Geochimica et Cosmochimica Acta*, 47, 1523-1532.
- Cranwell, P. A., 1984. Lipid geochemistry of sediments from Upton Broad, a small productive lake. *Organic Geochemistry*, 7, 25-37.
- Cranwell, P. A., 1990. Paleolimnological studies using sequential lipid extraction from recent lacustrine sediment: recognition of source organisms from biomarkers. *Hydrobiologia*, 23, 293-303.

- Deines, P., 1980. The isotopic composition of reduced organic carbon. *In*: Fritz, P., Fontes, J. Ch. (Eds), *Handbook of Environmental Isotope Geochemistry*, vol. 1, Elsevier, Amsterdam, 329-406.
- Dowling, N. J. E., Widdel, F., White, D. C., 1986. Phospholipid ester-linked fatty acid biomarkers of acetate-oxidizing sulphate-reducers and other sulphide-forming bacteria, *Journal of General Microbiology*, 132, 1815-1825.
- Duan, Y., Wen, Q., Zheng, G., Luo, B., Ma, L., 1997. Isotopic composition and probable origin of individual fatty acids in modern sediments from Ruergai Marsh and Nansha Sea, China. *Organic Geochemistry*, 27, 583-589.
- Edlund, A., Nichols, P. D., Roffey, R., White, D. C., 1985. Extractable and lipopolysaccharides fatty acid profiles from *Desulfovibrio* species. *Journal of Lipid Research*, 26, 982-988.
- Farrington, J. W., Quinn, J. G., 1973. Biogeochemistry of fatty acids in recent sediments from Narragansett Bay, Rhode Island. *Geochimica et Cosmochimica Acta*, 37, 259-268.
- Findlay, R. H., Trexler, M. B., Guckert, J. B., White, D. C., 1990. Laboratory study of disturbance in marine sediments: response of a microbial community. *Marine Ecology Progress Series*, 62, 121-133.
- Froelich, P. N., Klinkhammer, G. P., Bender, M. K., Luedtke, N. A., Heath, G. R., Cullen, D., Dauphin, P., Hammond, D., Harman, B., Maynard, V., 1979. Early oxidation of organic matter in pelagic sediments of the eastern equatorial Atlantic: suboxic diagenesis. *Geochimica et Cosmochimica Acta*, 43, 1075-1090.
- Fukushima, K., Kondo, H., Sakata, S., 1992a. Geochemistry of hydroxyl acids in sediments – I. Some freshwater and brackish water lakes in Japan. *Organic Geochemistry*, 18, 913-922.
- Fukushima, K., Uzaki, M., Sakata, S., 1992b. Geochemistry of hydroxyl acids in sediments: II. Freshwater and brackish water lake in Japan. *Organic Geochemistry*, 18, 923-932.
- Garcette-Lepecq, A., Largeau, C., Bouloubassi, I., Derenne, S., Saliot, A., Lorre, A., Point, V., 2004. Lipids and their modes of occurrence in two surface sediments from the Danube delta and northwestern Black Sea: implications for sources and early diagenetic alteration I. Carboxylic acids. *Organic Geochemistry*, 35, 959-980.
- Goosens, H., Rijpstra, W. I. C., Düren, R. R., de Leeuw, J. W., 1986. Bacterial contribution to sedimentary organic matter; a comparative study of lipid moieties in bacteria and Recent sediments. *In*: Leythäeuser, D., Rullkötter, J. (Eds),

Advances in Organic Geochemistry 1985. Pergamon Press, Oxford. *Organic Geochemistry*, 10, 683-696.

Goosens, H., de Leeuw, J. W., Rijpstra, W. I. C., Meyburg, G. J., Schenck, P. A., 1989a. Lipids and their mode of occurrence in bacteria and sediments – I. A methodological study of the lipid composition of *Acinetobacter calcoceticus* LMD 79-41. *Organic Geochemistry*, 14, 15-25

Goosens, H., Düren, R. R., de Leeuw, J. W., Schenck, P. A., 1989b. Lipids and their mode of occurrence in bacteria and sediments – II. Lipids in the sediment of a stratified, freshwater lake. *Organic Geochemistry*, 14, 27-41.

Guezennec, J., Fiala-Medioni, A., 1996. Bacterial abundance and diversity in the Barbados Trench determined by phospholipid analysis. *FEMS Microbiology Ecology*, 19, 83-93.

Hinrichs, K. –U., Summons, R. E., Orphan, V., Sylva, S. P., Hayes, J. M., 2000. Molecular and isotopic analysis of anaerobic methane-oxidizing communities in marine sediments. *Organic Geochemistry*, 31, 1685-1701.

Hunt, J. M., 1996. *Petroleum Geochemistry and Geology* (2nd ed), Freeman, New York, 743p.

Jørgensen, B. B., 1982. Mineralization of organic matter in the sea bed – the role of sulphate reduction. *Nature*, 296, 643-645.

Jørgensen, B. B., 2000. Bacteria and marine biogeochemistry, *In*: Schulz, H. D., Zabel, M. (Eds.), *Marine Geochemistry*. Springer, Berlin. 173-207.

Kaneda, T., 1991. Iso- and anteiso- fatty acids in bacteria: biosynthesis, function, and taxonomic significance. *Microbiological Reviews*, 55, 288-302.

Kawamura, K., Ishiwatari, R., 1982. Tightly bound β -hydroxy acids in a Recent sediment. *Nature*, 297, 144-145.

Kawamura, K., Ishiwatari, R., 1984. Tightly bound aliphatic acids in Lake Biwa sediments: their origin and stability. *Organic Geochemistry*, 7, 121-126.

Kawamura, K., Tannenbaum, E., Huizinga, B. J., Kaplan, I. R., 1986. Long chain carboxylic acids in pyrolysates of Green River kerogen. *In*: Leythäeuser, D., Rullkötter, J. (Eds), *Advances in Organic Geochemistry 1985*. Pergamon Press, Oxford. *Organic Geochemistry*, 10, 1059-1065.

Klok, J., Baas, M., Cox, H. C., de Leeuw, J. W., Rijpstra, W. I. C., Schenck, P. A., 1984. Qualitative and quantitative characterization of the total organic matter in a Recent marine sediment (Part II). *Organic Geochemistry*, 6, 265-278.

Klok, J., Baas, M., Cox, H. C., de Leeuw, J. W., Rijpstra, W. I. C., Schenck, P. A., 1988. The mode of occurrence of lipids in a Namibian Shelf diatomaceous ooze with emphasis on the β -hydroxy fatty acids. *Organic Geochemistry*, 12, 75-80.

Lehninger, A. L., 1975. *Biochemistry* (2nd edition), Worth Publishers Inc., New York, 543-558.

Londry, K. L., Des Marais, D. J., 2003. Stable carbon isotope fractionation by sulfate-reducing bacteria. *Applied and Environmental Microbiology*, 69, 2942-2949.

Londry, K. L., Jahnke, L. L., Des Marais, D. J., 2001. Stable carbon isotope ratios of lipid biomarkers and biomass for sulfate-reducing bacteria grown with different substrates. *11th Annual V. M. Goldschmidt Conference, Hot Springs, Virginia, May 20-24, 2001*.

Londry, K. L., Jahnke, L. L., Des Marais, D. J., 2004. Stable carbon isotope ratios of lipid biomarkers of sulfate-reducing bacteria. *Applied and Environmental Microbiology*, 70, 745-751.

Mancuso, C. A., Franzmann, P. D., Burton, H. R., Nichols, P. D., 1990. Microbial community structure and biomass estimates of a methanogenic Antarctic Lake ecosystem as determined by phospholipid analyses. *Microbial Ecology*, 19, 73-95.

Martens, C. S., Berner, R. A., 1974. Methane production in the interstitial waters of sulfate-depleted marine sediments. *Science*, 185, 1167-1169.

Martens, C. S., Klump, J. V., 1984. Biogeochemical cycling in an organic-rich coastal marine basin 4. An organic carbon budget for sediments dominated by sulfate reduction and methanogenesis. *Geochimica et Cosmochimica Acta*, 48, 1987-2004.

Matsuda, H., Koyama, T., 1977. Early diagenesis of fatty acids in lacustrine sediments – II. A statistical approach to changes in fatty acid composition from recent sediments and source materials. *Geochimica et Cosmochimica Acta*, 41, 1825-1834.

Mendoza, Y. A., Gülaçar, F. O., Buchs, A., 1987. Comparison of extraction techniques for bound carboxylic acids in recent sediments 2. β -hydroxyacids. *Chemical Geology*, 62, 321-330.

Meyers, P. A., Ishiwatari, R., 1993. Lacustrine organic geochemistry – an overview of indicators of organic matter sources and diagenesis in lake sediments. *Organic Geochemistry*, 20, 867-900.

- Monson, K. D., Hayes, J. M., 1982. Carbon isotopic fractionation in the biosynthesis of bacterial fatty acids. Ozonolysis of unsaturated fatty acids as a means of determining the intramolecular distribution of carbon isotopes. *Geochimica et Cosmochimica Acta*, 46, 139-149.
- Mudge, S. M., Norris, C. E., 1997. Lipid biomarkers in the Conwy Estuary (North Wales, UK): a comparison between fatty alcohols and sterols. *Marine Chemistry*, 57, 61-84.
- Mudge, S. M., Seguel, C. G., 1999. Organic contamination of San Vicente Bay, Chile. *Marine Pollution Bulletin*, 38, 1011-1021.
- Naraoka, H., Ishiwatari, R., 1999. Carbon isotopic compositions of individual long-chain n-fatty acids and n-alkanes in sediments from river to open ocean: Multiple origins for their occurrence. *Geochemical Journal*, 33, 215-235.
- Naraoka, H., Ishiwatari, R., 2000. Molecular and isotopic abundances of long-chain n-fatty acids in open marine sediments of the western North Pacific. *Chemical Geology*, 165, 23-36.
- Naraoka, H., Yamada, K., Ishiwatari, R., 1995. Carbon isotopic difference of saturated long-chain n-fatty acids between a terrestrial and a marine sediment. *Geochemical Journal*, 29, 189-195.
- Nichols, P. D., Mancuso, C. A., White, D. C., 1987. Measurement of methanotroph and methanogen signature phospholipids for use in assessment of biomass and community structure in model ecosystems. *Organic Geochemistry*, 11, 451-461.
- O'Leary, W. M., 1962. The fatty acids of bacteria. *Bacteriological Reviews*, 26, 421-447.
- Orphan, V. J., House, C. H., Hinrichs, K. -U., McKeegan, K. D., DeLong, E. F., 2001. Methane-consuming Archaea revealed by directly coupled isotopic and phylogenetic analysis. *Science*, 293, 484-487.
- Pancost, R., Sinninghe Damsté, J., 2003. Carbon isotopic compositions of prokaryotic lipids as tracers of carbon cycling in diverse settings. *Chemical Geology*, 195, 29-58.
- Parkes, R. J., Gibson, G. R., Mueller-Harvey, I., Buckingham, W. J., Herbert, R. A., 1989. Determination of the substrates for sulphate-reducing bacteria within marine and estuarine sediments with different rates of sulphate reduction. *Journal of General Microbiology*, 135, 175-187.

- Perry, G. J., Volkman, J. K., Johns, R. B., 1979. Fatty acids of bacterial origin in contemporary marine sediments. *Geochimica et Cosmochimica Acta*, 43, 1715-1725.
- Petsch, S. T., Edwards, K. J., Eglinton, T. I., 2003. Abundance, distribution and $\delta^{13}\text{C}$ analysis of microbial phospholipid-derived fatty acids in a black shale weathering profile. *Organic Geochemistry*, 34, 731-743.
- Rajendran, N., Matsuda, O., Imamura, N., Urushigawa, Y., 1992a. Determination of microbial biomass and its community structure from the distribution of phospholipid ester-linked fatty acids in sediments of Hiroshima Bay and its adjacent bays. *Estuarine, Coastal and Shelf Science*, 34, 501-514.
- Rajendran, N., Matsuda, O., Urushigawa, Y., 1992b. Distribution of polar lipid fatty acid biomarkers for bacteria in sediments of a polluted bay. *Microbios*, 72, 143-152.
- Rajendran, N., Suwa, Y., Urushigawa, Y., 1992c. Microbial community structure in sediments of a polluted bay as determined by phospholipid ester-linked fatty acids. *Marine Pollution Bulletin*, 24, 305-309.
- Ratledge, C., Wilkinson, S. G., 1988. Microbial lipids. Vol. 1, Academic Press, London.
- Reeburgh, W. S., 1980. Anaerobic methane oxidation: rate depth distribution in Skan Bay sediments. *Earth and Planetary Science Letters*, 47, 345-352.
- Rütters, H., Sass, H., Cypionka, H., Rullkötter, J., 2002. Phospholipid analysis as a tool to study complex microbial communities in marine sediments. *Journal of Microbiological Methods*, 48, 149-160.
- Saliot, A., Laureillard, J., Scribe, P., Sicre, M. A., 1991. Evolutionary trends in the lipid biomarker approach for investigating the biogeochemistry of organic matter in the marine environment. *Marine Chemistry*, 36, 233-248.
- Skerratt, J. H., Nichols, P. D., Bowman, J. P., Sly, L. I., 1992. Occurrence and significance of long-chain (ω -1)-hydroxy fatty acids in methane utilizing bacteria. *Organic Geochemistry*, 18, 189-194.
- Smallwood, B. J., Wolff, G. A., 2000. Molecular characterization of organic matter in sediments underlying the oxygen minimum zone at the Oman Margin, Arabian Sea. *Deep Sea Research II*, 47, 353-375.
- Stefanova, M., Disnar, J. R., 2000. Composition and early diagenesis of fatty acids in lacustrine sediments, lake Aydat (France). *Organic Geochemistry*, 31, 41-55.

- Summit, M., Peacock, A., Ringelberg, D., White, D. C., Baross, J. A., 2000. Phospholipid fatty acid-derived microbial biomass and community dynamics in hot, hydrothermally influenced sediments from Middle Valley, Juan De Fuca Ridge. *In: Zierenberg, R. A., Fouquet, Y., Miller, D. J., Normark, W. R. (Eds), Proceedings of the Ocean Drilling Program, Scientific Results*, 169, 1-19.
- Summons, R. E., Jahnke, L. L., Roksandic, Z., 1994. Carbon isotopic fractionation in lipids from methanotrophic bacteria: relevance for interpretation of the geochemical record of biomarkers. *Geochimica et Cosmochimica Acta*, 58, 2853-2863.
- Tolosa, I., Lopez, J. F., Bentaleb, I., Fontugne, M., Grimalt, J. O., 1999. Carbon isotope ratio monitoring-gas chromatography mass spectrometric measurements in the marine environment: biomarker sources and paleoclimate applications. *The Science of the Total Environment*, 237/238, 473-481.
- Vainshtein, M., Hippe, H., Kroppenstedt, R. M., 1992. Cellular fatty acid composition of *Desulfovibrio* species and its use in classification of sulfate-reducing bacteria. *Systematic and Applied Microbiology*, 15, 554-566.
- Valentine, D. L., Reeburgh, W. S., 2000. New perspectives on anaerobic methane oxidation. *Environmental Microbiology*, 2, 477-484.
- Wakeham, S. G., 1999. Monocarboxylic, dicarboxylic and hydroxyl acids released by sequential treatments of suspended particles and sediments of the Black Sea. *Organic Geochemistry*, 30, 1059-1074.
- Weckesser, J., Drews, G., 1979. Lipopolysaccharides of photosynthetic Prokaryotes. *Annual Review of Microbiology*, 33, 215-239.
- Wünsche, L., Mendoza, Y. A., Gülaçar, F. O., 1988. Lipid geochemistry of a post-glacial lacustrine sediment. *Organic Geochemistry*, 13, 1131-1143.
- Zegouagh, Y., Derenne, S., Largeau, C., Saliot, A., 2000. A geochemical investigation of carboxylic acids released via sequential treatments of two surficial sediments from the Changjiang delta and East China Sea. *Organic Geochemistry*, 31, 375-388.
- Zelles, L., 1999. Fatty acid patterns of phospholipids and lipopolysaccharides in the characterization of microbial communities in soils: a review. *Biology and Fertility of Soils*, 29, 111-129.
- Zelles, L., Rackwitz, R., Bai, Q. Y., Beck, T., Beese, F., 1995. Discrimination of microbial diversity by fatty acid profiles of phospholipids and lipopolysaccharides in differently cultivated soils. *In: Collins, H. P., Robertson, G. P., Klug, M. J.*

(Eds.), *The Significance and Regulation of Soil Biodiversity*, Kluwer Academic Publishers, Netherlands, 115-122.

Zhang, C., Li, Y., Wall, J., Larsen, L., Sassen, R., Huang, Y., Wang, Y., Peacock, A., White, D., Horita, J., Cole, D., 2002. Lipid and carbon isotopic evidence of methane-oxidizing and sulfate-reducing bacteria in association with gas hydrates from the Gulf of Mexico. *Geology*, 30, 239-242.

CHAPTER 6

Conclusions and Recommendations for Future Work

6.1 Concluding Remarks

Core MBH 54/2 consists of two sediment units, a dark greenish gray to black Holocene mud unit and a desiccated crust unit representing sediments from the upper unit of the late Pleistocene. Very little has been done on the detailed organic geochemical characterization of sediment cores around Hong Kong, which could provide a glimpse of changes to environmental conditions, changes in organic matter source contributions, and changes in bacterial communities throughout the late Quaternary.

Recent dredging activities around Hong Kong have resulted in the release of methane from the Recent sediments, initiating interest in the study of potential sources of methane in Victoria Harbour. The initial goal was to study the downcore variations in isotopic composition of methane in a 4m core section (MBH 54/2) from Kowloon Bay, in Victoria Harbour, Hong Kong. However, methane was not detected in the core sediments. Hence, a lipid marker approach was undertaken to determine the sources of organic matter, evaluate changes in organic matter composition and environmental conditions during the Quaternary, and to ascertain whether remnants of bacterial communities might be present to enlighten our understanding of processes that may have contributed to methane generation. Organic geochemistry tools such as bulk properties (*e.g.*, %C_{org}, %N, $\delta^{13}\text{C}_{\text{org}}$, and $\delta^{15}\text{N}$), lipid composition and profiles were applied to delineate and

map changes in organic matter sources deposited in the Kowloon Bay area of Victoria Harbour during the late Quaternary.

6.1.1 Summary of Bulk Parameter Measurements

Bulk properties (*i.e.*, %C_{org}, %N, $\delta^{13}\text{C}_{\text{org}}$, and $\delta^{15}\text{N}$) of sedimentary organic matter were measured in core MBH 54/2. Fluctuations in the sources of organic matter derived from terrigenous and aquatic sources can be assessed using the C/N ratio. Although the Holocene unit in core MBH 54/2 appears as a thick unit of dark greenish gray to black mud, the C/N ratio demonstrates significant changes in sedimentary organic matter sources at different periods in Hong Kong's history. Higher C/N ratios are observed between 0.7m and 1.6m (C/N ratios generally fall between 13.7 and 14.7). Sediments deposited at this depth interval correspond to calendar dates between ~1954AD and ~1977AD, a period after significant portions of Kowloon Bay had been reclaimed and when untreated sewage was discharged into the study site. Below this depth range (*i.e.*, 1.8m to 2.3m), Kowloon Bay was an open bay and the area did not receive significant amounts of raw sewage. A sharp shift towards lower C/N ratios (*i.e.*, between 8.4 and 9.8) is observed at these depths, indicating that there was a higher input of aquatically-derived organic matter. C/N ratios were more variable between 2.6m and 3.5m, with values shifting between 10.5 and 15.7. The frequent fluctuations suggested that these sediments received a mixture of aquatically and terrigenously derived organic matter. Spikes in the C/N ratio were observed at

1.4m, 2.6m, 3.3m, and 3.7m (where C/N ratios were 18.9, 15.7, 14.7, and 17.2, respectively). The sharp spikes in the C/N ratio may reflect periods of strong storms, carrying excess terrigenously derived organic matter into the area.

Bulk stable isotope compositions (*i.e.*, $\delta^{13}\text{C}_{\text{org}}$, and $\delta^{15}\text{N}$) between 0.7m and 1.6m ranged between -28.59‰ to -26.30‰ and 2.14‰ to 3.44‰ , respectively. These isotopic values are consistent with isotopic compositions reported in the literature for sewage contaminated sites. A shift towards isotopically heavier $\delta^{13}\text{C}_{\text{org}}$ values (-21.87‰) was observed at 3.7m in the desiccated crust. The enrichment in ^{13}C may reflect higher contributions from C4-type plants (*e.g.*, C4 seagrasses) thought to have once been present around Hong Kong. The base of the core (4.0m to 4.1m) had $\delta^{13}\text{C}_{\text{org}}$ values ranging between -33.17‰ and -30.18‰ , and a nitrogen isotope composition of 2.53‰ (at 4.0m). These isotopic compositions suggest contributions from C3-type terrigenous plants, fixating atmospheric nitrogen as their nitrogen source.

6.1.2 Summary of Free Lipid Composition and Profiles

Free lipids in sediments from core MBH 54/2 consisted of sterols, n-alcohols, fatty acids, and hydrocarbons. The lipids can be used to delineate sources of sedimentary organic matter and to provide a record of past environmental conditions. The relative abundance of stanols-to-sterols suggested that conditions in Kowloon Bay were anoxic. The stanols were significantly more

abundant than sterols between 1.1m and 1.6m (~1967AD and ~1954AD, respectively), and again around 3.4m (~4604BC). These two depth intervals represent periods when Victoria Harbour was highly anoxic. Lower stanol-to-sterol ratios were observed at 0.5m and between 2.0m and 3.0m, indicating that conditions were less anoxic. At 0.5m, the seawall-type sewage outfall was diverted further out into the channel of Victoria Harbour via a submarine-type sewage outfall. Between 2m and 3m, Kowloon Bay was an open bay and did not receive significant contributions of sewage waste. Conditions appear to have been more favorable for aquatic organisms during these periods. Sterols common to aquatic organisms (*e.g.*, brassicasterol and campesterol) were observed at these depths; however, they were not detected at 1.1m and 1.6m when conditions were more anoxic. Fecal sterols (*e.g.*, coprostanol, epicoprostanol, 24-ethylcoprostanol, and 24-ethylepicoprostanol) were identified at relatively high concentrations compared to cholesterol at 1.1m and 1.6m. These depths corresponded to periods of rapid population growth in Hong Kong, and periods of high sewage disposal into Kowloon Bay.

Free lipids commonly used to distinguish between aquatic and terrigenous sources include n-alcohols, fatty acids, and n-alkanes. Short chain n-alcohols and fatty acids (<C₂₀) denote an aquatic source, whereas long chain n-alcohols and fatty acids (>C₂₀) indicate a terrigenous source. The n-alcohols were dominated by the longer chain constituents, indicating that they were derived from cuticular waxes of terrigenous plant material. Fatty acids demonstrated bimodal distributions where short chain fatty acids were more prevalent at 1.1m

and 1.6m. More terrigenously derived organic matter appears to be more abundant than aquatically derived organic matter in the bottom half of the core. Branched fatty acids (*i.e.*, iso- and anteiso-C_{13:0}, C_{15:0}, and C_{17:0}) indicate a bacterial source. The n-alkanes in core MBH 54/2 had pronounced odd-over-even preference patterns at all depths. It is likely that these hydrocarbons originated from a biotic source, probably cuticular waxes of terrigenous plant material.

6.1.3 Summary of Ester- and Amide-Bound Lipids

Ester- and amide-bound lipids in Recent sediments have not been widely utilized but are well preserved and can provide a record of sources of organic matter. Ester-bound lipids in sediments from core MBH54/2 were dominated by carboxylic acids and β -hydroxy fatty acids, with smaller amounts of n-alcohols and ω -hydroxy fatty acids. While the carboxylic acids had a bimodal distribution, the short chain fatty acids (C_{12:0} to C_{20:0}) predominated over long chain fatty acids throughout the core. Branched fatty acids made up a significant fraction (7.6% to 29.3%) of the total short chain fatty acids and are associated with Gram-positive bacteria, sulfate-reducing bacteria, and other types of anaerobic bacteria. At depths of 1.4m, 1.6m, and 3.5m, the signature marker 10Me16:0 fatty acid was identified. The occurrence of 10Me16:0 fatty acids in the sediments indicate the presence of *Desulfobacter* species of sulfate-reducing bacteria.

The β -hydroxy fatty acids (C_{10} to C_{20}) are unique to bacteria and can be found at all depths of core MBH 54/2. At least two periods of high influx of β -hydroxy fatty acids occur between 0.8m and 2.0m, and around 3.5m. The interval between 0.8m and 2.0m was a period when excess raw sewage was discharged into Kowloon Bay, and conditions appear to have been highly anoxic. Around 3.5m, the event that occurred is not known, but environmental conditions around that depth appear to have been more anoxic.

Lipid markers for terrigenous plants were also identified in the ester-bound lipid fraction. These include ω -hydroxy fatty acids and n-alcohols, which are common components of cuticular waxes of land plant material. There were at least two periods of high influx of terrigenous plants, denoted by greater contributions of vascular plant material (*i.e.*, indicated by higher abundance of ω -hydroxy fatty acids and n-alcohols) at depths around 1.6m and 3.3m. Sharp fluxes in the C/N ratio were also observed around these depths. The higher flux of ω -hydroxy fatty acids and n-alcohols may support the idea that spikes in the C/N ratio are indications of the occurrence of strong storms in the area, which can carry in excess terrigenous plant material.

Amide-bound lipids are comprised of β -hydroxy fatty acids and n-alkanoic acids. The β -hydroxy fatty acids are the dominant compound group in the amide-bound form and are thought to be derived directly from the outer cellular membrane of bacteria. More detailed β -hydroxy fatty acid profiles of various strains of sulfate-reducing bacteria and other types of bacteria may provide a means to differentiate bacterial communities in marine sediments.

6.2 Recommendations for Future Work

Organic geochemical characterization of sediments from core MBH 54/2 demonstrated that bulk properties (such as the C/N ratio, $\delta^{13}\text{C}_{\text{org}}$ and $\delta^{15}\text{N}$ compositions), lipid marker composition, and profiles can be used to reconstruct past contributions of sedimentary organic matter and to infer environmental conditions as the organic matter was being deposited. This study looked at the deposition of sedimentary organic matter in an area of Kowloon Bay that has undergone significant environmental transformations (*e.g.*, reclamation activities, which in turn have increased sedimentation rates), experienced extreme conditions (*e.g.*, excessive raw sewage disposal directly into the study site), organic matter transported into the area from the Pearl River, and strong storms (which are capable of carrying in excess terrigenous plant material).

In order to gain a broader perspective and understanding of organic matter deposition throughout Hong Kong during the late Quaternary, detailed organic geochemical characterization should be carried out on cores throughout Victoria Harbour and in regions surrounding Hong Kong. A sediment core from the western border of Victoria Harbour might show a greater influence of sedimentary organic matter from the Pearl River, whereas sediment cores from the eastern rim may show a greater marine influence. Core sites should be selected in areas throughout Victoria Harbour that have experienced variable sedimentation rates, proximity to raw sewage disposal sites, and areas that have undergone changes in oxic/anoxic conditions. Each of these factors will have an

impact of the amount and type of sedimentary organic matter deposited and accumulated around Hong Kong.

The occurrence and identification of bacterial remnants in Victoria Harbour sediments should be studied further. If bacterial strains native to Victoria Harbour can be isolated and identified, their lipid profiles may allow us to gain better insights into the types of bacterial communities that were active in Victoria Harbour sediments (*i.e.*, to try and link bacterial lipid profiles to lipid profiles preserved in ester- and amide-bound forms in sediment samples). This may help us understand the roles of bacteria in organic matter remineralization and their role in the consumption and/or generation of carbon dioxide or methane.

Compound-specific carbon isotopes can be measured on ester- and amide-bound fatty acids in sediments. However, it is uncertain if isotopic fractionations occur during the cleavage of ester- or amide-linkages. Further work should be conducted to investigate potential fractionation effects on synthesized ester- and amide-bound fatty acids of known isotopic composition. This would provide better confidence in the possible application of compound-specific isotope compositions of bound fatty acids. The ester- and amide-bound fatty acids in sediments are likely derived from cellular membranes of bacteria. Recent groups (*e.g.*, Boschker *et al.*, 1998, 1999; Abraham *et al.*, 1998; Boschker and Middleburg, 2002; Petsch *et al.*, 2003; Londry and Des Marais, 2003; Londry *et al.*, 2004) have begun evaluating the compound-specific carbon isotope analysis of fatty acids in bacteria. This is a complicated task with many variables to consider in interpreting the isotopic composition of bound fatty acids (*e.g.*, type of

bacteria, metabolic pathway and carbon sources being metabolized). Each of these uncertainties will need to be addressed in order to better utilize and incorporate compound-specific isotope measurements of bound lipids as a tool to better understand processes recorded in Recent sediments.

6.3 References

Abraham, W., Hesse, C., Pelz, O., 1998. Ratios of carbon isotopes in microbial lipids as an indicator of substrate usage. *Applied and Environmental Microbiology*, 64, 4202-4209.

Boschker, H. T. S., de Brouwer, J. F. C., Cappenberg, T. E., 1999. The contribution of macrophyte-derived organic matter to microbial biomass in salt-marsh sediments: Stable carbon isotope analysis of microbial biomarkers. *Limnology and Oceanography*, 44, 309-319.

Boschker, H. T. S., Middelburg, J. J., 2002. Stable isotopes and biomarkers in microbial ecology. *FEMS Microbiology Ecology*, 40, 85-95.

Boschker, H. T. S., Nold, S. C., Wellsbury, P., Bos, D., de Graaf, W., Pel, R., Parkes, R. J., Cappenberg, T. E., 1998. Direct linking of microbial populations to specific biogeochemical processes by ¹³C-labelling of biomarkers. *Nature*, 392, 801-805.

Londry, K. L., Des Marais, D. J., 2003. Stable carbon isotope fractionation by sulfate-reducing bacteria. *Applied and Environmental Microbiology*, 69, 2942-2949.

Londry, K. L., Jahnke, L. L., Des Marais, D. J., 2004. Stable carbon isotope ratios of lipid biomarkers of sulfate-reducing bacteria. *Applied and Environmental Microbiology*, 70, 745-751.

Petsch, S. T., Edwards, K. J., Eglinton, T. I., 2003. Abundance, distribution and $\delta^{13}\text{C}$ analysis of microbial phospholipid-derived fatty acids in a black shale weathering profile. *Organic Geochemistry*, 34, 731-743.

APPENDIX I

A1.1. Bulk measurements of sediments from core MBH 54/2: total organic carbon (%C_{org}) and total nitrogen (%N).

Depth (m)	%C _{org}	Avg %C _{org} ± stdev	%N	Avg %N ± stdev
0.5	0.75	0.75 ± 0.00	0.07	0.07 ± 0.00
	0.75		0.07	
0.7	1.28		0.09	
0.9	1.51	1.68 ± 0.20	0.12	0.12 ± 0.01
	1.90		0.13	
	1.64		0.12	
1.2	2.74		0.20	
1.4	2.83		0.15	
1.6	1.62		0.11	
1.8	0.88		0.09	
2.1	0.75	0.83 ± 0.07	0.08	0.09 ± 0.00
	0.85		0.09	
	0.90		0.09	
2.2	0.59		0.07	
2.4	0.62		0.07	
2.6	1.03	0.94 ± 0.13	0.06	0.06 ± 0.00
	0.85		0.06	
2.8	0.77	0.73 ± 0.05	0.06	0.06 ± 0.00
	0.70		0.05	
3.1	0.67	0.63 ± 0.05	0.06	0.06 ± 0.00
	0.65		0.06	
	0.65		0.06	
	0.50		0.06	
	0.56		0.06	
3.4	0.89	0.88 ± 0.01	0.06	0.06 ± 0.00
	0.88		0.06	
3.5	0.87	0.83 ± 0.06	0.07	0.07 ± 0.00
	0.79		0.07	
3.7	0.87	0.86 ± 0.04	0.05	0.05 ± 0.00
	0.89		0.05	
	0.81		0.04	
	0.89		0.05	
3.9	0.48	0.42 ± 0.09	0.04	0.04 ± 0.00
	0.36		0.04	
4.0	0.26	0.22 ± 0.05	0.03	0.03 ± 0.00
	0.19		0.03	
4.1	0.45	0.39 ± 0.06	0.03	0.03 ± 0.00
	0.35		0.03	
	0.29		0.03	
	0.42		0.03	
	0.42		0.03	
4.2	0.27	0.23 ± 0.06	0.04	0.04 ± 0.00
	0.19		0.04	

^abad value – atmospheric nitrogen present

^bbad value – inorganic carbon present

A1.2. Bulk measurements of sediments from core MBH 54/2: $\delta^{13}\text{C}_{\text{org}}$ (‰) and $\delta^{15}\text{N}$ (‰).

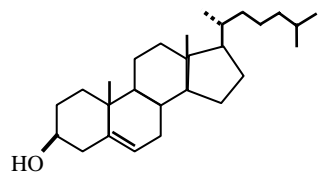
Depth (m)	$\delta^{13}\text{C}_{\text{org}}$	Avg $\delta^{13}\text{C}_{\text{org}} \pm \text{stdev}$	$\delta^{15}\text{N}$	Avg $\delta^{15}\text{N} \pm \text{stdev}$
0.5	-22.50	-22.60 ± 0.14		
	-22.70			
0.7	-23.86		6.19	
0.9	-28.93	-28.59 ± 0.30	2.66	2.57 ± 0.08
	-28.38		2.51	
	-28.46		2.55	
1.2	-26.62		3.44	
1.4	-26.30		2.14	
1.6	-27.49		3.13	
1.8	-27.74		4.49	
2.1	-28.20	-27.99 ± 0.18	3.19	3.05 ± 0.26
	-27.92		3.20	
	-27.87		2.75	
2.2	-27.12		4.30	
2.4	-26.92		4.27	
2.6	-26.40	-26.01 ± 0.54		
	-25.63		4.43	
2.8	-27.22	-27.25 ± 0.05		
	-27.29		3.61	
3.1	-26.84	-27.23 ± 0.29		
	-27.25			
	-27.26			
	-26.03		1.956 ^a	
	-27.56		4.60	
3.4	-24.71	-24.74 ± 0.04		
	-24.76		4.57	
3.5	-27.41	-27.50 ± 0.13		
	-27.58		4.33	
3.7	-16.24 ^b	-21.87 ± 0.08		4.51 ± 0.30
	-21.96		4.51	
	-21.80		4.81	
	-21.86		4.21	
3.9	-26.10	-26.27 ± 0.24		
	-26.43		4.26	
4.0	-30.56	-30.18 ± 0.54		
	-29.79		2.53	
4.1	-31.03	-31.85 ± 0.45 (if delete -29.94, then avg= -31.04 ± 0.03)		
	-31.09			
	-31.02			
	-31.03			
	-31.03			
	-29.94			
4.2	-33.10	-33.17 ± 0.10		
	-33.24			

^abad value – atmospheric nitrogen present

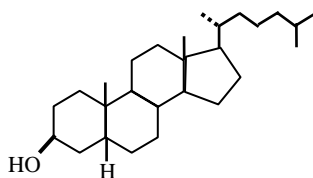
^bbad value – inorganic carbon present

APPENDIX II

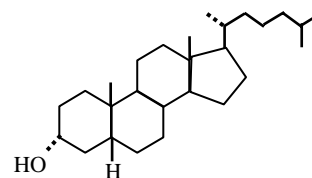
A2.1. Sterol structures, common names, IUPAC names, and chemical formula.



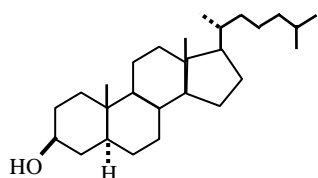
Cholesterol
(Cholest-5-en-3 β -ol)
 $C_{27}H_{48}O$



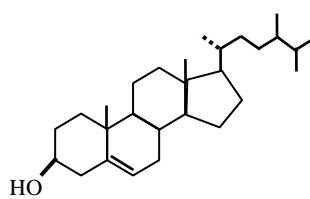
Coprostanol
(5 β -Cholestan-3 β -ol)
 $C_{27}H_{48}O$



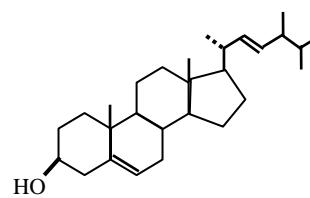
Epicoprostanol
(5 β -Cholestan-3 α -ol)
 $C_{27}H_{48}O$



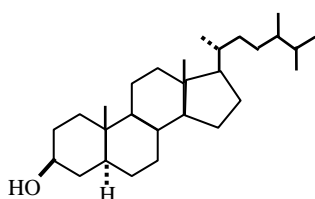
Cholestanol
(5 α -cholestan-3 β -ol)
 $C_{27}H_{48}O$



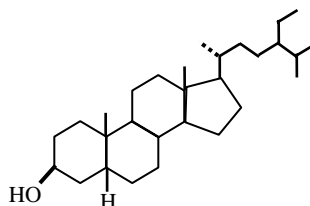
Campesterol
(24-methylcholest-5-en-3 β -ol)
 $C_{28}H_{48}O$



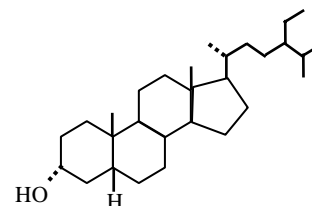
Brassicasterol
(24-methylcholesta-5,22E-dien-3 β -ol)
 $C_{28}H_{50}O$



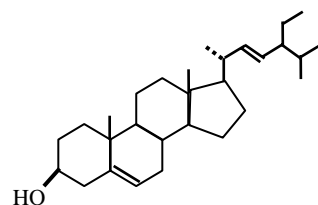
Campestanol
(24-methyl-5 α -cholestan-3 β -ol)
 $C_{28}H_{50}O$



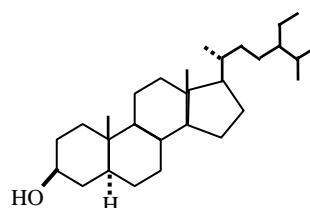
24-Ethylcoprostanol
(24-ethyl-5 β -cholestan-3 β -ol)
 $C_{29}H_{52}O$



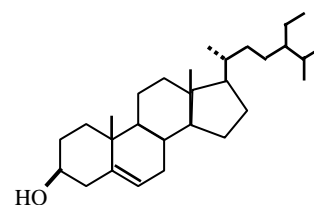
24-Ethylepicoprostanol
(24-ethyl-5 β -cholestan-3 α -ol)
 $C_{29}H_{52}O$



Stigmasterol
(24-ethylcholesta-5,22E-dien-3 β -ol)
 $C_{29}H_{48}O$



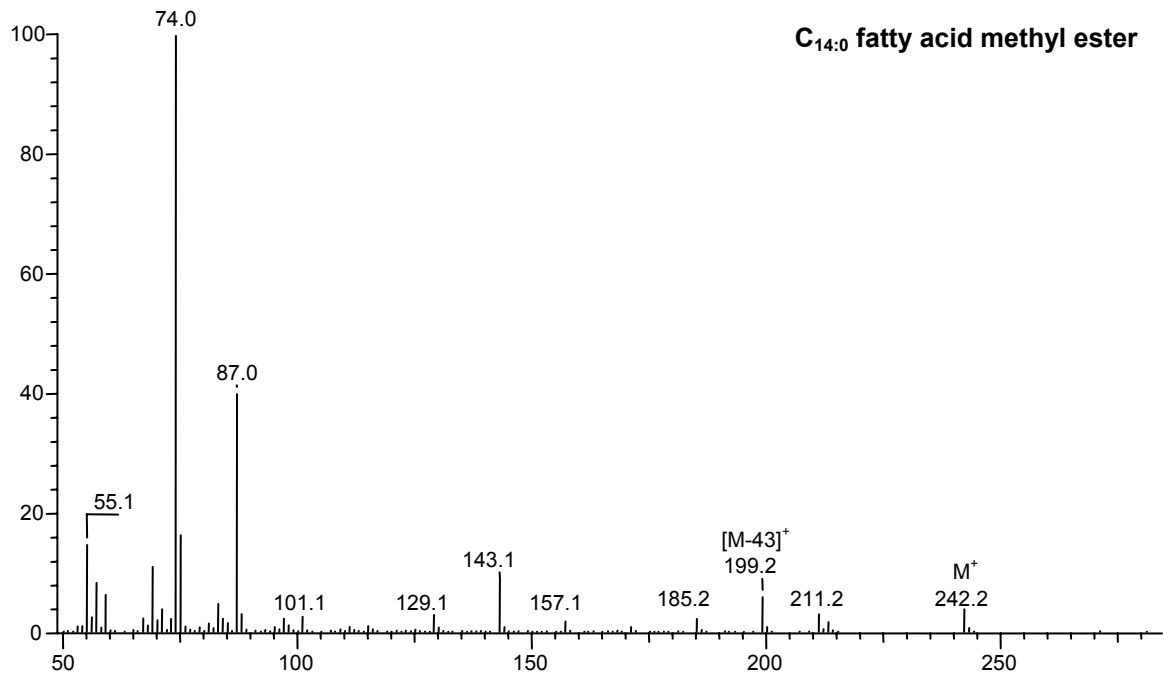
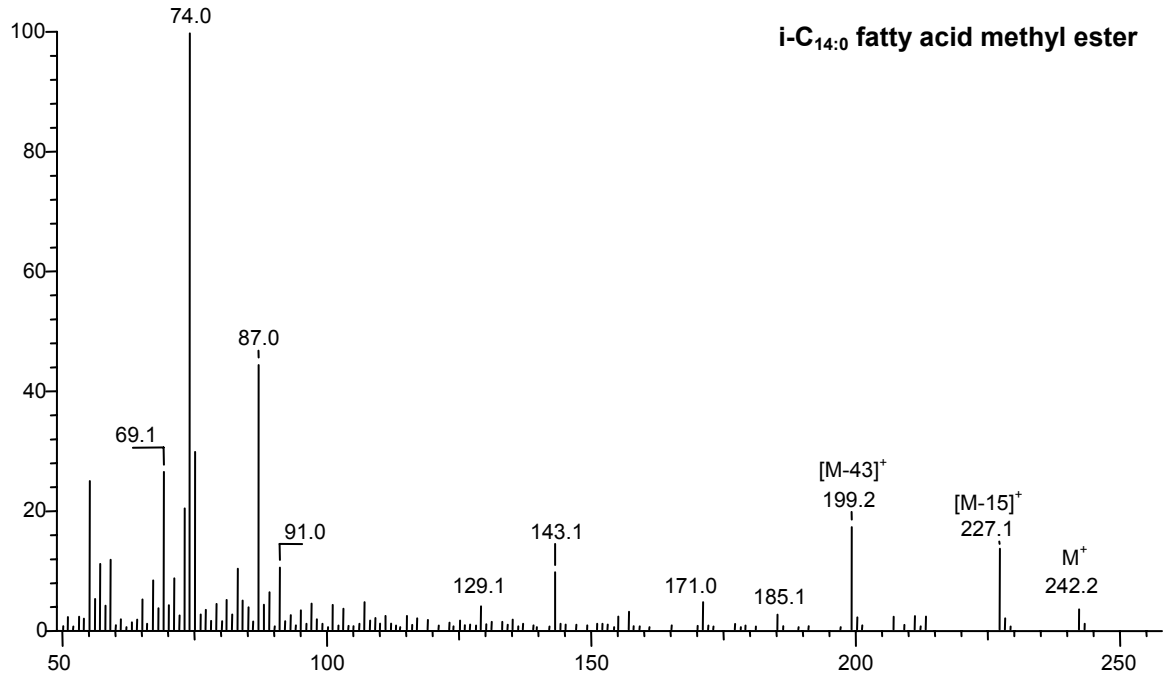
Stigmasterol
(24-ethyl-5 α -cholestan-3 β -ol)
 $C_{29}H_{52}O$

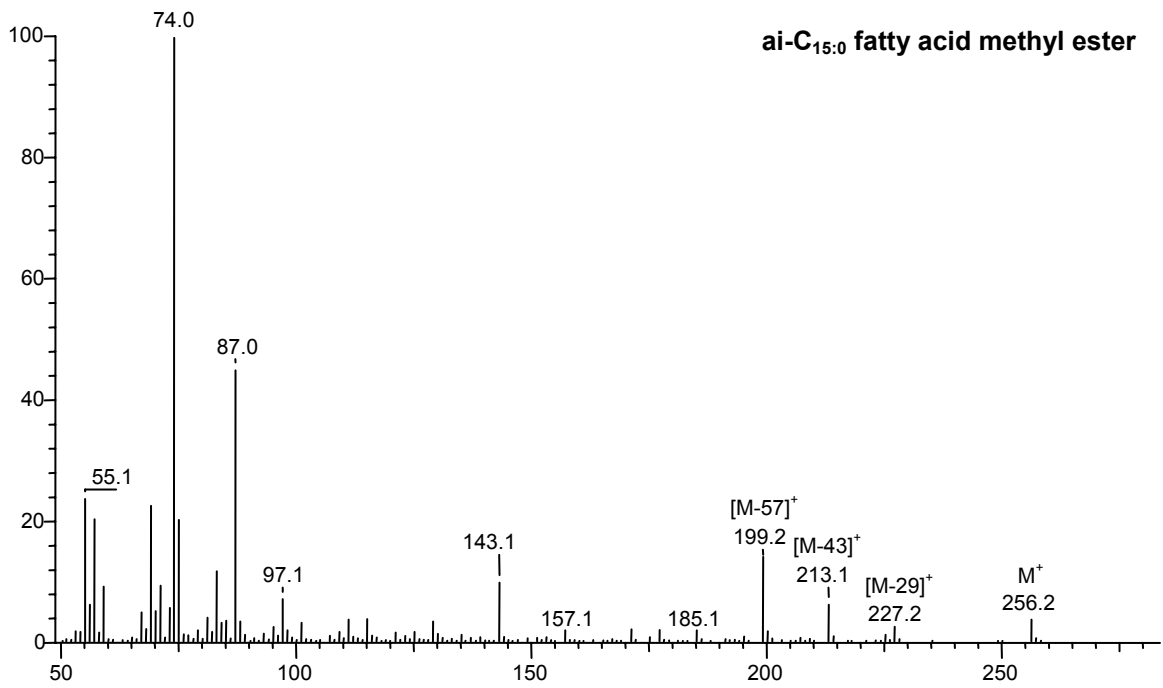
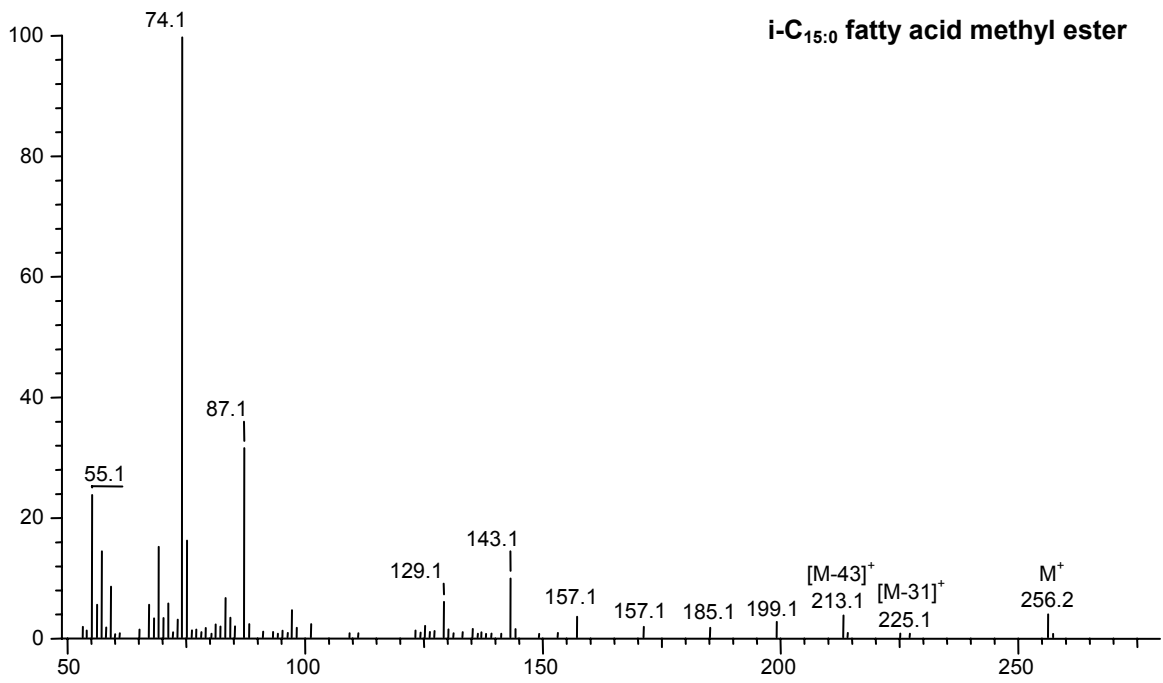


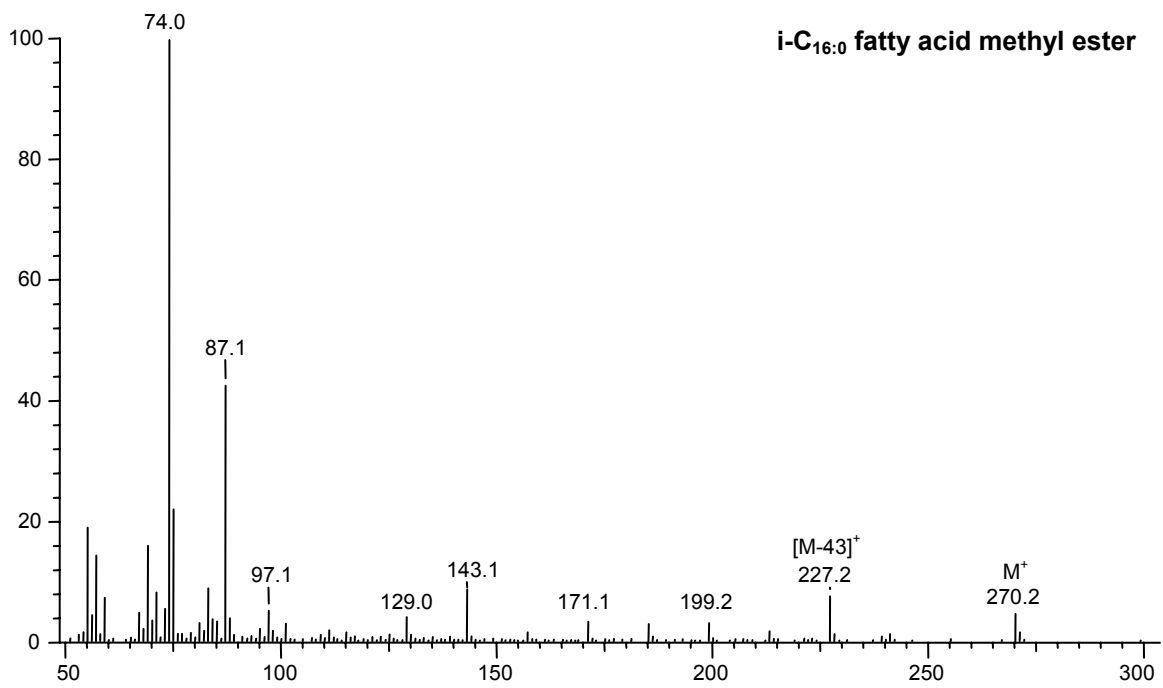
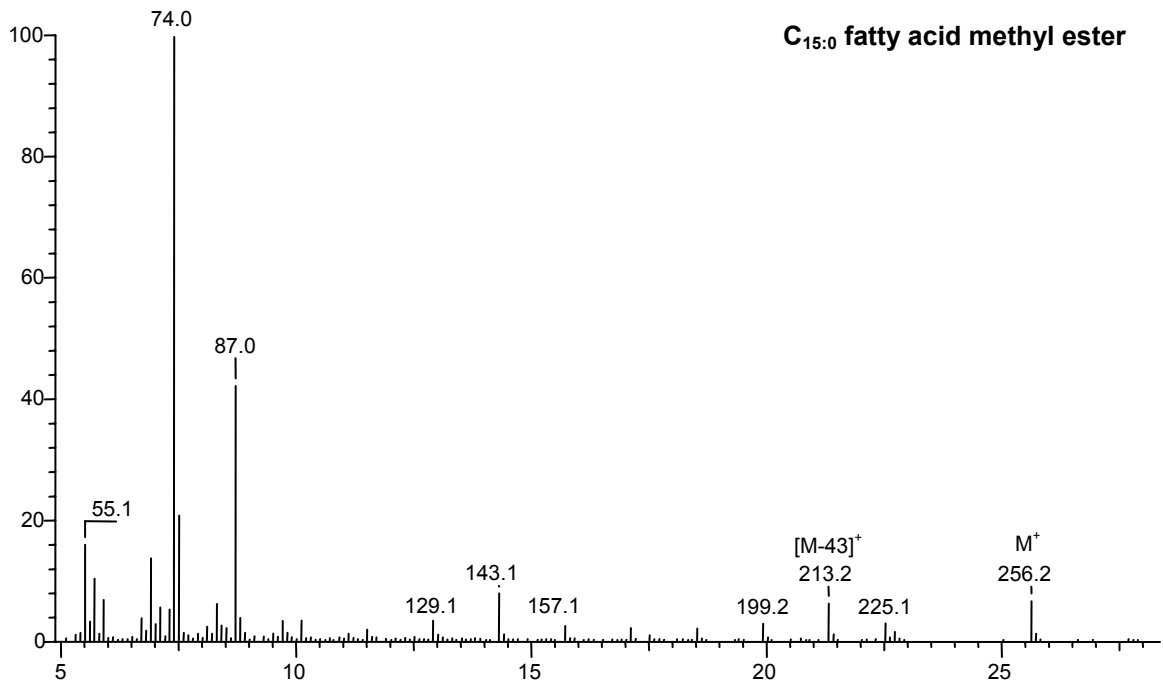
β -Sitosterol
(24-ethylcholest-5-en-3 β -ol)
 $C_{29}H_{50}O$

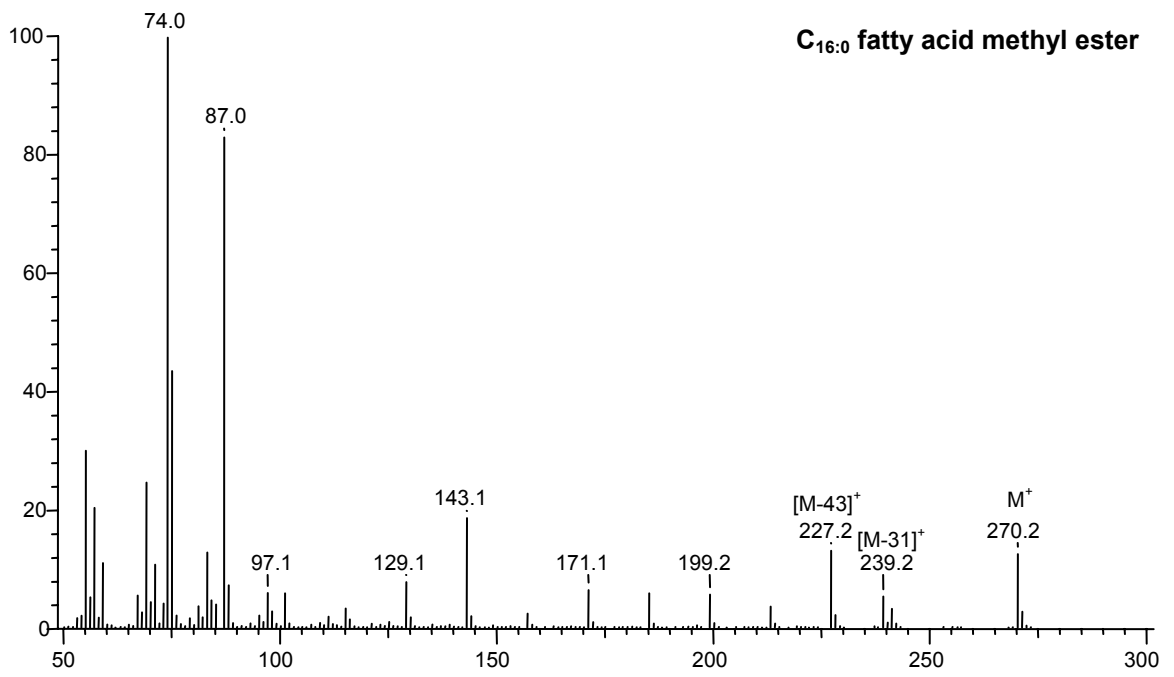
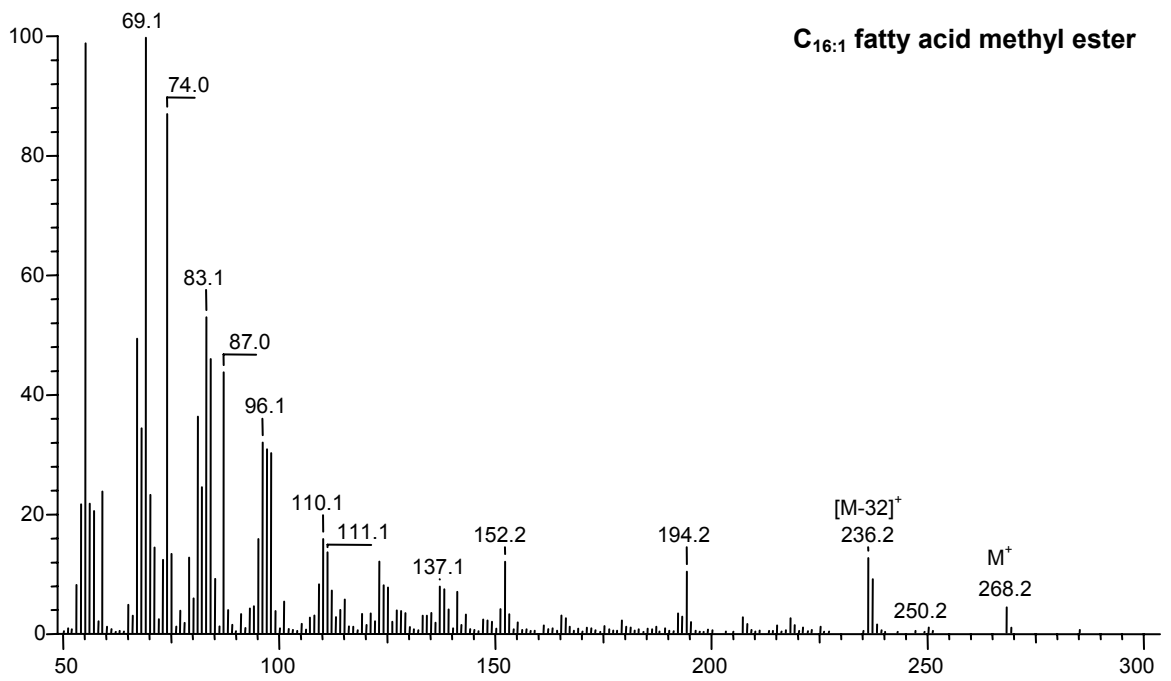
APPENDIX III

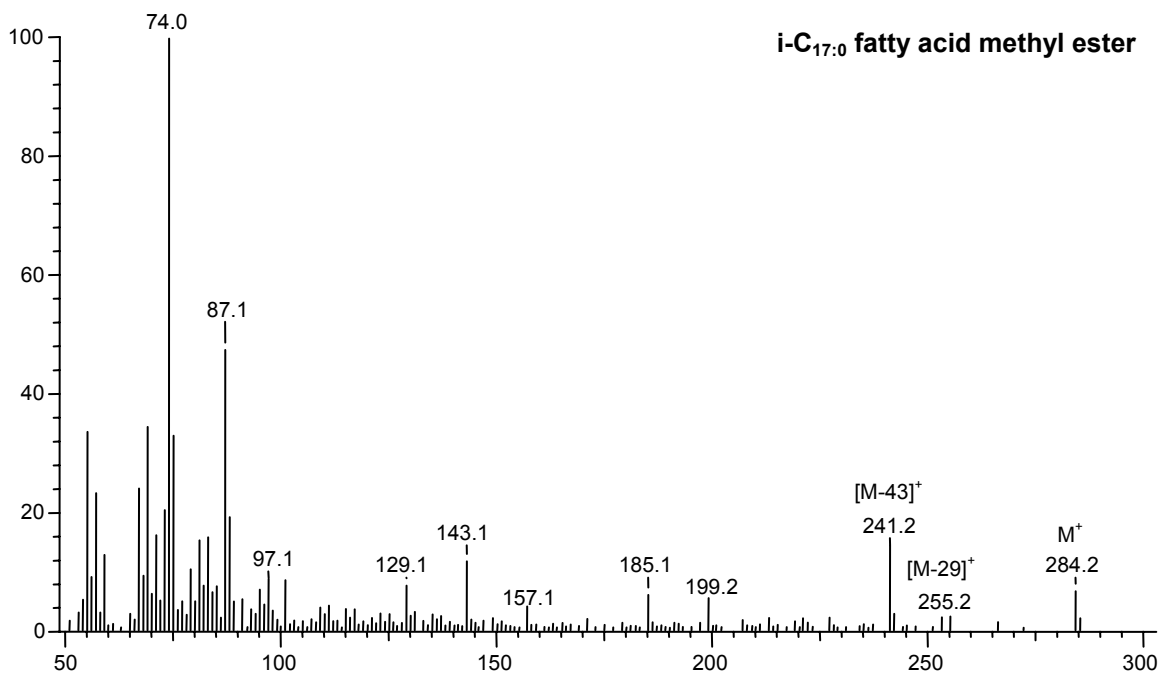
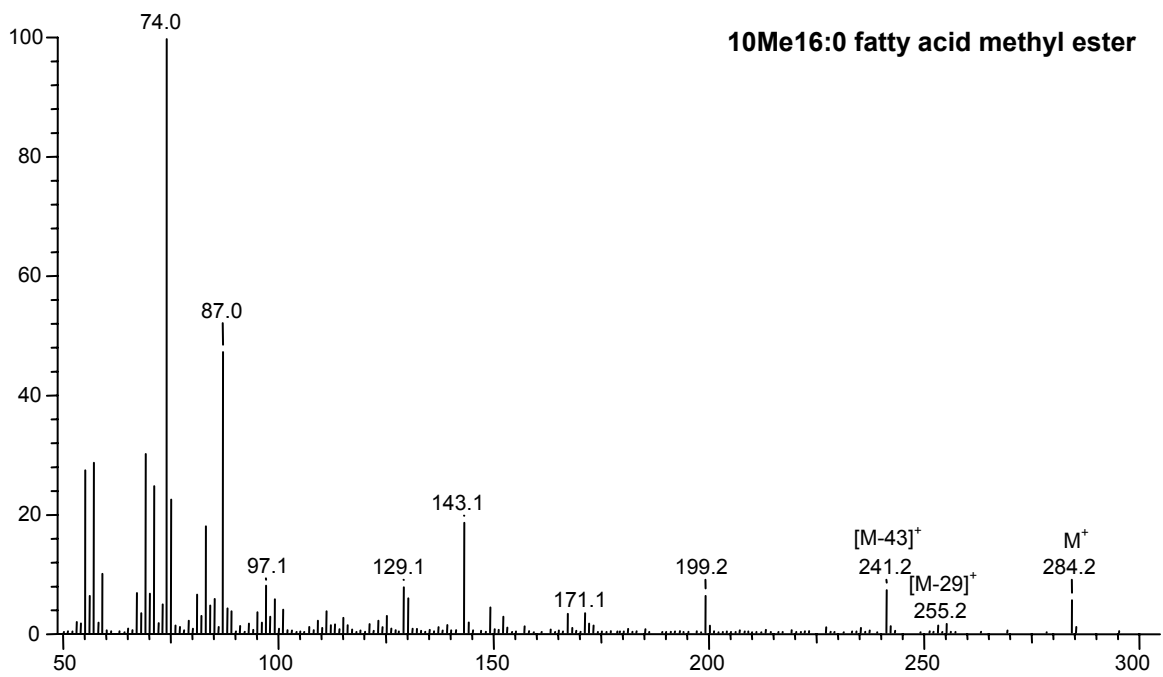
A3.1. Representative mass spectra for carboxylic acids, β -hydroxy fatty acids, α -hydroxy fatty acids, ω -hydroxy fatty acids, sterols, and stanols.

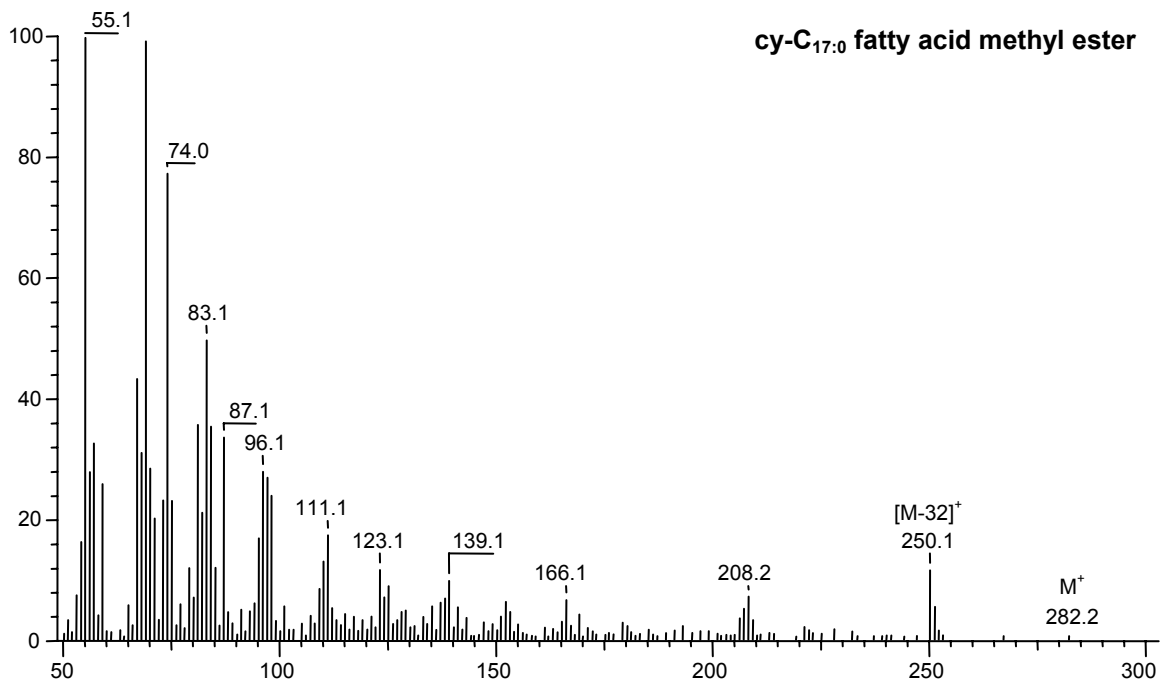
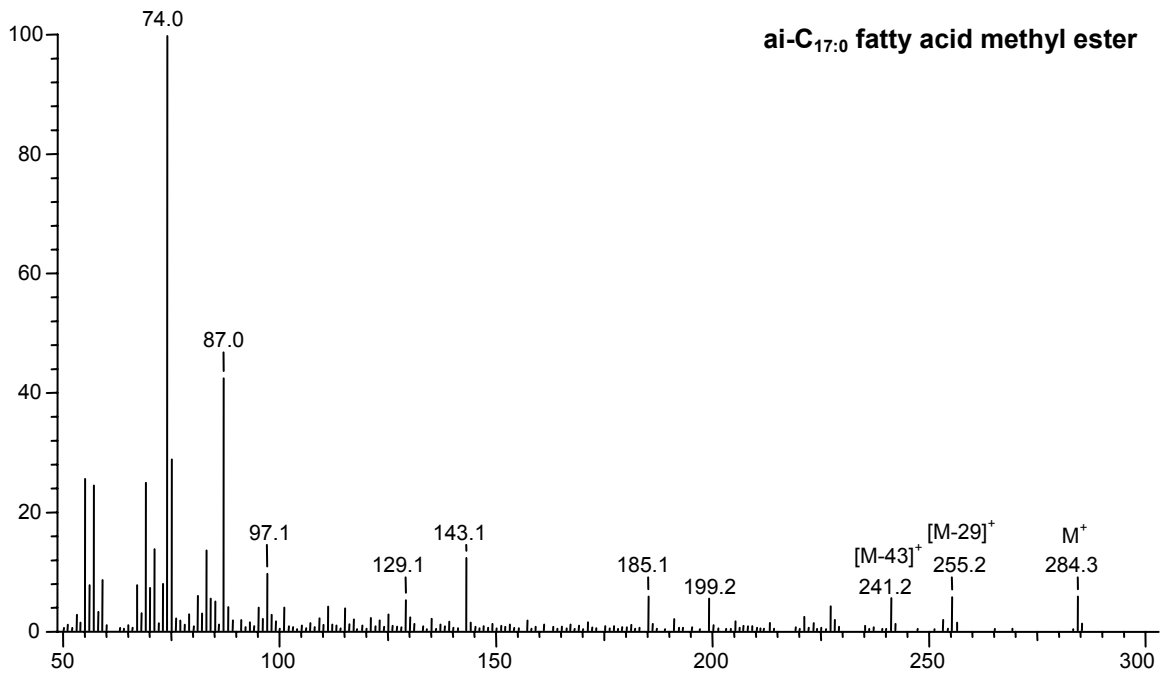


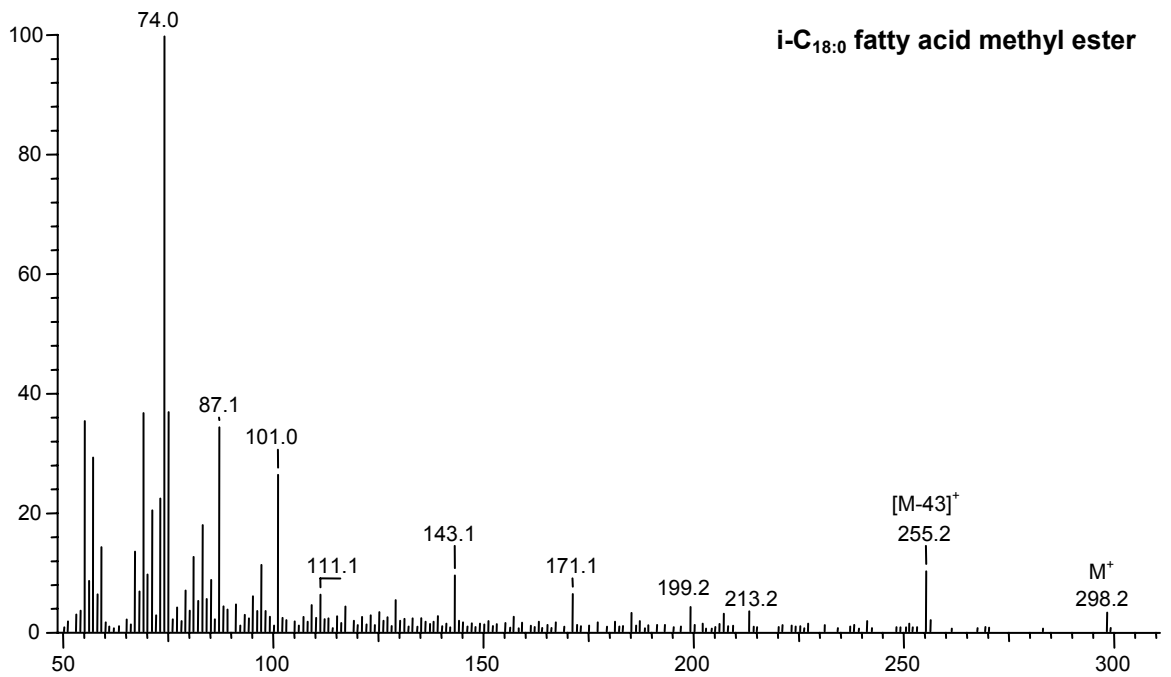
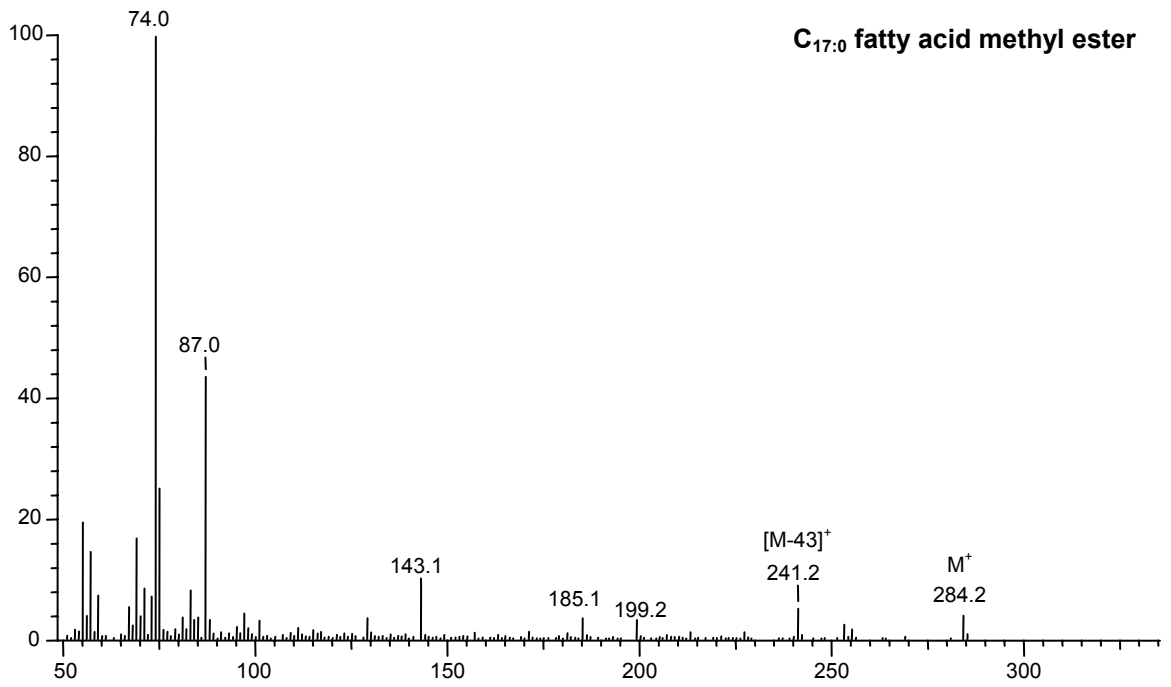


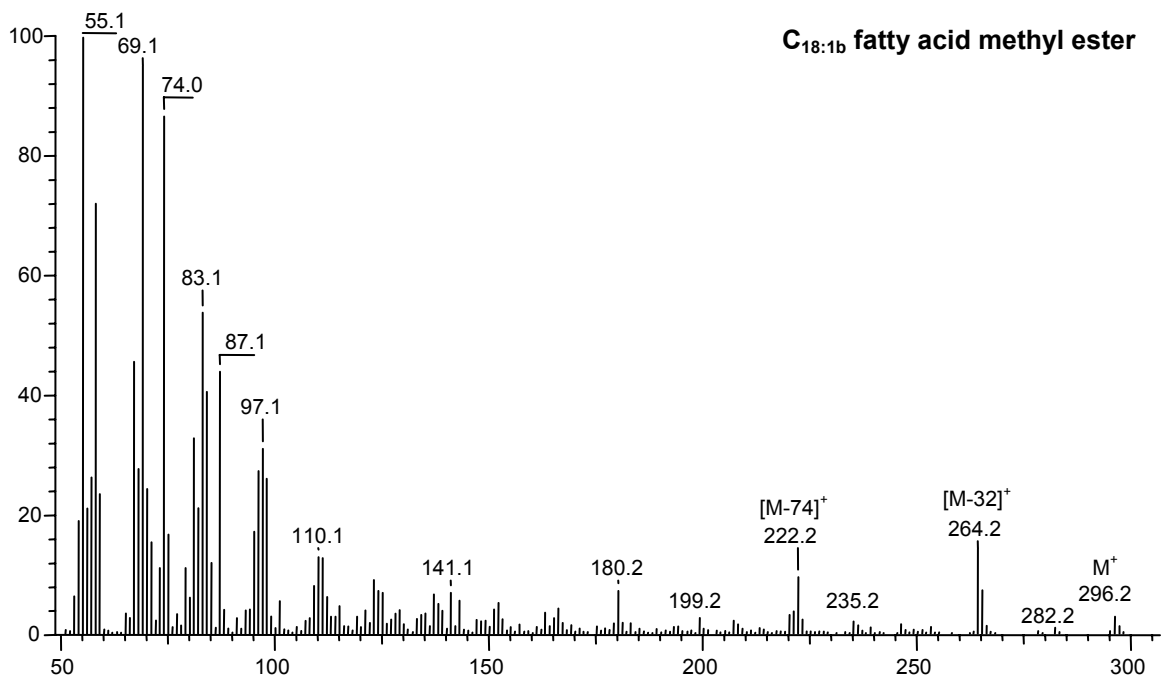
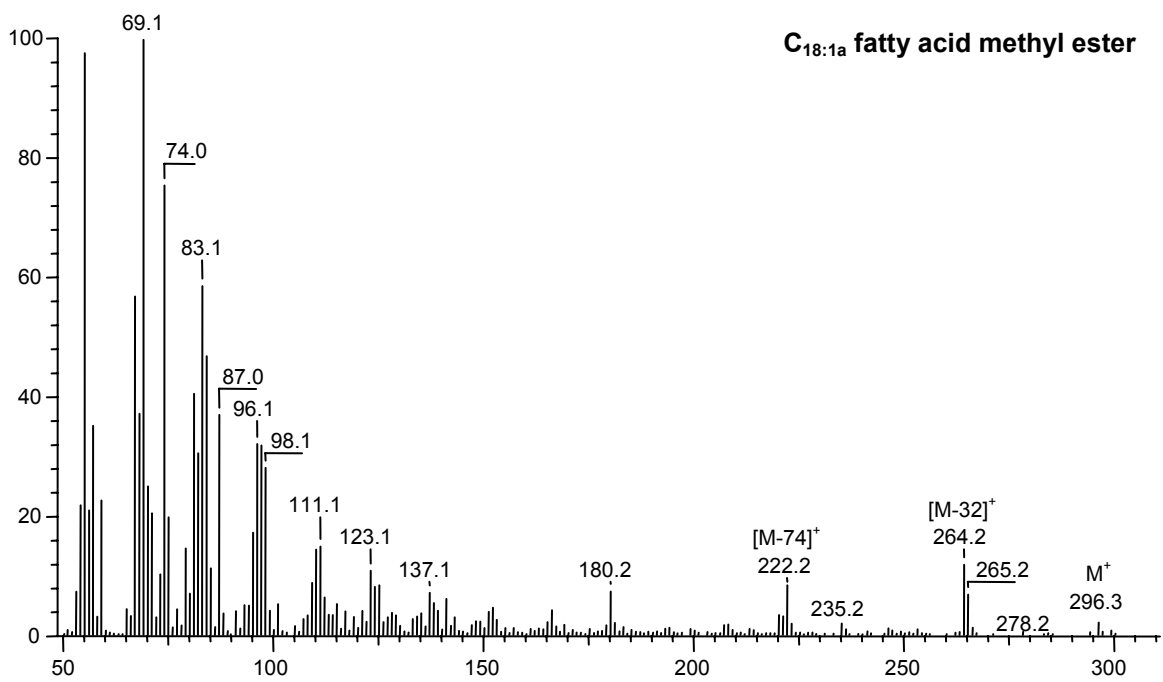


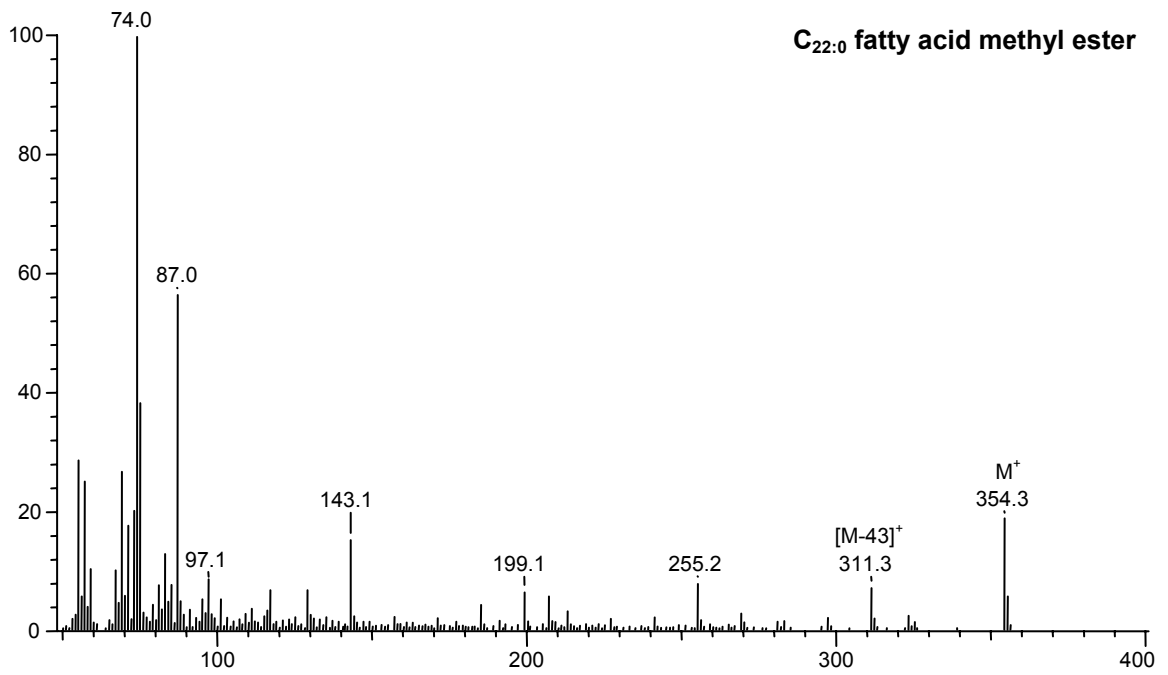
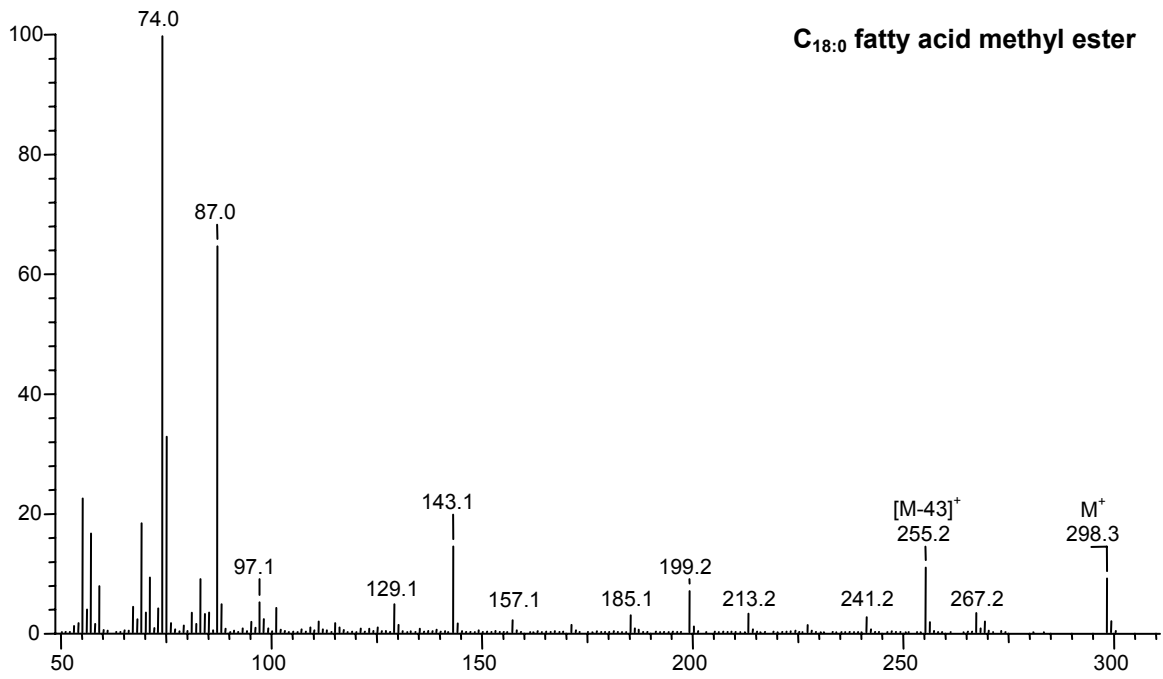


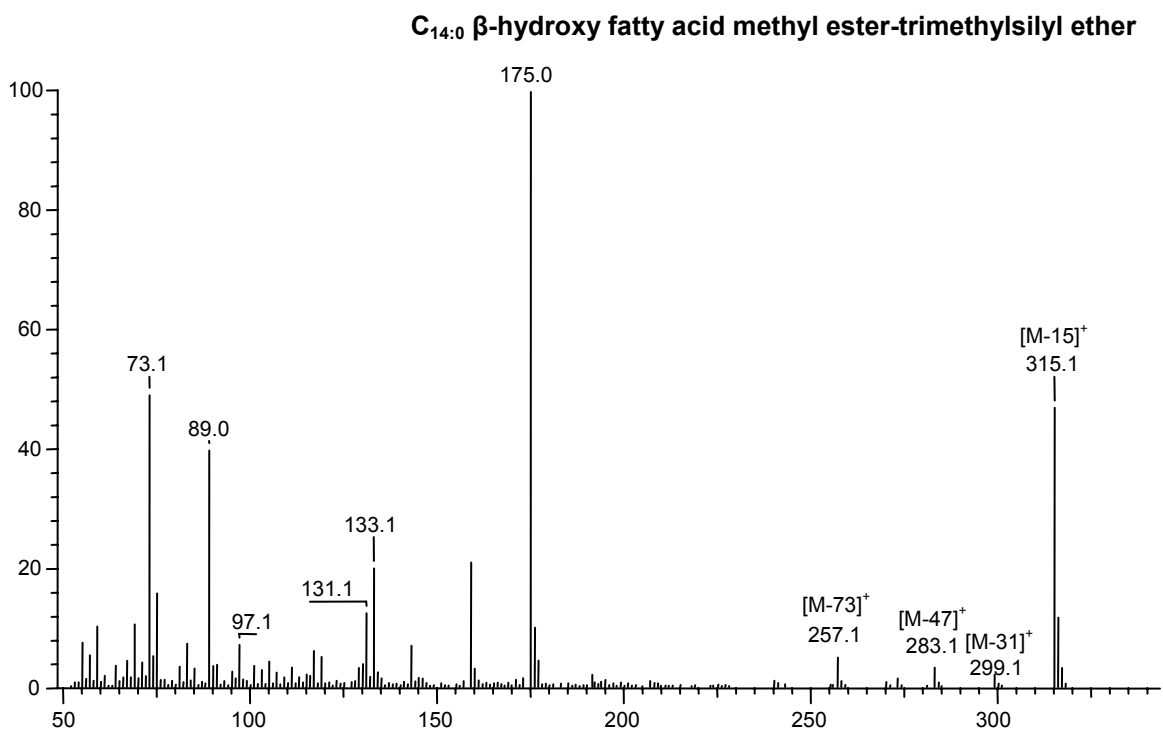
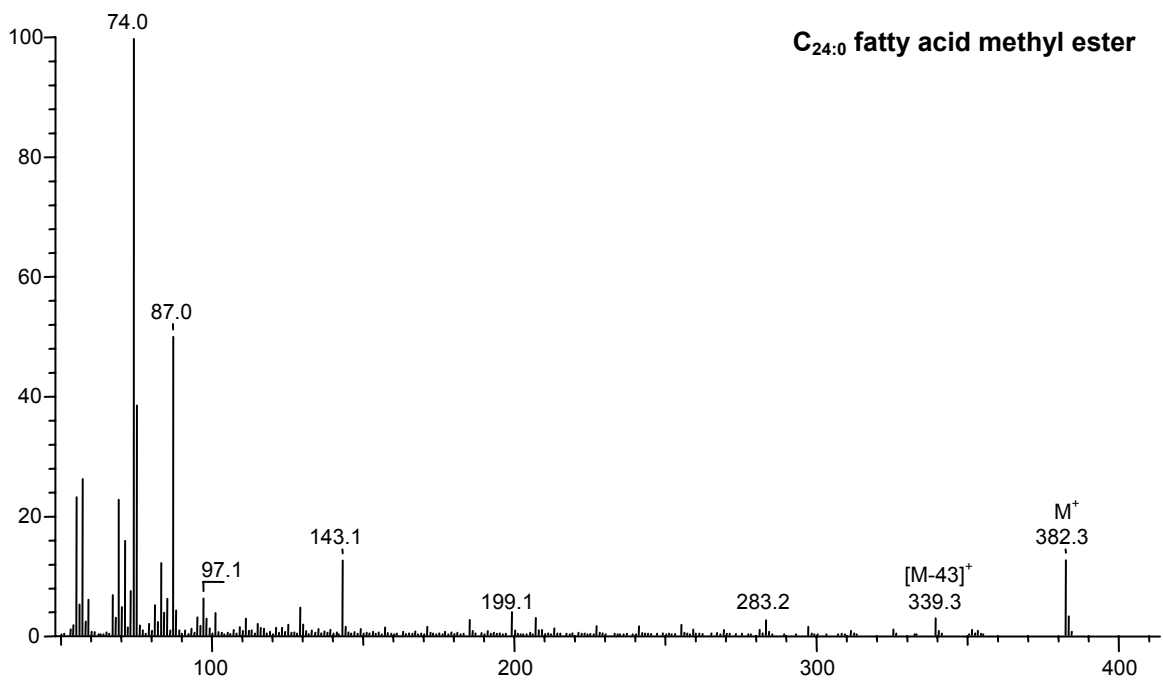




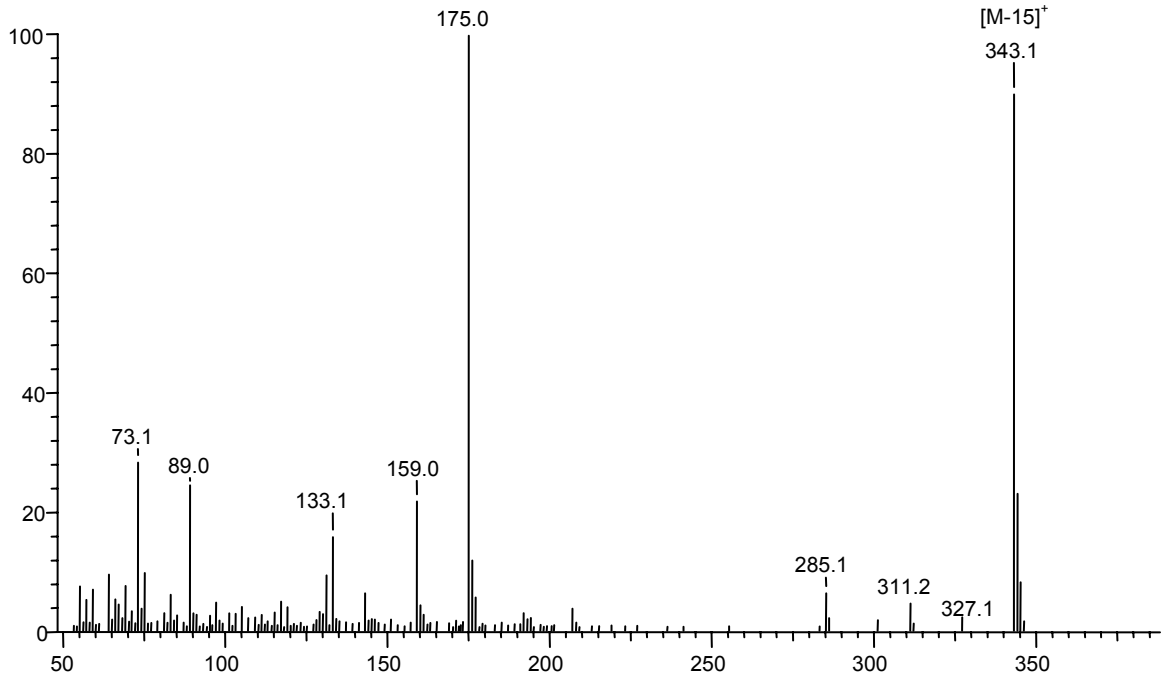




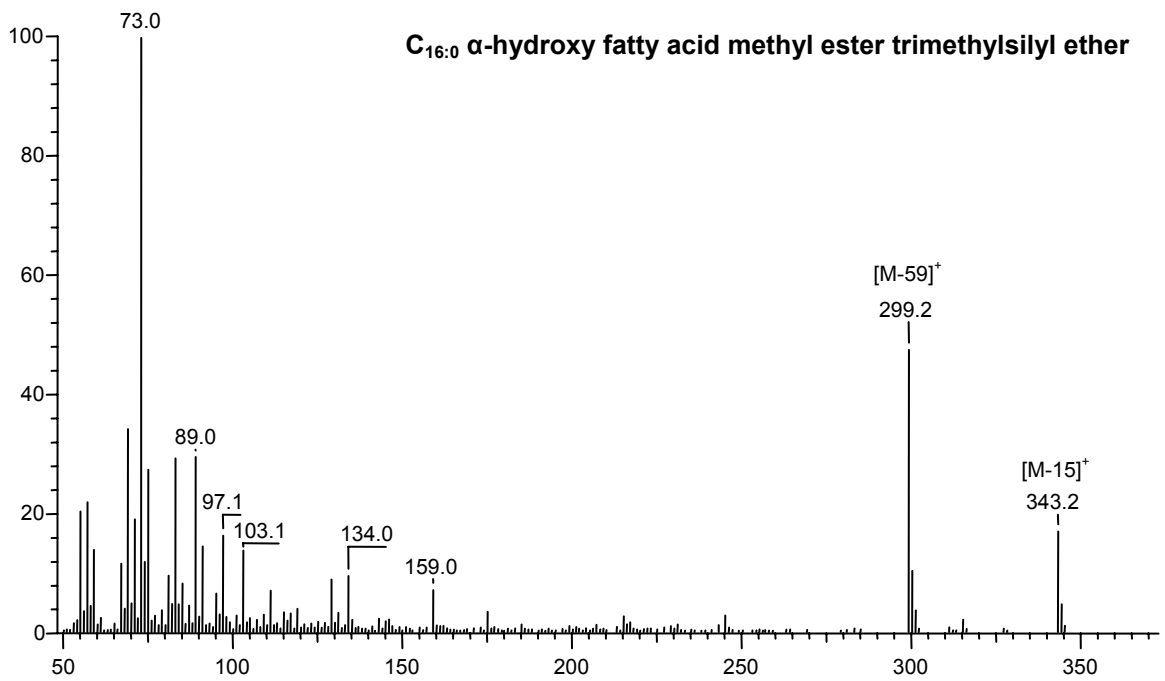


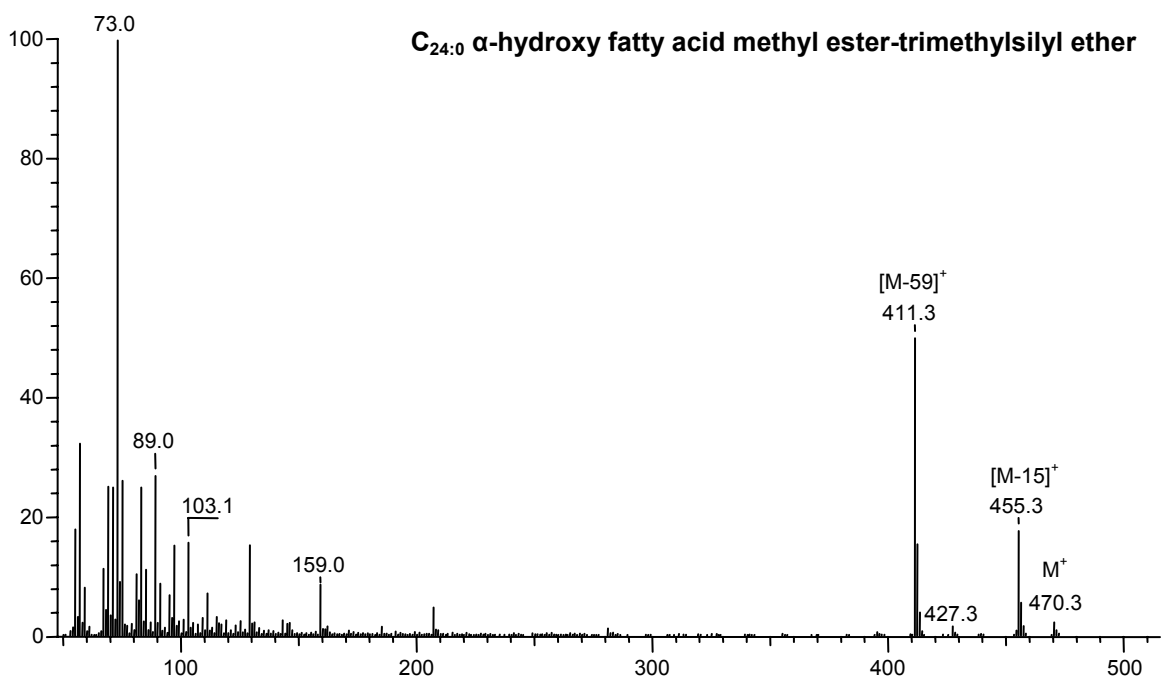
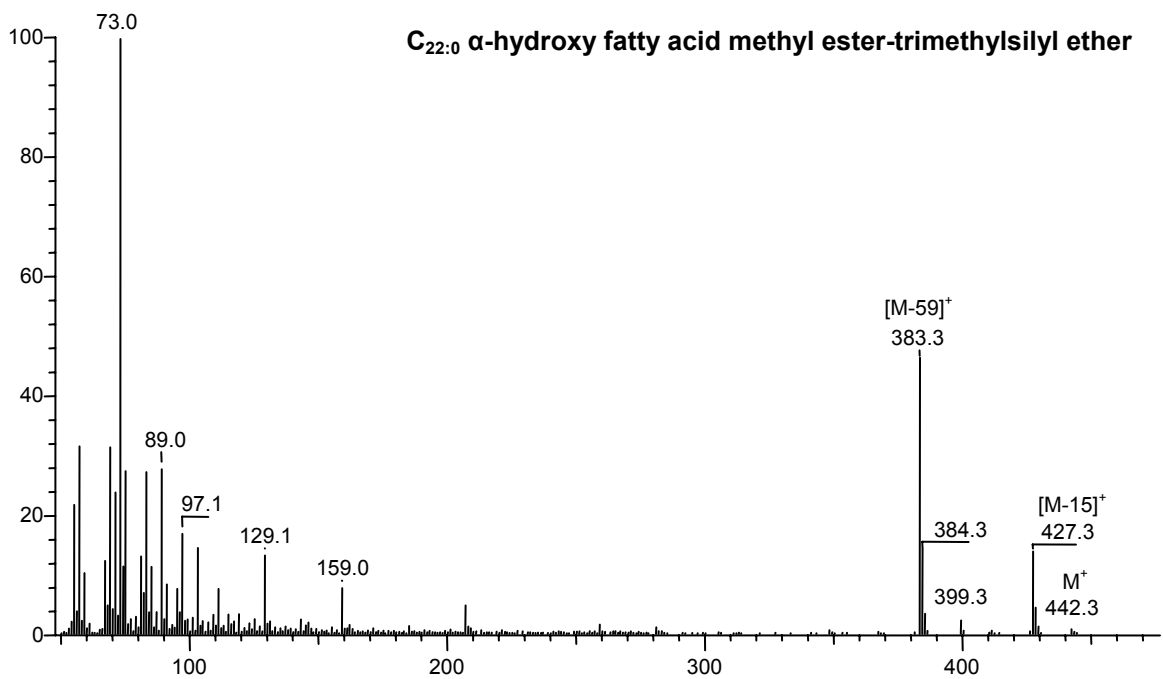


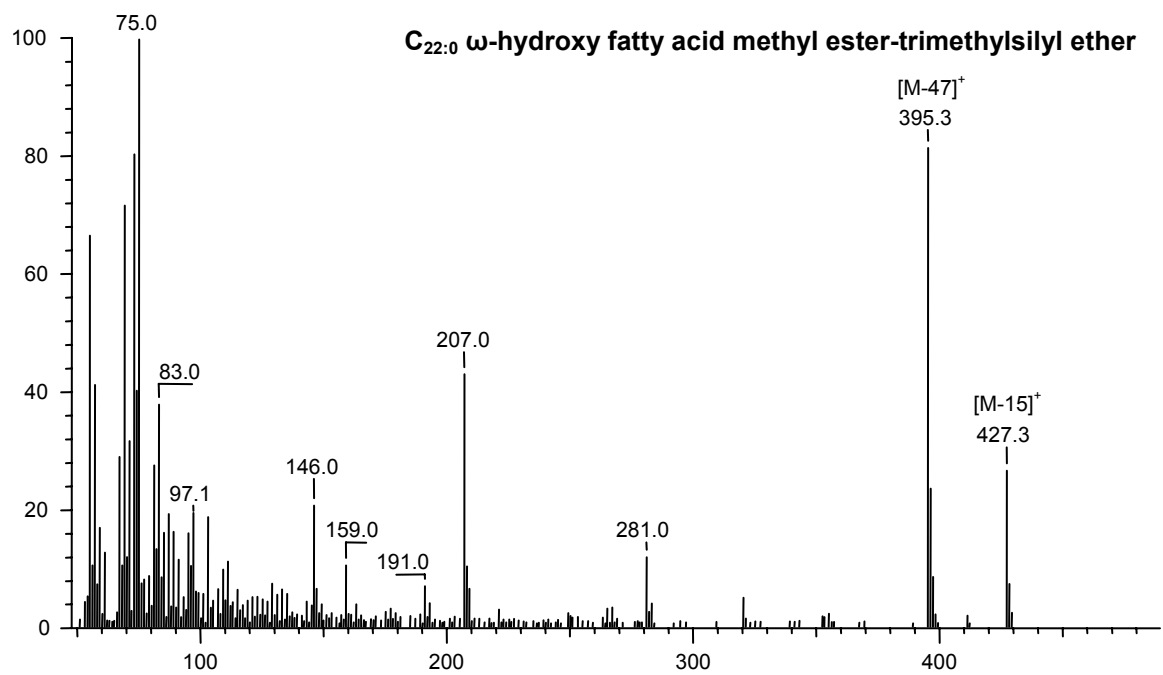
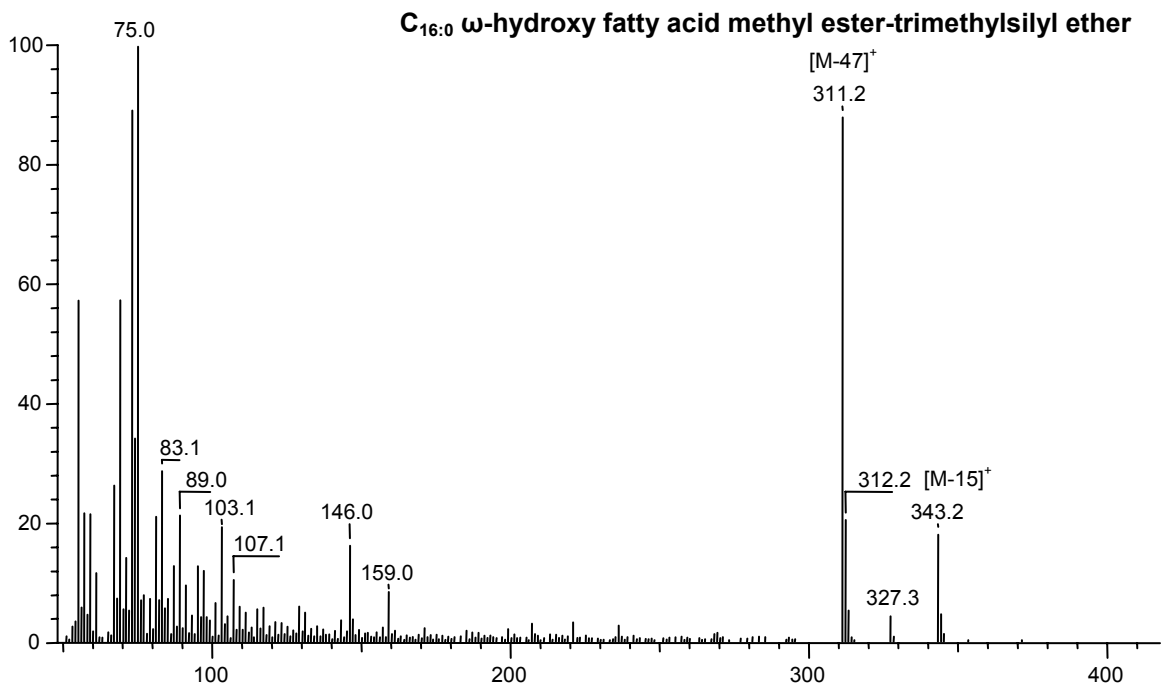
C_{16:0} β-hydroxy fatty acid methyl ester-trimethylsilyl ether

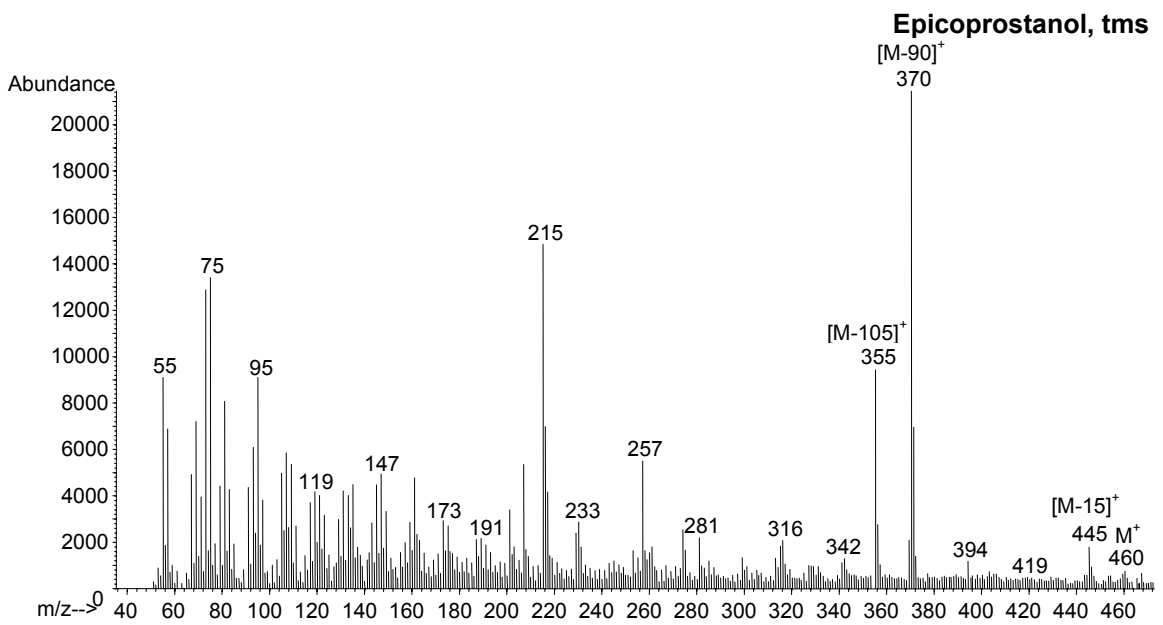
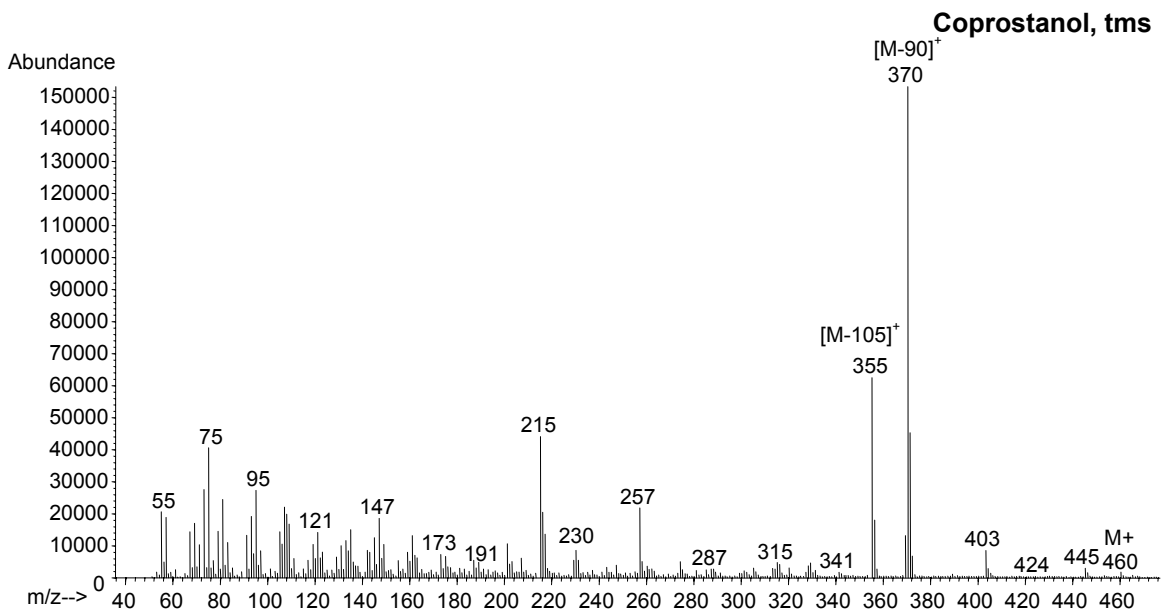


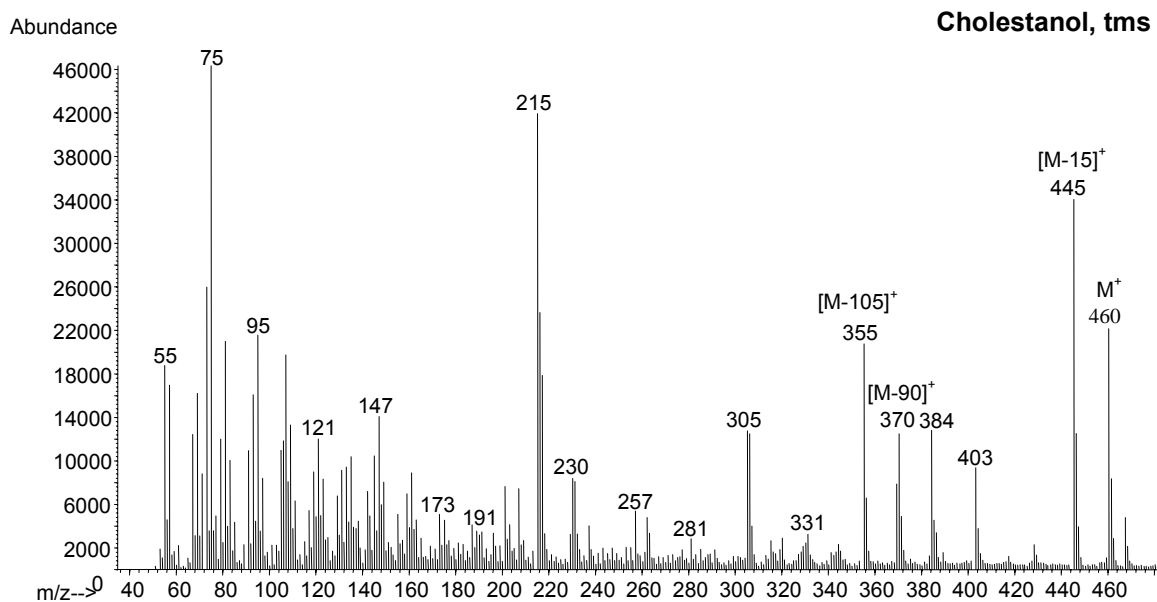
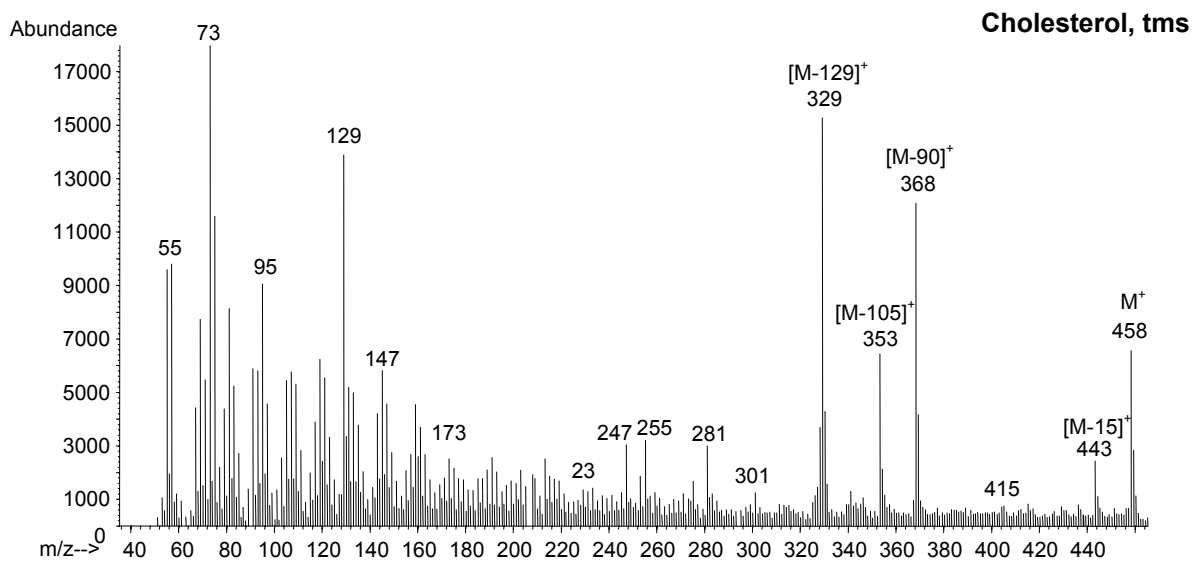
C_{16:0} α-hydroxy fatty acid methyl ester trimethylsilyl ether

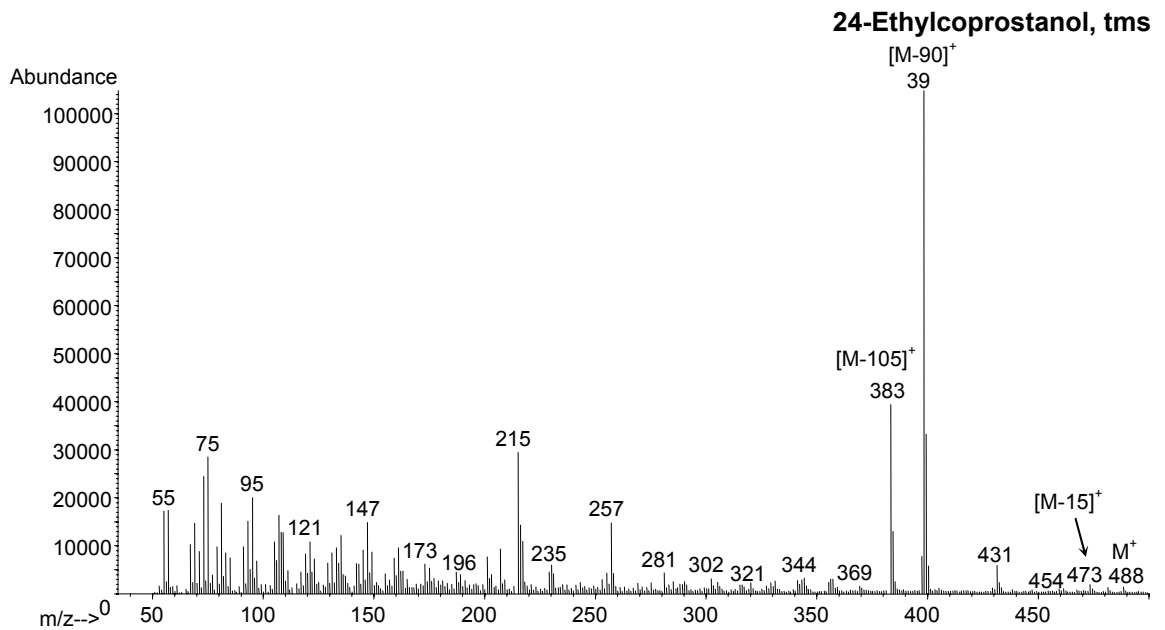
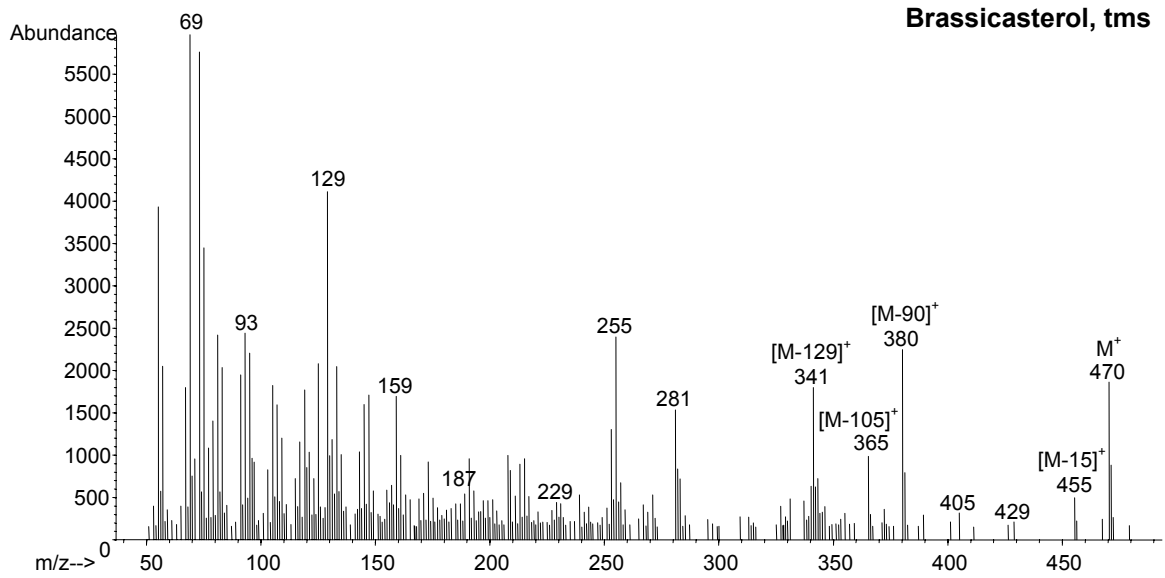


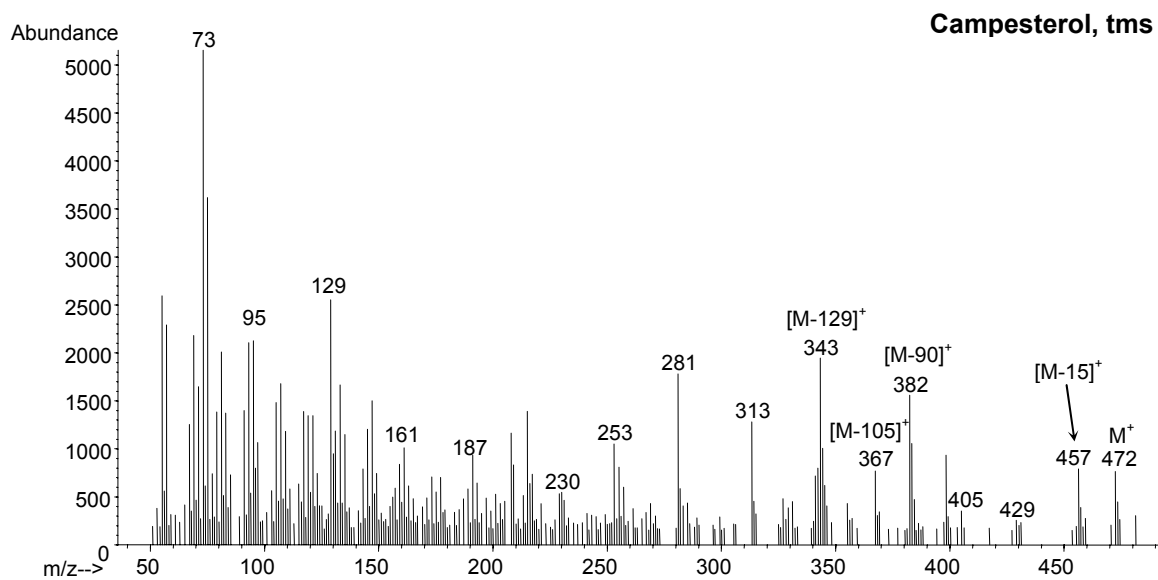
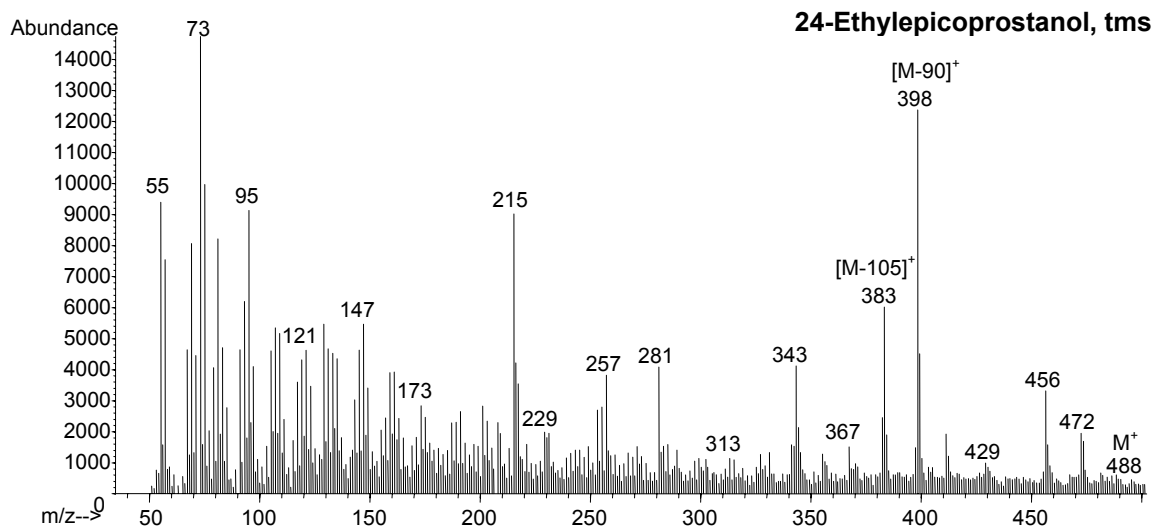


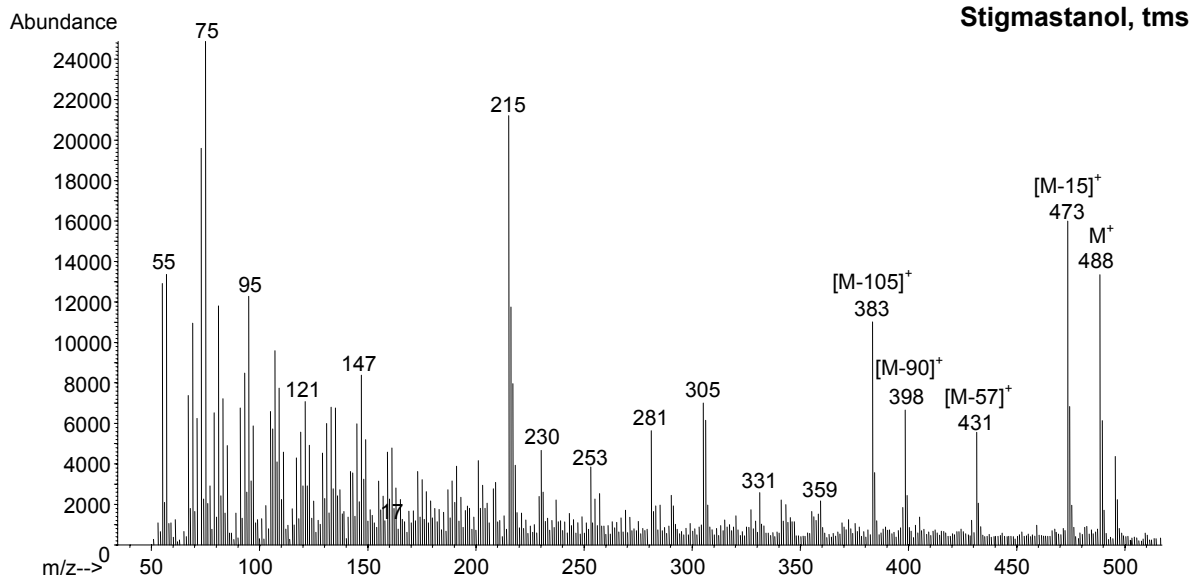
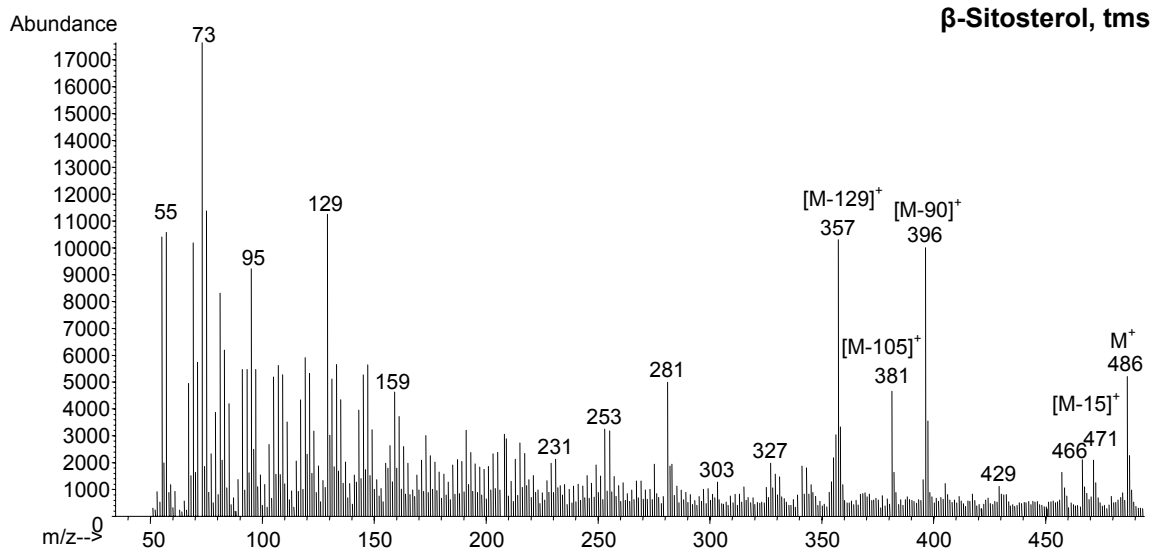












APPENDIX IV

A.4.1. Summary of sterol ratios in free lipids in core MBH 54/2.

Depth (m)	<u>brassicasterol</u> cholesterol	<u>sitosterol</u> cholesterol	<u>campesterol</u> cholesterol	<u>coprostanol</u> cholesterol	<u>epicoprostanol</u> cholesterol	<u>cholestanol</u> cholesterol
0.5	0.58	0.80	0.44	--	0.21	0.78
1.1	--	0.83	--	3.07	1.17	3.13
1.6	--	0.70	--	1.49	0.78	1.76
2.3	0.58	1.09	0.44	--	0.27	1.17
3.4	0.57	0.90	0.53	--	0.49	1.90

A.4.2. Summary of aquatic/terrigenous ratios for free lipids in core MBH 54/2.

Depth (m)	Saponifiable Fatty Acids $\Sigma(12:0-18:0)/\Sigma(22:0-28:0)$	Non-Saponifiable Fatty Acids $\Sigma(14:0-18:0)/\Sigma(20:0-24:0)$	Alcohol C_{18}/C_{28}	n-alkanes C_{19}/C_{31}
0.5	1.50	3.71	0.60	0.25
1.1	2.32	7.25	0.01	0.63
1.6	3.28	6.45	0.41	0.69
2.3	1.00	4.41	0.54	0.20
3.4	0.72	5.72	0.38	0.07

A.4.3. Summary of carbon preference indices for free lipids in core MBH 54/2.

Depth (m)	Saponifiable Fatty Acids $CPI_{(12:0-34:0)}$	Non-Saponifiable Fatty Acids $CPI_{(14:0-26:0)}$	n-Alcohols $CPI_{(C22-C32)}$	n-Alkanes $CPI_{(C19-C35)}$
0.5	7.4	7.0	6.49	2.58
1.1	10.4	9.1		1.24
1.6	9.5	15.9		1.22
2.3	7.1	9.6	7.99	2.24
3.4	5.0	7.5	9.70	3.01

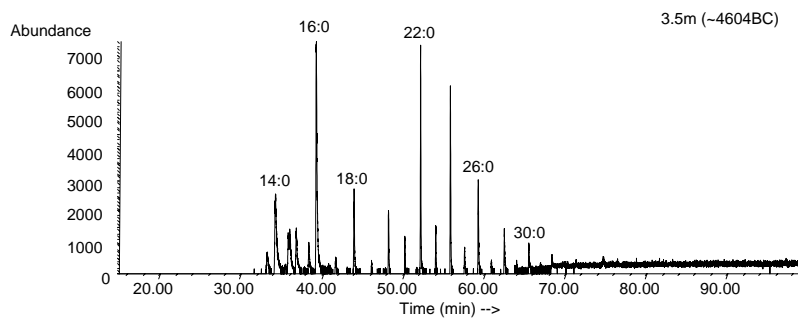
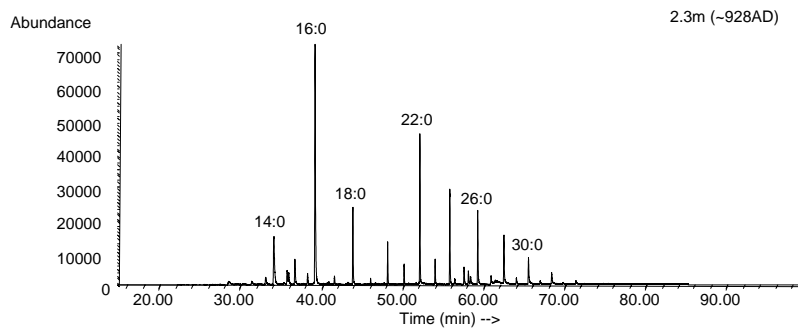
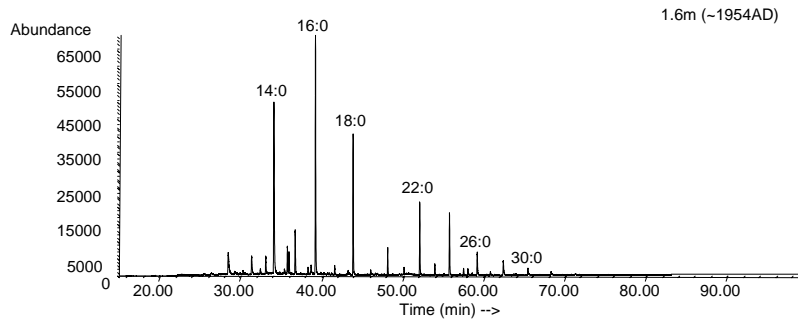
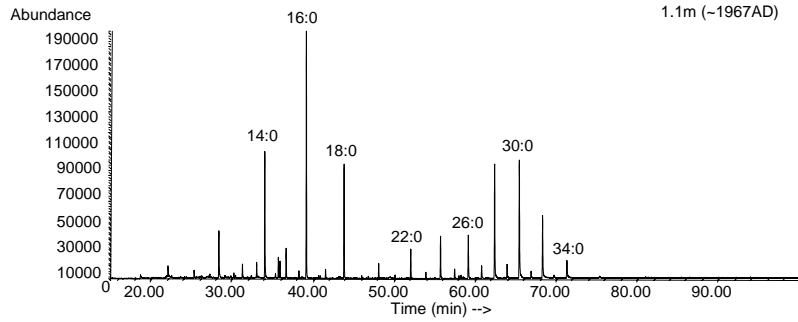
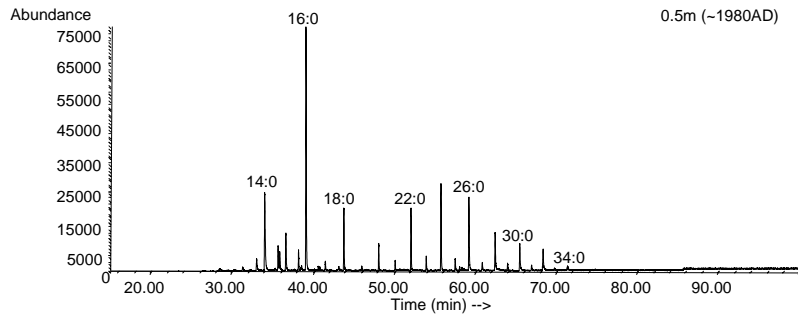
$$\text{Saponifiable fatty acids: } CPI_{(12:0-34:0)} = \frac{[C_{12:0} + 2 * (C_{14:0} + C_{16:0} + \dots + C_{30:0} + C_{32:0}) + C_{34:0}]}{[2 * (C_{13:0} + C_{15:0} + \dots + C_{31:0} + C_{33:0})]}$$

$$\text{Non-saponifiable fatty acids: } CPI_{(14:0-26:0)} = \frac{[C_{14:0} + 2 * (C_{16:0} + C_{18:0} + \dots + C_{22:0} + C_{24:0}) + C_{26:0}]}{[2 * (C_{15:0} + C_{17:0} + \dots + C_{23:0} + C_{25:0})]}$$

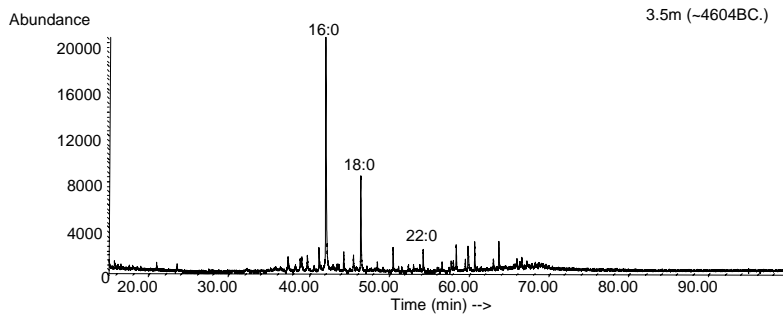
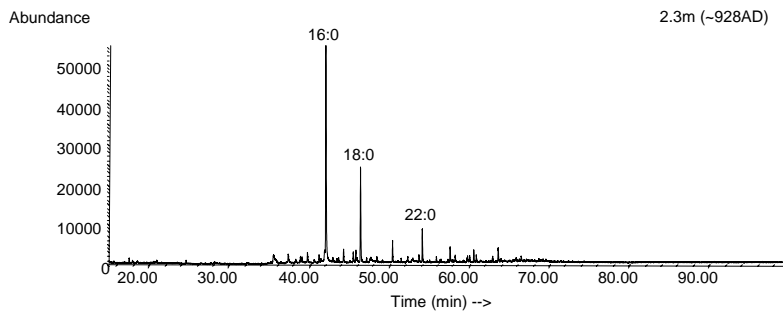
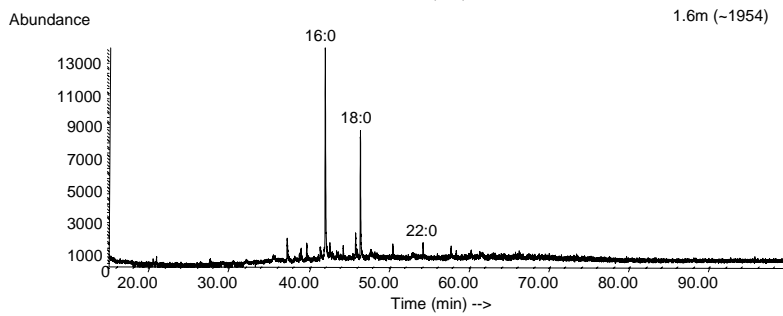
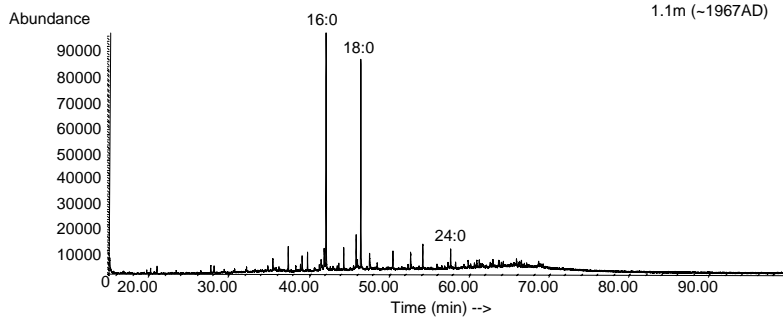
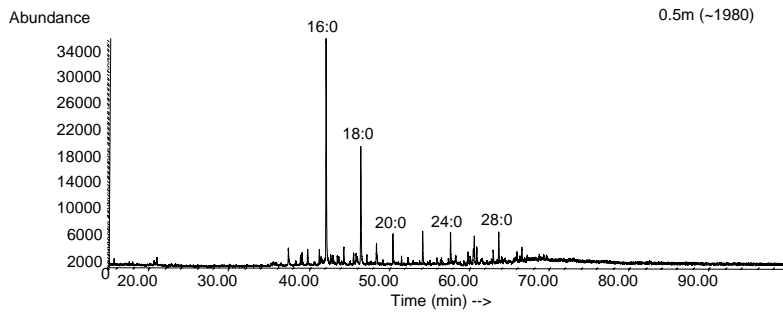
$$\text{n-Alcohols: } CPI_{(C22-C32)} = \frac{[C_{22} + 2 * (C_{24} + C_{26} + \dots + C_{28} + C_{30}) + C_{32}]}{[2 * (C_{23} + C_{25} + \dots + C_{29} + C_{31})]}$$

$$\text{n-Alkanes: } CPI_{(C19-C35)} = \frac{[C_{19} + 2 * (C_{21} + C_{23} + \dots + C_{31} + C_{33}) + C_{35}]}{[2 * (C_{20} + C_{22} + \dots + C_{32} + C_{34})]}$$

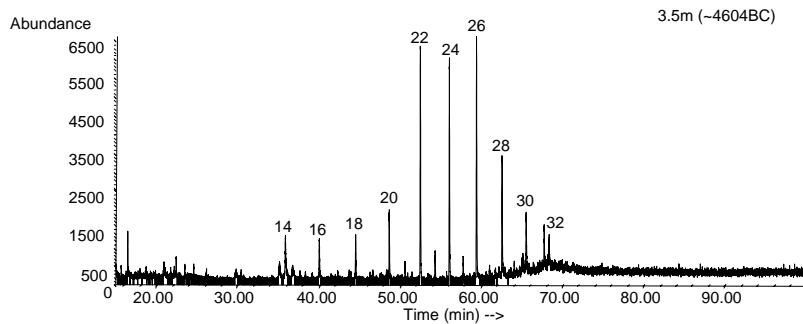
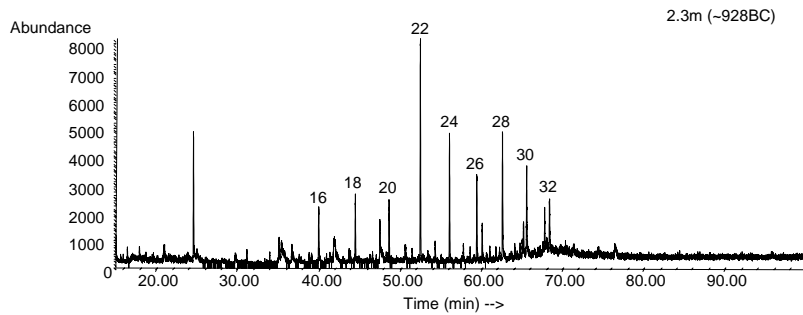
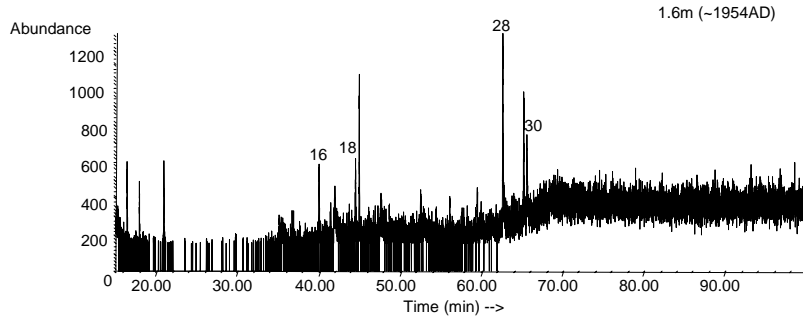
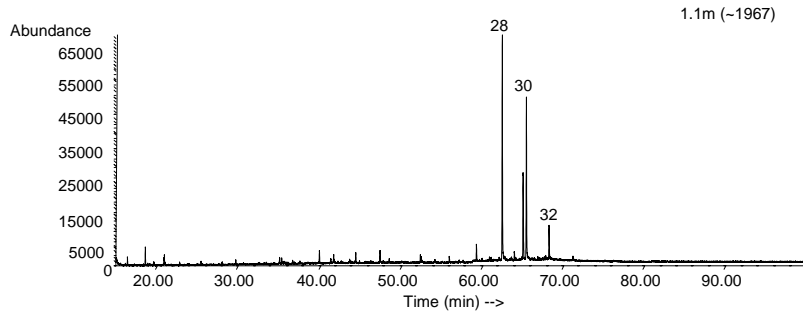
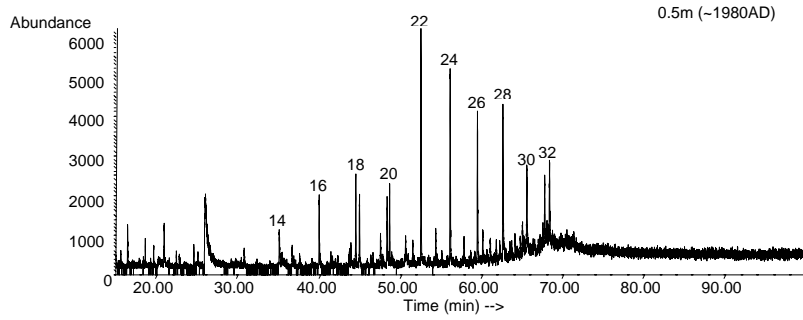
A4.4. Chromatograms of free fatty acids in the saponifiable lipid fraction.



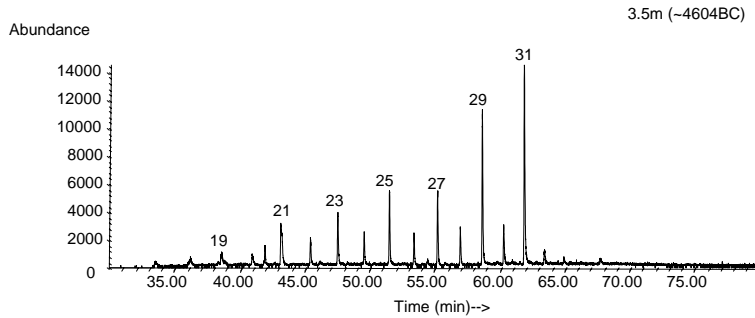
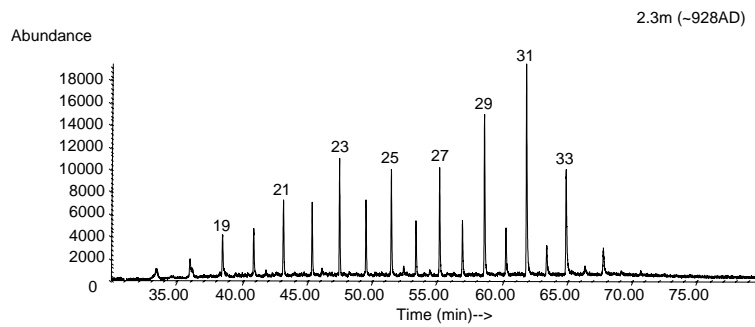
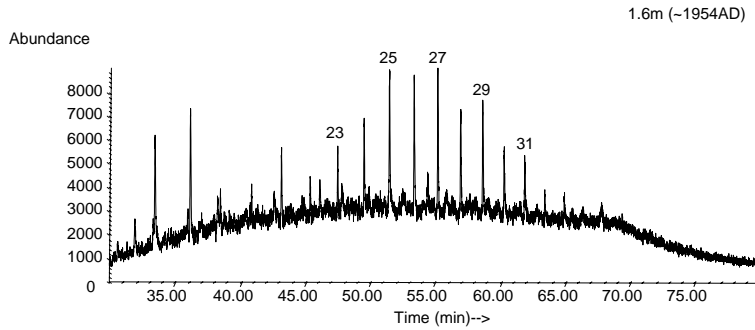
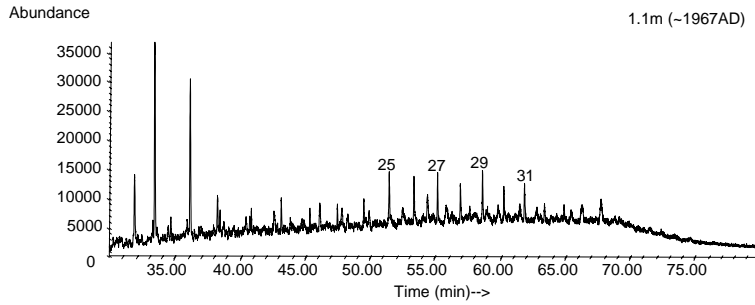
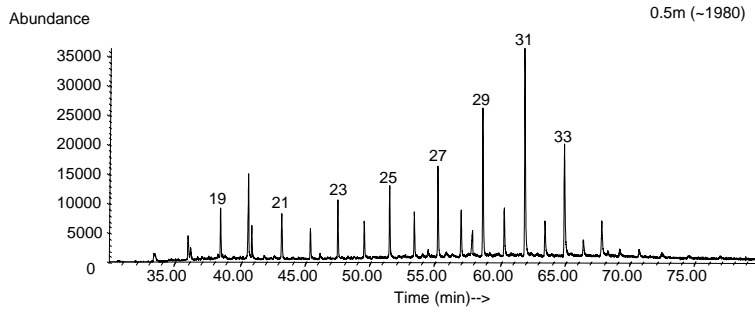
A4.5. Chromatograms of free fatty acids in the non-saponifiable lipid fraction.



A4.6. Chromatograms of free alcohols in the non-saponifiable lipid fraction.



A4.7. Chromatograms of free n-alkanes in the non-saponifiable lipid fraction.



APPENDIX V

A.5.1. Ester-bound fatty acid methyl esters ($\mu\text{g/g}$ sediment dry weight)

C#	0.5m	0.7m	1.2m	1.4m	1.6m	2.3m	3.0m	3.3m	3.5m	3.9m
12:0	0.168	0.047	1.376	0.127	3.285		0.051		0.003	
i13:0	0.039	0.029	0.345	0.085	0.123	0.011	0.012		0.001	
ai13:0	0.020	0.014	0.111	0.017	0.042	0.005	0.005		0.0004	
13:0	0.087	0.045	0.300	0.067	0.135	0.029	0.046		0.004	
i14:0	0.085	0.126	0.665	0.153	0.388	0.034	0.031	0.007	0.003	0.003
14:0	1.105	1.037	3.952	0.994	2.525	0.476	0.497	0.158	0.044	0.060
i15:0	0.291	2.304	2.304	0.697	1.819	0.128	0.110	0.043	0.017	0.017
ai15:0	0.159	0.435	1.576	0.458	0.972	0.073	0.039	0.014	0.005	0.007
15:0	0.336	0.332	1.157	0.432	1.050	0.195	0.190	0.093	0.021	0.042
i16:0	0.155	0.277	0.895	0.285	0.631	0.083	0.051	0.027	0.007	0.010
16:1		0.071	0.292						0.002	
16:0	2.574	4.035	14.63	5.950	8.702	1.755	1.684	0.936	0.188	0.345
10Me16:0				0.442	0.940				0.005	
i17:0	0.155	0.181	0.449	0.185	0.403	0.075	0.050	0.024	0.006	0.010
ai17:0	0.085	0.156	0.465	0.158	0.319	0.046	0.028	0.012	0.003	0.005
cy17:0				0.015	0.123					
17:0	0.240	0.281	0.867	0.313	0.759	0.155	0.143	0.088	0.016	0.038
18:1		0.340	1.262	0.087	0.826					
18:1		0.182	0.597		0.595					
18:0	1.089	2.689	8.324	2.801	5.490	0.916	0.593	0.355	0.074	0.164
19:0	0.099	0.085	0.233	0.096	0.172	0.064	0.071	0.045	0.007	0.015
20:0	0.480	0.431	1.260	0.389	0.876	0.241	0.217	0.153	0.021	0.045
21:0	0.096	0.058	0.185	0.098	0.172	0.057	0.070	0.046	0.007	0.015
22:0	0.487	0.534	1.780	0.579	1.277	0.261	0.304	0.253	0.028	0.054
23:0	0.105	0.837	0.314	0.152	0.228	0.060	0.070	0.050	0.006	0.014
24:0	0.738	0.528	1.194	0.445	1.170	0.313	0.440	0.371	0.038	0.068
25:0	0.082	0.061	0.142	0.065	0.178	0.036	0.042	0.038	0.004	0.011
26:0	0.589	0.268	0.549	0.180	0.674	0.174	0.300	0.411	0.026	0.054
27:0	0.051	0.040	0.118	0.042	0.133	0.019	0.027	0.032	0.002	0.010
28:0	0.191	0.212	0.578	0.299	1.062	0.059	0.092	0.158	0.010	0.031
29:0	0.047	0.036	0.065	0.035	0.111	0.019	0.022	0.035	0.002	0.007
30:0	0.142	0.148	0.451	0.152	0.967	0.036	0.061	0.126	0.006	0.023
31:0					0.055			0.024		0.005
32:0					0.451			0.081		0.016

A.5.2. Ester-bound β -hydroxy fatty acids (ng/g sediment dry weight)

C#	0.5m	0.7m	0.8m	1.2m	1.4m	1.6m	2.3m	3.0m	3.3m	3.5m	3.9m
10 β	8.08		40.38	86.33	54.34	81.26		7.72		14.20	
i12 β	1.93			26.12		31.74					
12 β	23.05		69.07	132.49	78.82	185.64	12.31	14.79	4.75	24.35	2.08
i13 β	23.57		53.45	121.36	10.80	68.89	20.44	4.77	4.32	9.70	1.37
ai13 β	4.17	31.19	26.40	16.48	5.95	19.85		2.09	1.60	5.28	1.54
13 β	6.93		8.59	4876	32.29	27.97		4.25	3.37	8.14	1.22
i14 β	11.14	5.69	165.82	47.72	8.29	24.43		5.25	3.94	8.69	1.27
14 β	50.65	47.92	72.81	239.18	95.57	208.08	35.90	35.09	18.31	49.87	7.26
i15 β	17.37	22.54	45.18	128.05	32.95	89.44	14.17	9.29	6.84	16.76	2.25
ai15 β	25.06	14.96	24.27	46.75	15.95	37.04	17.37	17.47	10.13	20.53	4.37
15 β	9.04	7.98	143.36	74.24	53.58	38.35	6.56	16.36	4.90	18.28	1.85
i16 β	6.10	7.21		36.86	7.96	23.39		4.60	2.45	5.07	0.81
16 β	57.25	44.73	72.80	244.67	168.51	170.45	40.31	51.87	22.93	67.44	9.83
i17 β	23.54	38.05	24.71	212.71	58.32	148.81	24.62	13.62	7.50	28.80	2.63
ai17 β	21.36	25.82	42.93	54.55	27.85	32.87	13.94	14.14	9.40	15.74	2.08
17 β	10.11	13.60	60.59	105.12	14.68	51.15	5.09	7.45	5.50	7.49	1.36
18 β	21.71	21.68		90.09		57.15	13.30	14.57	10.97	26.37	3.41
20 β	13.45						6.76	19.60	5.55	12.71	1.92

A.5.3. Ester-bound ω-hydroxy fatty acids (ng/g sediment dry weight)

C#	0.5m	1.2m	1.6m	2.3m	3.3m	3.5m	3.9m
16ω	14.40	31.02	273.8	2.93	33.36	37.25	9.90
18ω					27.62		4.28
20ω					9.38		2.36
22ω	26.23		228.9	3.86	53.75	16.29	7.20
24ω	17.43		154.4		37.41		3.14
26ω			122.5				

A.5.4. Ester-bound n-alcohols (ng/g sediment dry weight)

C#	0.5m	1.2m	1.6m	2.3m	3.0m	3.3m	3.5m	3.9m
16	41.0	183.8	214.5	24.5	38.18	40.53	70.68	17.89
18	29.2	110.1	170.7	11.0	12.31	30.92	48.79	34.19
20	11.6	64.3	109.1			41.0	33.1	12.78
22	27.0	65.0	160.3		9.85	68.32	49.29	17.51
24	13.8	19.9	110.5	3.34	6.43	39.28	10.15	8.65
26	2.90	10.0	73.7			12.63	1.56	1.96

A.5.5. Amide-bound fatty acid methyl esters (ng/g sediment dry weight)

C#	0.5m	0.8m	1.2m	1.4m	1.6m	3.3m	3.9m
i14:0	29.98	114.76	248.24	63.52	88.91	39.00	38.20
14:0	135.33	49.05	122.06	274.45	142.27	18.04	14.98
i15:0	56.79	30.14	86.02	147.47	119.80	5.54	10.29
ai15:0	23.12	77.37	141.92	59.55	3.64	30.04	38.31
15:0	64.23	41.00	150.70	204.47	144.34	22.51	6.53
i16:0	41.00	42.29	1358.15	95.26	96.06	192.65	225.19
16:0	555.55	684.02	211.34	2058.00	1729.11	33.98	20.57
i17:0	107.22	69.46	75.88	206.81	161.95	31.19	4.26
ai17:0	58.01	46.07	309.15	108.28	90.96	38.99	35.98
17:0	134.09	73.34	780.08	139.26	158.13	56.17	111.08
18:0	402.07	382.06	138.47	1183.41	1331.86	9.97	7.87
19:0	42.58	25.22	272.45	68.92	60.33	40.01	22.28
20:0	177.62	99.90	59.72	363.06	295.95	29.30	13.07
21:0	22.21	21.86	358.65	68.22	44.59	59.63	49.36
22:0	268.19	185.54	58.86	782.71	510.31	15.85	15.40
23:0	56.97	44.75	358.60	97.13	70.77	74	39.53
24:0	393.15	155.88	94.18	498.08	451.48	87	19.32
25:0	27.08	32.98	113.59	59.20	38.32	12.93	21.11
26:0	130.88	104.19	159.01	161.61	135.22	41.74	10.89
27:0	16.50	36.17		105.92	31.86	21.54	8.77
28:0	47.86			76.87	102.46		
29:0	17.51				23.34		
30:0	29.54				95.01		
31:0	10.72						
32:0					56.81		

A.5.6. Amide-bound β -hydroxy fatty acids (ng/g sediment dry weight)

C#	0.5m	0.8m	1.2m	1.6m	3.3m	3.9m
12 β	74.98	159.89	235.61	202.31	34.48	18.98
i13 β	58.38	67.26	81.18	82.02	13.78	20.64
ai13 β	20.39	23.52	9.36	24.39	3.73	5.14
13 β	24.93	36.43	78.12	57.50	2.46	4.74
i14 β	49.13	88.47	59.26	86.93	29.42	31.87
14 β	220.97	456.14	545.37	608.38	86.66	77.57
i15 β	75.42	123.64	231.90	206.21	28.97	35.02
ai15 β	168.66	151.74	110.88	113.91	69.53	63.32
15 β	63.92	95.97	127.32	66.65	17.84	24.55
i16 β		138.55	144.10	82.88	19.38	6.66
16 β	172.27	383.04	543.54	563.43	56.10	75.18
i17 β	52.34	192.25	406.71	420.69	1315	13.84
ai17 β	54.54	79.71	66.33	81.89	12.33	11.38
17 β		57.52	105.99	146.79	5.36	4.57
18 β	236.82	132.73	96.44	164.08	24.72	6.70
19 β				14.47		
20 β		63.01		48.41	15.48	11.47

A.5.7. Summary of carbon preference indices, aquatic-to-terrestrial ratio, and the (i-C_{15:0} + ai-C_{15:0})/C_{16:0} ratio for ester-bound fatty acids.

Depth (m)	CPI _(12:0-30:0)	CPI _(12:0-20:0)	CPI _(20:0-30:0)	$\frac{\sum(C_{120} - C_{180})}{\sum(C_{220} - C_{280})}$	$\frac{(iC_{15:0} + aiC_{15:0})}{C_{16:0}}$
0.5	6.48	6.68	6.09	2.46	0.18
0.7	9.63	10.78	6.56	5.07	0.25
1.2	9.82	11.04	6.02	6.90	0.27
1.4	9.06	11.01	4.54	6.57	0.19
1.6	8.14	8.88	6.21	4.78	0.32
2.3	6.64	7.38	4.93	3.90	0.11
3.0	6.15	6.46	5.54	2.49	0.09
3.3	6.72	6.75	6.67	1.21	0.06
3.5	6.31	6.71	5.43	3.04	0.12
3.9	5.51	6.25	4.26	2.76	0.07

A.5.8. Summary of carbon preference indices, and the aquatic-to-terrestrial ratio for amide-bound fatty acids.

Depth (m)	CPI _(12:0-30:0)	CPI _(12:0-20:0)	CPI _(20:0-30:0)	$\frac{\sum(C_{120} - C_{180})}{\sum(C_{220} - C_{280})}$
0.5	6.00	5.91	6.15	1.59
0.8	5.33	5.35	5.29	3.23
1.2	7.86	8.85	6.04	2.93
1.4	8.34	10.16	5.72	2.87
1.6	7.93	8.93	6.18	2.86
2.3	5.88	7.33	3.79	3.10
2.6	5.71	6.54	4.59	2.06
3.1	4.84	5.22	4.39	1.77
3.3	4.51	5.18	3.53	2.39
3.7	4.04	5.57	2.75	1.82
3.9	6.72	7.52	5.05	3.43

APPENDIX VI

A.6.1. $\delta^{13}\text{C}$ (‰) composition of ester-bound fatty acids in core MBH 54/2.

Depth (m)	14:0	i15:0	ai15:0	15:0	i16:0	16:0	i17:0	ai17:0	17:0	18:0	20:0	22:0	24:0	26:0	28:0	30:0
0.8	-27.66	-28.48	-28.83	-27.33	-30.36	-27.54	-27.40	-28.02	-27.15	-26.78		-29.24	-28.44	-28.77	-32.30	
1.2		-28.11	-29.15	-27.97		-27.20	-27.08	-27.11	-26.20	-26.66	-27.80	-28.58	-27.99	-29.26	-29.76	
1.4	-28.98	-29.26	-30.48	-28.08		-29.59				-27.37	-28.61	-29.97	-29.34			-32.68
1.6	-28.14	-28.67	-29.26	-27.92		-28.85	-27.45	-27.11	-26.09	-26.07		-28.06	-27.97	-29.26	-32.49	-32.35
2.3	-28.94	-29.13	-30.59	-28.81		-28.00			-26.18	-27.92	-26.82	-28.43	-28.29	-29.20	-30.08	-32.52
2.6	-29.12	-29.97	-29.01	-28.09		-29.05			-26.22	-26.68	-25.68	-26.95	-28.12	-29.33	-29.88	-33.19
3.1	-30.43			-26.19		-26.79				-26.24	-26.29	-28.06	-30.30	-31.30	-30.97	-32.90
3.3	-26.70	-23.69		-22.94		-25.27			-23.15	-23.91		-24.25	-26.51	-27.38	-26.92	-29.04
3.7	-28.17			-26.33		-28.22				-24.61	-25.52	-24.68	-26.66	-28.00	-28.89	-30.41
3.9	-25.80	-23.80		-22.65		-24.42	-24.66		-24.61	-23.53	-27.48	-24.20	-23.79	-25.62	-24.76	-28.74

A.6.2. $\delta^{13}\text{C}$ (‰) composition of amide-bound fatty acids in core MBH 54/2.

Depth (m)	14:0	16:0	18:0	20:0	22:0	24:0	26:0	28:0	30:0
0.5	-27.90	-26.52	-23.85	-25.64	-22.89	-23.10	-22.95	-24.41	-27.24
0.8		-25.50	-26.92		-25.82	-23.41			
1.2		-26.46	-26.90		-28.86	-27.31			
1.4		-29.12	-27.68	-29.98	-30.27	-27.55	-29.60	-34.84	
1.6	-28.56	-26.40	-27.23	-29.64	-28.37	-26.55	-29.53	-32.89	-33.80
2.3	-28.86	-27.66	-25.69	-27.96	-29.02	-25.16			
2.6	-29.34	-26.85	-24.69	-28.25	-27.52	-25.27	-24.87	-29.34	-32.17
3.1	-29.03	-28.17	-27.35	-27.19	-26.91	-26.18	-27.71		
3.3	-26.26	-25.95	-24.44	-27.46	-26.58	-24.41	-24.99	-27.63	-32.03
3.7	-27.06	-28.30	-26.82	-31.76		-30.35	-31.12		
3.9	-28.83	-27.05	-26.43	-28.41	-28.70	-24.79	-23.73	-29.24	-33.60